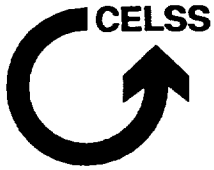

NASA Conference Publication 10040

Controlled Ecological Life Support Systems

Natural and Artificial Ecosystems

Sponsored by
Subcommission F.4
XXVII COSPAR meeting
Espoo, Finland
July 1989

NASA Conference Publication 10040

Controlled Ecological Life Support Systems

Natural and Artificial Ecosystems

Edited by
Robert D. MacElroy
Ames Research Center
Moffett Field, California

Brad G. Thompson
Alberta Research Council
Edmonton, Alberta, Canada

Theodore W. Tibbitts
University of Wisconsin
Madison, Wisconsin

Tyler Volk
New York University
New York, New York

Sponsored by
Subcommission F.4
XXVII COSPAR meeting
Espoo, Finland
July 1989

NASA

National Aeronautics and
Space Administration

Ames Research Center
Moffett Field, California

1989

TABLE OF CONTENTS

PREFACE

The 27th COSPAR meetings held in Espoo, Finland in July 1988 included a series of papers sponsored by Subcommission F.4, titled "Natural and Artificial Ecosystems." The scientific and technological interests of this group of investigators range from the study of *in situ* natural ecological systems, the development of biotechnology systems, through the generation of data on natural and artificial ecosystems by remote sensing technologies, to the development of artificial ecosystems. Underlying the studies presented are the participants' interests in developing life support systems for the use of human crews in space.

The diversity of ideas and approaches presented in the papers contained in this collection reflect the complexity of natural ecosystems and bioregenerative life support systems. It is anticipated that by increasing our knowledge of how the Earth's natural ecosystems function, we will gain insights into the requirements and function of artificial bioregenerative systems that will be used in space, either in orbit or on planetary surfaces. In turn, the development of bioregenerative systems may provide information leading to fuller definition of how natural systems function.

The majority of the papers presented in Espoo were concerned with research directed towards the development of Controlled Ecological Life Support Systems (CELSS). Topics include biotechnology, plant productivity studies, waste management issues, and ecosystem modelling. Contributions from Japan, France, Canada, the Soviet Union, and the United States have been edited by R. MacElroy (NASA Ames Research Center, California, U.S.A.), B. Thompson (Alberta Research Council, Alberta, Canada), T. Tibbitts (University of Wisconsin, Wisconsin, U.S.A.) and T. Volk (New York University, New York, U.S.A.). The editors wish to thank Sally Greenawalt at NASA Ames for her dedicated work in coordinating the manuscripts.

Robert D. MacElroy
July 1989

SECTION I

HIGHER PLANT GROWTH

UNDER CONTROLLED ENVIRONMENTAL CONDITIONS

CURRENT AND POTENTIAL PRODUCTIVITY OF WHEAT FOR A CONTROLLED ENVIRONMENT LIFE SUPPORT SYSTEM

B. G. Bugbee* and F. B. Salisbury**

*Assistant Professor, **Professor, Plant Science Department, Utah State University, Logan, UT 84322-4820

ABSTRACT

The productivity of higher plants is determined by the incident photosynthetic photon flux (PPF) and the efficiency of the following four physiological processes: absorption of PPF by photosynthetic tissue, carbon fixation (photosynthesis), carbon use (respiration), and carbon partitioning (harvest index). These constituent processes are analyzed to determine theoretical and potentially achievable productivity. The effects of optimal environmental and cultural factors on each of these four factors is also analyzed. Results indicate that an increase in the percentage of absorbed photons is responsible for most of the improvement in wheat yields in an optimal controlled environment. Several trials confirm that there is an almost linear increase in wheat yields with increasing PPF. An integrated PPF of 150 mol m^{-2} d^{-1} (2.5 times summer sunlight) has produced 60 g m^{-2} d^{-1} of grain. Apparently, yield would continue to increase with even higher PPF's. Energy efficiency increased with PPF to about 600 μmol m^{-2} s^{-1}, then slowly decreased. We are now seeking to improve efficiency at intermediate PPF levels (1000 μmol m^{-2} s^{-1}) before further exploring potential productivity. At intermediate and equal integrated daily PPF levels, photoperiod had little effect on yield per day or energy efficiency. Decreasing temperature from 23° to 17° increased yield per day by 20% but increased the life cycle from 62 to 89 days. We hope to achieve both high productivity and energy efficiency.*

INTRODUCTION

Several factors interact in complex ways to limit crop productivity. Crop physiologists have used correlation analysis to identify the environmental, genetic and cultural factors associated with high yields, but as we learn more about crop plant communities, it has become useful to identify and separately analyze the constituent processes that determine yield. The approach used in this paper is not unique and was developed from similar approaches used by J. H. M. Thornley /33/, John Monteith /23/, Penning de Vries and van Laar /28/, and especially D. A. Charles-Edwards /5/. We used the following determinants of crop growth in our analysis of productivity:

1. Incident photosynthetic photon flux (PPF; μmol m^{-2} s^{-1} or mol m^{-2} d^{-1}).
2. Percent absorption of the incident PPF by photosynthetic tissue.
3. Photosynthetic efficiency (moles of CO_2 fixed per mole of photons absorbed).
4. Respiratory carbon use efficiency (CUE, net carbon fixed in biomass per unit carbon fixed in photosynthesis).
5. Harvest index (edible biomass / total biomass).

Factor 1: Photosynthetic Photon Flux

PPF is the primary input to all plant production systems. All other environmental factors indirectly influence growth and yield by altering the efficiency of PPF utilization. Incident PPF level not only determines potential yield, but dictates (directly or indirectly) the energy fluxes in the plant production section of a Controlled Environment Life Support System (CELSS). PPF level determines the heat load and thus the cooling requirements in a CELSS.

Elevating CO_2 levels or lowering temperatures will increase the energy inputs to controlled environments on the earth, but changing these inputs will probably have insignificant effects on the energy requirements in a CELSS. Gas recycling means that it will not be

*Research reported in this paper was supported by the National Aeronautics and Space Administration Cooperative Agreement 2-139, administered through the Ames Research Center, Moffett Field, CA. Support was also received from the Utah Agricultural Experiment Station. This is Utah Agricultural Experiment Station paper no. 3653.

difficult to maintain elevated CO_2 levels. The challenge will be to control CO_2 at the desired concentration. Providing low temperatures in the plant chamber means that slightly lower grade waste heat will be produced, but biologically important temperature changes are relatively minor when measured as absolute temperatures. In the vacuum of space, cooling must be accomplished solely by radiation transfer, which is proportional to the fourth power of the absolute temperature of the radiating surfaces (Stefan-Boltzman Law). Reducing the temperature from 20° to 15°C would require 7.1% more radiating surface (293^4 / 288^4), but only a very small increase in energy input to circulate cooling fluids /1/.

Increasing heat loads require increasing convective air movement, which requires more energy, but even this is a small fraction of the PPF energy. In a preliminary analysis, Strickford et al. /32/ calculated that fans would require 4 to 10% of the total CELSS energy (lighting required about 65% and cooling about 25% of the total energy). Commercial growth chambers require 4 to 15% of the total energy to run the fans (depending on the PPF level), but commercial chambers have not been designed to minimize energy input to the fans.

Factors 2 to 5: Physiological Response

Four constituent physiological factors determine the efficiency with which photons are converted into food. They follow each other in chronological order:

Factor 2. Photons cannot cause photosynthesis until they are absorbed by green leaves, yet percent PPF absorption is often not included as a yield determinant. Measurement of PPF absorption of plant canopies is often highly correlated with yield (e.g. /12, 14/).

Studies using single plants usually determine plant response to the environment by measuring dry mass. These studies sometimes conclude that increased net photosynthesis per unit leaf area caused increased growth. Total leaf area, however, (and thus PPF absorption) is often the cause of improved growth. The factor causing increased plant growth becomes particularly important when single-plant studies are extrapolated to predict the performance of plants in communities /37/. Increased leaf area per plant causes increased competition among plants in communities, but increased photosynthetic rates per unit leaf area can translate into increased photosynthesis per unit ground area.

Factor 3. Photosynthetic carbon gains are usually integrated with respiratory carbon losses because plant dry mass is easily measured. Measuring plant dry mass is an excellent method of determining net carbon gain over periods of several days or weeks, but dry mass measurements cannot accurately separate photosynthesis from respiration. Photosynthesis is biochemically well characterized, and considerable progress has been made in determining the factors that limit carbon fixation in single leaves in optimal environments /30, 31/. Measurements of photosynthesis in intact plant canopies in a CELSS can be used to evaluate specific environmental effects on photosynthesis without the interacting effects of dark respiration.

Factor 4. During recent years much progress has been made in coupling models of dark respiration (excluding photorespiration) with physiological processes /16/. Several recent studies indicate that respiratory efficiencies deserve more study in plants /2, 16, 19, 20/. Respiration is best analyzed as the sum of two functional components: growth and maintenance respiration. These two components use the same substrates and biochemical pathways but provide energy for different physiological processes /2/. Respiratory efficiency has been widely studied in microorganisms and animals, so a large theoretical and empirical foundation can be applied to studies of plant respiration.

Factor 5. Carbon partitioning (harvest index) has been widely studied, and a large data base is available for comparison. Profuse vegetative growth (tallness, large leaves, etc.) increases competitive ability; but competitive ability is neither necessary nor desirable in controlled environments, and it decreases harvest index. There is thus considerable opportunity to increase the harvest index of crops in controlled environments. Donald and Hamblin /8/, in an excellent review of harvest index in grain crops, showed that yield increases (in the field) during the past 50 years have been primarily the result of increased harvest index.

Because theoretical maxima for each of these four physiological processes have been calculated (based on the underlying biochemistry), this analysis can be used to determine theoretical yield. Theoretical maxima, however, have never been achieved for any constituent process, so it is also useful to calculate the potentially achievable yield. This yield is based on the highest, instantaneous values ever recorded for each process. It assumes that all four processes could be maintained at this rate throughout the life cycle.

This type of component analysis makes it possible to separately analyze the processes that limit yield. Currently achievable productivity in a controlled environment, field produc-

tivity, and potential productivity are compared for each factor. This analysis not only provides an historical perspective on past accomplishments but is useful as a model to direct future research.

MEASUREMENT OF PHYSIOLOGICAL DETERMINANTS OF CROP GROWTH

Accurate PPF measurements are particularly important in CELSS research. Incident PPF is best measured with a recently calibrated quantum sensor (e.g. LiCor, model LI-190S). PPF is not uniform over a horizontal area in a growth chamber, and the average of many measurements should be used to determine PPF level.

Absorption of PPF cannot be measured directly but can be determined by measuring reflected and transmitted PPF and subtracting these components from incident PPF /12, 13/. Transmitted PPF is very nonuniform and must thus be averaged over a large area. We use an array of small (6 mm^2) gallium arsenide photodiodes (Hamamatsu, model G-1118; /6/, which are calibrated with a quantum sensor. The small size of these sensors minimizes interference with leaf position in the canopy.

Carbon fixation and carbon use efficiencies are best measured with a gas exchange system that measures carbon dioxide fluxes. Photosynthesis, photorespiration, and dark respiration all occur simultaneously in the light, so special measurement procedures must be followed. Many techniques for determining the magnitude of photorespiration have been developed, but photorespiration is not a separate part of this model; its effects show up as a reduction in the photosynthetic efficiency. Photorespiration is very important in a CELSS and is discussed in the final section of this paper.

Unlike photorespiration, dark respiration is a separate part of this model. Precise determination of respiratory carbon efflux is difficult because the effect of light on dark respiration is not fully understood. Dark respiration may be higher in the light because high levels of assimilates are known to increase respiration. Dark respiration may be lower in the light because photophosphorylation provides reducing energy, and may thus decrease dark respiration. The effect of light on dark respiration is reviewed by Amthor /2/. Most models assume that respiration does not vary with light or darkness, but several approaches to minimize the problem have been developed. They involve changing the photosynthesis rate, growth rate, and/or plant mass and measuring corresponding changes in the dark respiration rate /2/. An additional problem, common to all methods, is that the energy gained by photophosphorylation can substitute for dark respiration. In fact, photophosphorylation (which is driven by absorbed photons) is probably one of the reasons that the highest measured photosynthetic efficiencies are well below their theoretical potential. The merits and the problems of the methods for measuring dark respiration have been reviewed by Lambers et al. /20/. The problems mean that values reported for carbon use efficiency are close estimates rather than direct measurements.

Gas exchange measurements are frequently made either on single leaves or on single plants, but we wanted to measure these parameters on communities of plants. To this end, we sealed a growth chamber to allow the measurement of canopy gas exchange. A CELSS is a sealed environment and is thus uniquely adapted to routine measurement of photosynthesis and respiration.

Harvest index can easily be determined by separating edible plant parts from less edible stem and root tissue. This measurement is made on a dry mass basis and includes the dry root mass.

Although the individual determinants of yield are sometimes difficult to measure, the total system efficiency can be accurately determined. The fundamental measure of efficiency is the output of the system divided by the required input. The most useful measure of the efficiency of higher plant growth in a CELSS is grams of edible and total biomass per mole of photosynthetic photons. Calculations of efficiency per unit photosynthetic radiation will be 3 to 6 times higher than per unit total radiation (because artificial lamps are only about 15 to 35% efficient), but basing efficiency on photosynthetic photon flux is more appropriate because biologists should not be penalized (or rewarded) for differences in the efficiency of the lamps they are using. Expressing efficiency per photosynthetic photon also facilitates comparison of results among laboratories. The first goal of higher-plant CELSS research should be to determine optimal environments; a subsequent goal should be to help engineers build systems to deliver the desired environments.

Efficiency can be expressed on an energy basis by determining the energy content of the biomass and the photons. The total (bomb calorimeter) energy content of wheat straw is typically 17.0 kJ g^{-1}. Wheat seeds have a higher energy content at 18.6 kJ g^{-1}. Photosynthetic photons from the sun have an average wavelength of 550-nm and thus contain 217 kJ

mol^{-1} (E = hc/wavelength). Multiplying by these energy contents allows the calculation of percent efficiency /4/.

PHYSIOLOGICAL DETERMINANTS OF CROP GROWTH: EFFICIENCY

Estimates of the efficiencies of the four yield determinants are summarized in Table 1 for five situations: theoretical maximum, potentially achievable, Utah State University CELSS project, world record field, and typical field. The values are combined (by successive multiplication) to give an integrated efficiency for conversion of PPF to the chemical bond (bomb calorimeter) energy of edible grain (92 to 96% digestible energy). The following sections discuss the determinants as they apply in each situation.

TABLE 1 Efficiency of different growing environments for converting incident PPF into edible food

SITUATION	PPF ABSORPTION %	PHOTO-SYNTHETIC EFFICIENCY %	RESPIRATION EFFICIENCY %	HARVEST INDEX %		INTEGRATED PPF EFFICIENCY %
THEORETICAL EFFICIENCY	100	33.5	82	100	=	27.5
POTENTIALLY-ACHIEVABLE EFFICIENCY	98	18	75	90	=	11.9
UTAH STATE UNIVERSITY CELSS PROJECT	90	16	70	44	=	4.4
WORLD RECORD IN FIELD	65	12	63	45	=	2.2
TYPICAL FIELD	50	8	55	40	=	0.9

Theoretical Maximum

PPF absorption. At the theoretical level we assume that plants are perfect blackbodies and absorb 100% of the incident radiation.

Photosynthesis. One photon is required to excite one electron (Stark-Einstein Law), four electrons are required to split each water molecule (because excitation of both photosystems is essential), and two molecules of water are required to reduce each molecule of CO_2; this means that an absolute minimum of 8 photons (2 x 4) are necessary to fix CO_2 into a carbohydrate skeleton (CH_2O; /29/). Photons of red light (exactly 700 nm) have the lowest possible energy to excite electrons in photosynthesis, but the Emmerson enhancement effect (cooperation of the two photosystems) means that it is more appropriate to assume that photons must have an average wavelength of 680 nm /25/. At 680 nm, photons have an energy of 176 kJ mol^{-1} so 8 moles of photons contain 1408 kJ. The energy per mole of carbon in simple carbohydrate (sucrose) is 470 kJ mol^{-1}. Thus, the theoretical maximum efficiency of photosynthesis is 33.5% (470 / 1408).

Respiration. Plants consist of more than simple carbohydrates; additional energy is required to synthesize structural carbohydrates, proteins, and lipids. The theoretical minimum amount of nonstructural carbohydrate (e.g. sucrose, fructose, or starch) required to make other compounds in higher plants was analyzed in a classic paper by Penning De Vries et al. /28/. This paper, and another by DeWitt /7/, indicate that structural carbohydrates (cellulose and hemicellulose) can be made from hexose sugars with about 86% efficiency, and amino acids can be synthesized with 70% efficiency (from ammonia, Table 2). If we assume a plant that is 75% carbohydrate and 25% protein (RUBISCO for CO_2 fixation) it is possible to estimate a theoretical carbon use efficiency of 82%. This assumes that no carbon is used in maintenance respiration and that neither lipid nor lignin is present in the plant.

Harvest index. For theoretical purposes, we consider all the biomass to be edible (100% harvest index).

Combining these efficiencies (1.00 x 0.335 x 0.82 x 1.00 = 0.275) gives an overall theoretical maximum efficiency of 27.5%.

Potentially Achievable Yield

Percent absorption. A single leaf transmits about 5% of the incident PPF and reflects an additional 5% (when it is perpendicular to the light beam), so 90% of the PPF is absorbed. Multiple layers of leaves in a fully developed wheat canopy in an optimal environment result in a PPF transmission of about 0.1%. The vertical leaf orientation in wheat canopies also means that slightly less PPF is reflected than is reflected from horizontal leaves. We have measured less than 2% reflected PPF from a healthy canopy. The resulting absorption is thus 98%. The challenge is to quickly reach and then maintain this level of absorption until harvest.

Photosynthetic efficiency. The number of photons required to fix a molecule of CO_2 is known as the quantum requirement. The lowest quantum requirement measured in reliable studies (in a single leaf at a PPF level below 200 μmol m^{-2} s^{-1}) has been 12 moles of photons per mole of CO_2 fixed /9, 10, 26/.

As noted above, photosynthetic photons from sunlight contain 217 kJ mol^{-1}. The average wavelength of most artificial lamps (and the energy content of photosynthetic photons) is similar to sunlight, so a more realistic calculation for the conversion efficiency of photosynthesis in a CELSS environment is thus 18% {470/(12*217)}. Because maximum photosynthetic efficiency is only obtained at PPF levels below 200 μmol m^{-2} s^{-1}, the challenge is to obtain maximum efficiency in a plant canopy at higher PPF levels.

Respiratory Carbon Use Efficiency: Growth respiration. Growth respiration is the cost associated with the synthesis of new biomass. The conversion efficiency of simple sugars into plant dry mass depends on the compound synthesized. Table 2 indicates the efficiencies of conversion of glucose to the major categories of plant substances (from /7/). Glucose is an uncommon compound in plants but is energetically representative of the initial products of photosynthesis. Triose phosphates are the first products of photosynthesis; the predominant sugar transported and metabolized in plants is sucrose; and hexose sugars feed glycolysis and the Krebs cycle. Glucose was used in this study apparently because the original analyses were done with microorganisms, which utilize glucose. Fortunately, the energy per mole of carbon in glucose and sucrose are nearly identical (466.7 and 469.6 kJ mol^{-1}, respectively; Handbook of Chemistry and Physics 66th ed.) so the values of Table 2 do not change significantly with the substrate sugar.

TABLE 2 Grams of the major categories of plant tissue that can be synthesized from one gram of glucose.

COMPOUND	CONVERSION EFFICIENCY g per g
Structural carbohydrates	. . . 0.86
Lipids.	. . . 0.36
Lignin.	. . . 0.46
Organic acids	. . . 0.99
Organic N-compounds with NO_3. . .	. . . 0.47
Organic N-compounds with NH_3. . .	. . . 0.70
Inorganic minerals assimilated into organic molecules	. . . 0.93

Low-lipid, high-carbohydrate plants (wheat and potatoes) can have very high respiratory conversion efficiencies for new biomass. The carbon use efficiency for the synthesis of high-lipid biomass (e.g. peanuts and soybeans) is much lower than wheat and potatoes; such plants do have a correspondingly high energy content per unit mass of seed storage tissue.

Maintenance respiration. As noted earlier, it is useful to partition the dark respiratory carbon efflux into two functional components, a growth component and a maintenance component /19/. The carbon required for maintenance respiration is used to maintain existing biomass. A significant fraction of the carbon used in maintenance respiration is required to resynthesize compounds that help plants adapt to changing or harsh environmental conditions. The constant, optimal environmental conditions in a CELSS may thus significantly reduce the maintenance requirement /19/. Rapid growth rates should also reduce the maintenance requirement. Models by Johnson /16/ indicate that carbon use efficiency should asymptotically approach 75% as the growth rate increases, but the effect of rapid growth rates on maintenance respiration are still controversial /19/. Some models of potential crop production have assumed a carbon use efficiency of 75% for root and tuber crops /35/. We thus estimate a potential carbon use efficiency of 75%. The challenge is

to maximize total carbon use efficiency by minimizing unnecessary compounds (like lignin) and unnecessary biomass (roots and stems).

Harvest index. Crop plants vary widely among species in their harvest index. Some improvement in a species can be made with cultural and environmental manipulations, but major improvements require genetic manipulation of plant morphology. A harvest index of 100% would be possible only when combined with the refinement of technologies to convert cellulose, hemicellulose and lignin to digestible compounds /21/. Potatoes and lettuce grown in an optimal environment typically have harvest indexes of about 80% /18, 34/. Some super-dwarf wheat cultivars (20-cm tall) have a harvest index of over 60%, but they are not high yielding. Genetic improvement of head size (sink strength) in these cultivars might significantly increase both yield and harvest index, but this will not be easy to accomplish. Our experience with wheat indicates that the root system is consistently about 3% of the dry biomass at harvest. An additional 2% is in the stem base. We speculate that a harvest index of 90% might be achieved with appropriate genetic and environmental manipulations.

The potentially achievable efficiency, within the constraints as discussed, is thus about 11.9% (0.98 x 0.18 x 0.75 x 0.90 = 0.119).

Currently Achievable Efficiency: Utah State University CELSS Project

PPF absorption. Although 98% absorption occurs at full canopy development, an average of 90% of the PPF is absorbed over the life cycle (Figure 1). The high plant densities that are an important component of high yields in a CELSS cause PPF absorption to exceed 95% a few days after emergence (when the lights are turned on). Leaf senescence during the last part of the life cycle reduces absorption.

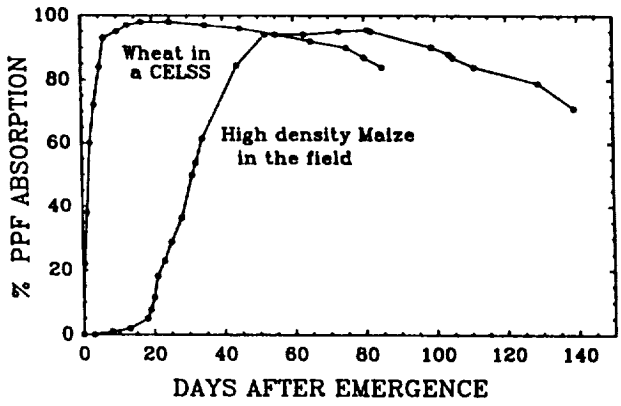

Fig. 1. A comparison of the percent absorption of PPF by wheat in a CELSS and maize in the field. The data for maize are taken from /13/. Similar data for wheat (over the entire life cycle) were not readily available, but cereal crops typically absorb PPF somewhat more rapidly during early growth than maize /12, 14/. This comparison indicates one of the primary reasons for increased yields in a CELSS.

Photosynthetic and respiratory efficiencies. Preliminary data from our canopy gas exchange system indicate that photosynthetic efficiencies of 17% are possible during the first half of the life cycle. Leaf senescence during the final stages of the life cycle reduces photosynthetic efficiency and thus reduces the average efficiency over the life cycle to about 16% /4/.

We do not yet have good measurements of the respiratory carbon use efficiency, but we hypothesize that rapid growth rates may reduce maintenance respiration and thus increase carbon use efficiency /4/. The respiration rate of roots is typically very high /19/, but an optimal root-zone environment (hydroponic culture) significantly reduces the size of the root system, thus improving carbon use efficiency, which we estimate to be 70%.

Harvest index. Our harvest indexes (40 to 45%) have not exceeded those in the field. High CO_2 concentrations and a continuous supply of nitrogen in the root-zone promote vegetative growth and may thus reduce the harvest index. Wheat forms multiple heads (called tillering) when environmental conditions favor vegetative growth. High photosynthetic environments cause excessive tillering, and late forming tillers have a 10% lower harvest index (Figure 2). Eliminating late (tertiary) tillers might increase the mean harvest index to 50%.

Our genetic manipulations have not eliminated tillering, but altering the red/far-red radiation ratio might be very effective. This ratio directly alters the phytochrome equilibria in plant tissue, which in turn regulates tillering /17/. We hypothesize that a high level of far-red radiation during the first 20 days of growth may be sufficient to eliminate late forming tillers. Charles Barnes, a Ph.D. student in our laboratory, is studying these effects.

Our highest current efficiency is 4.4% (0.9 x 0.16 x 0.7 x 0.44 = 0.044).

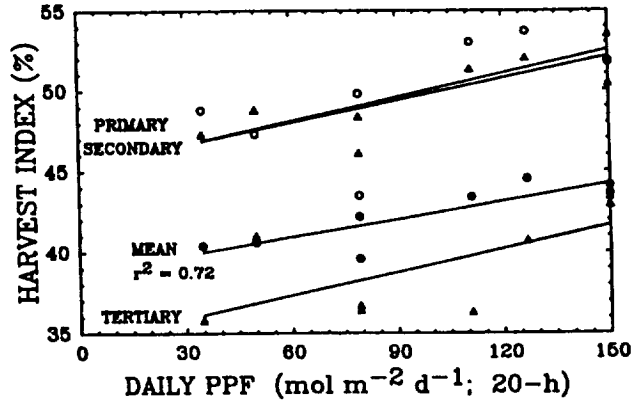

Fig. 2. The effect of daily PPF on harvest index. Note that primary (o) and secondary (▲) tillers have a much higher harvest index than tertiary (△) tillers. The harvest index increased slightly with increasing PPF. The root dry mass is included with the total plant biomass in these data. Root mass is not typically included in harvest index calculations in the field, but these plants had less than 5% root mass.

Field Efficiencies

Integrated efficiency. The data for the world record wheat efficiency are from a one hectare field in Washington State. This record, set in 1965, used the cultivar "Gaines", which is a winter wheat /36/. This report is similar to other reports of record yields in the literature. These reports were recently reviewed /4/. Record wheat yields are typically set with winter wheat, partly because it is in the field for about 9 months (over the winter). This makes it difficult to realistically estimate yield per day. We took the total grain yield as reported by Wittwer /38/ (216 bushels/acre) and assumed a 100 day period of active growth (yield/100 = yield per day). This probably overestimates the yield per day, but we prefer to give field yields the benefit of the doubt. This calculation, combined with average daily PPF data for Washington State, allows an estimate of integrated PPF efficiency (2.2%). The integrated PPF efficiency for a typical field is estimated in a similar manner.

PPF absorption. The data in Figure 1 for high density maize in the field is typical of highly productive field environments /13/. The PPF absorption integrated over the life cycle for the high density maize in Figure 1 is 53% of the incident PPF. High density wheat is planted in rows that are closer together than high density maize (15-cm vs. 30-cm, respectively) and thus more rapidly absorbs incident PPF during the first 20 days of growth. Hipps et al. /15/ found that a wheat crop in the field absorbed about 75% of the incident PPF at a leaf area index (LAI) of 2, and 95% of the PPF above an LAI of 5. Unfortunately, wheat does not reach an LAI of 2 for several weeks after planting. Average PPF absorption is typically about 65% over the life cycle /12, 14/.

Photosynthesis and respiration. Photosynthetic efficiency in the field was taken from values in the literature /5, 28/. Experimental evidence indicates that the respiratory cost of maintenance in annual plants in the field is about equal to the cost of growth respiration over the plant life cycle /2/. The overall carbon use efficiency has thus been about 60% for crop plants /16, 22/.

Harvest index. A harvest index of 50 to 55% can be obtained in field grown wheat, but a harvest index of 40 to 45% is more common. Harvest indexes below 40% are usually associated with plant stress.

TOTAL SYSTEM EFFICIENCY

The PPF Input / Efficiency tradeoff

Table 3 indicates how the total percent efficiency (from Table 2) interacts with PPF input to determine edible yield.

TABLE 3 The effect of PPF level on energy efficiency and edible yield.

SITUATION	PPF INPUT mol m^{-2} d^{-1}	EFFICIENCY %	EDIBLE YIELD g m^{-2} d^{-1}
POTENTIAL YIELD	45	11.9	73
UTAH STATE UNIVERSITY CELSS PROJECT	45	4.4	27
WORLD RECORD IN FIELD	45	2.2	14
TYPICAL FIELD	45	0.9	6
UTAH STATE UNIVERSITY CELSS PROJECT	150	2.9	60
TOTAL BIOMASS	150	7.2	137

High efficiency (4.4%) can be achieved at field PPF levels, but the most remarkable finding is that yields continue to increase as PPF increases. The average daily PPF in the field ranges from 35 to 60 mol m^{-2} d^{-1} during the summer months in different crop growing regions (depending mostly on cloud cover). A high PPF in controlled environments (3.3 times field PPF) resulted in a yield that was close to the potentially achievable grain yield in the field (60 vs. 73 g of seed m^{-2} d^{-1}; CELSS and field, respectively). This yield increase comes at the expense of efficiency (2.9% versus 4.4%). Figure 3 illustrates this tradeoff. The efficiency values in this figure are for total biomass, but the shape of the efficiency curve is nearly identical for edible biomass because harvest index changes only slightly with daily PPF.

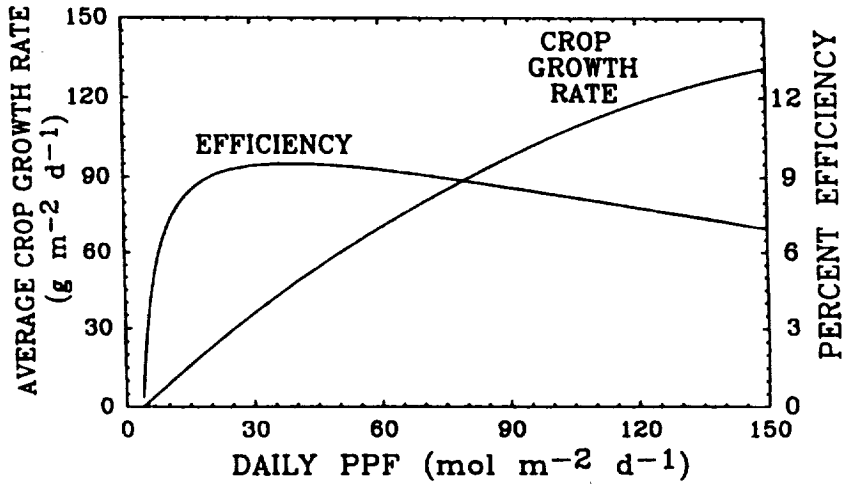

Fig. 3. The tradeoff between percent PPF efficiency and yield in a CELSS. Percent efficiency is calculated as discussed in the text. These data (from /4/) indicate that efficiency peaks at about 30 to 40 mol m^{-2} d^{-1} and then slowly decreases. When mass and volume are considered, peak efficiency should occur at a higher PPF level.

Potentially achievable productivity. Figure 4 graphically indicates field, CELSS, and potentially achievable productivity as a function of PPF input. The CELSS yield curve in this figure is the same as that in Figure 3, which is based on data from our laboratory. Record productivities are documented in the literature, and they vary widely for different crops in different environments (reviewed in /4/). The calculation of potentially achievable yield is based on the assumptions discussed earlier.

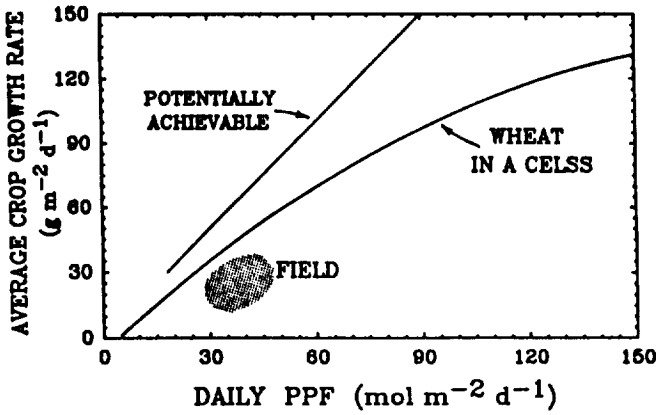

Fig. 4. A comparison of potentially achievable yield, current CELSS yield, and the range of record yields in the field (shaded area). All data are for total biomass. Potentially achievable yield assumes that PPF is the only limiting factor and is based on the calculations in the text. CELSS yield is from /4/. Summer PPF in the field is 30 to 50 mol m^{-2} d^{-1} and maximum field yields are from studies in the literature.

Reproducibility. How reproducible is the CELSS yield curve in Figure 4? Figure 5 shows the overall mean from eight separate studies and compares this mean with the yield from our best single study. The 8 studies include different environmental conditions (photoperiod and temperature); different cultivars (Yecora Rojo and Veery 10), and different cultural conditions (planting densities, etc.). The studies were also conducted in different types of growth chambers. Two of the studies were conducted in a special, CO_2-enriched greenhouse section. All studies were conducted in hydroponic culture. About half of the scatter in the data is the result of environmental parameters other than PPF, but much of the scatter is from unidentified causes (experimental error).

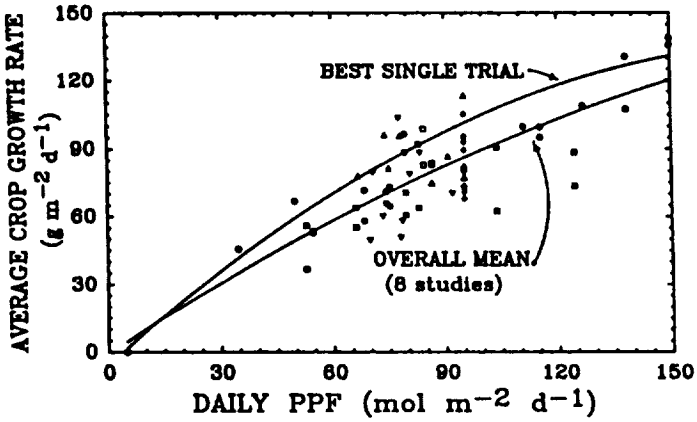

Fig. 5. Reproducibility in a CELSS: A comparison of our best single trial with the overall mean of 8 different trials. Symbols represent different studies. The eight studies involve environmental and cultural treatments conducted in different types of growth chambers. None-theless about half of the variability is the result of experimental error.

Reproducibility is critical in a CELSS, but variability is inherent in biology. As we identify the causes of low yields, we improve our ability to predict yields.

Figure 5 also indicates the lack of data at low and high PPF levels. Additional research at low PPF levels would help to precisely identify the PPF level at which peak energy efficiency occurs. Energy, however, is not the only input to a CELSS. Higher PPF levels are necessary to increase efficiency per unit mass and volume. Studies at both high and low PPF are important because PPF level often interacts with the other environmental, cultural and genetic factors that determine the PPF utilization efficiency.

Photoperiod effects. When the daily PPF is the same, low PPF levels and long photoperiods usually result in better growth than high PPF levels and short photoperiods. Wheat is a long-day plant for reproductive initiation and thus does not have an obligate need for a daily dark period. Wheat plants yield well and appear healthy in continuous light, but

long photoperiods might reduce efficiency per photon. Three recent studies with 16, 20, and 24 hour photoperiods indicated that wheat plants do not need or benefit from a daily dark period. Photoperiod, however, has large effects on plant height and length of the life cycle. Compared to a 16-h photoperiod, continuous light shortened the life cycle by 30% and shortened plant height by 25%. Both of these effects would be beneficial in a CELSS.

A NOTE ON PHOTORESPIRATION IN A CELSS

Although photorespiration can reduce photosynthetic efficiency by 30% at ambient O_2 and CO_2 levels, high CO_2 levels (1500 μmol mol^{-1}; characteristic of a CELSS) reduce photorespiration to less than 5% /9/. Indeed, photosynthetic efficiency is increased in a CELSS environment largely because of reduced photorespiration. In high CO_2 environments, all plants with C_3 photosynthesis have higher photosynthetic efficiencies than the four principal, C_4 crop plants (maize, millet, sorghum, and sugar cane; /9, 10/).

Are low oxygen concentrations necessary or useful in a CELSS? Theoretically, photorespiration can be eliminated either by decreasing O_2 levels or by increasing CO_2 levels /11/, but Musgrave and Strain /24/ found that wheat growth was increased at 5% O_2 compared to controls at ambient O_2 and 1000 μmol mol^{-1} CO_2. This CO_2 level (0.1%), however, is not high enough to eliminate photorespiration. Increasing the CO_2 concentration to 0.2% (2000 μmol mol^{-1}) is high enough to eliminate almost all photorespiration, but, although this CO_2 level increases photosynthesis for several days, it can reduce growth after several weeks /3, 18/. The physiological mechanism causing CO_2 toxicity is not yet clear and we are continuing our studies. Small CO_2 increases (0.1% of total atmosphere) have large effects on plant growth and are thus preferable to decreasing O_2, which is hazardous to humans.

REFERENCES

1. B.N. Agrawal, Design of Geosynchronous Spacecraft, Prentice Hall, Englewood Cliffs, NJ, 1986.

2. J.S. Amthor, The role of maintenance respiration in plant growth, Plant, Cell and Environment 7, 561-569, (1984)

3. B. Bugbee, When does CO_2 enrichment become toxic to plants? HortSci. 20, 549 (1985)

4. B.G. Bugbee and F.B. Salisbury, Exploring the limits of crop productivity: Photosynthetic efficiency in high irradiance environments, Plant Physiol. 88, 869-878 (1988)

5. D.A. Charles-Edwards, Physiological Determinants of Crop Growth, Academic Press, London, 1982.

6. R.L. Chazdon and C.B. Field, Photographic estimation of photosynthetically active radiation: Evaluation of a computerized technique, Oecologia 73, 525-532 (1987)

7. C.T. DeWit, Simulation of Assimilation, Respiration and Transpiration of Crops, Halstead Press, New York, 1978.

8. C.M. Donald and J. Hamblin, The biological yield and harvest index of cereals as agronomic and plant breeding criteria, Advances in Agronomy 28, 361-405 (1976)

9. J. Ehleringer and O. Bjorkman, Quantum yields for CO_2 uptake in C_3 and C_4 plants: Dependence on temperature, CO_2, and O_2 concentration, Plant Physiol. 58, 86-90 (1977)

10. J. Ehleringer and R.W. Pearcy, Variation in quantum yield for CO_2 uptake among C_3 and C4 plants, Plant Physiol. 73, 555-559 (1983)

11. G. Farquhar and S. VonCammerer, Modeling of photosynthesis to environmental conditions, Encyclopedia of Plant Physiology 12B, 549-587, Springer-Verlag, 1982.

12. J.N. Gallagher and P.V. Biscoe, Radiation absorption, growth and yield of cereals, Jour. Agric. Sci. 91, 47-60 (1978)

13. K.P. Gallo and C. Daughtry, Techniques for measuring intercepted and absorbed photosynthetically active radiation in corn canopies, Agron. Jour. 78, 752-756 (1986)

14. C.F. Green, Nitrogen nutrition and wheat growth in relation to absorbed solar radiation, Agric. and Forest Meteorology. 41, 207-248 (1987)

15. L.E. Hipps, G. Asrar, and E.T. Kanemasu, Assessing the interception of photosynthetically active radiation in winter wheat, Agric. Meteorology 28, 253-259 (1983)

16. I.R. Johnson, Models of respiration, in: Plant Growth Modeling for Resource Management Vol II, eds. K. Wisiol and J. Hesketh, CRC Press, 1987.

17. M.J. Kasperbauer and D.L. Karlen, Light-mediated bioregulation of tillering and photosynthate partitioning in wheat, Physiol. Plant. 66, 59-163 (1986)

18. S.L. Knight and C.A. Mitchell, Effects of CO_2 and photosynthetic photon flux on yield, gas exchange, and growth rate of Lactuca Sativa, J. Exp. Bot. 39, 317-328 (1988)

19. H. Lambers, Higher plant cell respiration: Respiration in intact plants and tissues, eds. R. Douce and D.A. Day, Encyclopedia of Plant Physiology 18, 418-473, 1985.

20. H. Lambers, R.K. Szaniawski, R. De Visser, Respiration for growth, maintenance and ion uptake: An evaluation of concepts, methods, values and their significance, Physiol. Plant. 58, 556-563 (1983)

21. M. Mandels and D.L. Kaplan, Conversion of inedible wheat biomass to edible products for space missions, Final Report to NASA Biomedical Office, KSC, 1986.

22. K.J. McKree, Sensitivity of sorghum grain yield to ontogenetic changes in respiration coefficients, Crop Sci. 28, 114-120 (1988)

23. J.L. Monteith, Climate and efficiency of crop production in Britan. Phil. Trans. R. Soc. Lond. 281, 77-294 (1977)

24. M.E. Musgrave and B.R. Strain, Response of two wheat cultivars to CO_2 enrichment under subambient oxygen conditions, Plant Physiol. 87, 346-350 (1988)

25. P. Nobel, Biophysical Plant Physiology and Ecology, Freeman, San Francisco, 1983.

26. B.A. Osborne and M.K. Garrett, Quantum yields for CO_2 uptake in some diploid and tetraploid plant species, Plant, Cell, and Environment 6, 135-144 (1983)

27. F.W.T. Penning de Vries, A. Brunsting, and H. van Laar, Products, requirements and efficiency of biosynthesis: A quantitative approach, Jour. Theoretical Biol. 45, 339-377 (1974)

28. F.W.T. Penning de Vries and H. van Laar (eds), Simulation of plant growth and production, Center for Agric. Publishing, Wageningen, 1982.

29. F.B. Salisbury and C. Ross, Plant Physiology, 3rd ed., Wadsworth, Belmont, CA, 1985.

30. T.D. Sharkey, M. Stitt, D. Heineke, R. Gerhardt, K. Raschke, and H. Heldt, Limitation of photosynthesis by carbon metabolism: Oxygen insensitive CO_2 uptake results from limitation of triose phosphate utilization, Plant Physiol. 81, 1123-1129 (1986)

31. M. Stitt, Limitation of photosynthesis by carbon metabolism: Evidence for excess electron transport capacity in leaves carrying out photosynthesis in saturating light and CO_2, Plant Physiol. 81, 1115-1122 (1986)

32. G.H. Strickford Jr., F.E. Jakob, and D.K. Landstrom, An engineering analysis of a closed cycle plant growth module, in: Controlled Environment Life Support Systems: CELSS '85 Workshop, NASA Tech. Memo. 88215, eds. R.D. MacElroy, N. Martello, and D. Smernoff, Ames Res. Cntr., (1986)

33. J.H.M. Thornley, Mathematical Models in Plant Physiology, Academic Press, NY, 1976.

34. T. Tibbitts, this issue.

35. M.N. Verstreg and H. van Keulen, Potential crop production prediction by some simple calculation methods, as compared with computer simulations, Agricultural Systems 19, 249-272 (1986)

36. O. Vogel, Washington State University, USDA, personal communication, (1988)

37. J.W. Wilson, Analysis of growth, photosynthesis and light interception for single plants and stands, Ann. Bot. 48, 507-512 (1981)

38. S.H. Wittwer, Food production: Technology and the resource base, Science 188, 579-584 (1975)

A90-15428

EFFECT OF CO_2 AND O_2 ON DEVELOPMENT AND FRUCTIFICATION OF WHEAT IN CLOSED SYSTEM

M. André*, F. Cotte**, A. Gerbaud***, D. Massimino*, J. Massimino*, C. Richaud*

*Institut de Recherche Fondamentale CEA. Département de Biologie, Service de Radioagronomie, CEN Cadarache, F 13108 ST PAUL LEZ DURANCE. **Boursier CNES, F 31000 TOULOUSE. ***INRA, Laboratoire des Symbiotes des racines, INRA Montpellier (France).

ABSTRACT

The cultivation of wheat (Triticum aestivum L.) was performed in controlled environment chambers with the continuous monitoring of photosynthesis, dark respiration, transpiration and main nutrient uptakes. A protocol in twin chambers was developed to compare the specific effects of low O_2 and high CO_2. Each parameter is able to influence photosynthesis but different effects are obtained in the development, fructification and seed production, because of the different effects of each parameter on the ratio of reductive to oxidative cycle of carbon. The first main conclusion is that low level of O_2, at the same rate of biomass production, strongly acts on the rate of ear appearance and on seed production. Ear appearance was delayed and seed production reduced with a low O_2 treatment (≈ 4 %). The O_2 effect was not mainly due to the repression of the oxidative cycle. The high CO_2 treatment (700 to 900 $\mu l.l^{-1}$) delayed ear appearance by 4 days, but did not reduce seed production. High CO_2 treatment also reduced transpiration by 20 %. Two hypothesis were proposed to explain the similarities and the difference in the O_2 and CO_2 effects on the growth of wheat.

INTRODUCTION

In space, plant life is free not only from gravity but also from factors linked to earth surface particularities such as : atmosphere composition, light cycles, and light intensity. In particular, planned farming for producing part of the food needed by the crew, especially on long duration missions /19/, can be optimized without regard to earth conditions.

The first planned modification has to do with the atmosphere. Experiments involving the growth of CO_2 content at three times the earth atmosphere level were put into practice at the Botany facilities /8/. It is because carbon dioxide stimulates the photosynthesis process, that experiments have been planned to provide information for the Biogeneration Life Support program /25/. From a physiological point of view, little is still known regarding the particular effects of this increase in CO_2.

Biochemistry studies show that the effect of CO_2 is inseparably linked to that of oxygen. The two react on the same substratum thus generating two antagonistic reactions, one of carboxylation and the other of oxygenation, catalyzed by the same enzyme : ribulose bisphosphate carboxylase/oxygenase or rubisco. The ratio of the two reaction speeds depends on the respective concentrations of CO_2 and O_2 /21/. The two reactions initiate two metabolic cycles /30/. The activity of the carbon reduction cycle which synthesizes hydrocarbons depends on the rate of carboxylation reaction. All activity enhancement obtained by increases in the CO_2 partial pressure, is detrimental to the oxygenation process. Oxygenation supplies the oxidative carbon cycle that is closely linked to nitrogen metabolism. Biochemical studies have shown this link /30/, but no physiological experiments have demonstrated this link. Even so, if it is established that the oxidative cycle generates amino acids (glycine and serine) it will still remain unknown if the cycle exports these substrates. Assuming that these are exported, either directly or by transaminase, it is equally unclear whether this emission is essential or useful to the plant.

Cultivation of plants under CO_2 enrichment /9, 20, 28, 29/ have shown a total biomass improvment but often a smaller increase in the reproductive parts, as the grain of wheat than in the vegetative parts. Because the grain is very rich in nitrogen compounds, a reduction in the ratio of grain to dry matter could be associated with a repression of the oxidative cycle /23/. However, accurate and systematic research on the effect of CO_2, in repressing the oxidative cycle, has not been undertaken. Equally significant is the

decrease of dark respiration activity when assimilation is increased by elevation of CO_2 /5, 10, 17/. This suggests that synthesis activity, which accounts for part of the respiration and is proportional to the assimilation activity, is reduced when CO_2 is increased.

Up to this time, oxygen content modification has not been studied in Bioregenerative Life Support research. Considering the activity of rubisco, /21/, the lowering of the oxygen content theoretically stimulates the photosynthesis process in the same way as an increase in the CO_2 content. In practice, the stimulation of growth is important during the vegetative phase /7, 27/. But accurate study of secondary effects of the repression of oxidative cycle by this way has not be implemented.

The potential opportunity to regulate oxygen concentration in space farming systems, together with the difficulties and the cost of a precise oxygen regulation in culture modules or in the bioreactors, are reasons for the study of the oxygen level effects.

The study of partial oxygen pressure is of particular importance if there are reductions in the total pressure in the plant growing modules. Considering the high volume required for cultivating plants for life support the weight, and hence the launching costs, can be considerably reduced by growing plants in a rarified atmosphere. It has been shown that germination and growth of plants for about 20 days can be undertaken in a pressure of .07 of the normal atmospheric pressure /4/. If the same low pressures can be utilized for the entire growth period, it is evident that the weight reduction within the depressurized modules would be extremely important and proportional to the depressurization factor.

This option should be examined, especially if the need for separating the plant growing modules from inhabited areas is required for pathological (microorganisms) and physiological (airborne pollutant) reasons. The reduction of pressure by eliminating all or part of the nitrogen in the atmosphere would facilitate the management and transfer of oxygen from the "plant" compartments to the inhabited areas /18/. However if the space vehicles are maintained at reduced pressures and thus at high oxygen concentrations, this involves additional risks to the humans present.

Interestingly, in contrast to humans, plants thrive in a partial oxygenated environment /7, 27/. The partial O_2 pressure could be decreased well below 250 mb, thus avoiding the risks of using pure oxygen at this pressure.

Carbon dioxide and oxygen effects account for numerous growth problems in plants when grown under special or extreme environments. The theoretical and practical motivations of long duration space farming can shed some light on the specific effects of oxygen and CO_2.

MATERIALS AND METHODS

Wheat (Triticum aestivum L. cv. Courtot, a semi-dwarf, spring cultivar) was used in two successive experiments. Each experiment used two growth chambers : a control chamber in standard atmosphere and a treated chamber where the atmosphere was modified to manipulate the rate of photorespiration, either by low O_2 or by high CO_2. In both cases the equality of CO_2 uptake between treated and control chambers was obtained by an electronic slaving of the valve of CO_2 injection of the treated chamber to the valve of control chamber.

Experiment in low O_2. One-week-old seedlings were planted in 3-cm holes in 20 x 90-cm polyvinylchloride tubes filled with sand and aerated with normal air. The stems of the seedlings were sealed with non-toxic putty (Teroson, France) to make the root compartment gas-tight, thus allowing independent control of root conditions and measurement of root respiration. Tillers emerged through the putty without difficulty. Details of this experimental system were described previously /14, 16/. Two tubes, each containing 20 plants, were placed in a 700 l reach-in chamber /1, 2/, giving a density of 80 plants m^{-2}. The volume of sand was approximately 1 liter per plant.

The photoperiod was 14 h, day/night temperatures were 23/18°C, and 400-700 nm photon flux density was 850 µmol $m^{-2}s^{-1}$ on the young plants, but rose to 1000 µmol $m^{-2}s^{-1}$ on plant tops when they reached their full height. CO_2 concentration in the control chamber was regulated at 340 µl l^{-1} by automatic injection from compressed air cylinder of CO_2 or trapping in a loop including soda lime with control by a computer. Photosynthesis and respiration were computed from the computer records of counts of injection or seconds of trapping CO_2.

Treated chamber. O_2 concentration in the shoot compartment was reduced to about 4 % by a nitrogen flushing and was maintained by coupling injections of nitrogen to the injections of CO_2, ensuring a dilution of the photosynthetic O_2 proportional to its production. Supple-

mentary nitrogen was also injected manually whenever necessary. The linkage of the valve of CO_2 injection for the low O_2 chamber to the valve of control chamber made the CO_2 level lower in the low O_2 chamber due to the higher affinity of the plants for CO_2 (Fig. 1B2).

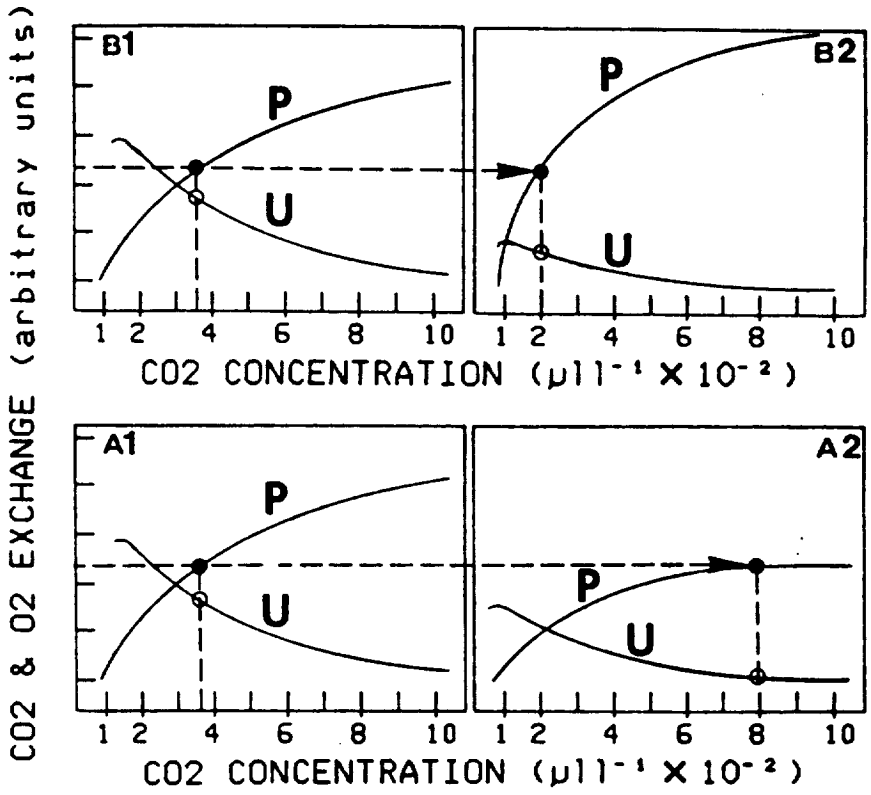

Figure 1 : Principle of the experiments in twin growth chambers directed toward manipulating photorespiration (O_2 uptake, U) with the same photosynthesis (CO_2 uptake, P). A : Comparison between photosynthesis and photorespiration versus CO_2 concentration at a "standard" irradiance (A1) or at a "low" irradiance (A2): for a same rate of photosynthesis, two rates of photorespiration depending on the level of irradiance could be achieved. B : Comparison between photosynthesis and photorespiration versus CO_2 concentration at 20.6 % O_2 (B1) and at ≈ 4 % oxygen partial pressure (B2). The dashed lines and arrows intersect points of equal rates of photosynthesis but significantly different rates of photorespiration. It symbolizes the slaving of the injection of CO_2 of the treated chamber to the injection of the control chambers.

Experiment in high CO_2. The conditions were similar to the experiment at reduced O_2 with the following exceptions. The roots were not in closed containers because there was no risk of hypoxy. In each chamber, twenty 1.45 dm^3 pots of sand were used instead of tubes filled with sand. Two seeds were directly sowed in each pot giving a density of 80 plants m^{-2}.

In the control chamber the irradiance was lower than the previous experiment, around 600 µmol $m^{-2}s^{-1}$ on the young plants and 800 µmol $m^{-2}s^{-1}$ on mature plants.

Treated chamber. The CO_2 was not monitored to a fixed concentration, but maintained between 700 and 900 µl l^{-1} to maintain a photosynthetic rate similar to that in the control chamber. The valves of CO_2 injection for the elevated CO_2 chamber were coupled to the valves of the control chamber. The irradiance was reduced to permit the equilibrium of CO_2 at a high level, for the same assimilation rate (Fig. 1A1). A change of irradiance was made periodically to maintain the balance in the range 700-900 µl l^{-1} of CO_2.

Nutrient conditions and mineral uptakes. For all experiments the control of nutrition was the same. Hoagland nutrient solution (Tab. 1) was regularly delivered to the plants by a small tube watering system (Gerbaud and Daguenet, 1984). The frequency of watering and the total volume delivered were calculated so as to ensure that the plants received twice as much water as lost by transpiration. The excess nutrient solution drained to a container from which samples were taken daily and chemically analyzed for determination of nutrient consumption /3/.

Transpired water was condensed on a cooled radiator in the chamber and collected in a container under the chamber. The transpiration rate was derived from the weight of condensed water measured with an electronic balance connected to the computer. We used the program "TRACER" (A. Daguenet) for part of the data processing.

TABLE 1 Composition of the nutrient solution

Macroelements, mM						
K^+	Mg^{2+}	Ca^{2+}	NH_4^+	NO_3^-	SO_4^{2-}	PO_4^{2-}
6.5	2.0	4.0	1.0	14.5	2.0	1.0

Microelements, µM							
BO_3^{3-}	Cl^-	Fe^{3+}	Mn^{2+}	Cu^{2+}	Na^+	MoO_4^{2-}	Zn^{2+}
46	18	16	9	0.32	0.21	0.10	0.087

RESULTS

The effect of the repression of oxidative cycle by low O_2 pressure on the life cycle of wheat has been described /15, 17/. The main results will be concisely presented in a first part to permit a comparison with the effect of high CO_2 treatment presented afterwards. Then the global comparison and discussion will take place.

I - Influence of low O_2 concentration

The wheat crop grown under low O_2 (4 %) did not significantly differ in shoot respiration, photosynthetic capacity of leaves, the chlorophyll content, from wheat grown under normal O_2. However under low O_2, there was a slight depression in transpiration and an increase in root respiration compared to normal O_2 levels. The main important change was a delay of 15 days in the appearance of ears and the total absence of grain under low O_2.

II - Influence of a high CO_2 concentration

A) Gas exchanges and mineral nutrition of the control culture crop.

The pattern of gas exchanges and mineral uptakes of the control plants maintained under 340 µl l^{-1} of CO_2 and 20.6 % of O_2 is presented in Fig. 2.

Net CO_2 assimilation. According to the pattern of net CO_2 fixation of the wheat crop, the life cycle can be divided in four phases : a quasi-exponential phase until the day 20, a linear increase from the day 20 to day 36, a saturating effect until a plateau although day 68, and a continuous decline at the end of the cycle.

The initial phase of rapid increase in photosynthesis resulted from the simultaneous increase in the surface of leaves, number of leaves, and number of tillers. The linear phase of photosynthesis expressed the equilibrium between tillering and the beginning of the competition for light. This competition was equalized when the plateau was reached. The beginning of the decreasing slope, corresponded to the time of ear appearance (Fig. 5).

Transpiration and Nocturnal Respiration. The transpiration of water vapor and the evolution of CO_2 in the dark followed the general pattern of CO_2 uptake (Fig. 2). One mole of fixed CO_2 required an average of 300 moles of transpired water. The dark respiration of the whole plant corresponded to a loss of carbon of 20 % of the light period uptake.

Mineral Nutrition. The uptake of nutrients did not strictly follow the pattern of CO_2 uptake (Fig. 2). The increase of the potassium and also nitrate uptake started earlier than the rapid increase in CO_2 uptake. Their increase was quasi-linear until the maximum of photosynthesis. The fast decrease of the nitrate uptake corresponded to the time of ear appearance. Potassium uptake also decreased during this period. Such a decrease was also reported at the beginning of the reproductive phase for maize /3/. The uptake of

ammonia and phosphorus, increased uniformly with a stabilization after 80 days of growth. The requirement of nutrients in m mole per mole of net CO_2 absorbed for 100 days of cultivation was 52.6 of NO_3^-, 4.3 of HPO_4^{2-}, 19.1 of K^+. The distribution of the uptake for the different nutrients was similar to that reported by Berezi et al. /6/.

The total uptake of anions did not equal cation uptake because certain cations were not included as Ca^{2++}, Mg^{2+}, Na^+. However their uptake was probably not great enough to equal the nitrate uptake to obtain ionic equilibrium. It is probable, as demonstrated by Gerbaud et al. /15/, that H^+ uptake compensated to obtain ionic equilibrium.

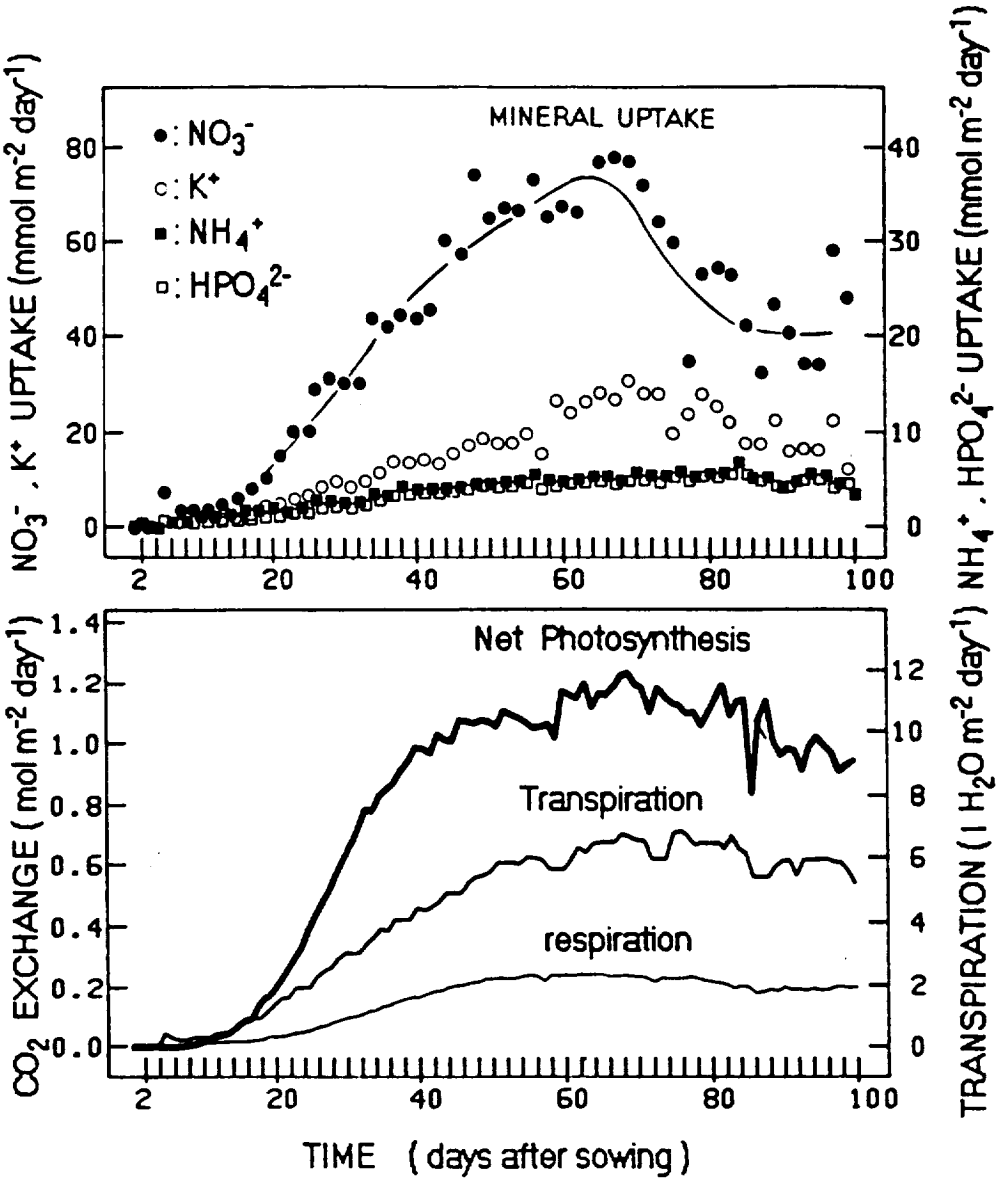

Figure 2 : Net photosynthesis, night respiration, transpiration and mineral nutrition of control plants of wheat (Triticum aestivum) plotted on the basis of the surface area of the growth chamber. Plants were grown under the following conditions. Photoperiod : 14 h light/10 h dark ; irradiance : 600 µmol $m^{-2}s^{-1}$; CO_2 concentration : 340 µl l^{-1} ; O_2 concentration : 20.6 % ; density of plants : 80 per m^2.

B) Gas exchanges, mineral nutrition and development of the crop cultivated under high CO_2 concentration

Gas Exchange. The diurnal CO_2 assimilation being by definition equal to that of the control, the variations observed in exchange of other gases, are only reported. They will be expressed in relative value in comparison with the control.

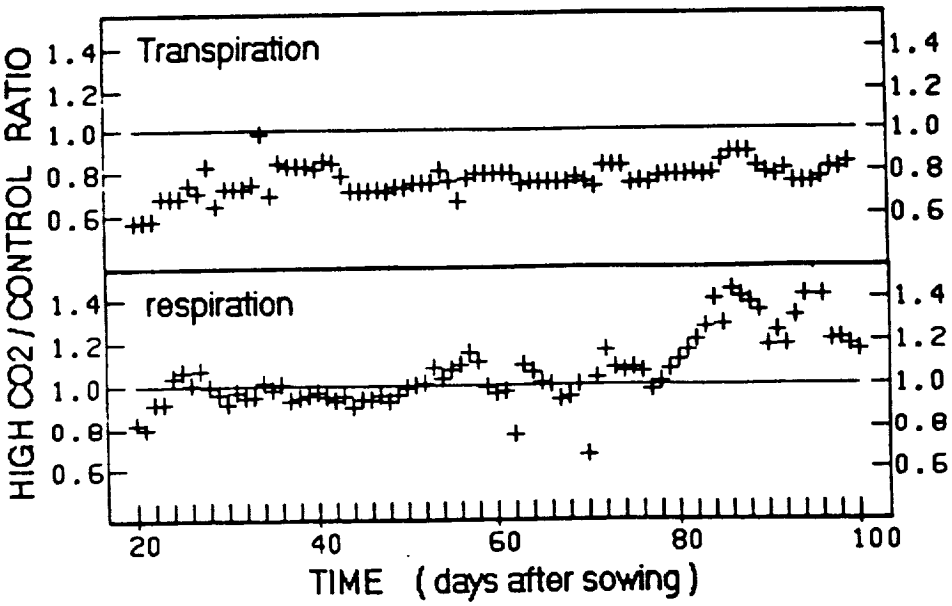

Figure 3 : Effect of elevated CO_2 (700-900 µl l^{-1}) on respiration and transpiration of wheat. Ratio values calculated for surface area of growing chamber.

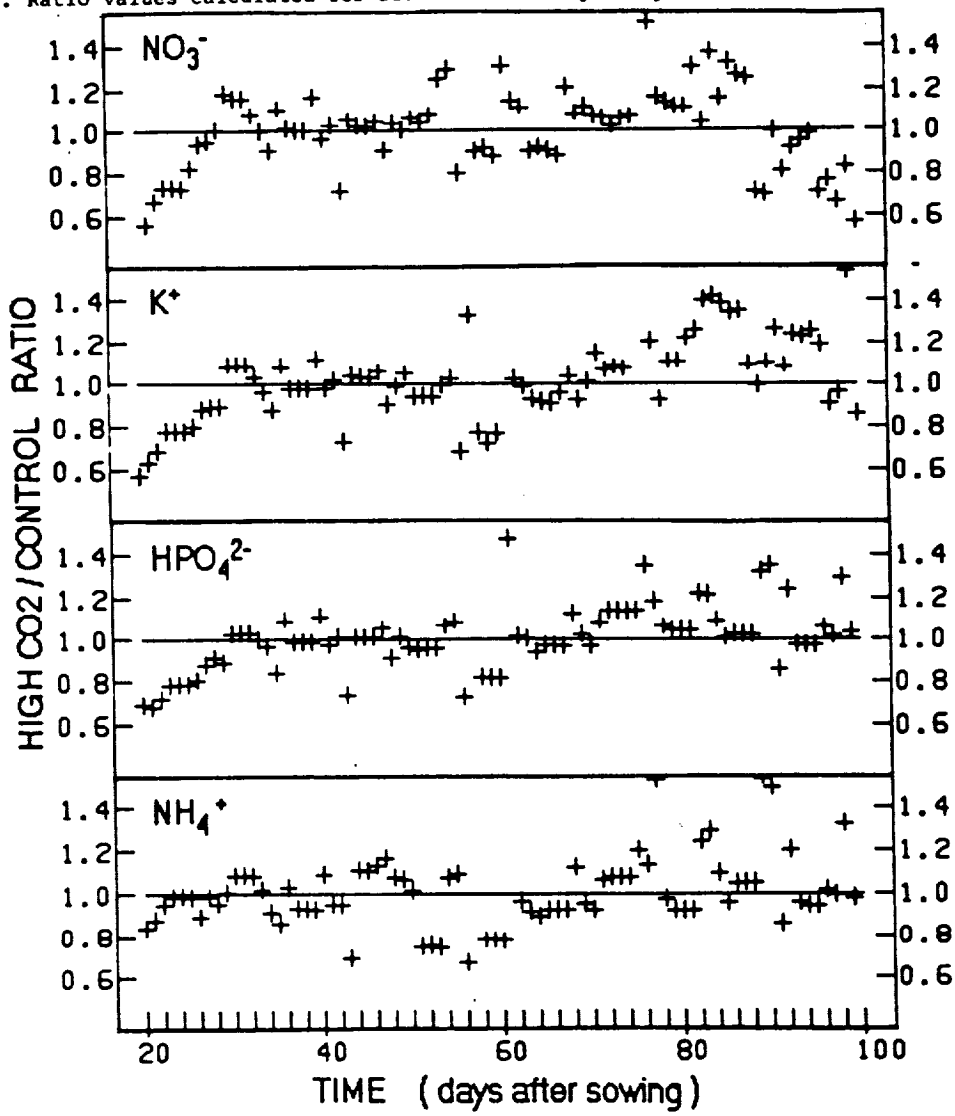

Figure 4 : Comparison of mineral nutrient uptake of wheat grown with a CO_2 concentration of 340 µl l^{-1} to that of wheat grown with a CO_2 concentration of 700-900 µl l^{-1}.

Transpiration rate was reduced 77 % by elevation of the CO_2 (Fig. 3). This figure was relatively stable along the entire 100 days of growth. This effect was probably the consequence of the increase of the stomatal resistance /12/. The nocturnal respiration of the crop under CO_2 enrichment was not very different from control plants under ambient CO_2 (Fig. 3). However, after day 75 an increase was noticed, corresponding to the period of grain formation. Other workers have shown that CO_2 enrichment causes stimulation of growth, but that the respiration rate was not stimulated in proportion to that of photosynthesis /10, 5/. In our case a lower rate of respiration was expected, but was not observed. The explanation proposed is that the CO_2 enrichment associated with higher light probably induced, in conventional experiments, an extra accumulation of glucosides which was stored and not used in respiratory metabolism.

Mineral nutrition. Figure 4 depicts the ionic uptake of NO_3^-, K^+, HPO_4^{2-}, NH_4^+ of wheat under CO_2 enrichment as a ratio of the uptake of wheat with ambient CO_2 level. It is not possible to observe a very significant difference between the two crops. During the 80 days of measurements, the averages of the ratio of uptake, for elevated CO_2/ambient CO_2, were 1.03, 1.06, 1.02, 1.04 respectively for nitrates, potassium, phosphate, and ammonium.

Development and Yield Characteristics at Harvest. The appearance of leaves was delayed by 1 to 2 days in high CO_2 compared to ambient CO_2. The appearance of ears was delayed 4 days by elevated CO_2 (Fig. 5A). In the crop under low O_2 treatment this delay was 15 days (Fig. 5B).

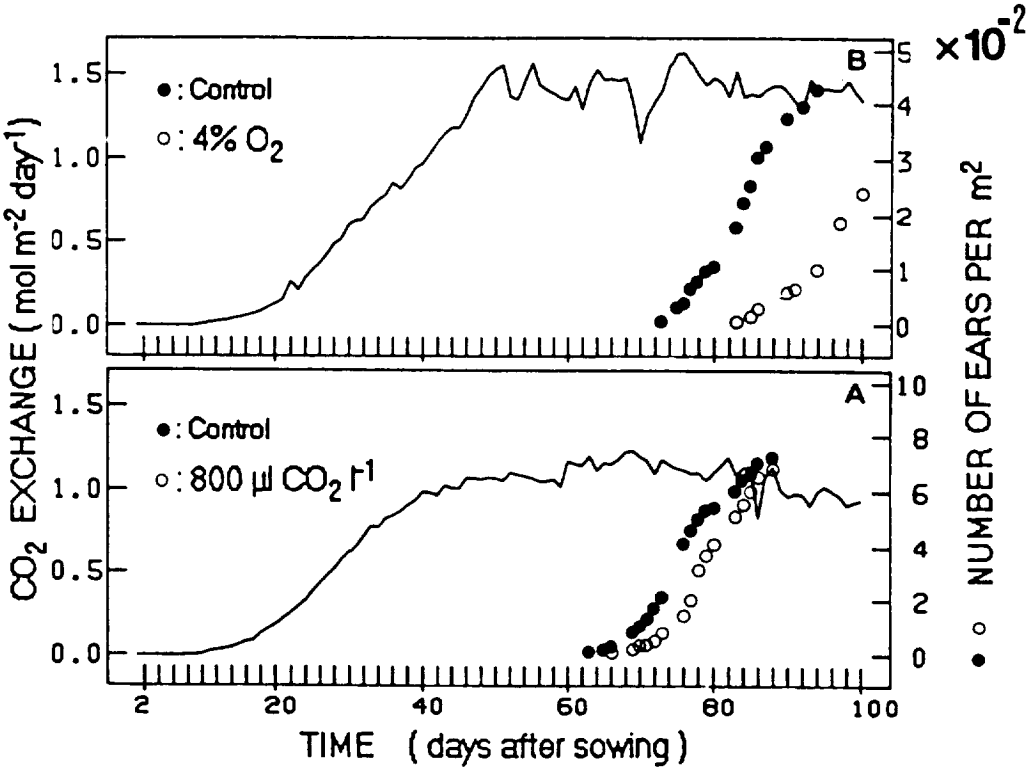

Figure 5. Time for appearance of ears for plants grown at an elevated CO_2 concentration (A) and for plant grown in low O_2 concentration (B). The control plant grown at 20 % of O_2 and 340 µl l^{-1} of CO_2. The photosynthetic CO_2 exchange (———) was maintained equal between control and treated plants.

Harvest data is shown in table 2. The distribution of dry matter in the different parts or organs was similar, but the roots were of less weight in high CO_2 than in ambient CO_2. This effect is surprising and must be confirmed. In contrast, CO_2 enrichment in conventional experiments induced an opposite effect, an increase of root allocation. As observed in respiration, the response was probably the consequence of the requirement for storage of extra assimilates. With low O_2, the main observed effect was the absence of grain. This effect was not observed with high CO_2.

TABLE 2 Harvest data for wheat crops grown at ambient and elevated CO_2 with photon flux balanced to obtain similar net photosynthesis at each CO_2 level. Each chamber was divided into three areas to permit statistical comparisons.

		Control		High CO_2	
Dry weights per plant	Leaves & stems	10.2 9.7 9.3	9.7	9.2 8.1 8.4	8.6
	Ears	7.8 7.2 7.4	7.4	6.3 6.9 6.3	6.5
	Seeds	3.2 2.7 3.6	3.2	2.7 3.3 3.1	3.0
	Roots	2.9 2.6 2.3	2.6	1.8 1.7 1.5	1.7
Number per plant	Tillers	23.5 18.8 20.2	20.8	19.1 18.5 18.5	18.7
	Ears	22.3 17.8 17.4	19.0	19.1 18.5 18.2	18.6
	Seeds	88.0 66.6 102.0	85.5	89.6 108.0 108.3	95.6
Harvest index		0.18 0.16 0.22	0.19	0.17 0.22 0.21	0.20

DISCUSSION

Harvest index. The harvest index was low in comparison with figures obtained in field or in similar cultures /24, 9/. That was primarily due to the low density used of 80 plants m^{-2}, compared with 1000 to 2000 plants m^{-2} used by Bugbee and Salisbury /9/. The low density was chosen so that roots of plants could be maintained in separate atmospheres during the low O_2 treatment. A consequence of this low density was an abnormal increase in the number of tillers. Ear appearance was distributed over a long period of time. The late developing tillers were shaded significantly and heads remained small and unfertile.

A "closure effect" may also have resulted, as found in Soviet studies (MELESHKO, private communication). Closure would permit the accumulation of volatile products emitted by plants, especially ethylene, which would interfere on the fertilization of the plants. In our case the closure was relatively complete. Our CO_2 supply, by a gas mixture of 20 % CO_2 and 80 % nitrogen, minimized the atmosphere renewal necessary to exhaust the oxygen produced by plants. Hence, the atmosphere renewing was lower than 10 % of the chamber volume per day. A trap for volatile products (activated charcoal) was inserted in the system loop provided for CO_2 trapping. However the efficiency of this trap for ethylene absorption was questionable.

Significance of the delay induced by CO_2 enrichment. The delay observed for ear appearance with CO_2 enrichment was small but was probably real because many precautions were taken to maintain equal average temperatures in twin chambers. The temperature probes recorded by a computer were frequently checked by standard thermometers introduced in shaded tubes beside the recorder probes. Considering that the development rate is proportional to the thermal time ($\int_0^T \theta\, dt$) with θ the dry temperature, dt the interval of time in days, T the age of the culture /11/. The daily temperature average being around 20°C, a difference

of 4 days corresponds to a difference of thermal time of 80 days, a systematic error of 80/75 days = 1.06°C is necessary to explain the discrepancy of the ear appearance. Thus temperature differences cannot explain the delay in ear appearance because the average temperature was 19.54°C for the control and 19.57 for the high CO_2 chambers.

Differences in irradiation levels may have increased leaf temperatures even though air temperatures were similar. However a differential effect of radiation on the shaded temperature probes would only concern the light period temperature. Hence, to have an effect of 1.06°C on the daily average, the error must be 1.81°C. The effect of increased radiation would tend to increase the temperature probe of the control chamber. Thus the actual effect of increased radiation would be to reduce the true temperature of air in the control chamber. A difference of 0.5°C on the probe would mask a difference of one day in the rate of flowering. That would minimize the observed difference.

Comparison with data of literature. It is known that a certain weight must be obtained by a plant to permit flowers to develop /22/. Studying the effect of CO_2 enrichment on growth and development of several plants, Marc and Gifford /26/, showed that the increase of dry weight by continuous CO_2 enrichment was accompanied by an advance in the date of flowering. In wheat, this advance was from 1 to 5 days. A short term enrichment (7-10 days) before the period of flowering was also sufficient to advance this process. The explanation can be either a trophic effect or a direct effect of CO_2. Nonetheless the availability of additional carbon dioxide generally contributes to a stimulation in the rate of flowering.

The discrepancy between these data and our observations could result from the two opposite actions of the CO_2 enrichment - the stimulation of the carboxylation and the repression of the oxidative cycle. The experiment cited above mixed the two effects, the stimulation being predominant. In our case the protocol was developed to avoid the stimulation effect of CO_2, insuring the same growth as the control. Thus it reveals an opposite effect, the repression of the oxidative cycle.

Comparison between low O_2 and CO_2 effects. It is clear that CO_2 enrichment, in the range of our experiments, does not modify the yield of grain. On the contrary reduction of O_2 did modify the yield of grain. A direct effect of O_2 was suggested rather than an indirect effect on the oxidative cycle /16/. It has been reported that a lowering of O_2 concentration can reduce the respiration of organs or organelles concerned with reproductive growth /13/. A direct effect of O_2 is also proposed to explain the effect of O_2 on the rate of development, however the small but significant effect of CO_2 on rate of development suggests that the oxidative cycle is the controlling factor in the low O_2 effect.

If the effect of low O_2 was larger than that of CO_2 enrichment, the two treatments would not have the same theoretical effect on the repression of the oxidative cycle. It was calculated /16/ that the vo activity at low O_2 was depressed from the control plant vo value of 0.4 P to a value of 0.09 P (vo being the oxygenation rate of rubisco giving the flow rate (activity) of the oxidative cycle, P being the net CO_2 assimilation). Thus the repression of oxidative cycle was 1.7 time less for CO_2 enrichment than O_2 reduction but the delay of the flowering was three times less important (4 days instead of 15 days). This would indicate that the repression of flowering is not proportional to the repression of the oxidative cycle. In fact there is no reason why the effects on the nitrogen metabolism, /30/ should be proportional to the repression of the oxidative cycle. Two different hypothesis can be proposed :

1) One hypothesis is that the oxidative cycle regulates the production of required nitrogen compounds. The nitrogen requirement, stated as a proportion of the carbon requirement, can be deduced from the classic ratio of N/C in organic matter and is around 0.09 g/g. Expressed in moles, and related to the rate of carbon assimilation P, this requirement is equal to 0.078 P. The stochiometry of the oxidative cycle indicates that the rate of amino acid synthesis is vo, the activity of the oxygenation of rubisco. Thus if one assumes that the requirement of nitrogen is totally satisfied by the production of glycine, then to obtain a limitation in the production of nitrogen compounds, the vo activity must be repressed below 0.078 P. A threshold effect could be expected when approaching this value. That actually was observed since, with low O_2, the value of vo was 0.09 P and is near the threshold. On the contrary, with elevated CO_2, the value of vo was 0.15 P and was far from the threshold and thus less reason to implicate this hypothesis. The same conclusion would be obtained if the serine was used in place of glycine.

2) Another hypothesis is that the glycine is a preferential substrate to support in vitro mitochondrial activity /31/. The basic activity of mitochondria should be totally saturated by the great availability of glycine which, as noted above, is 0.4 P in standard conditions. To perturbate the "normal" mitochondrial metabolism of the light period and to force it to use sugar as it uses in the dark, it is necessary to repress the glycine activity, i.e. vo, below the basal dark respiration. It is observed that a threshold effect can

be expected and that the response of low O_2 plants was at this threshold. However the elevated CO_2 response only approaches this limit.

CONCLUSION

The concentration of CO_2 did not modify the ratio of grain to dry matter, at the elevated level of 700 to 800 $\mu l\ l^{-1}$ of CO_2. The CO_2 effect on the rate of development also was small. The concentrations of CO_2 anticipated in space bases, around 1000 $\mu l\ l^{-1}$, are higher than levels studied but should not have any significant effect on the development of plants. However the basic question concerning the necessity for activity of the oxidative cycle was not solved by these investigations. The two hypothesis suggested by our data indicate that the action of CO_2 on the oxidative cycle is considerable compared to its effect on nitrogen metabolism. The inhibition of nitrogen metabolism by CO_2 was too small to have any significant effect on nitrogen metabolism. It can be calculated that 3000 $\mu l\ l^{-1}$ of CO_2 would be necessary to repress the amino acids synthesis below the 50 % of normal requirement of nitrogen compounds. Our hypothesis therefore could explain the toxicity of very high levels of CO_2.

Concerning the effect of low O_2 treatment, two negative responses were observed : absence of grain and delay of flowering. Only the last response could be related to the repression of oxidative cycle according to our hypothesis. The evidence for theses effects of O_2 reveals new limiting steps in the fertilization process that should be of use to geneticists and plant breeders for improvement of plant lines.

The effect of low O_2 on grain production poses a serious problem to solve if reductions of O_2 pressure are used in combination with a decrease of nitrogen pressure to maintain reduced pressure-plant cultivation modules in space.

ACKNOWLEDGEMENTS

We are grateful to M. Carral and to the staff of the laboratory for their contribution to the experiments. We thank Pr T.W. Tibbits for the improvement of the manuscript. This research was partly supported by C.N.E.S.

REFERENCES

1. M. André, A. Daguenet, D. Massimino, and A. Gerbaud, The $C_2$3A system, an example of quantitative control of plant growth associated with a data base, Proceeding of the Fifteenth Intersociety Conference on Environmental System. San Francisco Calif. Publisher : SAE The Engineering Resource for Advancing Mobility report n°85 1395 and NASA report TM 88 215 (July 1985)

2. M. André, H. Du Cloux, and C. Richaud, Wheat response to CO_2 enrichment : CO_2 exchange, transpiration and mineral uptake. Controlled Ecological Life Support Systems : CELSS'85 Workshop : Proceeding of a NASA Meeting held at Moffett Field Calif. NASA Report TM 88 215 (1986)

3. M. André, D. Massimino, and A. Daguenet, Daily patterns under the life cycle of a Maize crop. II Mineral nutrition, Root respiration and Root excretion, Physiol. Plant. 44, 197-204 (1978b)

4. M. André and C. Richaud, Can plants grow in quasi vacuum? Controlled Ecological Life Support Systems : Celss'85 Workshop, Mac Elroy R.O., Martello N.V. and Smernoff D.T. NASA report TM 88 215, AMES Research Center, Moffet Field, Calif. 94 035 (1986), p. 395-404

5. M. André, H. Du Cloux, C. Richaud, D. Massimino, A. Daguenet, J. Massimino, and A. Gerbaud, Etude des relations entre Photosynthèse Respiration Transpiration et nutrition minérale chez le blé, Advance in space Research 7, n°4 : 105-114 (1987)

6. A. Berezi, Z. Olah, and L. Erdei, Nutrition of winter wheat during the life cycle. I Yield and accumulation of dry matter and minerals, Physiol. Plant. 58 : 124-130 (1983)

7. O. Bjorkman, The effect of oxygen concentration on photosynthesis in higher plants, Physiol. Plant. 19 : 618-633 (1966)

8. Botany facility. Core payload for Eureca. ESA report référence ESA CR (P) 2510 vol.2 (1987)

9. B.G. Bugbee and F.B. Salisbury, Studies on maximum yield of wheat for the controlled environments of space. Controlled Ecological Life support systems : Celss'85 Workshop, 447-470, Mac Elroy R.D., Martello N.V. and Smernoff D.T., NASA, Ames Research Center, Moffett Field Calif. 94 035, NASA report TM 88 215 (1986)

10. H. Du Cloux, M. André, A. Daguenet, J. Massimino, Wheat response to CO_2 enrichment : growth and CO_2 exchanges at two plant densities, J. Exp. Bot. 38, 1421-1431 (1987)

11. R. Durand, Action de la température et du rayonnement sur la croissance, Ann. Physiol. vég. 9, 1, 5-27 (1967)

12. G.D. Farquhar and T.O. Sharkey, Stomatal conductance and photosynthesis, Ann. Rev. Plant Physiol. 33 : 317-345 (1982)

13. J. Gale, Oxygen control of reproductive growth : possible mediation via dark respiration, J. Exp. Bot. 25, 88, 987-989 (1974)

14. A. Gerbaud, M. André, Closed system physiology : Role of oxygen in the development of wheat. 3rd European Symposium on Life Sciences Research in Space, GRAZ, Austria, (1987)

15. A. Gerbaud, M. André, C. Richaud, Gas and nutrient exchange patterns during the life cycle of an artificial wheat crop, Physiol. Plant., in press (1988)

16. A. Gerbaud, M. André, J.P. Gaudillère and A. Daguenet, The influence of reduced photorespiration on long term growth and development of wheat. Physiol.Plant., in press (1988)

17. R.M. Gifford, H. Lambers, and J.I.L. Morison, Respiration of crop species under CO_2 enrichment, Physiol. Plant. 63 : 351-356 (1985)

18. P. Guérin de Montgareuil and M. André, Procédé de culture de végétaux à basse pression et application de ce procédé, Brevet n°EN 7108691 du 12 mars 1971

19. E. Gustan and T. Vinopal, Controlled Ecological Life Support System : Transpiration Analysis, NASA CR 166 420 (1982)

20. P. Jones, L.H. Allen, J.W. Jr Jones, K.J. Boote and W.J. Campbell, Soybean canopy growth photosynthesis and transpiration responses to whole-season carbon dioxide enrichment, Agronomy Journal. 76, 633-637 (1984)

21. W.A. Laing, W.L. Ogren, and R.H. Hageman, Regulation of soybean net photosynthetic CO_2 fixation by the interaction of CO_2, O_2 and ribulose 1.5-diphosphate carboxylase, Plant Physiol. 54 : 678-685 (1974)

22. A. Lang, Physiology of flower initiation. Encyclopedia of plant physiology. ed. W. Ruhland. Springer-Verlag, Berlin p. 1380-1536 (1965)

23. E.R. Lemon, CO_2 and Plants. A.A.A.S. Selected Symposia Serie 84. ed. E.R. Lemon. Westview Press, Boulder (1983)

24. R.S. Loomis and P.A. Gerakis, Productivity of agricultural ecosystems. In : Photosynthesis and productivity in different environments. ed. J.P. Cooper. Cambridge University press, 145-172 (1975)

25. R.D. Mac Elroy, N.V. Martello and D.T. Smernoff, Controlled Ecological Life Support Systems : Celss'85 Workshop. NASA report TM 88 215, Ames Research Center, Moffett Field, Calif 94 035 (1986)

26. J. Mark and R.M. Gifford, Floral initiation in wheat, sunflower, and sorghum under carbon dioxide enrichment, Can. J. Bot. 62 : 9-14 (1984)

27. B. Quebedeaux and R.W.F. Hardy, Reproductive growth and dry matter production of glycine max (L.) Merr. in response to oxygen concentration, Plant Physiol. 55, 102-107 (1975)

28. H.H. Rogers, G.E. Bingham, J.D. Cure, J.M. Smith and K.A. Surano, Response of selected plant species to elevated carbon dioxide in the field. Journal of Environmental Quality, 12, 569-574 (1983)

29. T.W. Tibbitts, Utilization of potatoes in cells : Productivity and growing systems. Controlled Ecological Life Support System : Celss'85 Workshop, 487-498, Mac Elroy R.D., Martello N.V. and Smernoff D.T., NASA, Ames Research Center, Moffett Field Calif. 94 035, NASA report TM 88 215 (1986)

30. N.E. Tolbert, Glycolate metabolism by higher plants and Algae, Photosynthesis II, ed. M. Gibbs and E. Latzko, Springer Verlag, Berlin : 338-352 (1979)

31. G.H. Walker, D.J. Olivier and G. Sarojini, Simultaneous oxidation of glycine and malate by pea leaf mitochondria, Plant Physiology 70, 1465-1468 (1982)

N90-15429

UTILIZATION OF SWEET POTATOES IN CONTROLLED ECOLOGICAL LIFE SUPPORT SYSTEMS (CELSS)

Walter A. Hill*, Philip A. Loretan, Conrad K. Bonsi, Carlton E. Morris, John Y. Lu and Cyriacus Ogbuehi

G. W. Carver Agricultural Experiment Station
Tuskegee University, Tuskegee, AL 36088, U.S.A.

ABSTRACT

A number of studies have selected the sweet potato as a potentially important crop for CELSS. Most hydroponic studies of sweet potatoes have been short term (<80 days). Full term (90 to 150 days) studies of sweet potatoes in hydroponic systems were needed to understand the physiology of storage root enlargement and to evaluate sweet potato production potential for CELSS. Early and late maturing sweet potato varieties were grown in hydroponic systems of different types--static with periodic replacement, flowing with and without recirculation, aggregate and non-aggregate. In a flowing system with recirculation designed at Tuskegee University using the nutrient film technique (NFT), storage root yields as high as 1790 g were produced with an edible growth rate of up to 66 g m^{-2} d^{-1} and a harvest index as high as 89% under greenhouse conditions. Preliminary experiments indicated high yields can be obtained in controlled environmental chambers. Significant cultivar differences were found in all systems studied. Nutritive composition of storage roots and foliage were similar to field-grown plants. The results indicate great potential for sweet potato in CELSS.

INTRODUCTION

Progress and problems associated with growing plants in controlled environments for future space missions have been described and summarized by Langhans and Dreesen /1/ and Salisbury and Bugbee /2,3/. To date, eight crops that provide a balanced diet have been selected by NASA for initial study: wheat, rice, white potato, sweet potato, soybean, peanut, sugar beet and lettuce /4/. The primary focus of scientists working with the NASA-CELSS program has been on four of these crops--wheat, lettuce, potato and soybean. Intensive research on the cultural and environmental conditions for optimum yield and quality of these crops in controlled environments at 1 G is being conducted. Limited data exists for the other crops. In 1985 NASA initiated studies of sweet potato for CELSS through Tuskegee University. This paper represents a progress report on some of the studies conducted in growing this crop for CELSS.

SELECTION OF SWEET POTATO FOR CELSS

A number of studies have developed criteria to select crops appropriate for CELSS /5,6,7,4/. Hoff et al. /7/ gave numerical values to 21 selection criteria so that their growth potential for CELSS could be quantified (Table 1). Sixteen of these criteria were assigned numerical values of 0, 1 or 2 for a low, medium or high rating. Because of their relative importance for CELSS, the other five criteria were given a weighting factor twice that of the other 16, i.e, 0, 2 or 4. These five criteria were: energy concentration, nutritional composition, processing requirements, proportion of edible biomass and yield of edible plant biomass. Of the 13 root and tuber crops evaluated, potato, carrot and sweet potato received the highest ratings of 35, 34 and 32 respectively.

---

*Author presenting paper. Contribution No. PS007 of the George Washington

Hill et al. /8/ modified this rating in view of the edibility of sweet potato foliage (which increases the weighted factors of both proportion and yield of edible biomass for this crop), the presence of solanine, saponins in combination with oxalate, and hydrocyanic acid in potato, taro and cassava, respectively, (which lowers the ratings for these crops in toxicity) and the horizontal (ageotropic) growth habit of sweet potato. This latter characteristic would be a positive factor in that it eliminates the need for gravitational cues for growth--an important factor in plant selection for CELSS /9/--and thus was added to the 21 criteria and given a weighted factor. These modifications have been incorporated in Table 2 with the resulting ratings of 43, 39 and 38 for sweet potato, carrot and white potato, respectively. These results agree with the conclusion by Nikishanova /6/ that sweet potato is the "crop most suited for CELSS".

Basic preparations of sweet potato storage roots and leaves are simple. The roots can be processed into flour, starch, hot cakes, gruel, noodles, pies, cakes, french fries, chips, candy, ice cream, milkshakes, jelly and syrup. Carotene, pectin, and a tempeh-like food can also be produced from sweet potato. The foliage tips may be prepared as a salad or a cooked green in a manner similar to spinach, mustard, turnips, and collard greens. Cultivars with dwarf-type foliage exist and potentially can be selected to minimize non-edible leaf and shoot portions /10,11,6,12/. The sweet potato roots are high in carbohydrates, protein (some cultivars), vitamins A (orange flesh cultivars), B_1 and C, iron and potassium. The leaves are high in protein, vitamins B_2 and C, calcium, iron, phosphorus and dietary fiber.

Sweet potato would be expected to have an oxygen production potential similar to other plants. Oxygen evolution can be assumed to be approximately proportional to dry matter accumulation, i.e., the oxygen production in liters $m^{-2} d^{-1}$ is approximately equal to dry mass production in g $m^{-2} d^{-1}$ when the dry mass consists of sugars /4,5/. Sweet potato has the second highest sugar production (next to sugar beet) of the root and tuber crops per unit of dry matter and thus can be expected to rank high in oxygen production. Also, if sweet potato can be produced with a harvest index of 89%, then a smaller percentage of the oxygen produced will be needed for oxidation of the inedible plant parts and a greater percentage available for breathing (food oxidation) by humans.

OVERVIEW OF EXPERIMENTAL METHODOLOGIES

Studies at Tuskegee University in growing sweet potatoes in soilless culture have involved three phases of experimentation with aggregates and recirculating flowing culture (NFT)--both in the greenhouse and in environmental chambers.

Aggregate Studies

Three, ten or fifteen L black-white vinyl-covered pots filled within 2 cm of the top with sterilized perlite, sand, sawdust, rockwool or gravel were planted with 15 cm sweet potato vine cuttings in a greenhouse. 'Jewel', 'Regal' and 'Georgia Jet' cultivars were studied with the latter used in most experiments because it is early maturing. Water or nutrient solution was provided to each plant via drip irrigation. A small submersible pump in the nutrient solution or water reservoir fed the header according to a programmed time sequence. A bypass line off the header and directed back to the reservoir provided for flow rate control and aeration. Some systems were designed as open hydroponic systems with the effluent solution simply wasted. Others were closed systems with the solution recycled. In either case, the nutrient solution was changed every two weeks. Typical nutrient solution application protocols applied approximately 50-60 ml of solution six times daily for one to two minute intervals.

Experiments using these aggregate systems provided some basic information essential to understanding the process of sweet potato storage root growth and enlargement. However, the heavy weight of some of these aggregates preclude their use in CELSS.

Carver Agricultural Experiment Station, Tuskegee University. This research was supported by funds from the U.S. National Aeronautics and Space Administration (Grant No. NAG10-0024) and USDA/CSRS (Grant No. ALX-SP-1). We wish to thank Mr. Ralph Prince and Dr. William M. Knott of the NASA/John F. Kennedy Space Center for technical assistance.

NFT Studies

Experiments were also conducted using NFT. This system required a reservoir, pump, growing channels and associated piping and structural materials. Within this system, the nutrient solution is pumped from a 45 L reservoir to the high end of a 1.2 m long channel which is sloped (1 cm in 100 cm) down to the reservoir. The nutrient solution spreads across the 15 cm wide channel as a thin film as it flows to the drain and returns to the reservoir. The flow rate to each channel is set by utilizing a bypass line back to the reservoir with a system of on-off valves. The 15 cm sweet potato vine cuttings are held upright within a growing channel by an assembly attached to the sides of the channel by vinyl (white on top, black below) which covers the channel. As the foliage grows, the vines are tied to vertical strings dropping 1 meter from above the channel. The storage roots develop within the growing channel in the space below the assembly and the assembly is raised either manually or by the roots themselves as they enlarge. The roots may be examined during the course of the experiment by simply opening the vinyl.

The third stage for the research was to locate Tuskegee University nutrient film systems within walk-in environmental chambers so that system conditions could be effectively controlled and more easily quantified.

Growing Conditions

Table 3 lists the growing conditions presently under study or in the research plan. Greenhouse conditions precluded holding some of these parameters at a fixed value from day to day or even hour to hour. The air temperature in the greenhouse varied between 22 and 35°C depending on the season of the year and the weather conditions. Within the growth chambers the temperature has been held at 28°C during the day and 22°C at night. The relative humidity ranged between 60 and 95% in the greenhouse but was set at 70±3% in the growth chambers. The daytime irradiance level in the greenhouse varied with the season of the year, time of day and the weather conditions; between the sunlight and the supplemental cool white fluorescent (CWF) lighting, the level ranged from 200 to 2000 umol $m^{-2}s^{-1}$. The environmental chambers are supplied with both incandescent (INC) and CWF lighting and the distinct irradiance levels utilized in the sweet potato studies to date include 300, 480 and 960 umol $m^{-2}s^{-1}$. The hours of light in the photoperiod can be easily controlled in the growth chambers and the two levels studied thus far are 12 and 24 hours of light. In the greenhouse the variation in hours of light was from 10 to 15 hours depending on the season of the year. All studies to date have been conducted with CO_2 at the ambient level.

The channels for all the sweet potato experiments carried out so far have been designed as described earlier but modifications in design are being planned. The nutrient solutions used for growing sweet potatoes have varied from quarter to full strength Hoagland solution with modifications in Fe, N and K. The application protocol for these nutrients has been intermittent in the aggregate studies and continuous in the nutrient film studies. Deionized water has been used to top off reservoirs in many experiments if the level of nutrient solution became too low for proper pumping prior to the biweekly changeover.

Cultivars selected for our studies to date have included: 'Jewel', 'Georgia Jet', 'Regal', '85-DW-8', 'TI 155', 'GA 120' and 'GA 121'. Plant spacings considered to date have included 0.03 and 0.12 m^2 per plant in aggregate studies and 0.05 and 0.13 m^2 per plant in the nutrient film system. The harvesting procedure for sweet potatoes for one study involved taking foliage samples every 15 days beginning with day 55 and until entire plant harvest at 120 days. In other experiments, both roots and foliage have been harvested at 70, 90, 105, 120 or 130 days.

RESULTS AND DISCUSSION

Yields and Yield Components

Table 4 shows yield data from a few selected experiments with several cultivars of sweet potatoes grown hydroponically in the greenhouse with sand as an aggregate or with NFT using a modified half Hoagland solution. Yields of up to 869 g/plant in sand and 1790 g/plant in the NFT system

(Fig. 1) were obtained. These data are also listed along with both field and greenhouse experiments of other investigators /13,14,15,16,17,18,6/ in Table 5. If the sweet potato clone study of Martin /16/ and the cultivar evaluation in the undefined growing system of Nikishanova /6/--both single plant results--are excepted, the yields obtained in this report are comparable to the highest yields obtained in other greenhouse or field studies on sweet potatoes by other researchers. The yields obtained in NFT are the highest ever recorded for sweet potatoes grown in an NFT system. The 5000 and 8000 g yields listed in Table 5 indicate the potential of the sweet potato that can serve as a goal for future work. More immediately, we expect fresh storage root yields of 2 to 4 kg/plant to be produced in controlled environmental systems.

Table 4 also provides yield data expressed in units necessary to determine growing potential on an area, time and photosynthetic efficiency basis. The growth rates of 'Jewel' and 'Georgia Jet' grown in sand and calculated on a canopy area basis (9.4-14.1 g $m^{-2}d^{-1}$) and root area basis (34.6 to 52.0 g $m^{-2}d^{-1}$) are considerably lower than growth rates of 'Georgia Jet' and 'TI 155' grown in NFT and calculated on a canopy area basis (13.7 to 23.1 g $m^{-2}d^{-1}$) and root area basis (39.1 to 66.0 g $m^{-2}d^{-1}$). The growth rates of sweet potato in NFT are comparable to those for wheat, potatoes, lettuce and soybeans (54.3, 24.3, 28.7, and 23.6 g $m^{-2}d^{-1}$, respectively) /3/. None of these growth rates for sweet potatoes takes into account the fact that the sweet potato foliage tips are edible and can be consumed. Thus the rates as calculated would be higher if this fact were considered. On the other hand, it should be noted that these values were obtained in greenhouse studies with day-to-day variable temperatures, relative humidity and light. The harvest indices for the sweet potatoes resulting from each of these selected experiments ranged from 60 to 89.2%; this is comparable to those for potatoes and lettuce but exceed those for wheat and soybeans. Edible portions of foliage have not been included in these harvest index calculations.

Environmental Growth Chamber Study

A recent study in a controlled chamber using NFT produced a storage root yield of 505 g/plant and 374 g/plant with 960 and 480 umol $m^{-2}s^{-1}$ irradiation, respectively, in 85 days (Table 6). These yields were obtained with the 'Georgia Jet' cultivar grown with 14:10 L:D photoperiod, 28°C day and 22° night temperature, and 70% RH. Although these were preliminary, unduplicated data, results show a higher storage root production under the higher light intensity.

Nutritive Proximate Analysis for NFT

Proximate analysis of sweet potato storage roots grown in NFT are shown in Table 7 as compared to that for field grown roots. The data indicate that hydroponically-grown roots provide comparable nutrition to field-grown plants /19/. Apparent differences in values can be attributed to the fact that the roots from the NFT system were analyzed immediately after harvest while the field grown sweet potatoes were cured, stored and baked prior to analysis. Carbohydrates and vitamins A and C are the major nutritional components from the roots.

CONCLUSIONS

Preliminary research data have shown that sweet potatoes can be produced hydroponically in both aggregate and NFT systems. Yields of up to 1790 g per plant in a 0.19 m^2 area (root basis) have resulted in an edible growth rate up to 66 g m^{-2} d^{-1} and a harvest index as high as 89%. Yields per plant obtained in the greenhouse were comparable to those obtained in the field with the same cultivar.

Nutritive content of hydroponically-grown sweet potatoes was similar to field-grown ones.

Optimization of environmental conditions, nutrient composition and application protocol leading to the best yields form our present and future research agenda. There is also a need to study the effects of various harvest practices on foliage quality and storage root development. Some of these practices include single or multiple root removal at various times during the life of the plant and harvest of edible shoots at various

frequencies, amounts and locations on the plant. More research is needed in order to obtain maximum sweet potato yields under controlled conditions and to grow the crop effectively in the 'Breadboard' facility at the NASA-John F. Kennedy Space Center /20/ and finally in CELSS in space.

REFERENCES

1. R. W. Langhans and D. R. Dreesen, Challenges to plant growing in space. HortScience 23 (2), 286-293 (1988)

2. F. B. Salisbury and B. Bugbee, Space farming in the 21st century. 21st Century Science and Technology 32-41, March-April (1988a)

3. F. B. Salisbury and B. Bugbee, Plant productivity in controlled environments. HortScience 23 (2), 293-299 (1988b)

4. T. W. Tibbitts and K. K. Alford, Controlled ecological life support systems - use of higher plants, Proceedings of two NASA workshops held at O'Hare Airport Conference Center, Chicago, IL Nov., 1979 and at the Ames Research Center, Moffett Field, CA, March, 1980. NASA Sci. and Tech. Info. Branch, Washington, D.C. (1982)

5. M. A. Milov and K. A. Balakireva, Problems of creating biotechnical systems of human life support, NASA Tech. Translation, NASA TTF-17533--Selection of higher plant cultures for biological life support systems (1975)

6. T. I. Nikishanova, Plants for space explorations, NASA-TM-75314 (Transl. from Priroda (USSR) 10:105-117) (1977)

7. J. E. Hoff, J. M. Howe and C. A. Mitchell, Nutritional and cultural aspects of plant species selection for a controlled ecological life support system, NASA Contractor Report 166324. NASA, Ames Research Center, Moffett Field, CA (1982)

8. W. A. Hill, P. A. Loretan and C. K. Bonsi, Eds, The sweet potato for space missions, Carver Research Foundation Inc. of Tuskegee University and George Washington Carver Agricultural Experiment Station, Tuskegee, AL (1984)

9. J. R. Keefe and A. D. Krikorian, Gravitational biology on the space station. Soc. Automotive Engineers (SAE), Tech. Paper Series 831133, Warrendale, PA (1983)

10. W. A. Hill, Detecting mineral nutrient deficiences that affect crop production in the temperate and tropical regions. In: D. L. Plucknett and H. Sprague (Eds.) Sweet Potato, Westview Press, Boulder, CO. Chapter 20 (1988)

11. G. W. Selleck, Symposium overview. In: R. L. Villareal and T. D. Griggs (Eds.) Sweet Potato. Proc. First International Symposium, AVRDC, Taiwan (1982)

12. A. Jones, P. D. Dukes and J. M. Schalk, Sweet potato breeding. In: M. J. Bassett (ed). Breeding Vegetable Crops. AVI Publishing Co., Inc. Westport, CN (1986)

13. M. N. Alvarez and S. K. Hahn, Sweet potatoes. In: Annual Report for 1982. The International Institute of Tropical Agriculture. Ibadan, Nigeria 1983, pp 110-111.

14. S. B. Lowe and L. A. Wilson, Yield and yield components of six sweet potato (Ipomoea batatas) cultivars. I. Contribution of yield components to tuber yield. Expl. Agric. 11, 39-48 (1975)

15. National Sweet Potato Collaborators Group, National Sweet Potato Collaborators Group Progress Report, University of Georgia Extension--Research Center, Attapulgus, GA (1985)

16. F. W. Martin, Variation of sweet potatoes with respect to the effects of waterlogging. Trop. Agric. (Trinidad) 60 (2), 117-121 (1983)

17. O. A. Leonard, W. A. Anderson and M. Geiger, Effect of nutrient level on the growth and chemical composition of sweet potatoes in sand cultures. Plant Physiology 23:223-235 (1948)

18. T. Uewada, On the solution culture of sweet potatoes (iv) - Effect of leaves and root temperature on root tuberization, Rep. Soc. Crop Sci. Breed., Kinki (Japan) 32:60-64 (1987)

19. J. Y. Lu, P. K. Biswas and R. D. Pace, Effect of elevated CO_2 growth conditions on the nutritive composition and acceptability of baked sweet potatoes, J. Food Science 51(2):358-359,539 (1986)

20. R. P. Prince, W. M. Knott III, S. E. Hilding and T. L. Mack, A 'Breadboard' biomass production chamber for CELSS. 33rd Annual Meeting. American Astronautical Society. AAS Preprint AAS-86-338, San Diego, CA (1986)

Table 1 Modified Candidate Species Selection Criteria*

Criterion No.	Use (or nutritional) Criteria
1	Energy concentration**
2	Nutritional composition**
3	Palatability
4	Serving size and frequency
5	Processing requirements**
6	Use flexibility
7	Storage stability
8	Toxicity**
9	Human use experience
10	Proportion of edible biomass**
11	Yield of edible plant biomass**
12	Continuous vs. determinate harvestability
13	Growth habit and morphology
14	Environmental tolerance
15	Photoperiodic and temperature requirements
16	Symbiotic requirements and restrictions
17	Carbon dioxide - light intensity response
18	Suitability for soilless culture
19	Disease resistance
20	Familiarity with species
21	Pollination and propagation
22	Ageotropism**

* Modified from Hoff et al./7/

** Criteria that were assigned a weighted factor twice that of other criteria

TABLE 2 Modified Ratings of Root and Tuber Crops Based on Nutrional and Cultural Criteria[+]

Common Name	Nutritional Criteria++										Cultural Criteria++													Grand Total
	1*	2*	3	4	5*	6	7	8	9	Total	10*	11*	12	13	(14)	(15)	(16)	(17)	(18)	19	20	21	22**	Total	
Artichoke, Jerusalem	4	0	1	0	2	0	0	4	1	12	2	2	1	1	1	1	1	1	0	1	1	1	2	15	27
Beet, garden	2	0	1	0	2	1	1	4	2	13	4	4	1	2	1	1	1	1	0	1	2	1	2	21	34
Carrot	2	2	2	1	2	1	2	4	2	18	4	4	1	2	1	1	1	1	0	1	2	1	2	21	39
Kohlrabi	2	2	1	0	2	0	2	4	2	15	2	2	1	1	1	1	1	1	1	1	1	1	2	16	31
Manioc	4	0	1	1	0	1	1	0	1	9	2	2	1	0	1	1	1	1	0	1	0	1	2	13	22
Parsnip	4	0	1	0	2	0	1	4	1	13	2	2	1	1	1	1	1	1	0	1	0	0	2	13	26
Potato	4	2	1	2	2	2	2	2	2	19	2	4	1	1	1	1	1	1	1	1	2	1	2	19	38
Radish	0	0	1	0	4	0	1	4	1	11	2	2	1	2	1	1	1	1	0	1	1	1	2	16	27
Rutabaga	2	2	1	0	2	0	1	4	1	13	2	2	1	2	1	1	1	1	0	1	1	1	2	16	29
Sweet Potato	4	4	1	1	2	1	2	4	2	21	4	4	1	1	1	1	1	1	0	1	2	1	4	22	43
Taro	4	0	1	1	2	1	1	0	1	11	2	4	1	1	1	1	1	(2)	2	1	1	1	2	20	31
Turnip	2	2	1	0	2	0	1	4	1	13	4	4	1	2	1	1	1	1	0	1	1	1	2	20	33
Yam	4	2	1	0	2	1	1	4	1	16	2	2	1	1	1	1	1	1	0	1	1	1	4	17	33

* Assigned a weighted factor twice that of other criteria

( ) Largely unknown

** Ageotropism

+ Modified from Hoff et al./7/

++ See Table 1 for identification of criteria number

TABLE 3 Sweet Potato Growing Conditions Under Consideration

Parameters	Range
Temperature	15° to 38°C
Relative Humidity	60 to 95%
Irradiance	200 to 2000 umol $m^{-2}s^{-1}$
Lamp Source	High-pressure sodium, cool-white fluorescent, incandescent, sunlight
Photoperiod	6 to 24 hours of light
CO_2	Ambient to 1500 ul per L
Nutrient Application Protocol	Continuous - intermittent
Plant Spacing	0.01 to 0.50 m^2 per plant

TABLE 4 Yield Data for Sweet Potatoes Grown in Sand and NFT Systems Maintained in Greenhouse

Growing System	Cultivar	Duration (days)	Fresh Wt. Per Plant ($g\ plant^{-1}$)	Dry Weight Per Plant ($g\ plant^{-1}$)	Dry Weight Canopy Area ($g\ m^{-2}d^{-1}$)	Dry Weight Root Area ($g\ m^{-2}d^{-1}$)	Harvest Index (%)
Sand, pot	Georgia Jet	120	869*	203	14.1	52.0	89.2
			748**	175	12.1	44.8	87.6
Sand, pot	Jewel	120	606*	162	11.3	41.5	82.4
			505**	135	9.4	34.6	79.6
NFT	Georgia Jet	105	1482*	297	21.4	61.1	70.1
			949**	190	13.7	39.1	60.0
NFT	TI 155	130	1790*	397	23.1	66.0	-
			1493**	331	19.3	55.0	-

*Highest plant yield
**Mean of four plants

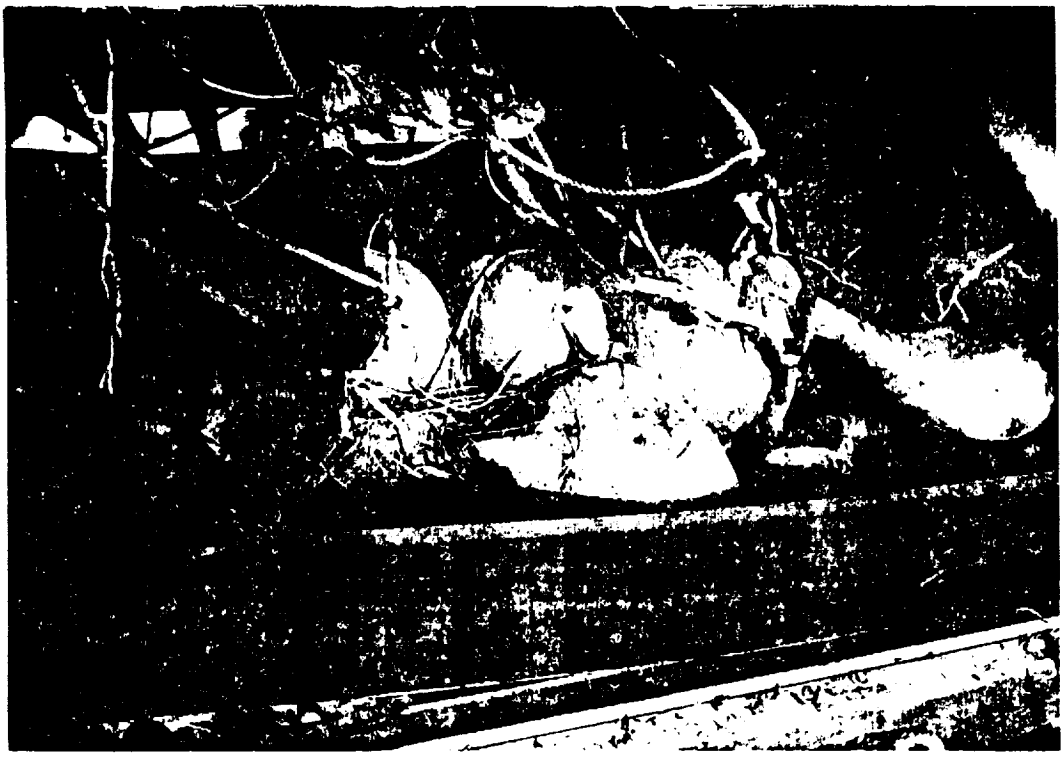

Fig. 1. Sweet potato roots grown in the Tuskegee University NFT system.

TABLE 5 Highest Sweet Potato Storage Root Yields Reported in Various Field and Greenhouse Studies

Fresh Wt/ Plant (g)	Cultivar	Specified Conditions	Growing Period (d)	Source
1627	TIS 9265	Field	120	Alvarez & Hahn, 1983
989	A28/7	Field, Dry season	140	Lowe & Wilson, 1975
1509	V5-113	Field, irrigated, humid region	133	National Sweet Potato Collaborators Group, 1985
8000	293 clones	Field	148	Martin, 1983
1300	Triumph	Greenhouse, pot, sand	132	Leonard et al., 1948
1550	#14 Tucker	Greenhouse, sand then static solution	30 100	Uewada, 1987
5000	60 varieties	Greenhouse, undefined hydroponic system	150	Nikishanova, 1977
869	Georgia Jet	Greenhouse, pot, sand	120	(This Report), 1986
1482	Georgia Jet	Greenhouse, Tuskegee NFT system	105	(This Report), 1987
1790	TI 155	Greenhouse, Tuskegee NFT system	130	(This Report), 1988

TABLE 6 Sweet Potato Storage Root Production in Environmental Growth Chambers

Storage Root Fresh Weight (g per plant)	Irradiance $PPF_{-2}s^{-1}$ (umol m^{-2})
374	480
505	960

Hydroponic System: Tuskegee University Nutrient Film System

Conditions:

Cultivar:	Georgia Jet
Duration:	85 days
Photoperiod:	14:10 Day:Night
Temperature:	28°C Day 22°C Night
Relative Humidity:	70%
CO_2:	Ambient
Nutrient Solution:	Half-Hoagland

TABLE 7 Proximate Analysis and Comparison[x] of 'Georgia Jet' Sweet Potato Storage Roots Grown in the Tuskegee University NFT System and Field Grown Roots

Component	NFT System Content* per 100g (g)	Field Grown Content* per 100g (g)
Moisture	78.5	80.4
Fat	-[+]	0.2
Ash	-[+]	0.6
Protein	1.0	1.1
Carbohydrate	-[+]	17.7[y]
Starch	12.9	-[+]
Sugar	-[+]	5.1
Vitamin B_1**	0.136	-[+]
Vitamin B_2**	0.064	-[+]
Vitamin C**	28.0	12.8
Carotenoids**	7.5	11.3

[x]NFT system measurements made on raw roots immediately after harvest; field grown measurements made on baked roots following curing and storage.
*Wet basis
**mg per 100g
[+]Not measured in this study
[y]Determined by difference

A90-15430

CARBON BALANCE AND PRODUCTIVITY OF *LEMNA GIBBA*, A CANDIDATE PLANT FOR CELSS

J. Gale, D.T. Smernoff *, B.A. Macler ** and R.D. MacElroy **

Institute of Life Sciences, Hebrew University of Jerusalem, 91904, Jerusalem, Israel
(Address for correspondence)

* Department of Biological Sciences, Stanford University, Stanford, CA 94305

** Ecosystem Sci. and Tech. Branch, NASA/Ames Research Center, Moffett Field, CA 94035

ABSTRACT

The photosynthesis and productivity of *Lemna gibba* were studied with a view to its use in Controlled Ecological Life Support Systems (CELSS). Photosynthesis of *L. gibba* floating on the nutrient solution could be driven by light coming from either above or below. Light from below was about 75% as effective as from above when the stand was sparse, but much less so with dense stands. High rates of photosynthesis (ca. 800 ηmol CO_2 g dry weight $(DW)^{-1}$ s^{-1}) were measured at 750 μmol m^{-2} s^{-1} PPF and 1500 μmol mol^{-1} CO_2. This was attained at densities up to 660 g fresh weight (FW) m^{-2} with young cultures. After a few days growth under these conditions, and at higher densities, the rate of photosynthesis dropped to less than 25% of the initial value. This drop was only partly alleviated by thinning the stand or by introducing a short dark period at high temperature (26°C). Despite the drop in the rate of photosynthesis, maximum yields were obtained in batch cultures grown under continuous light, constant temperature and high $[CO_2]$. Plant protein content was less than reported for field grown *Lemna*. When the plants were harvested daily, maintaining a stand density of 600 g FW m^{-2}, yields of 18 g DW m^{-2} d^{-1} were obtained. The total dry weight of *L. gibba* included 40% soluble material (sugars and amino acids), 15% protein, 5% starch, 5% ash and 35% cellulose and other polymers.

We conclude that a CELSS system could be designed around stacked, alternate layers of transparent *Lemna* trays and lamps. This would allow for 7 tiers per meter height. Based on present data from single layers, the yield of such a system is calculated to be 135 g DW m^{-3} d^{-1} of a 100% edible, protein-rich food.

INTRODUCTION

The development of Controlled Ecological Life Support Systems (CELSS) for use on long-duration and/or large population space missions has been described as a critical enabling technology by the National Commission on Space /1/. Proposed missions to the Moon, Mars, asteroids or large orbiting space stations demand reliable, largely autonomous systems to provide the life support requirements of the crew. The development of such bioregenerative systems will eliminate the need for expensive resupply strategies, which are incompatible with mission goals /2,3/. One of the main factors which determines the relative advantage of a CELSS based on plant growth, *versus* a chemical regeneration plus food storage system, is plant productivity per unit volume and per unit of required energy.

In theory, algae are among the most attractive higher plants for use in CELSS /4/. Their small size and small proportion of nonphotosynthetic tissue gives them extremely high relative growth rates (RGR) and they can be grown continuously in automated cultures. However, a variety of difficulties are associated with their use in a CELSS, including stringent growth requirements and the need for considerable processing before they may be eaten in quantity /5,6/.

Duckweeds, mainly from the *Lemnaceae* but also including *Spirodela* and *Wolffia* spp, are tiny (1-5 mm) higher plants, which grow as floating mats on still, fresh waters. Small size, a large percentage of photosynthetic tissue and permanently open stomates give them many of the qualities of algae, and RGR values are among the highest known for flowering plants /7,8/. They have a number of other characteristics which make them particularly attractive for CELSS:

- Reproduction is usually by vegetative budding, every one to three days. Flowering is rare /9/. This allows rapid, uniform growth.

- Axenic stock cultures can be maintained indefinitely in light, or in the dark on sugar /10/. This enables rapid restart of the standing crop after a prolonged period of dark, or after a system failure.

- They preferentially take up ammonia /11/, which may be present in the output of bioregenerative waste processors /12/.

- Their stomates are inactive /13/. This allows for photosynthesis during unusual photoperiods (unusual for terrestrially evolved plants) such as may be encountered in low Earth orbit (LEO) or on the moon.

- They have a 100% harvest index of highly nutritious material, reported to contain from 10-35% protein with a high content of most essential amino acids, about 5% lipids, 10% crude fiber /14/ and variable starch. There have been many animal feeding trials with duckweed spp which have shown high edibility and food value as compared to other high protein fodder crops /14,15,16,17/. There is at least one report on the use of *Wolffia* spp. for human consumption /18/.

On a very small scale, duckweed (mainly *Spirodela polyrrhiza*) has been studied and flown in the early days of space flight, with a view to their ultimate use in life support systems /19,20/ and /21,22/ (quoted by Landolt and Kandeler /23/). They have also been studied, for the same purpose, in submersed mass culture /24/.

Productivity figures for higher plants in bioregenerative systems are usually given on an area basis (e.g. /25/). It may be assumed that at least 1-1.2 m would be the minimum required height of substrate, plants and lighting system. *Lemna*, which can be grown floating on a few centimeters of nutrient solution in transparent trays, could be stacked with alternating layers of lamps, in many layers within a one meter height. The first purpose of the work reported here was to learn whether photosynthesis would respond to, and *Lemna* could be grown advantageously, with bilateral lighting, as could be used in such a stacked system.

As with other C_3 plants, photosynthesis and growth of *Lemna* increases with $[CO_2]$ rising from 350 ('normal') to 1500 ('high') μmol mol^{-1} $[CO_2]$ in air /26,27/. However, as for some other plants /28/, the response of *Lemna* has been found to drop after prolonged exposure to high $[CO_2]$ /27/. Thus our second purpose was to study RGR and changes in the rate of photosynthesis under conditions of continuous high $[CO_2]$ and light. Finally, we sought to determine the basic productivity (g m^{-2} d^{-1}) of a laboratory stand grown under these conditions and maintained at the stand density found to give maximum yield.

METHODS

Axenic cultures of *Lemna gibba* were grown in Erlenmeyer flasks, under continuous light: 150-200 μmol m^{-2} s^{-1} PPF, from Sylvania cool-white fluorescent lamps. This and all PPF values mentioned were measured with a LICOR Model LI-188 integrating quantum meter measuring photons of 400-700 ηm radiation. The culture medium was a modified Datko et al. (1980) nutrient #4 /10/, without sugar, having the following composition:

Macronutrients		Micronutrients	
NH_4NO_3	3.0 mM	H_3BO_3	16.2 μM
KNO_3	1.5 mM	Fe citrate	4.08 μM
$CaNO_3 \cdot 4H_2O$	1.5 mM	$ZnSO_4 \cdot 7H_2O$	3.48 μM
$MgSO_4 \cdot 7H_2O$	3.0 mM	$MnSO_4 \cdot 4H_2O$	0.592 μM
KH_2PO_4	3.0 mM	$Na_2MoO_4 \cdot 2H_2O$	0.41 μM
		$CuSO_4 \cdot 5H_2O$	0.12 μM
pH 6.5		EDTA (acidic)	0.01 M

Plants were transferred to four identical experimental chambers, which were alcohol-swabbed, contained sterile nutrient solution and were aerated with dry air. However, strictly axenic conditions were not maintained during the course of the experiments. The experimental chambers were rectangular at top and bottom with inwardly sloping sides, and were made of transparent polycarbonate. Polycarbonate lids were clamped to the tops, over gas-tight gaskets. Four liters of nutrient solution were added to each chamber, giving a depth of 6.0 cm and a surface area of 754 cm^2. Chamber temperatures were controlled by circulating controlled temperature water through transparent, plastic (Bev-a-line IV), heat-exchanging tubing, fitted at the bottom of the vessels. Temperatures were measured by thermistors set just below the surface of the nutrient solution.

Air was scrubbed of CO_2 by passing through two columns of indicating soda lime in series, and mixed with gas from cylinders containing 1 to 5% CO_2 via Side-Trak (Sierra Instruments) mass flow controllers/meters to obtain the desired concentration of CO_2. Air flow through each chamber was controlled by a set of four mass flow controllers. The rates of flow of CO_2, CO_2-free air, and flow through each chamber were manually adjusted during the course of experiments to give the desired $[CO_2]$ values within each chamber. The gas mixture entered

one side of the chamber, passed over the water surface and exited at the opposite side, via perforated stainless steel tubes. Within the chambers the air was stirred with fans fitted into the lids. As the air in the chambers was well stirred the $[CO_2]$ of the efflux air was taken as the average of the ambient air over the plants.

When the air leaving the chambers was being analysed, part of the efflux gas was passed through a condenser at 2-5°C and further dried by a column of magnesium perchlorate before reaching a LIRA (Mine Safety Appliances Co.) infra red gas analyzer (IRGA) for measurement of $[CO_2]$.

The chambers were irradiated from both above and below by banks of cool-white fluorescent lamps. The lamps could be raised or lowered to change the incident photon flux. Measurements of PPF were first taken at about 12 points in each chamber at the level of the liquid surface, with the quantum probe facing up or down. For these light measurements the chambers were fully configured, except for the presence of *Lemna* plants. The average values of the 12 points were correlated with levels measured at fixed points outside of and between the chambers. PPF readings at these external points were then used to calculate the photon flux incident on the plants, from above or below, within the chambers.

In the course of the experiments the nutrient pH was checked and periodically adjusted with ammonium hydroxide to pH 6.5. The solution was also periodically topped up with distilled water to replace transpired and evaporated water.

An Apple 512 computer, operating through a MacAdios model 411 analog to digital convertor, controlled the system and logged data. Under its control sequential samples of gas were taken as follows, and passed through the IRGA for $[CO_2]$ analysis: zero $[CO_2]$; calibration gas; air-in gas and air-out from chambers 1,2,3 and 4.

Each sample of gas was passed through the system for four minutes to allow for system and IRGA equilibration. Values of the IRGA, gas flow meters, clock and temperature thermistors were logged every four minutes. Initial (Di) and final (Df) dry weights were obtained. The IRGA was recalibrated and photosynthesis or respiration values were calculated for each chamber once every 28 minutes.

Photosynthesis or respiration were calculated from the rate of gas flow through the chambers and the difference between the $[CO_2]$ of the air-in and air-out. Results were expressed on either a per chamber or a per unit dry weight (DW) basis. The latter was calculated from Di (obtained from the measured fresh weight (FW), and the DW/FW ratio of a parallel sample) and Df. The dry weight at any time, t, was calculated from the RGR. Interpolation of t and Di into the rearranged RGR equation gave the instantaneous dry weight (D_t):

$$RGR = (lnDf - lnDi)/t \tag{1}$$

$$D_t = EXP(t * RGR + lnDi) \tag{2}$$

When photosynthesis was being measured as a function of $[CO_2]$ or PPF, changes in $[CO_2]$ and PPF were carried out manually. The order of PPF or $[CO_2]$ changes was always randomized to avoid time and hysteresis effects. Usually no more than a 5-10 minutes were required for the plants and system to equilibrate under the changed conditions. IRGA and other values were then noted and input into a data analysis program via the computer keyboard. The program calculated the $[CO_2]$ within the chambers, the incident PPF at the plant level, from above and below, and the rate of photosynthesis or respiration.

Protein content was measured by the method of Lowry et al. /29/. Starch content was measured by enzymatic degradation of starch to glucose followed by a colorimetric glucose assay /30/.

RESULTS

High vs. Low Assimilate levels

Net photosynthesis of *L. gibba* plants was determined as a function of PPF, with the light coming from above, below, or from both directions. Plants for this experiment were raised under conditions conducive to a low assimilate status: 200 μmol m^{-2} s^{-1} PPF, room air $[CO_2]$ and low nutrient levels ("low assimilate" means protein plus starch levels less than 100 mg g^{-1} DW). Prior to the measurements the plants were held in the dark

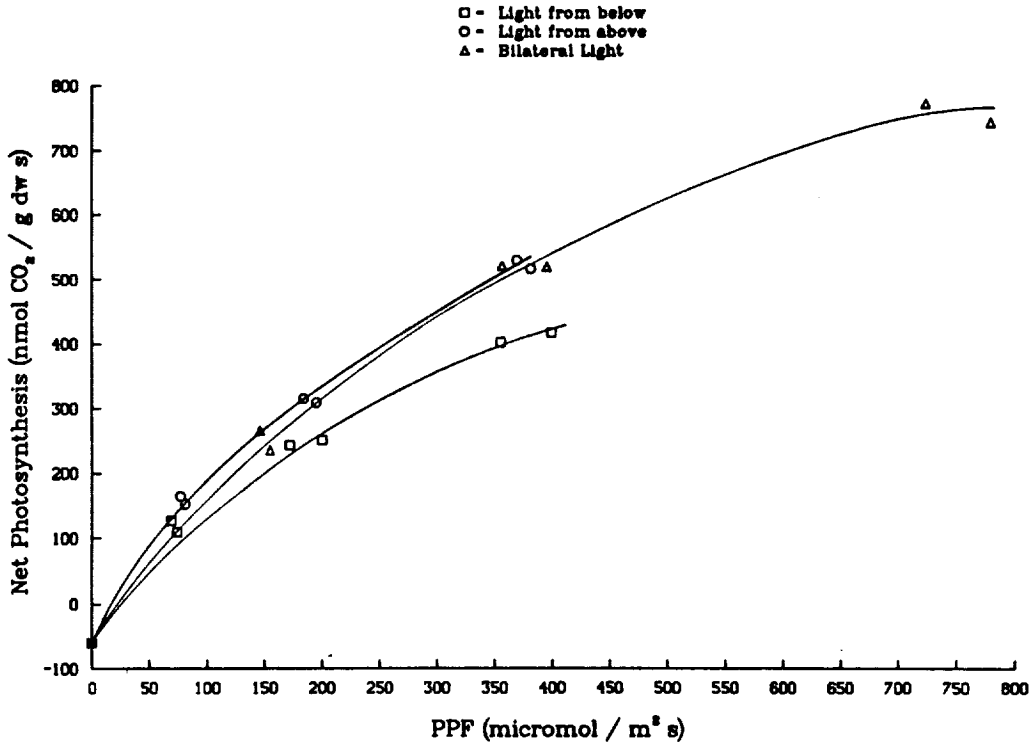

Fig. 1. Net photosynthesis response to bilateral lighting of a sparse stand of low assimilate *Lemna gibba*. Plants were grown with continuous light at 200-250 μmol m^{-2} s^{-1} PPF at ca. 350 μmol mol^{-1} $[CO_2]$. Measurements were made at saturating levels of $[CO_2]$ (> 1,400 μmol mol^{-1}).

for 15 hours. The measurements were made at photosynthesis-saturating $[CO_2]$ levels (> 1400 μmol mol^{-1}) using a sparse stand of plants (150 g FW m^{-2}).

As seen in Figure 1, light from below the floating *Lemna* plants could drive photosynthesis with about 75% of the efficiency of light from above. This experiment was repeated a number of times with *L. gibba* and also with *S. polyrrhiza*, with similar and consistent results.

The response differed when the plants were in a high assimilate status (protein plus starch greater than 100 mg g^{-1} DW). The plants were grown with ca. 1500 μmol mol^{-1} $[CO_2]$, a regime of 16 h light day^{-1} with bilateral lighting at a total flux of 750 μmol m^{-2} s^{-1} PPF, fresh nutrient media and at 26°C. After 5 days of growth under these conditions, the stand became very dense, reaching 1210 g FW m^{-2} and photosynthesis responded very little to light from below. This changed when the stand was thinned to 260 g FW m^{-2}.

The rate of photosynthesis at any given radiation level for plants grown at high light and $[CO_2]$ (high assimilate plants) was only one third that of plants grown at low light and $[CO_2]$. This can be seen by comparing the photosynthesis of the "sparse density, high assimilate" plants (Figure 2) with that of the low assimilate plants (Figure 1). Similar low rates of photosynthesis, after a period of growth at high light and $[CO_2]$, were found for *S. polyrrhiza* (data not shown). It should be noted that light saturation of photosynthesis was not attained in these experiments even at the highest bilateral lighting intensity used (750 μmol m^{-2} s^{-1} PPF).

The response of photosynthesis to changes in ambient $[CO_2]$ was also much reduced in plants grown under conditions of high light and $[CO_2]$ (Figure 3). This inhibition of photosynthesis could be partly offset by growing the plants with an 8 h day^{-1} dark period at 26°C. This partial offset of inhibition could also be seen in photosynthesis/light response curves. Similar responses to high light and $[CO_2]$ and to a 16h light day^{-1} regime were also found for *S. polyrrhiza* (data not shown).

Density effects

The data depicted in Figures 2 and 3 show that after a period of growth with continuous high light and $[CO_2]$ there was a very considerable reduction in the potential for photosynthesis as calculated on a dry weight basis. The loss of photosynthesis potential increased with time. This was a result of both an increase in stand density and internal plant factors (as also noted in field studies /28/). The optimal density within the present context is that which gives maximum carbon gain and hence growth per unit area. In batch experiments at high light and $[CO_2]$ photosynthesis per unit area tends to increase to a peak and then to decline, whereas the photosynthesis

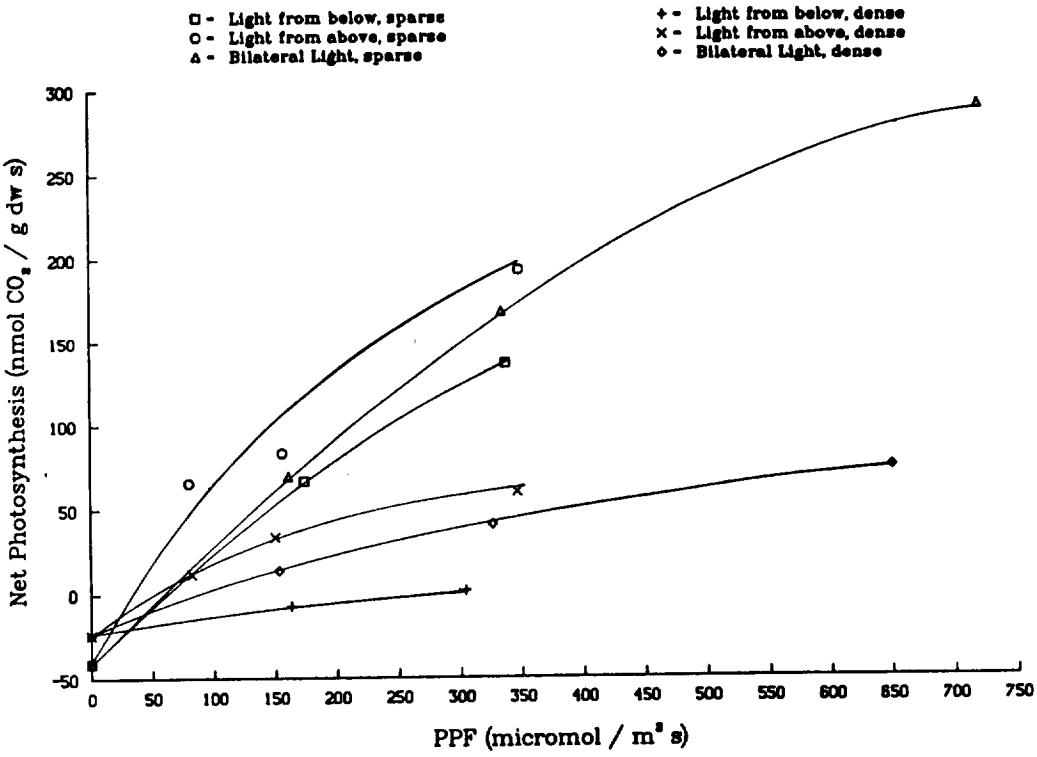

Fig. 2. The effect of stand density on the net photosynthesis response to bilateral lighting of high assimilate *Lemna gibba*.
The same plants were used in all experiments. Plants were grown at 1400 μmol· mol^{-1} $[CO_2]$, 720 μmol· m^{-2} s^{-1} PPF and 16 hour day length. Photosynthesis was first measured at a stand density of 1210 g FW· m^{-2}. The stand was then thinned to 260 g FW· m^{-2} and the measurements repeated.

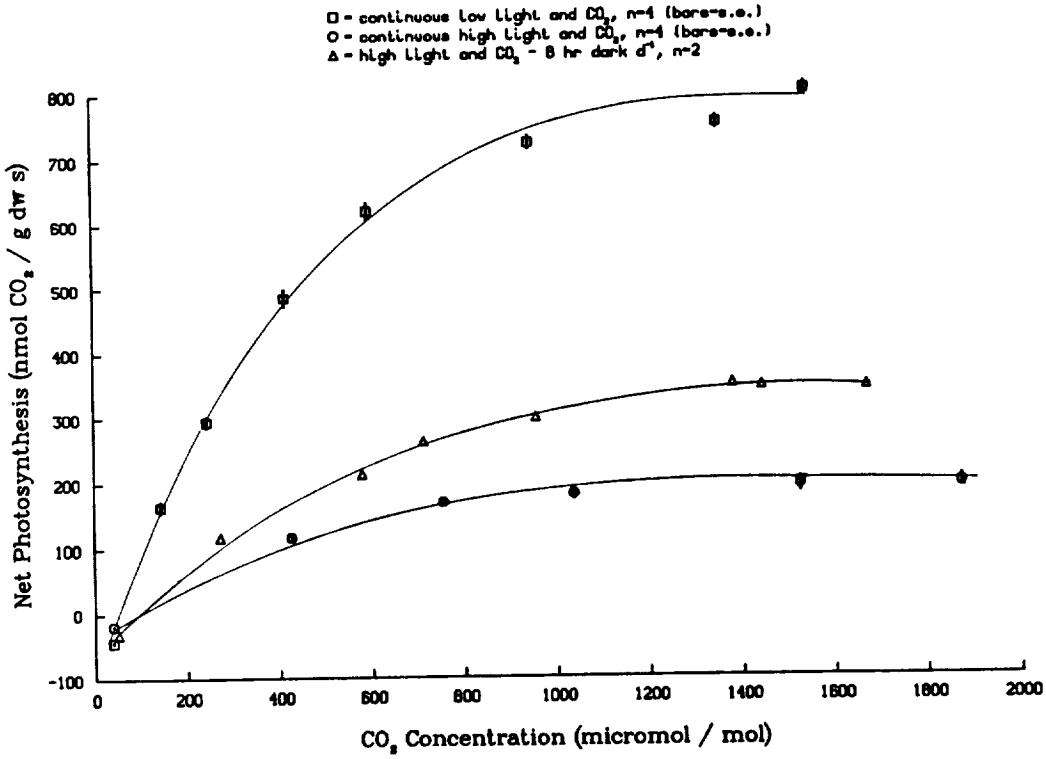

Fig. 3. Net photosynthesis response to ambient $[CO_2]$ of sparse stands of *Lemna gibba* after being grown for 5 days either at low $[CO_2]$ and continuous low radiation levels (bilateral, 200-250 μmol· m^{-2} s^{-1}), or at high $[CO_2]$ and either continuous or 16 h· d^{-1} high, bilateral radiation levels (720 μmol· m^{-2} s^{-1} PPF).

per unit plant material decreases with time. An example, from a batch run with *L. gibba*, grown with high light and $[CO_2]$, 16h light· day^{-1} and at 27°C, is shown in Figure 4. Note that there is a certain small, systematic error in the calculation of dry weight from RGR, as shown in Figure 4. The calculation of RGR assumes an equal g· g^{-1} d^{-1} growth, which is not exactly the case since photosynthesis per unit weight is decreasing.

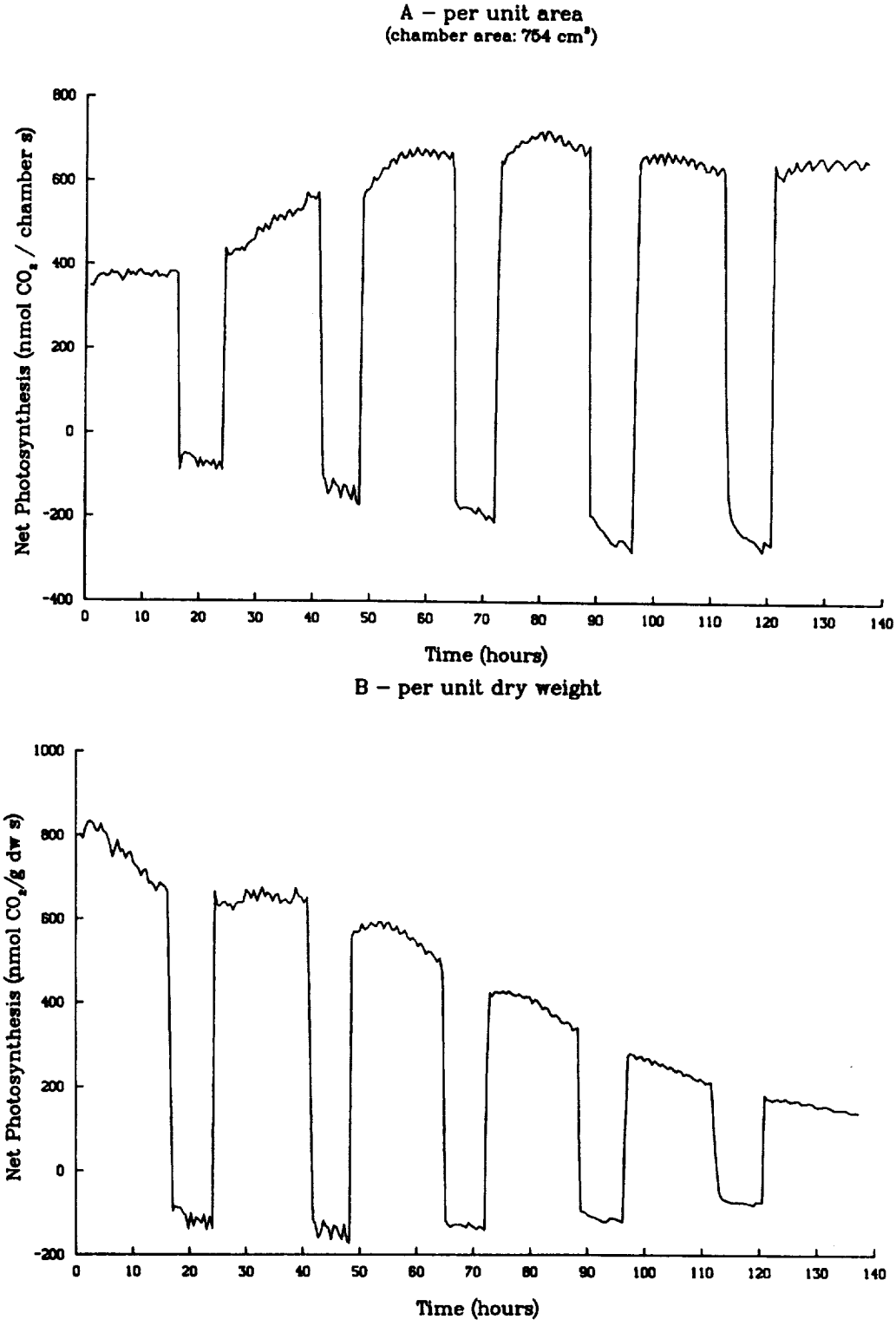

Fig. 4. Time course of net photosynthesis and respiration per unit chamber (area) and per unit dry weight of *Lemna gibba*.
Plants were grown at 26°C with 16 h· d^{-1} bilateral lighting at 720 μmol· m^{-2} s^{-1} PPF and photosynthesis saturating $[CO_2]$ (> 1,400 μmol· mol^{-1}). The surface area of the chambers is 754 cm^2.

Plant growth is directly related to net carbon gain (net photosynthesis, NP, less respiration in the dark, R). From the data given in Figure 4 the R/NP ratio can be calculated to increase from an initial value of 7.2% to a final value of 19%. In this case, the rate of maximum carbon gain was observed on the second day, when the stand density was 500-600 g FW $\cdot$ m^{-2}.

Maximum rates of photosynthesis per unit DW were higher in high light and [CO_2] grown plants when they were given an 8h $\cdot$ d^{-1} dark period (Figure 3), although daily yields were higher with continuous light. Subsequent experiments aimed at maximizing yield per unit area were therefore carried out with continuous light (750 μmol $\cdot$ m^{-2} s^{-1}) and high [CO_2] (> 2000 μmol $\cdot$ mol^{-1}). To determine the density for maximum yield per unit area under these conditions, plant stands were established at 8 different initial densities (in two separate experiments, each with four densities). The plants were grown for three days before harvesting. RGR (equation 1), yield and the logarithmic average FW density were calculated for each of the eight and data were plotted on this basis (Figure 5). Although there was some difference in the rate of growth of the two batches of four initial stands, both showed the expected drop in RGR with increasing stand density. The combined yield/density data could be fitted with a polynomial equation ($Y = -6.03 + 1.2x - 0.019x^2 + 0.00009x^3$) with an r value of 0.86. The polynomial curve indicated a standing density for maximum yield of 663 g FW $\cdot$ m^{-2} (50 g FW $\cdot$ $chamber^{-1}$ or 43 g DW $\cdot$ m^{-2}). At this density the daily yield was 18 g DW $\cdot$ m^{-2}.

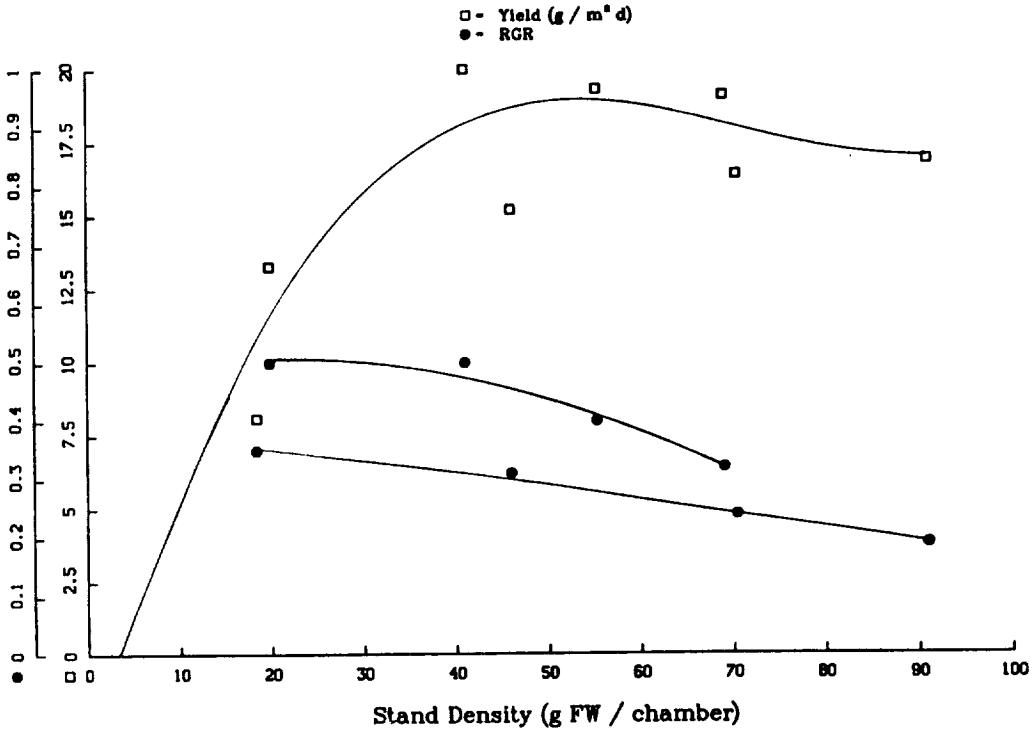

Fig. 5. RGR and yield (DW) of *Lemna gibba*, grown for three day periods under continuous, bilateral light at 720 μmol $\cdot$ m^{-2} s^{-1} PPF and ca. 2,000 μmol $\cdot$ mol^{-1} [CO_2], as a function of logarithmic average stand density.
The curve fitted to the square symbols, (yield/density) is pooled data from two experiments and, is the derived polynomial ($Y = -6.03 + 1.2X - 0.019X^2 + 0.00009X^3$, $r = 0.86$).
The RGR's are plotted separately for each experiment.

In order to confirm the potential yield, as indicated by the peak of the curve of the batch/density experiment (Figure 5), a continuously harvested system was set up with the four chambers. Light was continuous, bilateral at 720 μmol $\cdot$ m^{-2} s^{-1} PPF, and [CO_2] above the photosynthesis saturation level (> 1400 μmol $\cdot$ mol^{-1}). Temperature was held at 23°C. At day 5 density had reached about 50 g FW $\cdot$ $chamber^{-1}$ (663 g FW $\cdot$ m^{-2}). This density was maintained by daily harvesting. The harvested plants were analyzed for protein and starch content. The dry matter also contained 40% soluble material (sugars and amino acids), 5% ash and 35% cellulose and other polymers. Results are shown in Table 1. From day 5 to 10 it was possible to maintain a harvest averaging 18 g DW $\cdot$ m^{-2} d^{-1} and 13% protein. After day 10, protein and starch content decreased. Addition of fresh nutrient solution led to a partial recovery of growth and assimilates with a final harvest on day 14 of 4.3 g DW $\cdot$ $chamber^{-1}$.

Future projections

Based on the above data and 9 tiers of *L. gibba* in a stack 1.2 m high we calculate a potential yield of 135 g DW m^{-3} d^{-1} of a nutritious crop with a 100% harvest index. Although very high, this projection may be conservative. As discussed above, the rate of photosynthesis under the conditions of growth of the continuously harvested cultures is only 20-40% of the initial value. Manipulation of the environmental conditions, such as light intensity, nutrient solution composition, daylength and temperature, may allay part of this inhibition. Furthermore, although the parallel experiments noted above on *S. polyrrhiza*, showed no significant difference from *L. gibba*, it may be possible to select a species or strain of duckweed more adaptable to conditions conducive of extremely high rates of photosynthesis. Thus an increase of yield from 135 to 250 g DW m^{-3} d^{-1} does not seem to be an unreasonable target. Assuming a caloric value of dry duckweed equal to that of wheat and a requirement of 2800 Kcal man^{-1} d^{-1}, 3.3 m^3 of a CELSS plant growth unit could support the requirements of one man. However, a CELSS could not be based on a single plant species and there are many questions to be answered, such as the human acceptability and nutritional value of large quantities of duckweed.

Acknowledgment

This work was carried out while the first author held a National Research Council, Research Associateship, at NASA Ames Research Center. We wish to thank Ellen Moffatt for excellent technical assistance.

REFERENCES

1. National Commission on Space, Pioneering the Space Frontier, Bantam Books, New York, 1986.

2. R.D. MacElroy, H.P. Klein and M.M. Averner, The Evaluation of CELSS for Lunar Bases, in: Lunar Bases and Space Activities of the 21st Century, ed. W.W. Mendell, Lunar and Planetary Institute, Houston, 1985, p. 623.

3. R.D. MacElroy, CELSS and Regenerative Life Support for Manned Missions to Mars, in: Manned Mars Missions, Vol I, NASA M002, 1986, p. 363.

4. J. Meyers, Basic remarks on the use of plants as biological gas exchangers in a closed system, J. Aviation Med. 25, 407 (1954)

5. M. Averner, M. Karel, and R. Radmer, Problems associated with the use of algae in bioregenerative life support systems, NASA CR-166615 (1984)

6. Z. Nakhost, M. Karel, and V.J. Krukonis, Non conventional approaches to food processing in CELSS. I - Algal proteins; characterization and process optimization, Adv. Space Res. 7, #4, 29 (1987)

7. J.P. Grime and R. Hunt, Relative growth rate: Its range and adaptive significance in local flora, J. Ecology 63, 393 (1975)

8. E. Rejmankova, Comparison of *Lemna gibba* and *Lemna minor* from the production ecological viewpoint, Aquatic Bot. 1, 423 (1975)

9. R. Kandeler, Flowering in the *Lemna*-system, Phyton 24, 113 (1984)

10. A.H. Datko, S.H. Mudd, and J. Giovanelli, *Lemna paucicosta Hegelm.* 6746. Development of standardized growth conditions suitable for biochemical experimentation, Plant Physiol. 65, 906 (1980)

11. D. Porath and J. Pollock, Ammonium stripping by duckweed and its feasibility in circulating aquaculture, Aquatic Bot. 13, 125 (1982)

12. B.L. Onisko and T. Wydeven, Wet oxidation as a waste treatment in closed systems, ASME 81-ENAs-22 (1982)

13. J.S. McLaren and H. Smith, The effect of abscisic acid on growth, photosynthetic rate and carbohydrate metabolism in *Lemna minor L.*, New Phytol. 76, 11 (1976)

14. L.L. Rusoff, E.W. Blakeney, Jr. and D.D. Culley, Jr. Duckweeds (*Lemnaceae* Family): A potential source of protein and amino acids. J. Agric. Food Chem., 28, 848 (1980)

15. W.S. Hillman and D.D. Culley Jr., The uses of Duckweed, American Scientist, 66, 442 (1978)

16. D.D. Culley Jr., E. Rejmankova, J. Kvet and J.B. Frye, Production, chemical quality and use of duckweeds *(Lemnaceae)* in aquaculture, waste management and animal feeds, J. World Maricul. Soc. 12, 27 (1981)

17. J.G. Gaigher, D. Porath, and G. Granoth, Evaluation of duckweed (*Lemna gibba*) as feed for Tilapia (*Oreochromis niloticus x O. aureus*) in a recirculating unit, Aquaculture 41, 235 (1986)

18. K. Bhanthumnavin and M.G. McGarry, *Wolffia arrhiza* as a possible source of inexpensive protein, Nature 232, 495 (1971)

19. C.H. Ward, S.S. Wilks, and H.L. Croft, Use of algae and other plants in the development of life support systems, Am. Biol. Teacher, 25, 512 (1963)

TABLE I *Lemna gibba* Harvest Experiment

Time (days)	Harvest (g)		Assimilates (mg/g DW)	
	Wet weight	Dry weight	Protein	Starch
1	-	-	59.0 ± 4.0	5.2 ± 0.3
5	15.0 ± 2.0	1.4 ± 0.2	140.0 ± 10.0	30.0 ± 10.0
6	15.0 ± 2.0	1.2 ± 0.2	150.0 ± 10.0	20.0 ± 10.0
7	23.0 ± 2.0	2.0 ± 0.2	170.0 ± 10.0	25.0 ± 10.0
8	16.0 ± 1.0	1.3 ± 0.2	170.0 ± 10.0	21.0 ± 2.0
9	16.0 ± 2.0	1.2 ± 0.2	120.0 ± 10.0	25.0 ± 10.0
10	12.0 ± 1.0	1.0 ± 0.1	120.0 ± 20.0	19.0 ± 2.0
13	14.0 ± 3.0	1.0 ± 0.1	70.0 ± 10.0	15.0 ± 1.0
14	61.0 ± 4.0	4.3 ± 0.3	100.0 ± 20.0	20.0 ± 4.0

DISCUSSION AND CONCLUSIONS

The results shown in Figure 1 and the sparse stand data in Figure 2, indicate that, under suitable growth conditions, the photosynthesis of *L. gibba* will respond to light from below with about 75% of the response to light coming from above. This allows for the design of a multi-tiered CELSS plant growth unit for low gravity environments, such as prevail on the Moon or on Mars. Banks of relatively thin lamps, such as electric fluorescent or optical fibers bringing in filtered solar radiation /31/, could be alternated with layers of nutrient solution. The latter would be about 5 cm deep, with the duckweed plants floating on top. In this way 10 layers of lamps and 9 layers of duckweed could be stacked within a height of 1.2 m. 1.2 m is the least which would be required to provide space for the rooting medium, lamps and stand of a conventional crop such as wheat.

Light saturation was not attained in these experiments. Although, as can be seen in Figures 1 and 2, there was some indication that at high ambient [CO_2] (> 1000 μmol· mol^{-1}) saturation would be attained at about 1000 μmol· m^{-2} s^{-1} PPF when light is incident from above and below. This is considerably lower than has been used for maximizing productivity of most, if not all CELSS plants /32/. For wheat, Salisbury et al. /33/ reported using 1700 and Polanskiy and Lisovskiy /34/ used >5000 μmol· m^{-2} s^{-1} PPF. A nine tiered duckweed CELSS unit would use ten layers of lamps, each delivering 500 incident μmol· m^{-2} s^{-1} PPF in each direction. This may translate to considerable savings in terms of the energy and heat dissipation requirements per unit biomass produced.

When *L. gibba* or *S. polyrrhiza* were grown at low levels of light and [CO_2] their initial rates of photosynthesis, when measured with high bilateral light and high ambient [CO_2], were high as compared to values reported in the literature /7,8,16,17,20,26,27,35/. At 750 μmol· m^{-2} s^{-1} PPF and >1200 μmol· mol^{-1} [CO_2] rates approached 750 ηmol CO_2· g DW^{-1} s^{-1} (Figures 1 and 3). However, as shown in Figure 4B, when grown under these environmental conditions and even when the 24 hour day contained an 8 hour dark period, this rate declined rapidly. When the stand was thinned, the P_{max} rose but was still only 40% of the initial rate. When grown with continuous high light and [CO_2], P_{max} fell to 20% of the initial rate (Figure 3). Measurements of diurnal protein and starch levels indicated that starch was degraded over the first 4-6 hours of darkness, while protein was essentially constant over 24 hours. It is possible that the build up of starch in continuous light is detrimental. It can be expected that in addition to a daily 8h dark period, any regime which reduced photosynthesis per day, such as lower light intensity or lower ambient [CO_2] would also attenuate this drop in response of photosynthesis to light and CO_2.

As can be seen in Figs. 2 and 5, productivity was also reduced by high density. Farber et al. /36/ reported that ethylene production may be a detrimental factor in dense *Lemna* stands. Densely packed stands were also much less able to utilize light coming from below (Fig. 2). The highest productivity in this initial series of growth trials was obtained at a stand density of ca. 660 g FW· m^{-2} (Fig. 5). When plants were grown with relatively high, continuous bilateral lighting, saturating [CO_2] (> 1400 μmol· mol^{-1}) and were harvested daily, an average productivity of 18 g DW· d^{-1} could be maintained over a period of 10 days. This is only one third to one half of the productivity per unit <u>area</u> reported by Salisbury et al. /33/ for wheat, by Hill et al. for sweet potatoes /37/ and by Tibbitts and Wheeler for white potatoes (/32/ and this conference). However, as argued below, the comparison is very different on a <u>volume</u> basis.

20. C.H. Ward, S.S. Wilks, and H.L. Croft, Effects of prolonged near weightlessness on growth and gas exchange in plants, Develop. Indust. Microbiology 11, 276 (1970)

21. Y.A. Kutljachmedov, G.S. Sokurka and D.M. Grobzinsky, Investigation of the influence of cosmaunatic factors on the anabiotic stage of turons of *Spirodella polyrrhiza* (in Russian). Cosmic Invest. Ukraine, Kiev, 49 (1978)

22. A.T. Miller, Plant seeds in biological research in outer space (in Russian), Latr. Psr. Zinat. Akad. Vestis, 7.82 (1978)

23. E. Landolt and R. Kandeler, The family of *Lemnaceae* - a monographic study. Veroffentlichungen des Geobotanischen Institutes ETH, Stiftung Rubel, Zurich, p.638, 1987

24. R. Boudreault and B.G. Thompson, Fermentation based CELSS for microgravity operation, in: Abstracts of COSPAR XXVI, II.1.4. p. 153 (1986)

25. B. Bugbee, Exploring the limits of crop productivity, Plant Physiol, in press (1988)

26. G. Bjorndahl and S. Nilsen, Growth potential of *Lemna gibba*. Effect of carbon dioxide enrichment at high photon flux rate, Aquatic Bot. 22, 79 (1985)

27. J.H. Andersen, C. Dons, S. Nilsen, and M.K. Haugstad, Growth, photosynthesis and photorespiration of *Lemna gibba*: response to variations in CO_2 and O_2 concentrations and photon flux density, Photosyn. Res. 6, 87 (1985)

28. E.H. Delucia, T.W. Sasek, and B.R. Strain, Photosynthetic inhibition after long term exposure to elevated levels of atmospheric carbon dioxide, Photosyn. Res. 7, 175 (1985)

29. O.H. Lowry, N.J. Rosenbrough, A.L. Farr, and R.J. Randall, Protein measurement with the folin phenol reagent, J. Biol. Chem. 193, 265 (1951)

30. E. Raabo and T.C. Terkildsen, On the enzymatic determination of glucose, Scand. J. Clin. Lab. Invest. 12, 402 (1960)

31. K. Mori, H. Ohya, K. Matsumoto, and H Furune, Sunlight supply and gas exchange systems in microalgae bioreactor, in: Adv. Space Res. 7, #4, 47 (1987)

32. T.W. Tibbitts and R.M. Wheeler, Utilization of potatoes in bioregenerative life support systems, Adv. Space Res. 7, #4, 115 (1987)

33. F.B. Salisbury, B. Bugbee, and D. Bubenheim, Wheat production in controlled environments, Adv. Space Res. 7, #4, 123 (1987)

34. V.J. Polonskiy and G.M. Lisovskiy, Net production of wheat crop under high PAR irradiance with artificial light, Photosynthetica 14, 177 (1980)

35. M.Z.M. Said, D.D. Culley, L.C. Standifer, E.A. Epps, R.W. Myers, and S.A. Boney, Effect of harvest rate waste loading and stocking density on the yield of duckweeds, Proc. World Maricul. Soc. 10, 769 (1979)

36. E. Farber, H. Konigshoffer, and R. Kandeler, Ethylene production and overcrowding in *Lemnaceae*, Plant Physiol. 124, 379 (1986)

37. W.A. Hill, P.A. Loretan, C.K. Bonsi, C.E. Morris, R.D. Pace and J.Y. Lu, Utilization of sweet potatoes in Controlled Ecological Life Support Systems (CELSS), Adv. Space Res., this issue.

AAC-15431

Utilization of White Potatoes in CELSS

Theodore W. Tibbitts, Susan M. Bennett, Robert C. Morrow and Raymond J. Bula

University of Wisconsin, Madison, WI 53706 USA

ABSTRACT

Potatoes (Solanum tuberosum) have a strong potential as a useful crop species in a functioning CELSS. The cultivar Denali has produced 37.5 g $m^{-2}d^{-1}$ when grown for 132 days with the first 40 days under a 12-h photoperiod and a light:dark temperature cycle of 20°C:16°C, and then 92 days under continuous irradiance and a temperature of 16°C. Irradiance was at 725 µmol $m^{-2}s^{-1}$ PPF and carbon dioxide at 1000 µmol mol^{-1}. The dried tubers had 82% carbohydrates, 9% protein and 0.6% fat. Other studies have shown that carbon dioxide supplementation (1000 µmol mol^{-1}) is of significant benefit under 12-h irradiance but less benefit under 24 h irradiance. Irradiance cycles of 60 minutes light and 30 minutes dark caused a reduction of more than 50% in tuber weight compared to cycles of 16 h light and 8 h dark. A diurnal temperature change of 22°C for the 12-h light period to 14°C during the 12-h dark period gave increased yields of 30% and 10% for two separate cultivars, compared with plants grown under a constant 18°C temperature. Cultivar screening under continuous irradiance and elevated temperatures (28°C) for 8 weeks of growth indicated that the cvs Haig, Denali, Atlantic, Desiree and Rutt had the best potential for tolerance to these conditions.

Harvesting of tubers from plants at weekly intervals, beginning at 8 weeks after planting, did not increase yield over a single final harvest. Spacing of plants on 0.055 centers produced greater yield per m^2 than spacing at 0.11 or 0.22 m^2. Plants maintained 0.33 meters apart (0.111 m^2 per plant) in beds produced the same yields when separated by dividers in the root matrix as when no separation was made.

A. BACKGROUND

The white potato (Solanum tuberosum) is one of eight plant species being considered for inclusion in a CELSS. The crop has high productivity rates and a high ratio (.80) of edible to inedible biomass (high harvest index). Potato tubers are nutritious, consisting primarily of carbohydrates (82%), with a significant amount of protein (11%). There is sufficient protein to satisfy a person's total protein requirement if all that person's energy requirements are met by the consumption of potatoes. Potatoes are also easily stored for long periods, and can be prepared in a number of culinary forms.

The University of Wisconsin has been supported to evaluate potatoes for the CELSS program. To accomplish this, an extensive series of studies have been and continue to be carried out at the University of Wisconsin to determine maximum productivity; to determine the range of yield response under different environmental conditions, and to address the cultural aspects of growing potato plants in space. Brief summaries of these investigations will be provided.

B. RESEARCH

1. Maximum Productivity

Potatoes, cv Denali, were grown in a controlled environment room at the University of Wisconsin Biotron to maximize yield productivity in terms of grams per unit area per day (g m^{-2} d^{-1}). Plants were grown in 24 closely spaced containers to develop a solid stand 3.0 m x 2.0 m. The area was enclosed by a wire mesh fence to contain the plants. The sides were further enclosed by opaque but reflective siding to prevent side lighting of the plants. This siding was gradually raised during growth to be just below the top most part of the plants. Air movement in the room was horizontal from one end to the other end. Sixteen plants, excluding one row of plants on each end, were harvested for productivity calculations.

Growing conditions were as follows:

Irradiance Level	725 µmol $m^{-2}s^{-1}$ PPF
Carbon Dioxide	1000 µmol mol^{-1}
Relative Humidity	70%

	0-37 days	38-41 days	42-132 days
Temperature	20D:16N	19 to 17D:16N	16D:16N
Irradiance Duration	12 h	14 to 22 h	24 h

A 50% peat:50% vermiculite medium was used and plants watered to excess four times daily using a modified half strength Hoagland's solution. Plants were raised from tissue culture and grown for 18 days in 10 cm plastic containers to minimize the growing area when plants were small. Plants were then transferred to 30 cm plastic containers for the rest of the growing period. Spacing of each plant was as follows:

0.02 m^2 $plant^{-1}$ (day 0-18)
0.25 m^2 $plant^{-1}$ (day 19-132)
0.22 m^2 $plant^{-1}$ (overall average)

Plants were harvested after 132 days, and the following yield data obtained:

Total dry matter	5920 g m^{-2}
Edible dry matter	4352 g m^{-2}
Harvest index	73.5%
Tuber productivity	37.5 g m^{-2} d^{-1}
Nutritional Value of Tubers	
Protein	9%
Carbohydrate	82%
Fat	0.6%
Energy content	3.7 kcal/gDW
Nutritional Yield	139 kcal m^{-2} d^{-1}

Area for 1 human requiring 2800 kcal d^{-1} = 20.1 m^2

2. Environmental Responses

Irradiance and Carbon Dioxide Interactions

Three cultivars of potatoes, Denali, Norland and Russet Burbank, were grown for 90 days at 16°C, and 70% RH. Separate experiments were undertaken with 12 and 24-h durations of irradiation and with ambient ($\pm$ 350 µmol mol^{-1}) and enriched (1000 µmol mol^{-1}) carbon dioxide levels. In each experiment, plants were grown in one-half of the room at a PPF of 400 µmol $m^{-2}s^{-1}$ and in the other half at a PPF of 800 µmol $m^{-2}s^{-1}$.

The tuber yield of the three cultivars under the separate irradiance treatments and carbon dioxide levels is provided in Table 1. An increase from 400 to 800 µmol with a 12-h photoperiod increased yields of all cultivars. However, when grown under continuous (24 h) irradiance, only Denali showed an increase in yield with increasing PPF while Russet Burbank appeared to show a reduction in yield. Apparently the photosynthetic capability was exceeded for certain cultivars when 800 µmol $m^{-2}s^{-1}$ was provided for 24 h. It can be seen that the two treatments with similar total daily irradiance (400 µmol $m^{-2}s^{-1}$ for 24 h and 800 µmol $m^{-2}s^{-1}$ for 12 h) had rather similar yields when averaged over all cultivars and CO_2 levels.

Supplementation with carbon dioxide was a significant benefit to all cultivars when grown under 12-h of irradiance at both the low and high irradiance levels. This benefit amounted to an approximately 30% increase in yield, with the greatest benefit obtained by Denali. Carbon dioxide supplementation was much less of an advantage with 24-h irradiance durations and appeared to be a slight detriment at the high irradiance level. This response under 24 h irradiance durations was similar for all three cultivars (Table 1).

Light Duration Changes

Potatoes (cv Denali) were grown for 16 weeks at 16°C, 70% RH, ambient CO_2 (350 µmol mol^{-1}) and a PPF of 400 µmol $m^{-2}s^{-1}$. Plants were started under 12-h or 24-h light durations and switched to the opposite duration at 4, 8 or 12 weeks after planting.

Plants grown with 24-h light for 16 weeks gave the highest tuber yields and those grown at 12-h light for 16 weeks gave the lowest yields (Figure 1). Plants which were switched between light treatments gave intermediate yields, although plants grown first with 12-h of light followed by 24-h of light gave higher tuber yields than plants given the reverse treatment.

Table 1. Potato tuber dry weight[z] in response to irradiance and carbon dioxide concentration.

Cultivar	Carbon Dioxide (μmol mol^{-1})	Photoperiod 12-h Irradiance (μmol m^{-2}s^{-1} PPF) 400	800	Photoperiod 24-h Irradiance (μmol m^{-2}s^{-1} PPF) 400	800
Norland	Ambient	248	307	304	317
	1000	321	359	310	282
Russet Burbank	Ambient	225	262	339	311
	1000	321	335	388	272
Denali	Ambient	253	334	334	488
	1000	363	456	366	469

[z]Data represent mean of six plants expressed as grams by weight.

A second replicate of this experiment incorporated an elevated CO_2 concentration of 1000 μmol mol^{-1}. The CO_2 enrichment of this second replicate produced nearly 30% greater tuber yields on plants which received 12-h lighting for the entire 16 week growing period, but had little or negative effects on plants receiving 24-h lighting for the entire period and plants receiving changed lighting treatments (Figure 2). Carbon dioxide enrichment increased shoot growth by 50 to over 100% in all treatments.

Light/Dark Cycles of 90 Minutes

Potatoes (cvs Denali) were grown at 16°C, 70% RH and 400 μmol m^{-2}s^{-1} PPF for 16 weeks under a simulated low earth orbital (LEO) light:dark cycle of 60 minutes light and 30 minutes dark. Potatoes grown under a light:dark cycle of 16 hours light and 8 hours dark were used as a comparison. Both treatments were equivalent in terms of total irradiance over a 24 hour period. Potatoes showed a 49% reduction in total biomass and a 55% reduction in tuber yield when grown under the LEO light:dark cycle (Table 2). Reductions in total chlorophyll content of approximately 35%, and reductions in stomatal conductance and photosynthesis were associated with the biomass reductions observed under the LEO light:dark cycle. The flowers on plants in the LEO treatment failed to open fully, a response similar to that of flowers observed under continuous light exposures.

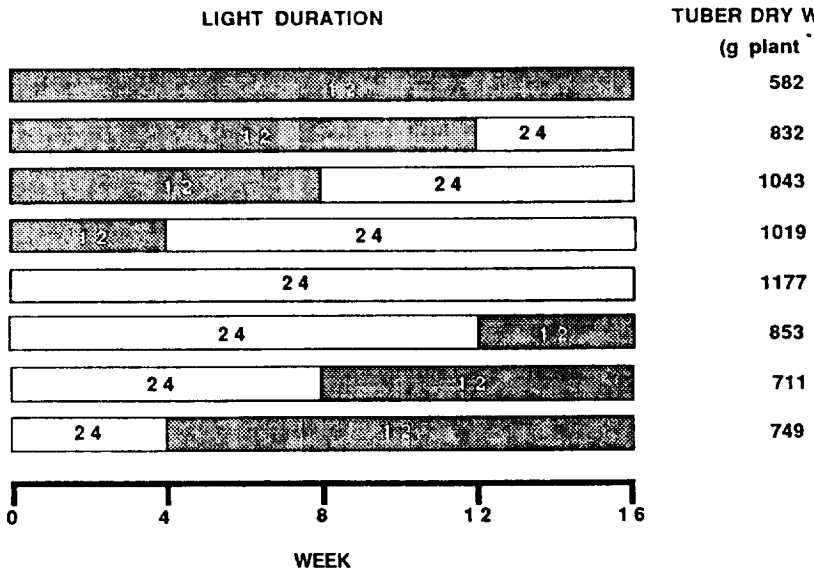

Fig. 1. Effect of light duration changes during growth on yield of potato tubers.

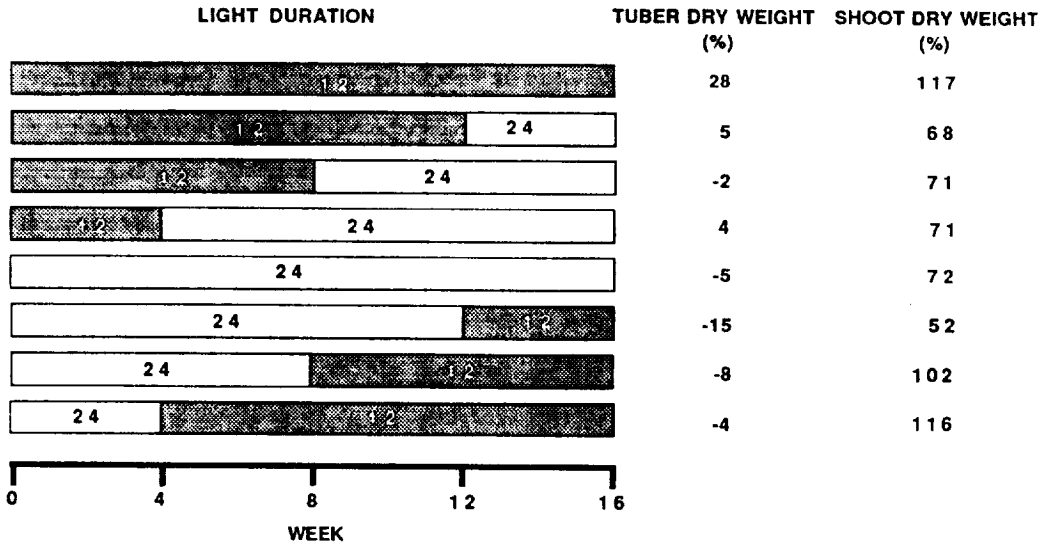

Fig. 2. Effect of carbon dioxide supplementation in combination with light duration changes on tuber and shoot dry weight.

Table 2. Weight of potato plants (cv. Denali) grown for 16 weeks under orbital light:dark cycles (60 minutes light:30 minutes dark) compared to plants grown under light:dark cycles of 16 hours light and 8 hours dark.

	Weight per plant (g)	
	60 MIN L:30 MIN D	16 HR L:8 HR D
Tubers	169	374
Total plant[z]	529	1030

[z]Includes shoots, tubers, roots, and stolons.

Subsequent experiments have provided evidence that the biomass reductions observed in potatoes under LEO light:dark cycles can be prevented by the addition of 75 μmol $m^{-2}s^{-1}$ PPF during the 30 minute "dark" portion of the cycle.

Diurnal Temperature Fluctuations

Potatoes (cvs Norland and Denali) were grown for 90 days under 12-h photoperiods with 440 μmol $m^{-2}s^{-1}$ PPF in two separate controlled environment rooms. One room was set at a temperature of 18°C during the light and dark periods, and a constant 70% RH. The other room was set with a diurnal temperature fluctuation of 22°C light and 14°C dark, with relative humidities adjusted to 77% light and 61% dark to maintain a constant vapor pressure deficit (0.59 kPa) in both treatments.

Tuber dry weights under diurnal temperatures were increased by 54% in Denali and 8% in Norland (Table 3). Total dry weight values were 30% higher for Denali grown in fluctuating temperatures and 10% higher for Norland. Both cultivars produced taller plants in the fluctuating temperature treatment. An experiment is currently in progress to determine if use of a low day/high-night temperature regime would reduce plant height without adversely affecting tuber yields.

Table 3. Effect of diurnal fluctuations in temperature on growth and tuberization of potato.

Cultivar	Temperature Treatment		Tuber Dry Weight	Total Plant Dry Weight	Plant Height
	Light	Dark	(g plant^{-1})	(g plant^{-1})	(cm)
	(°C)				
Norland	22	14	332	492	107
	18	18	309	449	94
Denali	22	14	405	649	120
	18	18	263	499	106

3. Cultivar Screening

Effort has been directed towards evaluating cultivars obtained from various growing regions for usefulness in a CELSS. Attempts have been made to obtain cultivars selected for long daylengths and for adaptation to high temperatures. Potatoes adapted to these conditions would extend the useful range of environmental conditions for potatoes in CELSS and possibly increase the maximum productivity that can be attained.

The cultivars were evaluated in continuous light at 600 µmol m^{-2}s^{-1} PPF, 1000 µmol mol^{-1} CO_2, 18°C and 70% RH in a continuous light screening study; and in 12-h lighting at 600 µmol m^{-2}s^{-1}, 1000 µmol mol^{-1} CO_2, 28°C and 70% RH in a high temperature screening study. Twenty three cultivars were grown for eight weeks and then observed for tuber initiation and plant vigor as shown in Table 4.

Table 4. Evaluation of selected cultivars at high temperature and with continuous irradiance.

Cultivar	Country of origin	Relative Tuber Initiation[z]	
		Continuous Light	High Temperature
Haig	US	**	**
Denali	US (Alaska)	** (slight chlorosis[y])	* (elongated stems)
Atlantic	US	**	*
Desiree	Holland	**	* (elongated stems)
Alaska 114	US (Alaska)	**	--
Rutt	Norway	* (slight chlorosis[y])	** (elongated stems)
Troll	Norway	* (slight chlorosis[y])	** (elongated stems)
Norland	US	--	**
R. Burbank	US	--	**
Kennebec	US	-- (chlorosis)	**
Bake King	US	--	**
Superior	US	-- (stunted, necrotic[y])	** (exposed tubers)
Alpha	Holland	-- (slight chlorosis[y])	*
Ottar	Norway	*	--
Snogg	Norway	* (chlorosis[y])	--
Bintje	Holland	*	--
NY81	US	* (slight chlorosis[y])	--
Snowchip	US (Alaska)	* (chlorotic[y], necrotic[y])	--
Gulauge	Norway	* (elongated stems)	-- (elongated stems)
Spunta	Holland	* (slight chlorosis[y])	--
Stately	US (Alaska)	-- (abscission[y])	--
ND860	US	-- (stunted plants)	--
NY72	US	-- (very stunted plants)	-- (very stunted)

[z]** high * some -- none
[y]leaves

Five cultivars, Haig, Denali, Atlantic, Desiree, and Rutt, were found to have the best potential under both continuous irradiation and high temperatures. These will be evaluated in growth studies of 120 days to determine their productivity potential.

4. Cultural Procedures

Substrates and Media

Investigations have been made of various substrates and media for use in a CELSS. These were studied using plants grown in inclined trays with nutrient solution flowing continuously along the bottom of the tray. The nutrient solution was recirculated and pH maintained at 6.0 with automatic pH controllers. Potatoes have been grown successfully both on capillary matting, as utilized for pot watering in greenhouses, and in a 1 cm layer of arcillite (calcined clay particles). In either case the matting or arcillite was covered with an opaque sheeting of plastic. These systems have achieved yields comparable to those obtained in deep containers filled with peat-vermiculite. However stolons have often grown under the fibrous root mat in these systems, and as tubers have enlarged the roots have been lifted and separated from the flowing liquid nutrient. Efforts are being directed toward finding substrate materials, such as finely woven screens and porous mats, that would allow downward root penetration but inhibit stolon penetration. Materials tested to date have been unsuccessful since newly initiated stolons have a sufficiently small diameter to penetrate the screens used. Also, it is possible that stolons may need to grow beneath a root mat, or within a substrate, in order to initiate tubers.

Continuous Harvesting

Continuous harvesting of tubers as they reach a usable size has been compared to a single harvest at plant maturity. Plants were grown in a 1 cm layer of arcillite, as described in the previous section. Plants were grown under 600 $\mu mol\ m^{-2}s^{-1}$ PPF of 12 h duration, a light:dark temperature of 22°C:16°C and 70% RH. At 8 weeks, and for each week until the final harvest at 16 weeks, enlarged tubers over 5 cm in diameter were removed by reaching under the cover (with the room dark) and separating the tuber from the stolon. The total weight of tubers harvested from trays over this 8 week period was compared to the weight of tubers harvested from trays that were undisturbed for 16 weeks. No yield advantage was obtained with the continuous harvesting practice, and there was no evidence that senescence of the plants was delayed. Tuber removal disturbed the source-sink balance in the plants as evidenced by the collapse of small areas of tissue on exposed leaflets within 24-h after the removal of the first tubers. Direct mechanical damage to stolons was also apparent in trays subjected to successive harvesting.

Plant Spacing and Container Configuration

Research has been directed toward determining the most effective spacing for potato plants and most desirable shape and size container for the plants.

One study was undertaken to determine the effect of plant spacing. Potatoes (cv Denali) were grown for 87 days under 400 $\mu mol\ m^{-2}s^{-1}$ PPF, of 24 h duration, 16°C and 70% RH. Plastic trays (54 cm wide and 83 cm long and 11 cm deep) were filled with a peat-vermiculite medium and planted with two, four and eight potato plants which provided .224, .112 and .056 m^2 (respectively) of growing area for each plant. Wire fencing was placed around each tray to contain the shoots to the tray area. Nutrient (modified half strength Hoaglands') was provided to the plants four times daily in excess.

The trays with eight plants developed a solid canopy to cover the surface of the trays in 20 days, whereas with four plants it required 25 days and with two plants 35 days. The shoot and dry weight increased with increasing numbers of plants in the trays with about a 40% greater yield at the close spacing (Table 5).

A second study was undertaken to determine if the depth of media and volume of media were significant factors in tuber yield. Plastic containers of 20.3 and 30.5 cm diameter were utilized. Four of the 20.3 cm containers were filled to within 1 cm of the top with peat-vermiculite (50:50) media. Four of the 30.5 cm containers were filled to the top with peat-vermiculite and eight of the 30.5 cm containers were fitted with false bottoms. Of these 8, four were fitted so that only the upper 17.8 cm was filled with media and the remaining four fitted so that only the upper 7.6 cm was filled with media. Potatoes (cv Norland) were grown under a continuous irradiance at 400 $\mu mol\ m^{-2}s^{-1}$ PPF, 16°C and 70% RH. Plants were watered to excess four times daily with modified half strength Hoagland's nutrient solution. Harvests made at 64 days indicated that tuber and total

plant production were proportional to the volume of media, with greatest production from plants that were provided with the largest quantity of media (Table 6). Although the differences in plant yield were not very large at this early harvesting date, it would be expected that if the plants had been grown to maturity the differences in yield would be much greater. It was of considerable interest that container shape appeared to have little influence on plant productivity, for plants grown in 30.5 cm wide x 7.6 cm depth had similar yields to those grown in 20.3 cm wide x 17.8 cm depth (containers with similar volumes of media).

Table 5. Effect of plant spacing on tuber weight, shoot weight, and plant height of potatoes (cv Denali) grown for 87 days.

Area per Plant (m^2)	Tuber Dry Weight ($g\ m^{-2}$)	Shoot Dry Weight ($g\ m^{-2}$)
.224	907	830
.112	1010	882
.056	1285	952

Table 6. Growth of Norland potatoes grown for 64 days in containers of different size and shape.

Diameter (cm)	Container Height (cm)	Volume (m^3)	Tuber Dry Weight ($g\ plant^{-1}$)	Total Dry Weight ($g\ plant^{-1}$)
30.5	7.6	.006	79.5	152.2
30.5	17.8	.013	86.0	171.3
30.5	30.5	.022	93.7	198.4
20.3	17.8	.006	79.4	160.5

A third study was undertaken to determine if containment of stolons and roots was a limitation to production of tubers. Trays were constructed of 0.3 cm thick polyvinyl chloride sheeting to develop growing areas that were 96 cm x 96 cm by 20 cm high. Two trays were constructed with dividers to partition the tray area into 9 separate compartments, each 32 cm x 32 cm. Two trays were left with no compartmentalization. The trays were filled with peat-vermiculite (50:50) media. Nine potato plants (cv Denali) were planted in each tray with a single plant positioned in the center of each compartment or in similar locations in the open tray. An automatic watering system was installed with four drip tubes positioned in each 'compartment' and waterings were made to excess four times each day. Wire fencing was placed around each tray to contain the shoots to the tray area. Plants were grown under 700 $\mu mol\ m^{-2}s^{-1}$ PPF at 16°C and 70% RH. Harvest of plants at 59 days showed no difference in potato growth or tuber yield between the two types of trays.

Summary: Research with potatoes continues to demonstrate that this species has a significant place in an operational CELSS, either alone or in combination with other food crops, and can fulfill a significant portion of the energy and protein requirements of humans in space. The high productivity of nutritious tubers, high harvest index and low irradiance requirement of the potato plant make it a particularly strong candidate for use in CELSS to provide food and oxygen, and to remove carbon dioxide for space inhabitants.

N90-15432

TRANSPIRATION DURING LIFE CYCLE IN CONTROLLED WHEAT GROWTH

Tyler Volk* and John D. Rummel**

**Earth Systems Group, Department of Applied Science, New York University, New York, NY 10003, U.S.A.*
*** Code EBR, Life Sciences, NASA Headquarters, Washington, D.C. 20546, U.S.A.*

ABSTRACT

We use a previously-developed model of wheat growth, which was designed for convenient incorporation into system-level models of advanced space life support systems. We apply the model to data from an experiment that grew wheat under controlled conditions and measured fresh biomass and cumulated transpiration as a function of time. We examine the adequacy of modeling the transpiration as proportional to the inedible biomass and an age factor, which varies during the life cycle. Results indicate that during the main phase of vegetative growth in the first half of the life cycle, the rate of transpiration per unit mass of inedible biomass is more than double the rate during the phase of grain development and maturation during latter half of the life cycle.

THE GROWTH MODEL

We developed a model for the growth of wheat /1/, which proved useful for coupling the wheat with other components in a system-level model of a Controlled Ecological Life Support System (CELSS). The rationale for the model's form is that growth curves of most crops prominently show the S-shaped or sigmoidal curve typical of biological systems. The solution to the logistic differential equation imitates this S-shape of exponential growth followed by a leveling-off. In the logistic equation, $dM/dt = rM(1-M/K)$, where M is the biomass and t is time, there are two parameters: r and K. The r is the growth rate for the purely exponential part of the system. K, the carrying-capacity in an ecological system, in this case is the maximum biomass reached by the crop. The logistic equation thus contains some biologically meaningful parameters.

While the logistic equation can be applied directly to the growth of the inedible biomass of a crop, the equation for the edible crop parts is here somewhat differently structured (see also /2,3/). Like the inedible cells, the edible cells reproduce and the total edible growth must be proportional to the edible mass (M_{ed}). However, the edible parts do not produce their growing mass through photosynthesis, but rather receive photosynthetic products from the inedible parts (in particular, the leaves); therefore, the inedible biomass (M_{ined}) should also appear in the edible equation. Furthermore, since the edible growth occurs substantially after the beginning of the inedible growth (about halfway through the life cycle for wheat), a time that initiates the growth of the edible mass (t^*) is incorporated into the edible equation. Before t^* the edible biomass is assumed equal to zero, and its growth is initiated at t^* with a minimum edible mass (E_{min}). The full set of equations is (see also /2,3/):

$$\frac{dM_{ined}}{dt} = r_{ined} M_{ined}\left(1 - \frac{M_{ined}}{K_{ined}}\right) \tag{1}$$

$$t < t^*: \quad \frac{dM_{ed}}{dt} = 0 \tag{2a}$$

$$t > t^*: \quad \frac{dM_{ed}}{dt} = r_{ed} M_{ined}\left(\frac{E_{min} + M_{ed}}{K_{ed}}\right)\left(1 - \frac{M_{ed}}{K_{ed}}\right) \tag{2b}$$

The parameters t and t^* are in units of time, r_{ined} and r_{ed} are in units of time^{-1}, and all other parameters (M_{ed}, M_{ined}, K_{ed}, K_{ined}, E_{min}) are in identical units of either dry mass or dry mass per unit area. The system of equations (1a-c) above was used for wheat, soybean, and potato /2/. The total fresh biomass (B) is the sum of the fresh edible and inedible masses, expressed using their respective ratios (w_i's) of their wet (fresh) mass to dry mass:

$$B = w_{ed} M_{ed} + w_{ined} M_{ined} \tag{3}$$

We compare the model to data provided by S. Schwartzkopf /4/. He grew wheat at the NASA Ames Research Center under controlled conditions of temperature, humidity, and atmospheric CO_2 (1200 ppm). Since we are not concerned here with how growth is affected by changes in these variables (except for humidity, see below), or other parameters (such as planting density), this data has been normalized to the total fresh biomass at day 60 (B_{60}), which in his experiment was the maximum total fresh biomass reached during the seed maturation. Figure 1a plots this normalized value of B/B_{60} as a function of time for the wheat data.

Equations (1, 2a-b, and 3) are run with w_{cd} = 1.13 (gm fresh per gm dry) /5/ and w_{incd} = 5.7 (gm fresh per gm dry) /6/. Other parameters used here are K_{cd} = 2500, K_{incd} = 3700, E_{min} = 80, initial M_{incd} = 10. In previous models these units have been gm dry mass m^{-2}, but here the units may be considered arbitrary since to facilitate comparison to Schwartzkopf's data, the model's output is normalized as a ratio between total fresh biomass and the total fresh biomass at day 60. This ratio, B/B_{60}, is plotted in figure 1a. Note also that the harvest index, defined as the fraction of the edible dry biomass—here approximately 2500/(2500+3700)—is consistent with the value of 0.4 from data /5/. The only major unknowns that can influence the shape of the growth curve significantly are the growth rates; these are adjusted to produce a reasonably accurate fit to data. The model curve shown in figure 1a uses $r_{cd} = r_{incd} = 0.2\ day^{-1}$.

TRANSPIRATION FORMULATION

Transpiration will probably account for about half the energy balance in the plant growth system of a CELSS. By definition, the total transpiration rate (Γ) is proportional to the transpiration rate per unit of inedible biomass (γ) and to the total inedible biomass. Therefore

$$\Gamma = \gamma\, M_{incd} \tag{4}$$

Following general reasoning such as that given in Gates /7/, γ is a function of the difference between the partial pressures of water vapor in the leaf ($P_{H2O,leaf}$) and atmosphere ($P_{H20,air}$) and a function of the stomatal resistance (f_s), which itself a complex function of various environmental factors including light, temperature, and CO_2.

$$\gamma = \gamma^*\, f_h\, f_s\, f_a \tag{5}$$

Here we have written γ as a product of a humidity factor (f_h is a function of $P_{H2O,leaf} - P_{H20,air}$), a stomatal resistance factor (f_s), a unit normalizing constant γ^*, and an age factor (f_a), which accounts for changes in the plant's transpiration rate per unit inedible biomass during its life cycle even when all environmental factors (f_h, f_s) are constant. A γ = constant = 2.4 gm H_20 per gm dry inedible biomass per day (this gives a rough average of typical wheat under controlled environments /8/) was used by Rummel and Volk /1/, but could not be tested against data during the plant's life cycle at that time. S. Schwartzkopf has been able to take detailed transpiration data from wheat /4/. To facilitate comparison between model and data the cumulated transpired water at time t ($\int_0^t \Gamma dt$) is normalized to the cumulated transpired water at day 60 ($\int_0^{60} \Gamma dt$). This ratio— $\int_0^t \Gamma dt \left(\int_0^{60} \Gamma dt\right)^{-1}$— is plotted as a function of time in figure 1b. It is also useful to consider the instantaneous transpiration rate Γ (here calculated from the data on cumulated water for any point using the previous and subsequent points), also normalized to the cumulated transpired water at day 60. This ratio— $\Gamma \left(\int_0^{60} \Gamma dt\right)^{-1}$—has the units of day^{-1}, and should be read as the fraction of the total transpired water during the life cycle transpired during a given day; this ratio is plotted in figure 1c.

$$\text{Normalized cumulated transpiration} = \frac{\int_0^t \Gamma dt}{\int_0^{60} \Gamma dt} \tag{6a}$$

$$\text{Normalized transpiration rate} = \frac{\Gamma}{\int_0^{60} \Gamma dt} \tag{6b}$$

Schwartzkopf's humidity controls kept the relative humidity (rh) at 0.35 at the beginning of the experiment, but only maintained rh near 0.45 at the end /4/; the change was gradual and approximately linear. Assuming leaf rh = 1.0 and air rh varied from 0.35 to 0.45, the humidity factor f_h, expressed in terms of rh and non-dimensionalized to the final condition, is taken here to have varied linearly from 1.18 at the beginning of the experiment ((1-0.35)/(1-0.45)) to 1.00 at the end. Furthermore, we set γ^*= 2.4 gm H_20 per gm dry inedible biomass per day, and since environmental conditions were approximately constant, f_s = 1.0 for the duration of the experiment. We test several cases of the age factor f_a.

The first case has f_a = 1.0 = constant (or, α = 0, see below). Output from the model for cumulated transpiration and transpiration rate is normalized to the cumulated transpiration at day 60 using equations 6a-b, like the experimental data. Note this normalization effectively eliminates dependence of the results on γ^*. Results with f_a

= constant are plotted against data in figures 1b and 1c. Although the general shape of the cumulated transpiration data is matched by the model (see figure 1b), the empirical value is significantly underestimated during the middle one-third of the life cycle. The underestimation is even clearer in the rate results, shown in figure 1c. For the first one-half of the life cycle, the transpiration rate in the model is much too low.

A second case explores the possibility that the transpiration rate per unit inedible biomass is substantially higher when the plant is younger than when mature. A convenient way of parameterizing this process that takes into account the apparent steadiness of the transpiration rate during the second one-half of the life cycle, when the inedible biomass itself is relatively maximum and constant, is to write f_a as a function of M_{incd}:

$$f_a = 1 + \alpha\left(1 - \frac{M_{incd}}{K_{incd}}\right) \qquad (7)$$

Here the term α is an enhancement of transpiration rate per unit biomass when the plant is young. Note $f_a = 1.0$ when $M_{incd} = K_{incd}$. The model output for cumulated transpiration and transpiration rate for this second model—which uses $\alpha = 1$, rather than $\alpha = 0$—is shown in figures 1b and 1c. Overall better fit to the data is apparent, in particular, improvement in the transpiration rate during the first one-half of the life cycle. However, also clear is that even higher rates (in other words, higher α's) are needed in the first one-third of the life cycle. Without fitting the data even further, we have nevertheless demonstrated the possibility of representing the transpiration to varying degrees of accuracy with formulations that have physical meaning.

CONCLUSION

Models such as these are the best way of examining the "interactions of assumptions" /9/. Considering the overall results, the logistic growth equations combined with the assumption that the rate of transpiration per unit inedible mass decreases during the life cycle of the crop will generally reproduce the data and will probably be adequate in highly aggregated models of a CELSS, for example, the BLSS model /1/. A physiological interpretation of this transpiration formulation and comparison of these findings to the transpiration formulations in more detailed models of non-hydroponic wheat /10,11/ (which, however, are presently not applicable to a CELSS model) will help the crop model shown here develop more complex dynamics and allow better preliminary designs of space agricultural systems.

ACKNOWLEDGEMENTS

Research time for T. V. was partially provided by NASA-Ames Joint Research Interchange NCA2-101. We thank T. Tibbitts for a thoughtful and important review.

REFERENCES

1. J. D. Rummel and T. Volk, A Modular BLSS Simulation Model, *Adv. Space Res.*, 7, # 4, 59-67 (1987).

2. T. Volk, Modeling the growth dynamics of four candidate crops for controlled ecological life support systems, Final report to NASA/ASEE Summer Faculty Fellowship Program at Johnson Space Center, NGT44-001-800, 33-1 to 33-17 (1987).

3. T. Volk and H. Cullingford, Crop growth and associated life support for a lunar farm, *Lunar Bases and Space Activities of the 21st Century*, in press (1989).

4. S. Schwartzkopf, private communication (1987).

5. B. G. Bugbee and F. B. Salisbury, Studies on maximum yield of wheat for the controlled environments of space, in *Controlled Ecological Life Support Systems: CELSS '85 Workshop*, eds. R. D. MacElroy, N. V. Martello, and D. T. Smernoff, NASA-TM-88215, p. 447-486 (1986).

6. B. G. Bugbee, private communication (1988).

7. D. M. Gates, *Biophysical Ecology*, Springer-Verlag, New York (1980).

8. B. G. Bugbee, private communication (1986).

9. J. F. Reynolds and B. Acock, Modeling approaches for evaluating vegetation responses to carbon dioxide concentration, eds. B. R. Strain and J. D. Cure, *Direct Effects of Increasing Carbon Dioxide on Vegetation*, DOE/ER-0238, U. S. Dept. of Energy, Wash., D. C., p. 33-51 (1985).

10. T. Hodges and E. T. Kanemasu, Modeling daily dry matter production of winter wheat, *Agronomy Journal*, *69*, 974-978 (1977).

11. S. J. Maas and G. F. Arkin, TAMW: A wheat growth and development simulation model, (Research Center Program and Model Documentation. No. 78-1), Blackland Research Center at Temple, Texas Agriculture Experiment Station, College Station, Texas (1980).

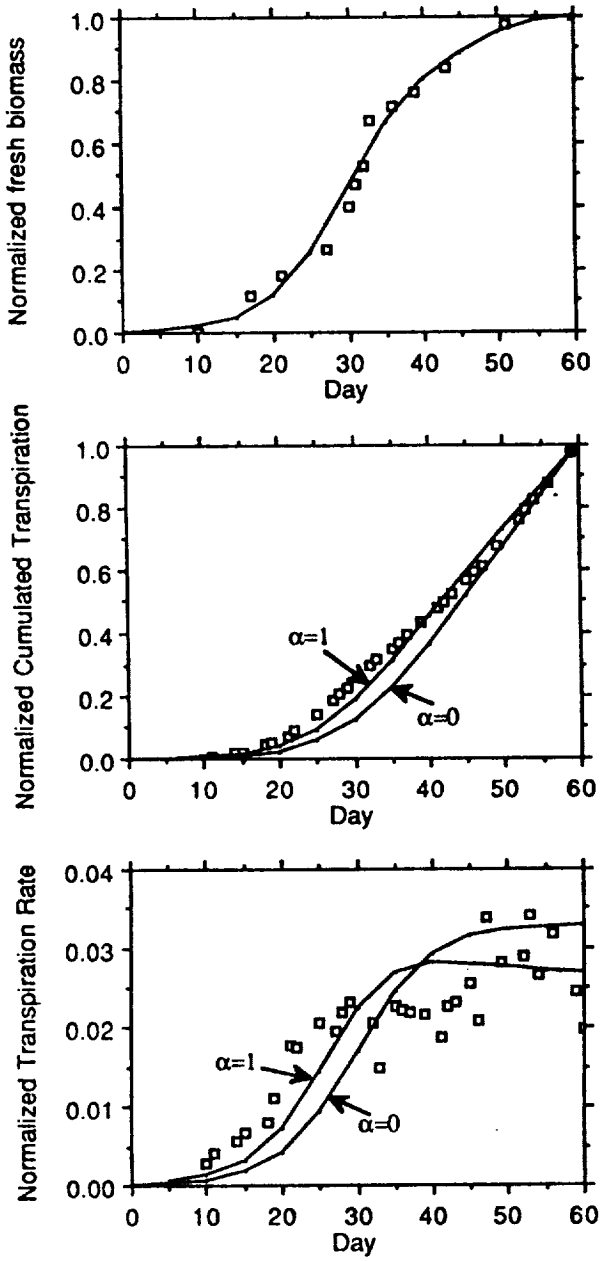

Fig. 1. Model results (lines) and empirical data (points) of (a, top) fresh biomass, (b, middle) cumulated transpiration, and (c, bottom) transpiration rate, all normalized as described in the text. Results in (b) and (c) are shown for two values of α; α controls the time-dependence of the age factor f_a in the transpiration rate. When $\alpha = 0, f_a$ is constant; when $\alpha = 1, f_a$ decreases non-linearly from about 2 in early growth to about 1 in late growth (see text). Results for biomass in (a) do not vary as a function of α. See equations 6a-b for definition of the normalized cumulated transpiration and normalized transpiration rate.

A-90-15433

LONG-TERM EXPERIMENTS ON MAN'S STAY IN BIOLOGICAL LIFE-SUPPORT SYSTEM

Gitelson I.I., Terskov I.A., Kovrov B.G., Lisovskii G.M., Okladnikov Yu.N., Sid'ko F.Ya., Trubachev I.N., Shilenko M.P., Alekseev S.S., Pan'kova I.M., Tirranen L.S.

Institute of Biophysics, USSR Academy of Sciences, Siberian Branch, Krasnoyarsk, 660036 USSR

ABSTRACT

We describe the experimental system having maximal possible closure of material recycling in an ecosystem, including people and plants, which was carried out in a hermetically sealed experimental complex "BIOS-3", 315 m^2 in volume. The system included 2 experimentators and 3 phytotrons with plants (total sowing area of 63 m^2). Plants were grown with round-the-clock lamp irradiation with 130 Wm^{-2} PAR intensity. The plants production was food for people. Water exchange of ecosystem, as well as gas exchange, was fully closed excluding liquids and gas samples taken for chemical analysis outside the system. The total closure of material turnover constituted 91%. Health state of the crew was estimated before, during and after the experiment. A 5-months period did not affect their health. The experiments carried out prove that the closed ecosystem of "man-plants" is a prototype of a life-support system for long-term space expeditions.

INTRODUCTION

The development of cosmonautics nowadays is directed to the preparation of spacecraft flights of long duration and distance with many crew members on board. The development also implies the creation of large space stations, Moon bases and extraterrestrial settlements inhabited by people. One of the key problems in the development of space technology of the next generation is the elaboration of biological life-support systems intended for a long stay of people beyond the Earth, independently of the supply from the Earth.

The analysis of the problem shows that the optimal solution for long-operating inhabited space objects is the creation of essentially closed ecological systems with substances turnover. The basis for these closed systems is photosynthesis of plants using the energy of sunlight. Such ecosystems including man, are the new product of civilization, in principle, being the instrument to permit the spreading of human civilization beyond the Earth biosphere. Since there are no complete analogues of these systems, neither in nature nor in technology, the possibility of their implementation makes theoretical analysis and experimental proof necessary.

The aim of our presentation is to consider one of the solutions which was put into practice through creation of an operating experimental ecosystem including man. The experimentators lived in this system for several months, obtaining oxygen, water and a part of food, by means of a controlled biological turnover of the substances inside the system. In the process of the work with this complex, we have become convinced that we can create an effective closed ecological system with man and providing a mechanism to reveal specific problems that arise. It presents an effective instrument for the experimental solution of these problems as well.

Experimental work on the development of such ecosystems was started by scientists in several research centres of the USSR, with scientists of the Siberian Branch of the USSR Academy of Sciences from Krasnoyarsk included. This particular work was guided from the very beginning by academician L.V. Kirensky with the project originally sponsored by academician S.P. Korolyov.

In the 1960's we developed and studied a closed "man-algae" system using the techniques of that time and involving continuous intensive cultivation of the unicellular algae, chlorella /1,2/. The experiments, which lasted 6 weeks, proved the algae to be able to fulfill successfully the functions of gas- and water-exchange in the system for man. However they failed to serve as the source of useful food for man. Thus we initiated experiments that included the traditional higher plants in a closed system /3,4,5/.

In the early 1970's, the experimental pilot complex "BIOS-3", for long-term experiments in a closed ecosystem, has been designed and built (Figure 1). The sealed system, with a volume of about 300 cubic meters, is fully isolated from the environment and has a closed cycle of circulation of air, water, and partly for nutrients.

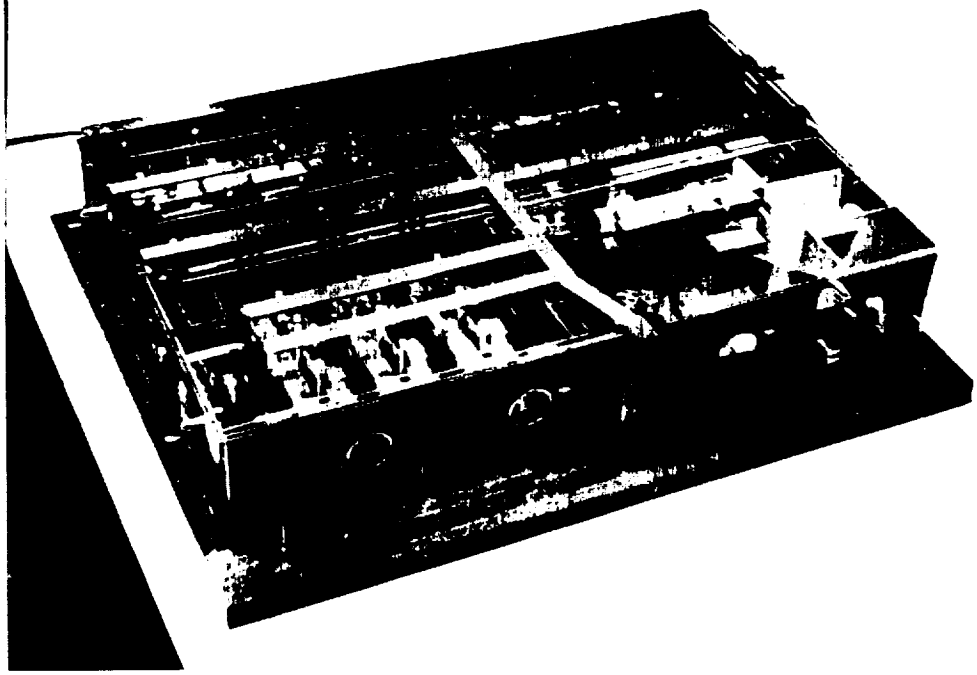

Fig. 1. The general view of the complex "BIOS-3" (The model is shown without ceiling). The right lower quarter is the living section with private cabins for the crew. The other sections are phytotrons for plants.

Three of the 4, equal in area and interconnected sections of the complex, could be called phytotrons and are used to grow plants (Fig. 2). The 4th section houses the crew in 3 single cabins, a galley-commissary, a lavatory and a control room for the phytotrons. This room also contains the equipment for processing of wheat, utilization of inedible biomass, repairs, weighing, and measurements.

During the series of experiments (1972-1984), 2- and 3-man crews of volunteers, selected by medical experts, manned "BIOS-3" over periods of 4 to 6 months /6-10/.

The crews planted crops, cultivated and harvested them, processed the harvest, and operated the complex in all other ways. This made the "BIOS" complex different from all the other similar experimental life-support systems in which all these jobs are done by the auxiliary personnel outside the complex.

The air of the crew module of the complex was pumped into the phytotrons to reduce the concentrations of carbon dioxide and other gases and vapors. Here it was enriched with oxygen generated by the green plants in the process of photosynthesis and then pumped back into the living quarters.

The plants did not clean the circulating air completely and a thermocatalytic filter was used to combust all the organic admixtures.

Water vapor discharged by plants was the source of water inside the complex. Drinking water was additionally purified by passing it through ion exchange filters and water for other uses was simply boiled.

While on board the "BIOS", the crew could communicate with the outside world by phone or view through the glass portholes which helped to relieve the psychological stress. When off duty, the crew members were able to spend time in their cabins where only electrophysiological monitors kept watch over them.

Crews who stayed inside the complex for periods of 6 months, did not manifest any signs of deterioration of their health, including allergies from contact with plants or any infection of the skin, mucous membranes or the intestine. Tests also revealed that the air and water inside the complex or edible food from plants did not undergo any unhealthy effect.

The driving force for the substances turnover in the closed ecosytem was plant photosynthesis.

Fig. 2. Wheat of different age in the phytotron of "BIOS-3".

During the experiments with man which lasted from 4 to 6 months in the sealed system, the crews cultivated a set of 10-12 cultures (wheat, sedge-nut, beet, carrots and others) under round-the-clock lamp illumination at photosynthetically active radiation (PhAR) level of 130-180 W/m² (380-720 nm). Wheat was cultivated with the help of an air subirrigational methods (Fig. 3), the sedge-nut and vegetables, by means of hydroponics. The nutrition of plants was supplied with salts and acids from storage. Each plant species was grown on a culture conveyer with 2 to 10 plantings of different ages simultaneously. This provided needed stability in photosynthesis and smoothed over the age fluctuations in photosynthetic rates of different cultures.

It should be noted that under optimized growth conditions nearly all the species showed a level of average daily productivity of similar value. This level of plant photosynthesis was conditioned by physical and technological limitations rather than by biological limitations. That is why the possibilities of further increase of photosynthetic productivity of higher plants is seen mainly in the improvement of technology of cultivation and not in the search for species with unusually high photosynthetic rates.

No negative interactions between different plants were revealed in the course of the experiments. During the 4-months period with man in the experimental closed system all the cultures went through 1.3 to 4 complete cycles.

The experiment carried out showed that under the chosen conditions of plants irradiance, 13 m² area occupied by plants is sufficient for a continuous supply of one man's oxygen, water (at the expense of transpirational moisture condensate) and for 40-45% of his food.

If one of the experiments, in which the crew was fed only by food produced by the plants, we increased the sowing area (for one man) up to 30 m² /11/. But it resulted in an excess of oxygen in the atmosphere and accumulation of alot of inedible plant biomass. This inedible part of biomass was combusted inside the system to produce additional carbon dioxide necessary for photosynthesis and reduce the oxygen level in the atmosphere. The sanitary water used in this experiment (shower, wash-basin etc.) after filtration, along with the urea of the experimentators without treatment or storage, was introduced into the wheat nutrient medium. Thus wheat's needs were met 59% in nitrogen, 28% in sulphur, 19% in potassium, 17% in phosphorus and 19% in magnesium. The rest of the biogenic elements for wheat and the nutrients for all other plants was introduced into the nutrient medium in the form of mineral compounds (acids and salts).

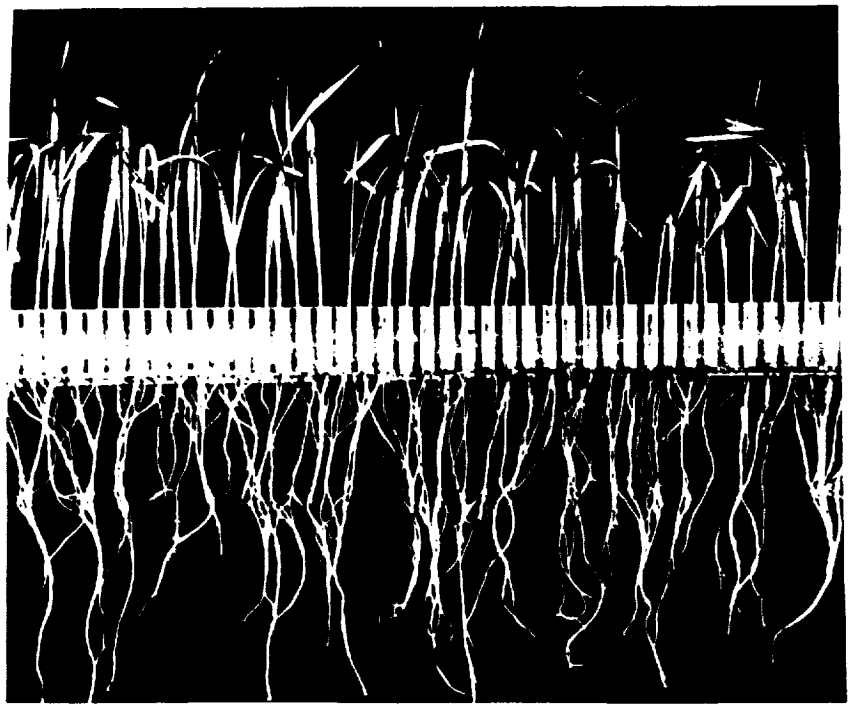

Fig. 3. Wheat on the plastic racks. The roots are periodically wet with nutrient solution.

The kitchen wastes, and the solid excretions of the experimentators were dried within the ecosystem to return water into the closed system and this dried material, along with the ash from the combustion of the plants' inedible biomass was then removed from the ecosystem.

The experiment showed that the average daily requirement of the crew for oxygen, water, food, etc. was met 95% (in weight) with the resources inside the system (Tables 1, 2). Only 5% of substances (animal products, sodium chloride for man and nutrients for plants, as well as personal hygiene requirements) were stored in advance for the duration of the experiment. The further increase in the degree of closure of substances turnover would be related mainly to animal product regeneration in the system. But this implies much greater consumption of energy because animal demands are nearly two-fold greater than demands for biomass production by plants.

TABLE 1. Requirements of the crew without recycling and with recyling in BIOS-3.

Substances Requirements of the Crew Without Recycling	(g per day)	Substances Requirements of the Crew With Recycling in BIOS-3	(g per day)
1. Dry food (without water)	924	1. Dry food	208
2. Oxygen	1220	2. Chemical compounds for the nutrient medium	350
3. Drinking water	5133	3. Sanitary materials	9.5
4. Sanitary water	5696	4. Absorbents for water purification	2.7
5. Sanitary materials	9.5	5. Cooking salt	28
6. Cooking salt	28		
TOTAL	13010.5		598.2

Note: The sampling of a substance for investigation outside the system isn't presented in this table.

TABLE 2. System recycling of food consumption by humans.

Turnover of substances for nutrition purposes	Absolutely dry substance g	Proteins g	Lipids g	Carbo-hydrates g	Caloric value kcal
Consumed by the crew during the month of the experiment					
TOTAL	27716	4369	4679	16030	119699
Edible biomass provided by plants grown in the system	21484	2851	1652	15290	83609
Portion of crew consumption being recycled (%)	77.5	65.2	35.3	95.4	69.8

A system that completely provides man with oxygen and water but provides only 40-45% of food is more advantageous energetically than a system providing 95% of man's food needs. To provide 40-45% of the food needs, it is necessary to have an area under crops of 13 m^2 for one man, and round-the-clock irradiation of 150-160 W/m^2 PhAR. This PhAR flux was provided by 200 watts of power from lamps. This is the flux of PhAR in Earth orbit beyond the limits of the atmosphere (and on the Moon) that incidents every 3.5 m^2 of surface perpendicular to the suns rays. At the orbit of Mars such a flux embraces 8 m^2. It goes without saying that the introduction of light into a life-support system would face the loss of a part of energy and require a definite increase of light-accumulating surfaces compared to the areas mentioned above. But this problem isn't of biological character, it is rather a technical one and is solvable in all probability.

The spacecraft flying by the Sun is irradiated by it continuously. In a cosmic settlement on the Mars the day lasting for 12 hours will be replaced by the night of the same duration. Neither 12-hours days nor the continuous illumination would pose any significant restriction to culture of the selected species.

More complicated is the problem of plants cultivation on the Moon surface because of the duration of the Moon day and the Moon night, i.e. 15 terrestrial days of continuous light and the same period of darkness. The Moon rhythm of night and day alternation does not occur under the Earth conditions. Growing plants usually can not bear the long period of continuous darkness. So the necessity arises to stop the growth of plants during long periods of darkness corresponding to the Moon nights in duration.

To solve the problem of the growth of plants under the conditions of Moon photoperiods, we carried out a series of experiments with wheat, barley, peas, turnips, dill, carrots, beet, radish, tomatoes, cucumbers, and sedge-nut /12,13,14/. The principal idea was to maintain plant vitality during the 15 day dark period by decreasing the temperature. Temperatures were lowered to 2.5 to 3.0°C during the darkness.

The experiments showed that all the cultures under study (except tomatoes, cucumbers, and sedge-nut) survived the Moon night safely and resumed grow normally during the Moon day. A partial injury of leaves was noted to occur in the course of Moon nights. As a result nearly all the cultures had the edible part of the crop reduced 30-50% compared to the control (Table 3). This indicates that the chosen regime of "conservation" of plants during the Moon nights is far from being optimal, but on the whole the data obtained provided evidence for the possibility of obtaining the traditional plant products under the conditions of Moon photoperiods, with a biochemical composition being essentially analogous to the control plants.

TABLE 3. Yield of plants grown under Moon photoperiods with a temperature of 24°C to during the light period and 2.5 to 3.0°C during the dark period.

Species	Cultivar	Irradiation regime[a]	Total biomass (kg m^{-2})	Edible biomass (kg m^{-2})	Economic coefficient (%)
Carrot	Chantanet	75 light days	15.92	10.80	67.8
		(5 m.d. + 4 m.n.)	13.82	7.93	57.3
Beet	Bordo	75 light days	8.38	5.32	63.5
		(5 m.d. + 4 m.n.)	13.77	6.51	47.2
Turnip	Petrovskaya	60 light days	12.32	5.71	46.0
		(4 m.d. + 3 m.n.)	7.6	3.25	42.5
Dill		30 light days	3.04	2.73	89.9
		(2 m.d. + 1 m.n.)	2.30	1.97	85.7
Radish	Virovsky (white)	22 light days	8.66	5.95	68.7
		(1.5 m.d. + 1 m.n.)	7.55	3.66	48.5

[a] m.d. - Moon day; m.n. - Moon night

REFERENCES

1. L.V. Kirensky, I.A. Terskov, I.I. Gitelson, G.M. Lisovsky, B.G. Kovrov, and Yu.N. Okladnikov, Experimental Biological Life Support System. II. Gas exchange between man and micro-algae culture in a 30-day experiment, Life Sciences and Space Research VI, 37 (1968).

2. L.V. Kirensky, I.I. Gitelson, I.A. Terskov, B.G. Kovrov, G.M. Lisovsky, and Yu.N. Okladnikov, Theoretical and Experimental Decisions in the Creation of an Artificial Ecosystem for Human Life Support in Space, Life Sciences and Space Research IX, 76 (1971).

3. G.M. Lisovsky, B.G. Kovrov, I.A. Terskov, and I.I. Gitelson, Method and Technique of Wheat Continuous Culture as a Link of Life Support System, Proc. 8th Intern. Symp. on Space Technology and Science, Tokyo, 1189 (1969).

4. L.V. Kirensky, I.I. Gitelson, I.A. Terskov, et al., Biological Life-Support System including Lower and High Plants, Proc. 20th Intern. Astronautic Congress, 825 (1972).

5. I.A. Terskov, I.I. Gitelson, B.G. Kovrov, G.M. Lisovsky, Yu.N. Okladnikov et al., The experiment on introducing vegetable plants in a closed gas-exchange biological life-support system, Space Biology and Airspace Medicine (USSR), N. 3, 33 (1974).

6. I.I. Gitelson, B.G. Kovrov, G.M. Lisovsky, Yu.N. Okladnikov, M.S. Rerberg, F.Ya. Sid'ko, and I.A. Terskov, Problems of Space Biology. Vol. 28. Experimental Ecological Systems Including Man, Moscow: Nauka, 1975.

7. I.I. Gitelson, I.A. Terskov, B.G. Kovrov, F.Ya. Sid'ko, G.M. Lisovsky, and Yu.N. Okladnikov, V.B. Belyanin and I.N. Trubachev, Life Support System with Autonomous Control Employing Plant Photosynthesis, Acta Astronautica, 3, 9-10, 633-650 (1976).

8. G.M. Lisovsky (The Editor), Closed System: Man - Higher Plants, Novosibirsk: Nauka (1979).

9. G.M. Lisovsky, I.A. Terskov, I.I. Gitelson et al., Experimental Estimation of the Functional Possibilities of Higher Plants as Medium Regenerators in Life Support Systems, Proc. XXXII Intern. Astron. Congress, (1981).

10. I.I. Gitelson, I.A. Terskov, B.G. Kovrov, G.M. Lisovsky et al., Closed Ecosystems as the Means for the Outer Space Exploration by Men (Experimental Results, Perspectives), Proc. XXXII Intern. Astron. Congress (1981).

11. B.G. Kovrov, I.A. Terskov, I.I. Gitelson, G.M. Lisovsky et al., Artificial Closed Ecosystem "Man-plants" with a Full Regeneration of Atmosphere, Water and Ration Vegetable Part, Proc. XXXII Intern. Astron. Congress (1981).

12. S.A. Mizrakh, G.M. Lisovsky, and I.A. Terskov, Growth and Development of Plants under the Moon Photoperiod, Proc. USSR Acad. Sci., 210, 2, 475-477 (1973).

13. I.A. Terskov, G.M. Lisovsky, S.A. Ushakova, et al., The Possibility to Use Higher Plants in Life-Support System at the Moon, Space Biology and Airspace Medicine (USSR), 3, 63-66, (1978-).

14. G.M. Lisovsky, O.V. Parshina, S.A. Ushakova, et al., Productivity and Chemical Composition of Some Vegetable Cultures, Grown under the Moon Photoperiod, Izv. SO AN SSSR, biol.ser., 1, 104-108 (1979).

SECTION II

WASTE OXIDATION

WASTE RECYCLING ISSUES IN BIOREGENERATIVE LIFE SUPPORT

R. D. MacElroy* and D. Wang**

* Ecosystem Science and Technology Branch NASA Ames Research Center, Moffett Field, CA 94035 U.S.A.

** TGS Technology Inc., Ecosystem Science and Technology Branch NASA Ames Research Center, Moffett Field, CA 94035 U.S.A.

ABSTRACT

Research and technology development issues centering on the recycling of materials within a bioregenerative life support system are reviewed. The importance of recovering waste materials for subsequent use is emphasized. Such material reclamation will substantially decrease the energy penalty paid for bioregenerative life support systems, and can potentially decrease the size of the system and its power demands by a significant amount. Reclamation of fixed nitrogen and the sugars in cellulosic materials is discussed.

INTRODUCTION

As the duration of space journeys and the number of crew members increase, future space missions will face the difficulty of ensuring a constant supply of life support consumables. The need to supply air, water and food, and to remove wastes from the crew environment represents a potential weight penalty of the order of 43 kg/day/person for consumables, such as drinking, hygiene and wash water for dishes and clothing, food, oxygen and carbon dioxide absorbers, and the packaging associated with these materials (Table 1). This sums to about 23,000 kg for a crew of 6 during a 90 day stay in space. Without alternative methods of dealing with life support, masses of this magnitude would have to be transported into orbit and, except for materials that leak into space, returned to Earth. Because such masses are close to the Shuttle's carrying capacity, life support could pose a significant logistics problem.

RESEARCH DIRECTIONS

NASA has conducted research and development activities for the past 20 years to address the issue of regenerating the O_2, water and food that crews require. Regeneration schemes are being developed based on physical - chemical and biological processes to regenerate waste materials, for example, collecting CO_2 and processing it to generate O_2 for crew use /1/, and oxidizing organic materials to generate CO2 and water /2/ /3/. These kinds of approaches separately address specific recycling and regeneration issues, and will probably be utilized early in human space exploration. However, the most ambitious and complete solution to life support recycling and regeneration is to develop a single integrated system capable of performing all of the necessary functions for life support. Bioregenerative systems are potentially useful in this regard and can use sunlight, plants or algae, and microorganisms to recycle wastes in much the same way as occurs on Earth (Figure 1).

TABLE 1 Use of Consumables and Packaging for Life Support per Person, per Day

Material	Consumables Mass (Kg)	Packaging Mass (Kg)
Water	22.08	6.87
Food	1.18	0.45
Oxygen	0.83	0.36
Waste		
CO_2	--	2.90
Liquid/solid	--	8.24
TOTAL	24.09	18.82

In concept, a very small "ecological" system will be developed for use in space (on orbit, in transit to Mars, or on the Lunar or Martian surfaces) to generate food, oxygen and potable water from waste materials, such as CO_2, organic materials and contaminated water produced by the crew. The system will not, in fact, rely on processes that are "natural" or "ecological" because they are slow, too poorly understood for adequate control, and do not necessarily respond to the goal of a life support system, which is to support a human crew. The term Controlled Ecological Life Support System (CELSS) is used to emphasize the need to operate a controlled system that fits crew needs and the space environment.

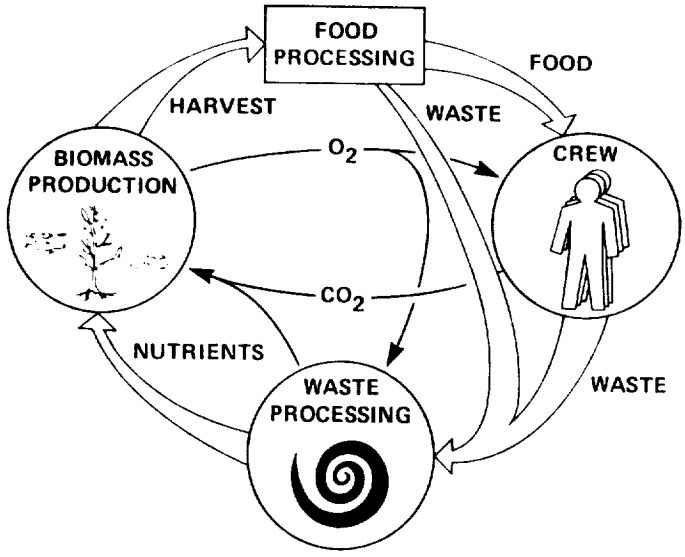

Fig. 1. Materials Cycling in a Closed System

Among the requirements of a CELSS are continuous regeneration of life support consumables in a system with long-term stability and with an efficiency, based on the use of mass, volume and power, such that most of the materials in the system are completely recycled in the shortest time possible. The constraints on such systems for use in space include limitations on mass and volume, on power and human labor availability, and on stable operation in lowered or micro-gravity and in radiation fluxes that are higher than on Earth. The requirements and constraints are summarized in Table 2.

TABLE 2 Requirements and Constraints for Life Support System Use in Space

Requirements:

- To produce the materials required for LIFE SUPPORT
- To RECYCLE and regenerate life support materials
- To function RELIABLY for extended periods of time

Constraints:

- Launch vehicle capabilities: MASS and VOLUME
- Mission capabilities: POWER and HUMAN LABOR availability
- Space environment effects: GRAVITY and RADIATION flux

TABLE 3 Progress in CELSS: 1982 - 1987

Material	Mass per Person 1982* (Kg)	Mass per Person 1987* (Kg)
Water	1867	896
Water (nutrient) Tanks	584	280
Structures (plant growth)	180	86
Ancillary equipment	1336	641
Harvest/Process equip.	134	**134
Waste process equip.	56	**56
Power (lighting) (electric, 43 Kw/person, 45.3 kg/kw)	1970	945
TOTAL	6127	3038

*Initial launch mass of components of a BLS system
**Not affected by plant growth efficiency improvements

To address the requirements and constraints the CELSS research program has, for the past 7 years, focussed heavily on the issue of how to supply a crew in space with a diet of food grown as rapidly and in as small a volume as possible. Significant progress has been

made in this area, resulting in a decrease in the required mass (Table 3), as well as better developed concepts of life support requirements (Table 4). Information of this kind allows estimates to be made as to whether the general approach is feasible, and which kinds of missions in space could benefit from a CELSS. The growth of plants involves the removal of CO_2 from the crew environment, the production of oxygen, and also the production of relatively large amounts of very pure water. All of these factors must be considered when measuring the fit of a CELSS to future space missions.

While considerations of biomass (food) growth within a life support system have occupied the major efforts of the CELSS research program to date, issues associated with proving the concept, and with scaling-up the system to human size /4/ have also been addressed. In the future it is likely that the CELSS research program will focus on issues of recycling the chemical elements that constitute the system. In general, the processes involved in recycling materials are termed 'waste processing' and are essential to the goal of 'loop-closing' upon which the concepts and the economics of regenerative life support systems are based.

TABLE 4 Life Support Consumables Produced by BLS System (per Person, per Day, assuming 97% regeneration of food)

Material	Consumables Mass per person (Kg)	Percent of Crew Requirements
Food	1.2	97
Water	300.0	322
Oxygen	3.6	97
CO_2 removal	3.4	97

RECYCLING, REGENERATION AND LOOP-CLOSURE

The term recycling refers to the process of continual re-use of the chemical elements of a life support system, and is the basis of the economies realized in a regenerative life support system. Such a system requires an initial charge of chemical elements: C, N, H, O, S, P, K, Na, Cl, I, Ca, Fe, Mn, Mg, Mo, Cu and Zn and possibly others, such as Si, B, F, Se and Co. Other elements, such as Ni, Cr, V, As, Ru, Rh, Pd, Au, Pt, Ba, Bi, Pb, Hg, Br, Ag and W, as well as the rare earth elements are likely to be present in the machinery and electronics that space systems depend upon. The goals of a bioregenerative life support system will be to recycle the elements that are essential for the correct functioning of the biological systems and to remove those elements that are poisonous or deleterious to them. It is clearly recognized that while complete recycling is a goal, it is one that is tempered by economic realities: when recycling is more expensive than resupply, in terms of mass carried into orbit, volume, power or human labor, it will not be practised.

Regeneration refers to the processes of re-forming life support consumables from elemental constituents and simple compounds. For purposes of life support regeneration involves relatively few classes of materials: air (O_2 supply and CO_2 removal), food and water. Regeneration requires energy input. When photosynthetic organisms (higher plants, algae, cyanobacteria, photosynthetic bacteria) are used to drive the system the energy source is sunlight. When other organisms drive the system, for example, hydrogen

oxidizing bacteria (e.g. *Pseudomonas saccharophila*) energy enters through processes that electrolyze water to H_2 and O_2. Because a supply of energy is one of the major constraints on operating a bioregenerative life support system, its economics are highly dependent on how efficiently it uses energy to achieve life support goals.

The term 'loop closure' has been used to describe the extent to which elements and compounds are recycled within a life support system. In terms of mass H and O (as water) are by far the largest constituents of a life support system. Carbon is next, followed by nitrogen. Each of these elements is freely transferred by organisms among gaseous, liquid and solid states, and from one compound to another. It will be economically advantageous to recycle these elements as rapidly and completely as possible, and to minimize their mass in the system.

WASTE PROCESSING

The term waste processing in the context of bioregenerative life support refers to those processes involved in converting materials that are not usable as human consumables into the reactants that can be regenerated into consumables. This definition covers a variety of materials: non-edible biomass, atmospheric contaminants (volatiles and particulates), organic and inorganic materials dissolved in water, CO_2 produced from metabolism (crew and microbial), urine, feces and surface contaminants (condensed volatiles, solids (including hair, skin, bacteria, etc.) and liquids). In addition to these wastes, which are directly associated with crew life support, other materials from sources such as scientific experiments, hygiene operations and machinery repairs must be considered as wastes to be processed.

Each class of waste [Table 5] to be processed is likely to undergo several different treatments depending on the characteristics of the waste materials. The input process stream may undergo physical separation, mechanical treatment (e.g. grinding, milling etc.), chemical treatment (e.g. pH adjustment, extraction), enzymatic or catalytic treatment (e.g. partial or complete hydrolysis, deamination etc.), fermentation (aerobic or anaerobic) and oxidation. Final (post-oxidation) output streams may undergo processes such as precipitation, mineral removal, filtration, ultrafiltration or reverse osmosis.

WASTE RECLAMATION

Because the consumption of energy will be a very strong constraint on the use and operation of a bioregenerative life support system, it will be essential to rescue usable organic materials from the waste stream as efficiently as possible. Two examples of the advantages of waste reclamation will be given below. The first, focussing on the recovery of fixed nitrogen, is brief; the second, dealing with reclamation of inedible biomass, will include a more extensive discussion.

FIXED NITROGEN RECOVERY

The growth of higher plants and of algae depends upon a relatively constant source of nitrogen in the 'fixed' (covalently bonded to other atoms) forms of ammonia (NH_3), nitric acid (HNO_3), nitrous acid (HNO_2) and in some cases urea (NH_2-CO-NH_2). These materials are required by the plant for the construction of protein and other molecules, and are accessible to the plants as ions (except for urea) and taken up primarily through the roots of higher plants, or through the membranes of algae. In the natural environment such fixed nitrogen is produced by lightning discharges during electrical storms, by decaying vegetation, by artificial processes that generate fertilizers and by the actions of bacteria. The two most significant bacterial sources of nitrogen are Cyanobacteria (blue-green algae), which are photosynthetic organisms that live freely in aquatic environments (e.g. *Nostoc* sp.), and non-photosynthetic bacteria (such as *Azotobacter* sp. or the Clostridia) that live symbiotically within nodules in association with the roots of certain kinds of

higher plants. In general, the process of nitrification can be summarized as:

$$N_2 + 3\ [H] + \text{energy (app. 16 ATP)} \leftrightarrow 2\ NH_3$$

Certain organisms that participate in the nitrogen cycle in the terrestrial environment also conduct a denitrification reaction, converting NH_3 to N_2. Such organisms (for example the Pseudomonads) are expected to be present in bioregenerative life support systems, and studies are in progress to understand how their denitrification activities can be inhibited /5/. Another locus of denitrification will be the physical-chemical oxidation processes that are likely to be used in a bioregenerative life support system. In this area, as well, studies are being conducted to minimize the extent to which oxidation processes convert fixed nitrogen to N_2 /3/.

In a bioregenerative life support system most of the fixed nitrogen will enter the waste streams through crew wastes, in particular, in the form of urea in urine. While direct use of urine as a source of fixed N for plants may be possible, urine also contains salts and other organic materials, such as sugars and degraded heme compounds. The latter are not used by higher plants, and are excellent substrates for bacterial growth. To minimize bacterial growth in the root environment it will be necessary to remove or separate the fixed N from the bulk of the urine. One process that may be studied for use in a bioregenerative system will be to concentrate urine solids, decompose the urea to CO_2, water and NH_3 with an enzyme (urease), and to extract volatile NH_3 from an acidified solution.

TABLE 5 Waste Streams in a Bioregenerative Life Support System

Waste Stream	Source	Content	Fate
1.Solid waste	Crew activities	Paper, plastics, feces, undefined trash	Oxidation
2.Urine	Crew	Urine, urinal flush water	NH_3 recovery, then oxidation
3.Domestic	Crew	Shower water, dish washing, clothes washing, oral hygiene	Removal of organics, then nutrient soln. makeup
4.Nutrient	Plant growth	Spent plant and algae nutrient solutions	Oxidation
5.Inedible biomass	Plant food processing	Roots, shoots, food process waste, water	Digest cellulose, remove sugars, then oxidize
6.Volatiles	Crew and plant volatiles, materials outgassing	Small organic molecules	Oxidation

INEDIBLE BIOMASS RECLAMATION

Salisbury, Bugbee and Bubenheim /6/ have estimated, based upon experimental data, that about 12 square meters of plant growing area will be required to produce enough wheat to support the caloric demands, although not the nutrient requirements, of one crew member for each day in space. This data assumes daily planting and harvesting of the crop, and results in the production of about 850 g of wheat berries, equivalent to about 2800 Calories, at each harvest. A wheat crop grown under stringently controlled environment conditions produces about 40 to 45% of its total biomass as edible food. The waste materials (about 1040 g) include leaves, stems and roots, the major constituents of which are cellulose, hemicellulose and a small amount of lignin (about 6 to 10% of the waste). The approximately 900 g of cellulose and hemicellulose in the waste represents an energy investment in materials potentially usable to the crew. However, except as inert dietary fiber, cellulosic materials do not contribute to human metabolic energy.

By conversion of celluloses and hemicelluloses to simple sugars the energy and carbon stored in them could be made available to a crew, either directly as sugars, or indirectly through conversion of the sugars into other food materials. If even 50% of the carbon and energy in the cellulosic materials could be reclaimed for use by the crew a substantial decrease (as much as 25% or 3 square meters) in food growing area could result. Such a potential increase in the efficiency of a bioregenerative life support system, based on volume and energy use, must be measured against the volume and energy required to process and digest the cellulosic materials, to utilize the sugars to produce alternative food sources, and the processing that might be required for such foods.

CHARACTERISTICS OF CELLULOSES

The cellulosic materials consist of high molecular weight carbohydrates, namely, cellulose and hemicellulose. Together these polysaccharides constitute about 90% of the total non-edible biomass structure. Cellulose is the major component of cell walls and is a linear polymer of D-glucose with a molecular weight of approximately half a million. Individual cellulose molecules are linked together by beta-1,4 linkages to form a highly crystalline material that is resistant to enzymatic hydrolysis.

Hemicellulose is composed of shorter chain polysaccharides, and it is the principal non-cellulose fraction of polysaccharides. The role of this component is to provide a linkage between lignin and cellulose. In its natural state, it exists in an amorphous form and can be divided into two categories, cellulosans and polyuronides.

Cellulosans are polymers whose building blocks are monomers of single sugars, including hexosans, such as mannan, galactan and glucosan, and pentosans, such as xylan and araban. Polyuronides are hemicelluloses which contain large amounts of hexuronic acids and some methoxyl, acetyl, and free carboxylic groups.

To make the sugars in cellulosic materials available to metabolism the sugars in the high molecular weight polymers must be separated by hydrolysis, that is by chemically or enzymatically adding water to the chemical bonds linking the sugars. Chemical processing usually requires high concentrations of acids, and recycling acids within a closed system in space is likely to present major obstacles. Enzymatic digestion is slower and less complete, but may be more controllable and easier to accomplish in space.

The obstacles to enzymatic hydrolysis of cellulose include: 1. the binding of lignin and hemicellulose to the cellulose, thus forming a physical barrier to enzymatic attack; 2. the crystallinity of native cellulose, which makes it highly resistant to enzymatic hydrolysis; 3. the limited number of enzymatic reaction sites that result from the structure of even separated cellulose fibres; 4. products that arise during hydrolysis that inhibit enzymatic

THE CELLULOLYTIC ENZYMES

Three enzyme complexes, Cx, C1, and beta-glucosidase, are responsible for the conversion of cellulosic materials to glucose. For the most efficient conversion, enzyme ratios of 1:2:4 of Cx:C1:beta-glucosidase are required. The component enzymes of the complexes are classified as:

1) Endo-beta 1,4 glucanases - several components varying in degree of randomness, the old Cx. One component may be the enzyme that acts first on crystalline cellulose. Specific activity (SA) is greater than 60 units/mg.

2) Exo-beta 1,4, glucanases - several varieties:
a) Beta 1,4 glucan glucohydrolase - removing single glucose units from the nonreducing end of the chain.
b) Beta 1,4 glucan cellobiohydrolase (CBH) - removing cellobiose units from the nonreducing end of the chain. The CBH was equated with the old C1 enzyme and has a specific activity of 0.7 units/mg. This is also the component having the greatest affinity for cellulose.

3) Beta-glucosidase (cellobiase) - converts cellobiose and short chain oligosaccharides to glucose. Some unknown factor converts native cellulose into an activated state which is attacked by endo- and exo- - glucanases to liberate diglucose units. Native cellulose in the presence of endo-glucanase goes to cellulose. Cellulose in the presence of exo-glucanase goes to cellobiose. Cellobiose in the presence of beta-glucosidase goes to 2-glucose.

THE ENZYME SOURCES AND FERMENTATION

Trichoderma viride (Tv) is the best source of active cellulase, although many other actively cellulolytic organisms exist and variations in media or growth conditions may result in good cellulase preparations from other organisms /7/. It is possible to use a combination of different sources of enzymes to increase the yield of glucose from cellulosic materials. Because the pH for maximum growth of Tv is 4.5, while maximum enzyme production occurs at pH 3.5, it is convenient to have one reactor at each pH.

Temperature, pH, substrate concentration, and enzyme concentration are important factors in determining the rate of hydrolysis of the substrate. For a Tv cellulase substrate system a temperature of 50 °C and pH of 4.5 - 5.5 are optimal. Rates of hydrolysis increase with enzyme and substrate concentrations. Cellulase can be inhibited at high concentrations by some of its substrates. Generally, end products exhibit inhibitory effects on the rate of the forward reaction. Glucose inhibition is generally weak. Cellobiose is the main inhibitor of the C1 factor in the enzyme complexes. The breakdown of the cellobiose by beta-glucosidase increases the reaction rate /7/.

The ultrafiltration technique relies upon the physical size of the molecules. The sugar molecular weight is less than that of the cellulose, the enzyme, and the lignin. A molecular sieve is placed in a position to filter liquid drawn off of the hydrolysis tank. The sugar solution is separated and saved for further concentration, purification, or use.

CONCLUSIONS

The elements of waste processing in a bioregenerative life support system will include collection of materials, separation to allow reclamation, reclamation of usable materials, oxidation of organics and post-treatment of oxidation products. While the final recycling process will be oxidation, the efficient functioning of a bioregenerative life support system will depend on reclamation of materials, such as organics and fixed nitrogen, into which a considerable amount of the system's energy has been invested.

REFERENCES

1. P.D. Quattrone, F.H. Schubert, and D.B. Heppner, SAE Technical Paper Series 840959, ICES, San Diego, Ca, (1984).

2. T.J. Wydeven, J. Tremor, C. Koo, and R. Jaquez, These proceedings (1988).

3. Y. Takahashi, T. Wydeven, and C. Koo, These proceedings (1988).

4. R.D. MacElroy, J. Tremor, D.T. Smernoff, W. Knott, and R. Prince, Adv. Space Research,7, 53-58 (1987).

5. L.I. Hochstein, M. Betlach, and G. Kritikos, Arch. Microbiol. 137, 74-78 (1984).

6. F.B. Salisbury, B. Bugbee, and D. Bubenheim, Adv. Space Research, 7, 123-132 (1987).

7. M.J. Malachowski, Cellulose Conversion Handbook, C.E.I. 17-70 (1980).

SOURCES AND PROCESSING OF CELSS WASTES

T. Wydeven,* J. Tremor,** C. Koo,** and R. Jacquez***

*Ecosystems Science and Technology Branch, NASA/Ames Research Center, Moffett Field, CA 94035, USA
**TGS Technology, Inc., Ames Research Center, Moffett Field, CA 94035, USA
***New Mexico State University, Las Cruces, NM 88003, USA

ABSTRACT

The production rate and solid content of waste streams found in a life support system for a space habitat (in which plants are grown for food) are discussed. Two recycling scenarios, derived from qualitative considerations as opposed to quantitative mass and energy balances, tradeoff studies, etc., are presented; they reflect differing emphases on and responses to the waste stream formation rates and their composition, as well as indicate the required products from waste treatment that are needed in a life support system. The data presented demonstrate the magnitude of the challenge to developing a life support system for a space habitat requiring a high degree of closure.

INTRODUCTION

Renewed interest in long duration human space missions, particularly the establishment of a Lunar base or a mission to Mars, has prompted a critical evaluation of advanced life support systems /1/. This evaluation has revealed that current methods available for nearly complete recycling of water, oxygen, and food in space are technologically and economically impractical. Such limitations prevent humans from spending long periods of time in space. Therefore, current research emphasis is placed on developing improved recycling techniques to overcome these limitations.

Nearly complete recycling can be theoretically accomplished by life support subsystems which are dependent either on physical or chemical (P/C) principles or by subsystems which include a living or biological component. (A life support system that relies heavily on biological subsystems for recycling is becoming defined as a Controlled Ecological Life Support System (CELSS) or bioregenerative system.) A subsystem which is based on a physical or chemical principle, for example, is a water electrolysis unit which provides oxygen for respiration by using electrical energy to decompose water into hydrogen and oxygen. Higher plants are an example of a biological subsystem that produces oxygen for respiration through photosynthesis, using sunlight for its source of energy. If a high degree of closure of the life support system is required, wherein most of the water, oxygen, and food is recycled, then a hybrid system consisting of a combination of P/C and biological subsystems will undoubtedly be needed.

Recycling in a space habitat implies the conversion of waste streams derived from several different sources into useable products. Some of the waste streams are common to both the P/C and CELSS based life support systems. For example, all of the wastes derived from a human are common to both systems. Certain waste streams are present only in space habitats that use living subsystems as an integral part of the life support system. To illustrate: if higher plants are used to produce food, then inedible biomass (in substantial quantity), water derived from the transpiration of plants, and the spent, organically rich plant nutrient solution are wastes not found in a solely P/C life support system.

Not only are the input waste streams different in P/C and biological systems, but the required outputs are also different. A CELSS requires plant nutrients as an output

stream, a requirement unique to a photosynthetic-based food production and life support system.

For either the development of a computer model of a waste treatment or recycling subsystem or the functional design itself, it is desirable to have well defined input feed streams, including production rates and composition. In this paper, recent data are presented, as specifically as possible, on the nature of the waste streams that would be encountered in a human space habitat. Those streams that are characteristic of a given type of life support system are identified, and two representative scenarios for recycling wastes and nitrogen in a bioregenerative life support system are described.

TABLE 1. Waste Feed Stream Production Rates and Solids Content in a Manned Space Habitat Containing a Higher Plant Growth Chamber

Stream ID	Wet Weight Formation Rate, kg/person-ks (lb/person-day)	Dry Weight Formation Rate, kg/person-ks (lb/person-day)	Weight Percent Solids, %
toilet waste			
urine /2/,/3/	2.41×10^{-2} (4.59) [a]	7.4×10^{-4} (0.14)	3.1
feces /2/	1.11×10^{-3} (0.210)	2.37×10^{-4} (0.0452)	21.4
wipes /2/	4.8×10^{-4} (0.091)	unknown	unknown
urinal flush water /5/	5.72×10^{-3} (1.09)	NA	NA
hygiene water			
dish /6/	6.3×10^{-2} (12)	1.4×10^{-5} (2.6×10^{-3})	0.022 [b]
shower and hand wash /6/	6.3×10^{-2} (12)	1.8×10^{-5} (3.4×10^{-3})	0.028 [c]
laundry /6/	0.15 (28)	7.9×10^{-6} (1.5×10^{-3})	0.0054 [b]
humidity condensate /6/	4.34×10^{-2} (8.26)	6.6×10^{-6} (1.3×10^{-3})	0.016
food preparation waste /3/	6.9×10^{-4} (0.13)	2.3×10^{-4} (0.044)	34
trash	1.2×10^{-2} (2.2)	unknown	unknown
respired CO_2 in air /5/	NA	1.15×10^{-2} (2.20)	NA
contaminated cabin air /11/	See Table 3 and Appendix I.		
inedible biomass (wheat chaff)	7.1×10^{-2} (14)	7.1×10^{-3} (1.4)	10
transpiration water /7/	0.71-3.56 (136-678)	See note (d).	

Footnotes

(a) The density of urine was taken as 1.008 g/ml /4/ to convert urine volume from reference /2/ to weight.
(b) Detergent only; sodium dodecyl benzene sulfonate (an anionic detergent).
(c) Cleansing agent only; Economics Laboratory Cleansing Agent Formulation 6503.54.4 (an anionic detergent).
(d) The contaminant load in transpired water from plants is unknown.

WASTE SOURCES

In determining the treatment to be applied to any waste stream of a life support system, at least three pieces of information must be considered: 1) stream composition, 2) rate of stream production, and 3) required end product(s). Tables 1, 2, 3, and Appendix I, summarize some of the important information concerning waste stream composition and production rate for streams derived from a number of sources in a life support system. A discussion of the data presented in Table 1 follows.

Wastes from General Human Activities

Parker and Gallagher /2/ reported results from a comprehensive study of human wastes in which over 25,000 person-days of data was analyzed. They reported mean values for the dry and wet weight of human feces, the volume of human urine (2,066 milliliters/person-day), solids per menstrual period (10 grams), the average number of pads or tampons used per period (15.2), the average weight of pads (10.65 grams) and tampons (2.60 grams) from different manufacturers, and the total amount of toilet paper usage for women for bowel movements and urination (41.1 grams/woman-day). The solids content of human urine shown in Table 1 was obtained from reference /3/. It should be noted that the values reported by Parker and Gallagher are mean values and these authors emphasize that a space habitat waste handling and treatment subsystem must be designed to accomodate extremes and should not be designed on the basis of mean values.

The type and amounts of organic and inorganic constituents in human urine can be found in references /3/ and /4/. The elemental composition of human feces derived from subjects fed a specified diet can also be found in reference /3/.

The amount of urinal flush water shown in Table 1 is being used for designing or sizing the environmental control and life support system (ECLSS) for the US Space Station /5/. The volumes of dish, laundry, shower, and hand wash water were obtained in a private communication /6/ and these amounts are also being used for designing the Space Station ECLSS. The amount of cabin humidity condensate and its contaminant concentration were derived from Space Shuttle data and are also part of the design load for the Space Station ECLSS.

The amount of food preparation waste and details concerning its composition were taken from reference /3/ and references cited therein. Reference /3/ cited the work of M. Karel of the Massachusetts Institute of Technology, who was responsible for designing a model food processing and preparation waste for the US CELSS program. In designing this model waste, it was assumed that the CELSS population would be small, that plants would be grown hydroponically, and that animals would not be part of a CELSS.

In 1985, the NASA-Ames laboratory analyzed the trash brought back to Earth aboard Space Shuttle Flight 51D. The objective of this analysis was to gain insight into the composition, amount, and volume of trash produced during a representative human space mission. This type of information will be needed for the design of long term human space mission waste handling and treatment subsystems. The results from this analysis are shown in Table 2.

Air Contaminants

Contaminated air from crew quarters is another waste stream that must be treated in the closed environment of a space habitat. Wastes in cabin air include water and carbon dioxide from perspiration and respiration, volatile contaminants from people and equipment, and airborne particles. The average amount of carbon dioxide produced by an adult each day (Table 1) was taken from reference /5/. A contaminant load model (including contaminant type and concentration) is a prerequisite for the design and sizing of the contaminant control subsystem for a space habitat. The load model being used for designing the Space Station contaminant removal subsystem is given in Appendix I. We have included the extensive list of representative volatile contaminants shown in Appendix I to illustrate the broad spectrum of compounds one can expect to find in a closed habitat. Appendix I also shows the space maximum allowable concentrations (SMAC) for continuous exposure to a given contaminant.

TABLE 2. Composition and amount of trash derived from Space Shuttle Flight 51D (49 person-day flight)

Trash Constituent	Weight, kg (lbs)	Volume, m^3 (ft^3)
Food containers [a]	23.0 (50.8)	0.093 (3.3) [b]
Paper	6.4 (14)	0.037 (1.3)
Biomedical	6.4 (14)	0.028 (1.0)
Leftover food & garbage	4.8 (10.5)	0.008 (0.3)
Plastic bags	3.2 (7)	0.062 (2.2)
Grey or duct tape	1.6 (3.5)	0.008 (0.3)
Cans, aluminum & bimetallic	1.2 (2.8)	0.014 (0.5)
Miscellaneous	2.6 (5.8)	0.023 (0.8)
Total	49.0 (108)	0.280 (9.9)

Footnotes

(a) Includes 12.2 kg (27 lbs) of uneaten food and beverages.
(b) After cleaning and stacking.

The estimated concentration and size of airborne particles which are expected to be found aboard the Space Station are given in Table 3. These estimates are being used for the design and sizing of the contaminant control subsystem. In estimating the rate of generation of airborne particles expected aboard the Space Station, it was assumed that about 90 percent of the particles would be derived from humans and their activities. To obtain the total generation rate of particles or dust expected aboard the Space Station, the numbers in Table 3 must be multiplied by the crew size and the factor 1.1 to account for particle generation by sources other than people (assumed to be 10 percent of the total).

TABLE 3. Estimation of Space Station Particle or Dust Generation Rate by Humans /11/

Particle Size (microns)	Particle Generation (particles/hr/person)
0.3 - 0.5	81,341,426
0.5 - 1	34,570,164
1 - 2	4,270,366
2 - 5	1,565,870
5 - 10	211,548
above 10	40,626

Wastes from Plant Production Activities

In estimating the amount of inedible biomass and transpiration water (Table 1) that must be handled by the waste treatment subsystem in a CELSS, the following

assumptions were made: a) the average amount of dry food required by each adult per day is 0.617 kilograms /5/, b) wheat alone can meet a person's daily caloric but not necessarily nutritional requirement, c) only 50 percent of the dry mass of a mature wheat plant is inedible (i.e., an optimistic harvest index of 50 percent), d) 90 percent of the wet weight of the inedible portion of a wheat plant is comprised of water, and e) depending upon carbon dioxide concentration, the amount of transpired water ranges from 50-250 grams per gram of plant (edible plus inedible) dry weight /7/.

Transpiration water may contain volatile organic compounds that must be removed before recycling the water. These compounds may come from plants or materials in the plant growth chamber. Currently, the type and concentration of contaminants in transpiration water are poorly defined and therefore this stream must be considered as a waste stream that will require some processing.

Wastes from Experimental Systems

Experiments being conducted in a space habitat will also contribute waste of varying types and amounts that will require handling and treatment. The broad spectrum of wastes that might be derived from experiments precludes this source of waste from being considered here. However, a study has been conducted in which waste derived from potential flight experiments is defined /8/.

WASTE PROCESSING

Given the quality and quantity of the waste streams presented in Table 1, there are a number of different waste processing methods that one might consider for handling and treating these wastes. These methods include both biological and physical/chemical processes. The optimum combination of processing technologies remains to be determined. However, a scenario based on qualitative considerations (as opposed to detailed mass and energy balance calculations, tradeoff studies, etc.) is shown in Figure 1.

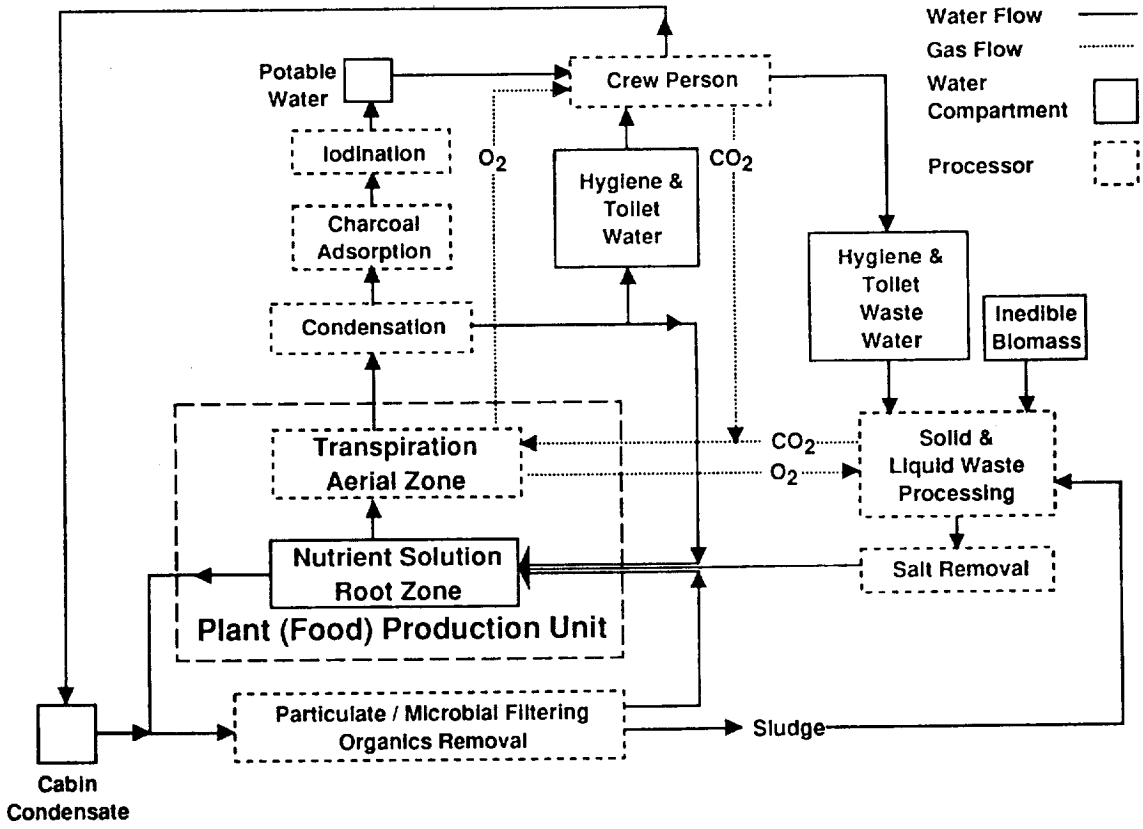

Fig. 1. Representative Water Pathways in a CELSS.

General Water and Gas Processing Scenario

Figure 1 graphically depicts a water pathway scenario in a CELSS. The scenario shows how water may be processed or treated in order to attain the required quality standards of each of the depicted water compartments. The different sizes of the solid boxes in Figure 1 reflect proportional volumes (derived principally from Table 1) of the major water compartments on a per day per person basis (actual sizes are dependent upon the rate of throughput and storage considerations).

It should be noted that the range for transpiration water production set forth in Table 1 is determined by the environmental conditions, predominantly the concentration of carbon dioxide (CO_2) in the plant growth chamber. Transpiration water production is inversely proportional to the CO_2 partial pressure. When the CO_2 pressure is low, the stomates, openings in the leaves through which gas and water exchange occur, open, and the transpiration rate is high (up to 250 grams water transpired per gram of dry biomass produced); the reverse is true for high CO_2 concentrations.

The ability to change the transpiration rate by varying the CO_2 concentration can be an important control factor in a CELSS. For example, under optimal plant growth conditions, more than enough water is provided to meet crew requirements even though the transpiration rate is low. Should an emergency occur whereby more water is needed by the crew, the transpiration rate and the amount of water provided to the crew can be quickly increased, by merely decreasing the CO_2 concentration in the plant growth chamber.

It is expected that transpiration water, having been derived from a phase change process, will be relatively clean. Therefore, this waste stream may need only minimal filtering and bacterial control to yield high quality water for drinking and other applications. However, most of the condensed transpiration water will be used to replenish water lost from the plant nutrient solution. This cycle as illustrated in Figure 1 shows nutrient solution make-up water also being introduced from other processors.

The condensate collected from the cabin environmental control system, having passed through a phase change, is also expected to be quite clean (see Table 1). However, humidity condensate may contain a high population of microbes derived from microbial growth on the condenser or heat exchanger. Although the amount of condensate collected is not enough to meet the hygiene and toilet water requirement, the water recovered here can be combined and treated along with transpiration water and spent nutrient solution. The nutrient solution will contain an unknown number of microbes as well as organic compounds produced by root metabolism and detritus breakdown. These contaminants can be filtered out and useable salts can be returned to the nutrient solution. The filtrate or sludge would be treated in the solid waste processor.

Toilet water containing feces and the inedible biomass waste streams have relatively high solids concentrations and also may contain potentially harmful microbes. Therefore, these streams will require a more rigorous treatment. High temperature and pressure processes, such as wet oxidation or supercritical water oxidation may be used to treat these more concentrated streams and to assist in closing the water cycle between the crew person and plant production unit. The water produced by the solid and liquid waste processor (see Figure 1) includes the yield from inedible biomass, hygiene and toilet water treatment, and also from a certain amount inherent in some of the items listed in Table 2, as well as from the root zone filtrate. This water is not necessarily potable, but after salts and potentially toxic metals (derived from corrosion) are removed, it is benign to the plants growing from the nutrient solution to which it is returned.

Gas exchange between the plant growth chamber and other parts of a CELSS is also an important part of recycling. For example, oxygen produced by photosynthesis in the plant growth chamber may be used for oxidation in the waste processor and for respiration by the crew. Likewise, the CO_2 produced by both crew and waste oxidation is needed by the plants for their growth.

The crew consumes water-containing edible biomass, drinks potable water, and produces waste. Consequently, the crew closes the life support loop in this generally described scenario.

Nitrogen Recycle through a Hybrid Waste Processing System

Figure 2 illustrates a more specific waste recycling scenario which includes methods for recycling nitrogen and converting it into forms desirable for plant metabolism. In this scenario, organic nitrogen is converted into ammonia (NH_3) and nitrate ions (NO_3^-) which are species desired by plants for their nutrition.

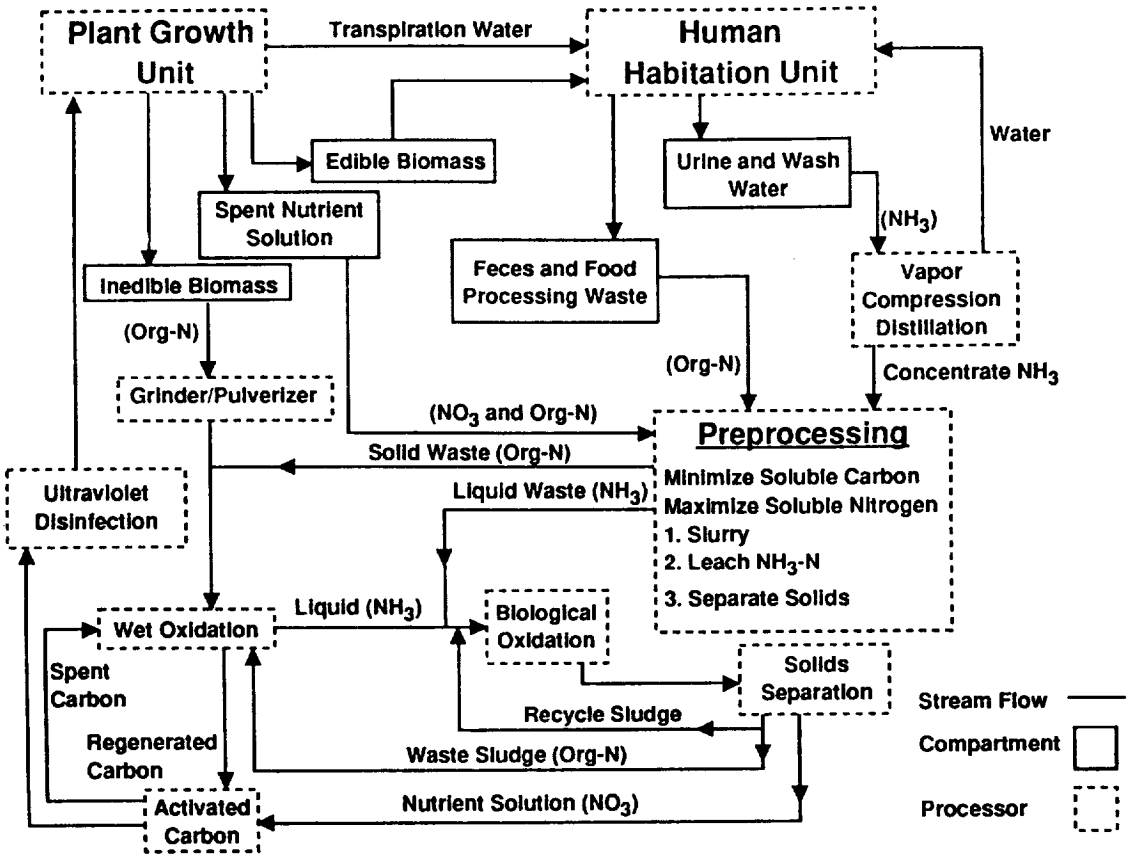

Fig. 2. Waste Processing in a CELSS: Nitrogen Recovery.

As mentioned previously, waste processing, applied to closing a life support system, can be achieved by three basic methods: physical/chemical processes, biological processes, or a hybrid of the two. Processing of wastes by physical/chemical methods is directly applicable to handling liquids as well as large quantities of solid materials but suffers a significant limitation: the inability to produce a form of nitrogen which is reuseable directly by higher plants. The physical/chemical waste processing methods characteristically produce nitrogen gases (N_2 and N_2O) while growing plants for a CELSS require either nitrate or ammonium ions (NH_4^+) as a source of nutrition. Aerobic biological waste processing systems can produce either or both ions as a final end product but do not handle solid wastes efficiently. With the above requirements and characteristics in mind, a scenario of an integrated waste processing system is discussed below. The hybrid system includes vapor compression distillation, wet oxidation, biological oxidation, activated carbon adsorption, and ultraviolet disinfection. A schematic diagram of the proposed system is presented in Figure 2. The treatment scheme is simplified to show the flow of nitrogen only.

The treatment scenario assumes processing of wastes generated by the plant growth and human habitation units. Wastes from the plant growth unit include the inedible biomass and the spent nutrient solution. The inedible biomass is principally solid waste (wheat chaff, etc.) low in organic nitrogen (Org-N) content /3/ but overall represents a potentially high mass of nitrogen due to the large amount of material generated. The inedible biomass will first be ground and pulverized to reduce the total volume and particle size. Final processing will be handled by wet oxidation operated at a

temperature less than 300°C and a pressure of 1500 psig to minimize loss of nitrogen as N_2 gas and maximize recovery of ammonia nitrogen (NH_3-N) /9/. The spent nutrient solution is primarily water, inorganic salts, and organic residues exuded by the plants. The spent nutrient solution will be sent to the preprocessing stage to act as a wetting agent to slurry and maximize leaching of Org-N and NH_3-N from the solid wastes generated at the human habitation unit. Nitrogen leaching can be accomplished through a combination of physical solids disintegration and an anaerobic fermentation-like process.

The solid wastes from the human habitation unit include feces and food preparation or processing waste. After preprocessing of the solid wastes, the slurry will be physically separated into liquid and solid streams. The solid portion containing Org-N will be further processed by wet oxidation to convert the Org-N to NH_3-N. Liquid wastes from the human habitation unit include urine and hygiene or wash water. These two waste streams will be combined for processing by vapor compression distillation (VCD). The final product of vapor compression distillation will be returned to the human habitation unit as drinking and hygiene water. Current state-of-the-art vapor compression distillation technology requires that pre- and post-treatment be implemented to optimize treatment efficiency and insure potable water quality /10/. Pretreatment by pH adjustment will maximize separation of NH_3-N and other salts while post-treatment by ultraviolet (UV) disinfection will significantly improve the bacteriological quality of the final product. Additional potable water will be supplied by water condensed from the evaporation/transpiration process occurring in the plant growth unit. The concentrate from vapor compression distillation will be sent to the preprocessing stage to be combined with the concentrated NH_3-N liquid leachate. The liquid leachate from the preprocessing stage as well as the liquid effluent from the wet oxidation step, both of which will contain highly concentrated NH_3-N, will be processed by biological (microbial) oxidation such as suspended growth (activated sludge) or fixed film (rotating biological contactor, trickling filter, etc.) systems. Carbon and nitrogen oxidation will occur, transforming the majority of the organic carbon to CO_2 and water and the NH_3-N and Org-N to nitrate nitrogen (NO_3-N). Following separation of the microbial solids, the liquid effluent from the biological oxidation unit will be returned to the plant growth unit to supply water, as well as nitrogen and other necessary nutrients. The microbial solids will be processed by wet oxidation to convert Org-N to NH_3-N. Due to the incomplete oxidation of carbon and separation of microbial cells during biological processing, the liquid effluent will require additional polishing by activated carbon adsorption and UV disinfection before being transferred to the plant growth unit. The activated carbon system will remove residual carbon which can stimulate the growth of bacteria while UV disinfection will destroy bacteria and viruses including potential plant pathogens. The wet oxidation system will also be used to regenerate the spent activated carbon.

CONCLUSION

The production rate and solid content of waste streams found in a life support system for a space habitat (in which plants are grown for food) have been discussed. Two recycling scenarios (Figures 1 and 2), derived from qualitative considerations as opposed to quantitative mass and energy balances, tradeoff studies, etc., have been presented; they reflect differing emphases on and responses to the waste stream formation rates and their composition, as well as indicate the required products from waste treatment that are needed in a life support system. The data presented here also demonstrate the magnitude of the challenge to developing a life support system with a high degree of closure.

Appendix I Preliminary Space Station Trace Contaminant Load Model (8 crewmembers) /11/

Contaminant	Alternate Names	Molecular Weight	Metabolic Rate (a) mg/man-day	SP ST (b) Gen. Rate (mg/day)	SMAC (h) (mg/m3)	Method of (c) Control
ALCOHOLS						
Methanol	Methyl alcohol	32.04	1.50	707	52.40	F,M
Ethanol	Ethyl alcohol	46.07	4.00	5216	94.00	F,M
2-Propenol	Allyl alcohol	58.08	.00	3.2	1.00	F,M
1-Propanol	N-propyl alcohol	60.09	.00	25.3	98.30	F,M
2-Propanol	Iso-propyl alcohol	60.09	.00	2022	98.30	F,M
1,2-Ethanediol	Glycol or Ethylene glycol	62.07	.00	9.5	127.00	F,M
1-Butanol	N-butyl alcohol	74.12	1.33	6922	121.00	F,M
2-Methyl-2-propanol	Tert-butyl alcohol	74.12	.00	15.8	121.00	F,M
2-Methyl-1-propanol	Iso-butyl alcohol	74.12	1.20	728.4	121.00	F
2-Butanol	Sec-butyl alcohol	74.12	.00	.7	121.00	F
1,2-Propanediol	Propylene glycol	76.10	.00	.5	0.10	F,M
1-Pentanol	N-amyl alcohol	88.15	.00	134	126.00	F
3-Methyl-1-butanol	Iso-amyl alcohol	88.15	.00	18	126.00	F
Phenol	Benzol or Carbolic acid	94.11	.00	7.9	7.70	F,M
Cyclohexanol	Hexahydrophenol	100.16	.00	1288	123.00	F,M
2-Ethyl-1-butanol		102.17	.00	.2	0.10	F
2-Hexanol	2-Hexyl alcohol	102.18	.00	1.2	167.00	F
2-Butoxy-ethanol	Glycol monobutyl ether	118.18	.00	.005	24.20	F,M
2-Ethyl-hexanol	2-Ethyl-1-hexanol	130.23	.00	4.5	186.40	F
Nonanol	Nonyl alcohol	144.26	.00	6.5	236.00	F
1-Decanol	Capryl alcohol	159.29	.00	9.5	259.00	F
ALDEHYDES						
Methanal	Formaldehyde	30.03	.00	.02	0.12	C,I
Ethanal	Acetaldehyde	44.05	.09	48.18	54.00	F
Propenal	Acrolein	56.06	.00	.06	0.11	F
Propanal	Propionaldehydde	58.08	.00	87	95.00	F
Methacrolein	2-Methyl-propenal	70.09	.00	.2	0.10	F
Butanal	Butyraldehyde	72.10	.00	1470	118.00	F
Pentanal	Valeraldehyde	86.13	.83	22.66	106.00	F
2,4-Hexadienal	Sorbaldehyde	96.13	.00	1.5	4.70	F
Hexanal	Caproic aldehyde	100.16	.00	43	4.70	F
Benzaldehyde	Benzene carbonal	106.12	.00	11	173.00	F
Heptanal	Enanthaldehyde	114.19	.00	4	0.10	F
Tolualdehyde		120.15	.00	.4	0.10	F
Octanal	Capril aldehyde	128.22	.00	3.2	210.00	F
KETONES						
Acetone	2-Propanone	58.08	.20	4212.4	712.50	F,M
Methyl vinyl ketone	3-Butene-2-one	70.00	.00	.3	0.10	F
Methyl ethyl ketone	2-Butanone or MEK	72.11	.00	3760	59.00	F
Cyclopentanone	Ketopentamethylene	84.11	.00	845	29.20	F
Methyl propenyl ketone	3-Penten-2-one	84.12	.00	.05	0.10	F
Acetyl cyclopropane	Methyl cyclo propyl ketone	84.13	.00	.08	0.10	F,M
Methyl propyl ketone	2-Pentanone	86.13	.00	4.7	70.40	F
Isopropyl methyl ketone	3-Methyl-2-butanone	86.13	.00	4.7	70.40	F
Cyclohexanone	Ketohexamethylene	98.14	.00	292	60.20	F
Mesityl oxide	4-Methyl-1-pentene-3-one	98.14	.00	47	40.10	F,M
Tetramethyl oxirane	2,3-Epoxy-1,4-dimethyl-butane	100.12	.00	1.6	0.10	F,M
Methyl isobutyl ketone	4-Methyl-2-pentanone	100.16	.00	1335	82.00	F
Pinacolone	3,3-Dimethyl-2-butanone	100.16	.00	6.3	81.90	F
5-Methyl-2-hexanone		114.18	.00	.6	23.50	F
2,4-Dimethyl 3-pentanone		114.18	.00	2.4	23.50	F
2-Heptanone		114.18	.00	.4	23.50	F,M
3-Heptanone		114.18	.00		35.50	F
Acetophenone	Acetyl benzene or 1-Phenyl ethanone	120.14	.00	1.6	245.00	F
5-Methyl-3-heptanone		128.21	.00	1.6	0.10	F
2-Octanone		128.21	.00	.3	105.00	F
Di-Isobutyl-ketone	2,6-Dimethyl-4-heptanone	142.20	.00	711	58.10	F
ALIPHATIC HYDROCARBONS						
Methane		16.04	160	1620(e)	1771.00	C
Acetylene	Ethyne	26.04	.00	26	532.00	C

Appendix I (continued)

Contaminant	Alternate Names	Molecular Weight	Metabolic Rate (a) mg/man-day	SP ST (b) Gen. Rate (mg/day)	SMAC (h) (mg/m3)	Method of (c) Control
Ethylene	Ethene	28.05	.00	.4	344.10	C
Ethane		30.07	.00	166	1230.00	C,F
Methyl acetylene	Propyne	40.07	.00	8.7	409.50	F
Propadiene	Allene or Dimethylene methane	40.07	.00	180	81.90	C,F
Propylene	Propene	42.08	.00	.5	860.30	F
Propane		44.09	.00	.5	901.40	F
1,3-Butadiene		54.09	.00	4.7	221.20	F
1-Butene		56.10	.00	40	458.00	F
Butane	N-Butane	58.12	.00	1.6	237.60	F
Iso-Butane	2-Methyl-propane	58.12	.00	95	237.60	F
Cyclopentene		68.11	.00	130	167.00	F
Isoprene	2-Methyl-1,3-butadiene	68.11	.00	148	557.00	F
1-Pentene	1-Pentylene or Propylethene	70.13	.00	35	186.00	F
Pentane		72.15	.00	134	590.00	F
Iso-Pentane	2-Methyl-butane	72.15	.00	3.2	295.00	F
Cyclohexene	1,2,3,4-Tetrahydro-benzene	82.14	.00	35	86.00	F
Methyl cyclopentane		84.16	.00	51	51.60	F
Cyclohexane		84.16	.00	624	206.00	F
2-Hexene		84.16	.00	.8	172.00	F
2,2-Dimethyl butane		86.17	.00	3.2	88.10	F
3-Methyl pentane		86.18	.00	2.8	1762.00	F
Hexane		86.18	.00	81	176.00	F
Methyl cyclohexene	4-Methyl cyclohexene	96.17	.00	253	393.20	F
Methyl cyclohexane		98.18	.00	69	60.20	F
1-Heptene		98.18	.00	113	201.00	F
2,2-Dimethyl pentane		100.21	.00	86	408.60	F
2,4-Dimethyl-pentane		100.21	.00	.4	201.00	F
3-Ethyl pentane	Triethyl methane	100.21	.00	.1	201.00	F
Heptane		100.21	.00	79	201.00	F
1,1-Dimethyl-cyclohexane		112.22	.00	24	115.00	F
Trans-1,2-dimethyl-cyclohexane		112.22	.00	95	115.00	F
6-Methyl-1-heptene		112.22	.00	.02	229.00	F
2-Octene		112.22	.00	22	229.00	F
2,2,3-Trimethyl-pentane		114.23	.00	1	229.00	F
3,3-Dimethyl-hexane		114.23	.00	1.3	229.00	F
3-Ethyl-hexane		114.22	.00	.4	229.00	F
Octane		114.23	.00	66	350.00	F
4-Ethyl-heptane	Ethyl-dipropyl-methane	128.26	.00	.06	129.00	F
Nonane		128.26	.00	1.7	315.00	F
Limonene	Citrene	136.23	.00	6	557.00	F
2-Methyl-3-ethyl-heptane		142.28	.00	2	116.00	F
Decane		142.28	.00	.08	223.00	F
Undecane	Hendecane	156.31	.00	14	319.00	F
Dodecane		170.34	.00	5.5	278.00	F
AROMATIC HYDROCARBONS						
Benzene	Phene or Benzol	78.11	.00	27	0.32	F
Toluene	Methyl-benzene	98.13	.00	1351	75.30	F
Styrene	Ethenyl-benzene	104.14	.00	9.5	42.60	F
o-Xylene	1,2-Dimethyl-benzene	106.16	.00	106	86.80	F
m-Xylene	1,3-Dimethyl-benzene	106.16	.00	3539	86.80	F
p-Xylene	1,4-Dimethyl-benzene	106.16	.00	780	86.80	F
Ethyl-benzene		106.16	.00	182	86.80	F
Indene	Indonaphthene	116.16	.00	118	9.50	F
Methyl-styrene	Methyl-ethenyl-benzene	118.18	.00	1.2	145.00	F
1,3,5-Trimethyl-benzene	Mesitylene	120.20	.00	2	15.00	F
1,2,4-Trimethyl-benzene	Pseudocumene	120.20	.00	16	15.00	F
Propyl-benzene		120.20	.00	269	49.10	F
Cumene	Iso-Propyl-benzene	120.20	.00	11	73.70	F
1-Ethyl-2-methyl-benzene		120.20	.00	5	25.00	F
Naphthalene		128.18	-	-	0.10	F
N-Butyl-benzene		134.12	.00	2.4	55.00	F
1-Methyl-3-propyl benzene		134.12	.00	2.7	11.00	F
p-Cymene	1-Isopropyl-4-methyl-benzene	134.22	.00	.5	0.10	F
HALOCARBONS						
Methyl chloride	Chloro-methane	50.49	.00	.3	41.30	C,F
Vinyl chloride	Chloro-ethene	62.50	.00	1.6	0.26	F
Ethyl chloride	Chloro-ethane	64.52	.00	545	263.70	F
3-Chloro-propylene	Allyl chloride	76.53	.00	34	0.63	F

Appendix I (continued)

Contaminant	Alternate Names	Molecular Weight	Metabolic Rate (a) mg/man-day	SP ST (b) Gen. Rate (mg/day)	SMAC (h) (mg/m3)	Method of (c) Control
Dichloro-methane	Methylene chloride	84.93	.00	1746	86.80	C,F
Freon 22	Chloro-difluoro-methane	86.47	.00	467	353.60	C,F
1-Chloro-butane		92.57	.00	3	151.00	F
1,1-Dichloro-ethene	Vinylidine chloride	96.95	.00	.02	7.90	F
1,2-Dichloro-ethane	Ethylene dichloride	98.97	.00	20	40.50	F
Freon 21	Dichloro-fluoro-methane	102.90	.00	5.5	21.00	F
Propylene dichloride	1,2-Dichloro-propene	106.97	.00	47	42.20	F
1,2-Dichloro-propane		112.99	.00	4	42.20	F
Chloro-benzene	Phenyl chloride	112.56	.00	1240	46.00	F
1-Chloro-1,2,2-trifluoro-ethane		118.50	.00	2.4	484.50	F
Chloroform	Trichloro-methane	119.38	.00	9.5	4.90	F
Freon 12	Dichloro-difluoro-methane	120.91	.00	14	494.40	F
Iso-Butyl chloride	1,2-Dichloro-2-methyl-propane	127.01	.00	.8	0.10	F
1,3-Dichloro-2-propanol		128.99	.00	.01	0.10	F
Trichloro-ethylene	Trichloro-ethene	131.39	.00	40	0.54	F
1,2-Dichloro-1,2-difluoro-ethene		132.93	.00	.8	136.00	F
Methyl chloroform	1,1,1-Trichloro-ethane	133.41	.00	229	164.00	F
1,1,2-Trichloro-ethane		133.41	.00	2.4	5.50	F
Freon 124	Chloro-tetrafluoro-ethane	136.48	.00	750	555.00	F
Freon 11	Trichloro-fluoro-methane	137.40	.00	174	561.80	F
1,2-Dichloro-benzene		147.01	.00	11	30.00	F
3-Chloromethyl-heptane		148.68	.00	.3	0.10	F
Halon 1301	Bromo-trifluoro-methane	148.90	.00	474	608.80	F
Carbon tetrachloride	Tetrachloro-methane	153.82	.00	1.6	13.00	F
Tetrachloro-ethylene	Tetrachloro-ethene	165.83	.00	553	34.00	F
Freon 114	1,1-Dichloro-1,2,2,2-tetrafluoro-ethane	170.92	.00	.01	702.90	F
Freon 113	1,1,2-Trichloro-1,2,2-trifluoro-ethane	187.40	.00	9180	383.00	F
Freon TF	1,1,2-Trichloro-1,2,2-trifluoro-ethane	187.40	.00	13801	383.00	F
Freon 112	1,1,2,2-Tetrachloro-1,2-difluoro-ethane	204.00	.00	103	834.20	F
ESTERS						
Methyl formate	Formic acid methyl ester	60.05	.00	.06	12.30	F
Ethyl formate	Formic acid ethyl ester	74.08	.00	.8	90.90	F
Methyl acetate	Acetic acid methyl ester	74.08	.00	11	121.00	F
Ethyl acetate	Acetic acid ethyl ester	88.11	.00	371	180.00	F
2-Ethoxy-ethanol	Glycol monoethyl ester	90.12	.00	1035	73.70	F,M
Allyl acetate	Acetic acid allyl ester	100.12	.00	5	51.20	F
Methyl methacrylate	2-Methyl-propenoic acid methyl ester	100.12	.00	24	102.00	F
N-Butyl formate	Formic acid butyl ester	102.13	.00	.05	83.50	F
Propyl acetate	Acetic acid propyl ester	102.13	.00	585	167.00	F
Iso-Propyl acetate	Acetic acid isopropyl ester	102.13	.00	3.2	209.00	F,M
Ethyl methacrylate	2-Methyl-propenoic acid ethyl ester	114.15	.00	36	116.70	F
Butyl acetate	Acetic acid butyl ester	116.16	.00	948	190.00	F
Iso-Butyl acetate	Acetic acid iso-butyl ester	116.16	.00	245	190.00	F
Ethyl lactate	2-Hydroxy-propanoic acid ethyl ester	118.13	.00	205	193.00	F,M
2-Methoxy ethyl acetate	Acetic acid 2-methoxy-ethyl ester	118.36	.00	5	24.20	F
N-Amyl acetate	Acetic acid pentyl ester	130.18	.00	79	160.00	F
Iso-Amyl acetate	Acetic acid-3-pentyl ester	130.18	.00	3.2	159.50	F
Cellosolve acetate	2-Ethoxyethyl acetate	132.16	.00	545	162.00	F
1,2-Ethane diacetate		146.14	.00	.7	0.10	F
Dibutyl oxalate	Oxalic acid dibutyl ester	202.25	.00	.04	0.10	F
ETHERS						
Furan	1,4-Epoxy-1,2-butadiene	68.07	.00	1.6	0.11	F
Tetrahydro furan	1,4-Epoxy butane	72.11	.00	95	118.00	F
Allyl methyl ether	3-Methoxy-1-propene	72.11	.00	.06	0.10	F
Diethyl ether	Ethoxy-ethane or Ether	74.12	.00	52	242.00	F
2-Methyl furan		82.10	.00	1	0.13	F
2,3-Dihydro-pyran		84.13	.00	.4	0.10	F
p-Dioxane	1,4-Dioxane or Glycol ethylene ether	88.11	.00	63	1.80	F,M
1,3,5-Trioxane		90.08	.00	.02	0.10	F,M
1-Propoxy butane	Butyl propyl ether	116.21	.00	55	186.80	F
SILANES & SILOXANES						
Siloxane dimer	Disiloxane	78.10	.00	32	52.40	F
Trimethyl silanol	Trimethyl silicol	90.21	.00	12	1.80	F
Diphenyl silane		184.32	.00	.02	0.10	F
Siloxane trimer	Trisiloxane	124.30	.00	24	83.40	F

Appendix I (continued)

Contaminant	Alternate Names	Molecular Weight	Metabolic Rate (a) mg/man-day	SP ST (b) Gen. Rate (mg/day)	SMAC (h) (mg/m3)	Method of (c) Control
Hexamethyl-disiloxane		162.48	.00	.08	96.60	F
Siloxane tetramer	Tetrasiloxane	170.40	.00	237	114.00	F
Hexamethyl-cyclo-trisiloxane		222.40	.00	47	227.00	F
Octamethyl-trisiloxane		236.54	.00	379	114.00	F
Octamethyl-cyclo-tetrasiloxane		296.62	.00	71	151.70	F
Decamethyl-tetrasiloxane		310.58	.00	-	150.70	F
Decamethyl-cyclo-pentasiloxane		370.64	.00	316	150.70	F
Decamethyl-cyclo-hexasiloxane		444.71	.00	403	150.70	F
Tetradecamethylcycloheptasiloxane		519.09	.00	555	150.70	F
Hexadecamethylcyclooctasiloxane		593.24	.00	126		F
ORGANIC NITROGENS						
Acetonitrile	Ethane-nitrile or Methyl cyanide	41.05	.00	83	6.70	F,M
Mono-methyl hydrazine	Methylhydrazine	46.07	.00	2.4	0.08	F
Nitromethane		61.04	.00	8	0.10	F
N,N-Dimethyl-formamide	Formic acid-N,N-dimethyl amide	73.10	.00	.6	6.00	F,M
Nitroethane		75.07	.00	.02	0.10	F
N-Ethyl-morpholine	4-Ethyl-morpholine	115.18	.00	213	16.00	F
Indole		117.15	25	100 (d)	0.48	F
SULFIDES						
Carbonyl sulfide	Carbon oxisulfide	60.07	.00	5.4	12.00	F,C
Ethylene sulfide	Thiirane	60.07	.00	.06	0.10	F
Dimethyl sulfide	Methyl sulfide	62.14	.00	.3	2.50	F
Carbon disulfide		76.14	.00	44	16.00	F
Pentamethylene sulfide	Tetrahydro pyran	102.20	.00	.08	0.10	F
MISCELLANEOUS ORGANICS						
Acetic acid	Ethanic acid	60.05	.00	.02	7.40	F,M,L
Epichlorohydrin	1-Chloro-2,3-epoxy-propane-dl	92.53	.00	5	1.20	F
2-Ethyl-hexanoic acid		144.21	.00	.6	0.10	F
INORGANICS						
Hydrogen		2.02	26	208 (f)	247.30	C
Ammonia		17.03	475	3806	17.40	PA
Carbon monoxide		28.01	23	1843 (g)	28.60	CO,C
Nitric oxide		30.01	.00	0.044	6.10	PU
Hydrazine		32.05	.00	1.68	0.05	F,M
Hydrogen sulfide		34.08	.09	.7	2.80	C
Nitrogen dioxide		46.01	.00	0.02	0.94	F,L
Nitrogen tetroxide		92.01	.00	48	1.90	F,M
Mercury		200.59	.00	1.2	0.006	F

Footnotes

(a) Metabolic generation rate per man.

(b) SP ST= Space Station. Predicted Space Station generation rate: 4 modules and 8 crewmembers.

(c) Contaminant removal methods:

- F - Fixed activated charcoal bed
- M - Sorption by moisture (condensing heat exchanger)
- PA - Sorption by phosphoric acid (impregnated on charcoal)
- L - Sorption by $LiOH/Li_2CO_3$ (pre- and post-sorber)
- CO - Low temperature catalytic oxidizer
- C - High temperature catalytic oxidizer
- CI - CI type charcoal
- PU - Purafil

(d) Only 50% of metabolic rate was used to obtain total Space Station rate.

(e) For total methane generation rate add 43,334 mg/day from Bosch reactor bleed.

Footnotes (continued)

(f) For total hydrogen generation rate add 7,334 mg/day from Bosch reactor bleed.
(g) For total carbon monoxide generation rate add 109,344 mg/day from Bosch reactor bleed.
(h) SMAC=Space Maximum Allowable Concentration.

REFERENCES

1. S. K. Ride, Leadership and America's Future in Space, A Report to the NASA Administrator, (August 1987)

2. D. B. Parker and S. K. Gallagher, Distribution of Human Waste Samples in Relation to Sizing Waste Processing in Space, Conference on Lunar Bases and Space Activities in the 21st Century, Paper No. LBS-88-107, Houston, Texas, (April 5-7, 1988)

3. T. Wydeven, Composition and Analysis of a Model Waste for a CELSS, NASA Technical Memorandum 84368, (September 1983)

4. D. Putnam, Composition and Concentrative Properties of Human Urine, NASA Contract NAS1-8954, Langley Research Center Contract with McDonnell Douglas Astronautics Co., (June 1970)

5. F. H. Schubert, R. A. Wynveen, and P. D. Quattrone, Advanced Regenerative Environmental Control and Life Support Systems: Air and Water Regeneration, Adv. Space Res., Vol. 4, No. 12, pp. 279-288 (1984)

6. D. Putnam, private communication, Umpqua Research Co., Myrtle Creek, Oregon, (1988) The amounts given are the same as those used for the Space Station Phase B Study Specifications.

7. Utah Science, Vol. 46, No. 4, pp. 145-151 (1985)

8. PMMS Water Management for the Space Station United States Laboratory, Report Number MDC E3224, McDonnell Douglas Astronautics Company, Saint Louis, MO, (1987)

9. C.C. Johnson and T. Wydeven, Wet Oxidation of a Spacecraft Model Waste, SAE Technical Paper Series, Fifteenth Intersociety Conference on Environmental Systems, San Francisco, CA, (July 1985)

10. T. Slavin, F. Liening, M. Oleson, and R.L. Olson, Controlled Ecological Life Support Systems (CELSS): Physiochemical Waste Management Systems Evaluation, NASA Contractor Report 177422, Boeing Aerospace Company, Seattle, WA, (June 1986)

11. Space Station Trace Contaminant Control, NASA Contract NAS8-36406, Marshall Space Flight Center Contract with Lockheed Missles and Space Co., Sunnyvale, CA, (1988)

A 90-15436

Subcritical and Supercritical Water Oxidation of CELSS Model Wastes

Y. Takahashi,* T. Wydeven,** and C. Koo,***

*Department of Civil Engineering, Niigata University,
8050 Ikarashi-2-nocho, Niigata City, 950-21, Japan
**Ecosystems Science and Technology Branch,
NASA/Ames Research Center, Moffett Field, CA 94035, USA
***TGS Technology, Inc., Ames Research Center,
Moffett Field, CA 94035, USA

ABSTRACT

Controlled-Ecological-Life-Support-System (CELSS) model wastes were wet-oxidized at temperatures from 250 to 500°C, i.e., below and above the critical point of water (374°C and 218 kg/cm^2 or 21.4 MPa). A solution of ammonium hydroxide and acetic acid and a slurry of human urine, feces, and wipes were used as model wastes.

Almost all of the organic matter in the model wastes was oxidized in the temperature range from 400 to 500°C, i.e., above the critical conditions for water. In contrast, only a small portion of the organic matter was oxidized at subcritical conditions. Although the extent of nitrogen oxidation to nitrous oxide (N_2O) and/or nitrogen gas (N_2) increased with reaction temperature, most of the nitrogen was retained in solution as ammonia near 400°C. This important finding suggests that most of the nitrogen in the waste feed can be retained in solution as ammonia during oxidation at low supercritical temperatures and be subsequently used as a nitrogen source for plants in a CELSS while at the same time organic matter is almost completely oxidized to carbon dioxide and water.

It was also found in this study the Hastelloy C-276 alloy reactor corroded during waste oxidation. The rate of corrosion was lower above than below the critical temperature for water.

INTRODUCTION

Subcritical water oxidation (wet-oxidation, WO) and supercritical water oxidation (SCWO) are presently the most hopeful candidate techniques for the waste management subsystem in a controlled-ecological-life-support-system (CELSS). Though many efforts have been concentrated on these research fields /1 to 7/, the waste treatment techniques of WO and SCWO still have many problems to be solved. Among the concerns for a waste treatment system in a CELSS are the fates of organic carbon and nitrogen in a raw waste material. The fates of carbon and nitrogen are important because WO or SCWO is intended to work as a complete oxidizer of organic matter and because the nitrogen product is planned to be used as fertilizer for higher plants in a CELSS.

Subcritical water oxidation is a process where an aqueous slurry and/or dissolved organic matter is oxidized in a pressure vessel. In CELSS related studies using WO, the temperature range studied was from 110 to 310°C and the pressure range was from 60 to 115 kg/cm^2 (5.88 to 11.3 MPa) /1,3/. Oxidation with and without catalysts has been studied.

Historically, WO without a catalyst, which was developed in the 1950's in the U.S.A. as the "Zimpro Process" for the treatment of industrial wastewater and sewage sludge, is the oldest technique /8/. The WO temperatures used for CELSS studies are given above and the oxidation efficiency ranged from 70 to 80% /3/. This means that organic matter in raw materials cannot be oxidized completely under these conditions, and it

was found that refractory or non-combustible organic acids like acetic acid are produced. On the other hand, most of the nitrogen in the raw material remained in solution in the form of ammonia. This fact is favorable for a CELSS because the nitrogen can be used as a liquid fertilizer for plants which are grown hydroponically in a CELSS.

In the case of WO with a catalyst /2, 4/, noble metal(s) such as gold (Au), ruthenium (Ru), rhodium (Rh), palladium (Pd), and platinum (Pt), which are supported on aluminum oxide (Al_2O_3) or titanium dioxide (TiO_2) pellets, or a ceramic honeycomb, are used as catalysts. Though copper (Cu) is a well known oxidation catalyst for organic carbon, it cannot be used for a CELSS because copper is dissolved in solution and forms a complex with ammonia. When noble metal(s) are used, the oxidation efficiency of organic matter is near 100%, and almost all nitrogen in a raw material is oxidized to nitrogen gas (N_2). This denitrification occurs with much smaller amounts of catalyst than is necessary for a high oxidation efficiency of organic matter. While the high oxidation efficiency of carbon is desirable for a CELSS, denitrification is undesirable because most plants cannot fix N_2.

In addition to the issue of denitrification, another disadvantage of catalytic wet-oxidation is that slurries which contain suspended organic matter generally cannot be used as a raw material because of catalyst poisoning. A third disadvantage of catalytic WO is that there is the possibility of deterioration or dissolution of the noble metal catalyst and subsequent poisoning of living things, such as higher plants and algae, in a CELSS recycle loop.

In the case of supercritical water oxidation (SCWO), which has been studied by Modell, Hong and others /6, 7/, oxidation is carried out over the temperature range of 500 to 700°C, and the pressure range from 220 to 250 kg/cm^2 (21.6 to 24.5 MPa). These conditions may be too stringent for human safety in a space habitat. Though the oxidation efficiency of organic matter is near 100% under these conditions, almost all nitrogen in a raw material is gasified, which is not good from a plant-growth point of view in a CELSS. At 650°C, 40% of the nitrogen in a raw material of mixed urine and feces was oxidized to nitrous oxide (N_2O) and the rest to N_2 /7/.

The most important thing to note from the above discussion is that comparative studies have not been carried out under experimental conditions in the transition region between WO and SCWO. In other words, the subcritical and supercritical conditions ranging from 300 to 500°C have not yet been thoroughly investigated. Therefore, using an ideal waste (a solution of acetic acid and ammonium hydroxide) and a typical spacecraft waste stream (a slurry of human feces, urine, and wipes) as model wastes, the authors performed experiments covering the WO and SCWO transition temperature range. It was anticipated prior to performing the experiments that a high oxidation efficiency of organic matter would be attained, but the nitrogen products in the reactor output were not predictable. This paper will describe the details and results of these experiments.

EXPERIMENTAL METHOD

Reactor: Each experiment was carried out as a batch test using a stirred cylindrical reactor made of Hastelloy C-276. The chemical composition of the reactor material is shown in Table 1.

The reactor inside dimensions were 89 mm in diameter and 318 mm in depth. After raw material and a stoichiometrically excess amount of oxygen were introduced to the reactor, it was heated to a designated temperature. A mixture of oxygen and neon was used as the oxygen source /1/. Residence time for oxidation as used here refers to the time at the designated temperature and does not include the time needed for heating and cooling. When the reaction period was over, the reactor was cooled by a fan to room temperature. After cooling, the headspace gas in the reactor was analyzed by gas chromatography and the liquid content was analyzed for chemical oxygen demand (COD) and ammonia. Periodically the liquid was analyzed for corrosion products and Kjeldahl nitrogen.

Experiment 1: Two series of experiments were carried out. In "Experiment 1", a mixture of acetic acid and ammonium hydroxide was used as raw material. The effects of the reaction temperature and/or residence time on carbon and nitrogen oxidation and on metal corrosion from the reactor material were studied. The pH of the raw

Table 1 Chemical Composition of Hastelloy C-276.

Element	Percent
Molybdenum	15.00-17.00
Chromium	14.50-16.50
Iron	4.00-7.00
Tungsten	3.00-4.50
Cobalt	2.50[2]
Manganese	1.00[2]
Vanadium	0.35[2]
Silicon	0.08[2]
Phosphorus	0.04[2]
Sulfur	0.03[2]
Carbon	0.02[2]
Nickel	Balance

(1) Cabot Corporation, Hastelloy alloy C-276, High Technology Materials Division, 1980
(2) Maximum

material was adjusted to 7.02 by adding ammonium hydroxide to a calculated amount of acetic acid in distilled water. Chemical oxygen demand (COD), total organic carbon (TOC) and ammonia in the feed as determined by analysis were 44.5 O_2 g/l, 16.5 C g/l, and 8.72 N g/l, respectively. COD as used here means grams of oxygen required to oxidize waste dry weight.

In studying the effects of temperature, five subcritical temperatures above 250°C and seven supercritical ones below 500°C were selected. The residence time at each temperature was fixed at 60 minutes. At subcritical temperatures, a constant amount of the raw material and oxygen was added to the reactor (200 ml and 200 psi, 14.1 kg/cm^2 or 1.38 MPa). 3.7 times the stoichiometrically required amount of oxygen was added to the reactor at the start of an experiment. The pressure at each selected temperature ranged from 679 to 2560 psi (47.7 to 180 kg/cm^2 or 4.68 to 17.7 MPa). At supercritical temperatures, the highest pressure was limited to 3500 psi (246 kg/cm^2 or 24.1 MPa) because of the safety limits of the reactor. The average pressure ranged from 3370 to 3490 psi (237 to 245 kg/cm^2 or 23.2 to 24.0 MPa). 1.1 to 1.7 times the stoichiometric amount of oxygen required for complete oxidation was introduced to the reactor for the supercritical temperature experiments.

In studying the effects of time on conversion efficiency, the temperature was set at 400 and 500°C. At each temperature, five different residence times were selected (0, 15, 30, 45 and 60 minutes) and a corresponding five batch tests were carried out. (0 residence time means the reactor was heated to the desired temperature and immediately cooled.) 1.2 and 1.7 times the stoichiometric amount of oxygen required was introduced to the reactor for the reactions at 400 and 500°C, respectively.

In order to know the extent of metal corrosion products derived from the reactor, the concentration in solution of the major components of Hastelloy C-276 (nickel, molybdenum, and chromium) and other elements, Table 1, were measured by atomic absorption spectroscopy. In addition, the elemental composition of the suspended matter (which apparently arose from charring of the acetic acid) in a sample (400°C, 60 minutes) was also analyzed by X-ray photoelectron spectroscopy (ESCA).

Experiment 2: In "Experiment 2" a slurry made from freeze dried human feces and urine, wipes, and distilled water was used as a raw material. The effects of reaction temperature on carbon and nitrogen conversion and on metal corrosion from the reactor material were studied.

Freeze-dried human feces and urine which had been prepared and analyzed by John L. Carden, Jr., of the Georgia Institute of Technology /9/, and wipes, which were representative of those used in the space shuttle missions, were used as components of the raw material. The amount of each is shown in Table 2.

Table 2 Toilet Waste Feed Solution.

	Wastes (dry weight) g/person/day	Nitrogen, %	COD	Amount in 1 liter of solution		
				Waste constituent, g	Nitrogen, g	COD
Urine	64[1]	22.0	0.267	28.6	6.29	7.6
Feces	44[1]	10.2	1.09	19.6	2.00	21.4
Wipes	41[2]	0.15	1.09	18.3	0.03	19.9
Total	149	-	-	66.5	8.32	48.9

(1) Freeze-dried and stored in a dessicator prior to weighing.
(2) Stored in dessicator prior to weighing.

The total solid (TS), total nitrogen, COD, and pH of the raw material were 66.5 g/l, 8.32 N g/l, 48.9 O_2 g/l, and 6.25, respectively.

Three subcritical temperatures above 250°C and five supercritical ones below 450°C were selected as desired oxidation temperatures. The residence time for these experiments was fixed at 60 minutes with the exception of the 400°C run, where an additional 120 minute batch test was added. At subcritical temperatures, the same volume of raw material and oxygen as "Experiment 1" was added to the reactor (200 ml and 200 psi, 14.1 kg/cm^2 or 1.38 MPa, respectively). The amount of oxygen was 3.0 times the stoichiometric amount required for complete oxidation. The pressure at each designated temperature ranged from 739 to 2575 psi (52.0 to 181 kg/cm^2 or 5.10 to 17.8 MPa). At supercritical temperatures the average reaction pressure ranged from 3360 to 3510 psi (236 to 247 kg/cm^2 or 23.1 to 24.2 MPa). For these experiments 1.1 to 1.8 times the stoichiometric amount of oxygen required was added to the reactor.

The head space gas of the reactor was analyzed by gas chromatography after each batch test. The gas chromatograph was equipped with a thermal conductivity detector (TCD) and helium was used as the carrier gas. A column with an inner diameter of 0.085 inch and a length of 20 feet packed with HayeSep D (100-120 mesh) was used at room temperature. Nitrogen gas (N_2), nitrous oxide (N_2O), methane (CH_4), carbon dioxide (CO_2), neon (Ne), and oxygen (O_2) were separated and measured by this column. In these experiments efforts were concentrated on closing the carbon and nitrogen balance.

As in "Experiment 1", corrosion products were measured using atomic absorption spectroscopy and the elemental composition of the suspended matter remaining after oxidation was analyzed using ESCA.

Analytical Methods: The methods for analysis of COD, Kjeldahl nitrogen, and ammonia were based on Environmental Protection Agency (EPA) Method 410.1, Standard Methods for the Treatment of Water and Wastewater (SMWW) 417D, and Japanese Industrial Standard (JIS) K 0102, respectively. In the measurement of nitrate, a modified Brucine-nitrate assay based on EPA Method 352.1 was used. The atomic absorption analyses were done by Carter Analytical Laboratory, Inc., Campbell, California. ESCA was done by Surface Science Laboratories, Mountain View, California.

RESULTS AND DISCUSSION

Experiment 1

C and N Conversion: Figure 1 shows the oxidation efficiency for carbon and nitrogen, which are defined as follows:

$$\text{Oxidation efficiency of carbon (\%)} = [(COD_{initial} - COD_{final})/COD_{initial}] \times 100$$
$$\text{Oxidation efficiency of nitrogen (\%)} = [(NH_{3,initial} - NH_{3,final})/NH_{3,initial}] \times 100$$

where NH_3 refers to ammonia concentration in solution (N g/l).

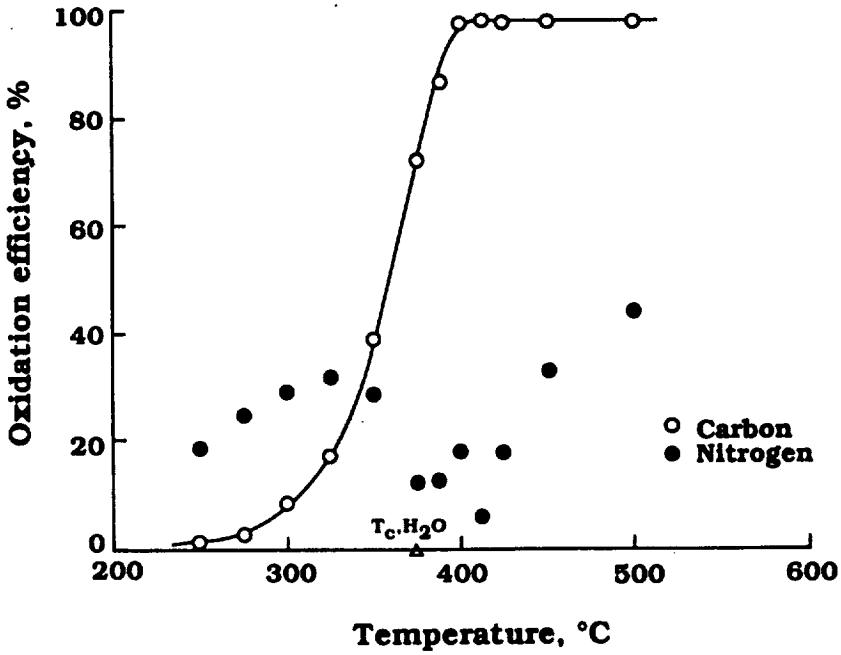

Fig. 1. Effect of temperature on the oxidation efficiency of ammonium hydroxide and acetic acid.

In the case of carbon, the oxidation efficiency at 250°C was very low (less than 2%). But with an increase in temperature, the oxidation efficiency increased and reached near 100% at 400°C. After that, the oxidation efficiency remained essentially constant.

In the case of nitrogen, the oxidation efficiency at 250°C was about 20%. With an increase in temperature, the oxidation efficiency increased to about 30% at 325°C and then apparently decreased to less than 10% at 410°C. In the range 325 to 410°C, which includes the transition temperature from subcritical to supercritical water at 374°C.

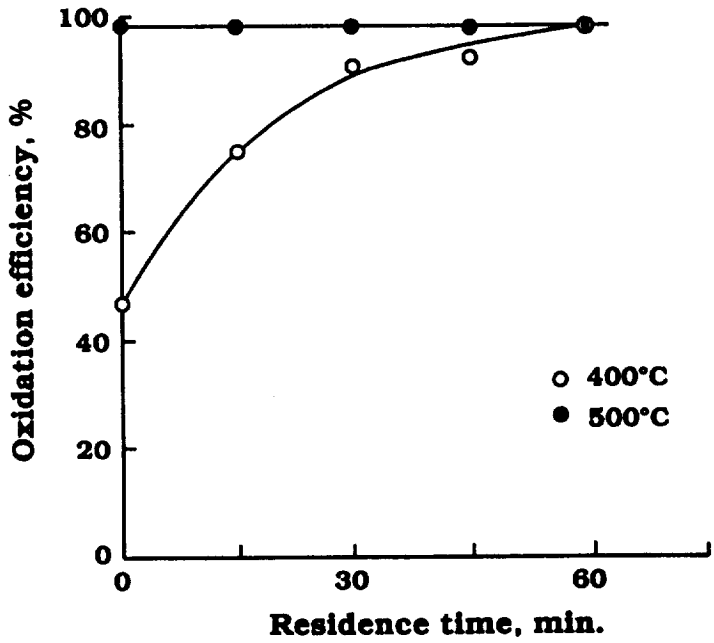

Fig. 2. Effect of residence time on the oxidation efficiency of acetic acid (based on COD); ammonium hydroxide and acetic acid model waste feed.

there was considerable scatter in the analytical data for ammonia. We have no explanation to account for the apparent decrease in ammonia oxidation to lower values around the critical temperature. Beyond 410°C, the oxidation efficiency continuously increased with an increase in temperature.

At 410°C, the oxidation efficiency of carbon was greater than 95% and the oxidation efficiency of nitrogen was only 30% or less. This means that most of the nitrogen in the raw material was retained in solution as ammonia. It is possible for this nitrogen to be used as a liquid fertilizer for plants grown hydroponically in a CELSS. Consequently, the observed oxidation efficiency for carbon and nitrogen in the vicinity of 410°C has important implications for a CELSS.

Figure 2 shows the effect of residence time on the oxidation efficiency of carbon.

At 500°C and 0 minutes residence time (defined earlier), the oxidation efficiency reached almost 100%. After that, it remained constant with increasing residence time. At 400°C, the oxidation efficiency increased with residence time and eventually reached the same efficiency as 500°C. At 400°C, in order to attain the same oxidation efficiency as 500°C, the residence time had to be increased to at least 60 minutes.

Figure 3 shows the effect of residence time on the oxidation efficiency of nitrogen.

At 500°C, the oxidation efficiency appeared to increase slightly with time. But, at 400°C, the oxidation efficiency was almost constant or increased only slightly with duration of oxidation. These findings mean that the nitrogen oxidation had almost finished at 0 minutes residence time or during the heating up period for the experiment. It appears that after 0 minutes residence time, carbon oxidation and nitrogen oxidation proceed separately.

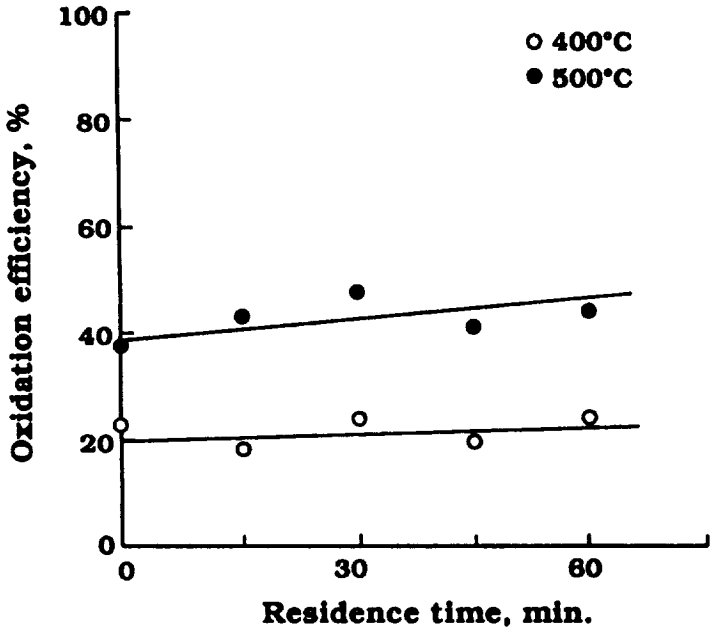

Fig. 3. Effect of residence time on the oxidation efficiency of ammonia; ammonium hydroxide and acetic acid model waste feed.

Metal Corrosion: Figure 4 shows the effects of temperature on metal corrosion from the reactor material.

Nickel (Ni), molybdenum (Mo) and chromium (Cr) shown in Figure 4 are the main components of Hastelloy C-276 (see Table 1). The concentration of each metal in solution after 60 minutes oxidation ranged from 10 to 80 mg/l.

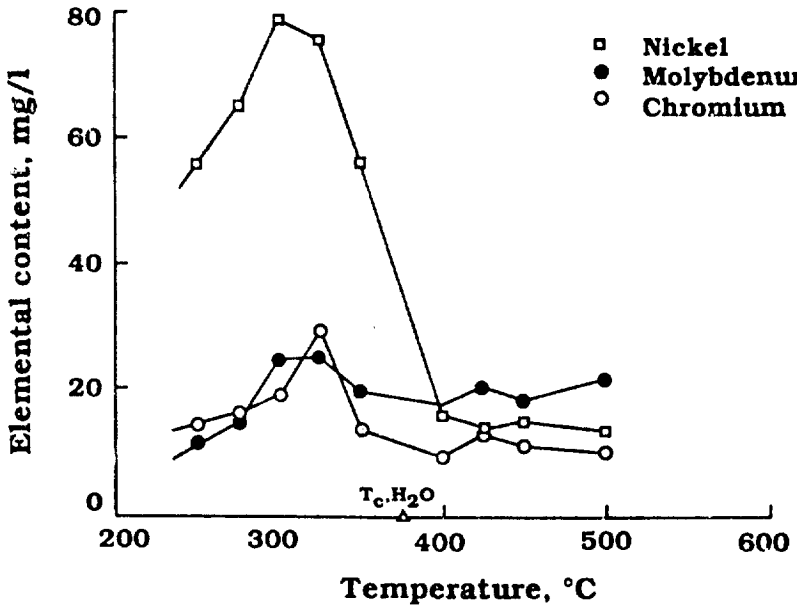

Fig. 4. Effect of temperature on the corrosion of the Hastelloy C-276 reactor; ammonium hydroxide and acetic acid model waste feed.

The change in the corrosion rate of nickel with oxidation temperature was most dramatic. Below the critical point of water, the corrosion rate of nickel first increased with reaction temperature and reached a maximum near 300°C. Beyond 300°C, it decreased significantly, particularly near the critical point of water. Above the critical point, the corrosion rate of nickel remained almost constant. Molybdenum and chromium behaved similar to nickel, but their fluctuations were not as large as nickel.

When distilled water was used as a raw material and oxidation was carried out at 450°C for 60 minutes, the concentrations of nickel, molybdenum and chromium were 2.60, 4.80 and 6.75 mg/l, respectively (Table 3). In contrast, when a mixture of acetic acid and ammonium hydroxide was used as the raw material, the corresponding concentrations were 15.0, 18.1, and 11.5 mg/l, respectively. These results show that the corrosion rate of the reactor was 1.7 to 5.8 times higher in the presence of acetic acid and ammonium hydroxide than in distilled water and the rate varied with the metal alloy component.

Results from the analysis by ESCA of the particles filtered from the product liquid showed that after water oxidation at 400°C, 4.1 atom percent nickel was present in the suspended solid (Table 4). This nickel came from the corrosion of the reactor material. The remaining main components in the suspended matter were carbon and oxygen. Judging from the carbon ESCA spectrum, it appeared to be in the form of graphitic or amorphous carbon.

Experiment 2

C and N Conversion: Figure 5 shows the oxidation efficiency for carbon and nitrogen.

The definition of the oxidation efficiency for carbon is the same as for "Experiment 1". Below the critical point of water, the oxidation efficiency for carbon increased with reaction temperature. The rate of its increase was much faster than in the case of acetic acid and ammonium hydroxide model waste (see Figure 1). This difference was probably due to the catalytic effect of minerals in the urine, feces, and wipes. Near the critical point of water, the oxidation efficiency reached higher than 95%. After that, the efficiency remained high and essentially constant.

In order to identify the chemical forms of nitrogen in solution, three indicators were used in this work: Kjeldahl nitrogen before filtration (total), Kjeldahl nitrogen after filtration (filtrate), and ammonia. Generally, results from these three analyses so close to each other that almost all nitrogen in the solution was considered to be in the form of ammonia. But, since the reproducibility of the Kjeldahl nitrogen analysis was better

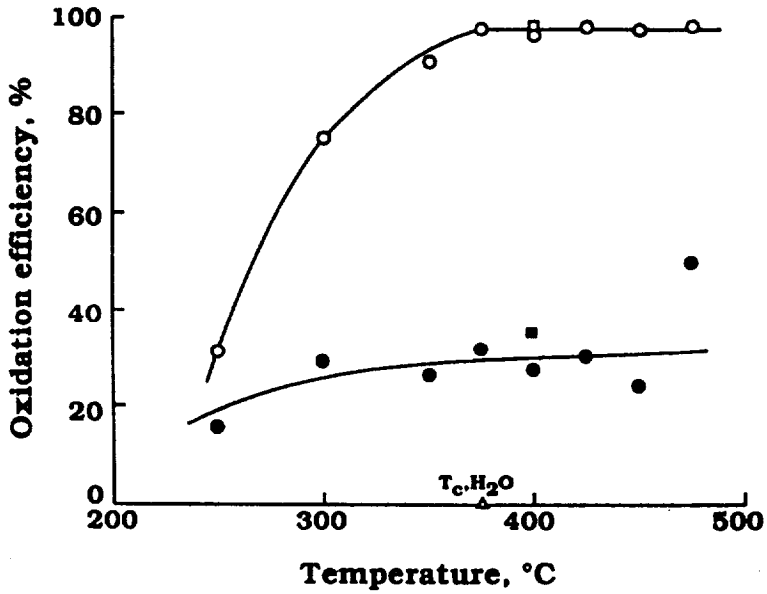

Fig. 5. Effect of temperature on the oxidation efficiency of human urine, feces, and wipes. Residence time was 60 minutes (o carbon, • nitrogen) and 120 minutes (▫ carbon, ▪ nitrogen).

than the ammonia analysis, the oxidation efficiency for nitrogen as used here is based on Kjeldahl nitrogen (total) and defined as follows:

$$\text{Oxidation efficiency of nitrogen (\%)} = [(\text{Kj-N}_{\text{initial}} - \text{Kj-N}_{\text{final}})/\text{Kj-N}_{\text{initial}}] \times 100$$

where Kj-N is defined as Kjeldahl nitrogen in solution (N g/l).

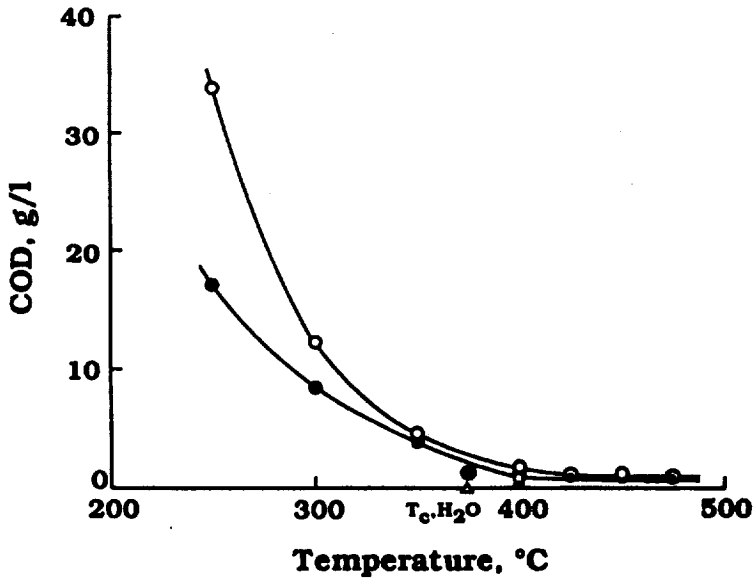

Fig. 6. Effect of temperature on the COD of human urine, feces, and wipes. Residence time was 60 minutes (o total, • filtrate only) and 120 minutes (▫ total, ▪ filtrate).

Though the oxidation efficiency for nitrogen in the human waste samples was higher than in the case of the acetic acid and ammonium hydroxide model waste, a substantial amount of nitrogen (about 70%) still remained in solution as ammonia between 300 and 450°C. This finding again confirms the usefulness of supercritical water oxidation in the vicinity of 400°C for CELSS wastes. The black dot (l) and square (n) in Figure 5 show

the results of oxidation for 120 minutes. Even with an increase in residence time from 60 to 120 minutes, the oxidation efficiency of both carbon and nitrogen did not increase significantly.

Figure 6 shows the temperature dependency of COD in the filtrate as well as total COD.

For reference, in Figure 5, the oxidation efficiency of carbon was based on total COD. In Figure 6, below the critical point of water, the ratio of COD in the filtrate to total COD increased with oxidation temperature. Above the critical point, COD in the filtrate was almost the same as COD total.

Figure 7 shows the results of total (TS) and suspended solids (SS) after oxidation of urine, feces, and wipes.

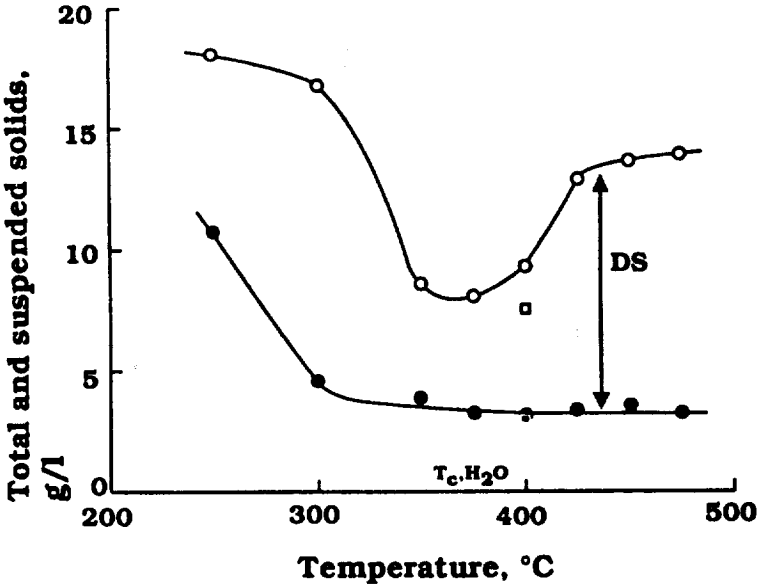

Fig. 7. Effect of temperature on the total (TS) and suspended solids (SS) of human urine, feces, and wipes. Residence time was 60 minutes (o TS, • SS) and 120 minutes (▫ TS, ▪ SS).

TS minus SS can be thought of as dissolved solid (DS). At subcritical temperatures, both TS and SS decreased with reaction temperature and reached a minimum near the critical point of water. At supercritical temperatures, though SS remained constant, TS *increased* with temperature, reaching its maximum at 430°C and remaining constant after that.

This increase in TS above 400°C was unexpected. Since almost all organic matter was oxidized above the critical point (see Figure 5 and 6), the content of DS above this point should be only inorganic. Perhaps, at the time of the TS measurement, decomposition and volatilization of some part of TS occurred in those samples taken from the 350 to 400°C runs yielding a low TS value in this range, or water was retained as water of crystallization and measured as part of TS for runs above 400°C, yielding high values. This phenomenon suggests that the chemical forms or situations of DS are different below and above about 400°C.

Metal Corrosion: Figure 8 shows the concentration of chromium (Cr) in solution after wet oxidation of urine, feces, and wipes.

Analysis of a representative sample of the feces used for the raw material contained no chromium while a representative sample of the urine used had 0.5 mg chromium per kilogram of dry urine /9/. We assumed wipes do not contain measurable amounts of chromium. Therefore, the chromium concentration in Figure 8 could not have come from the raw material and its origin was thought to be the reactor material. The Cr concentration reached a maximum at 350°C. On the other hand, nickel was not found

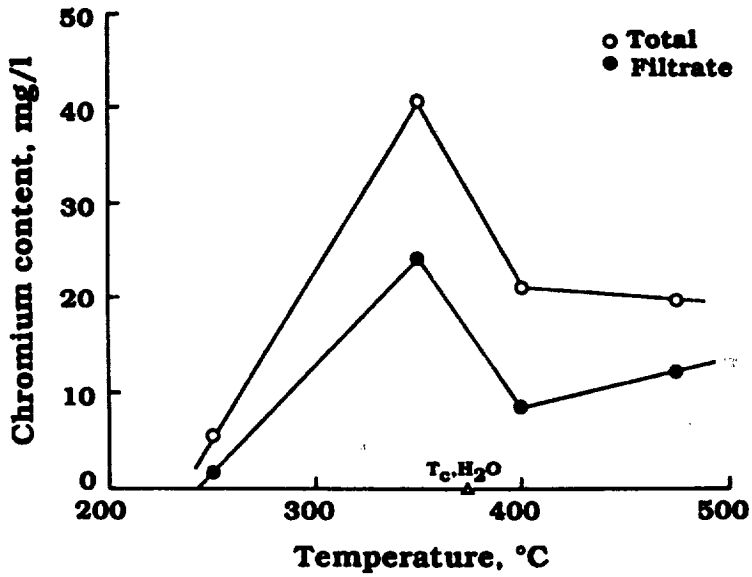

Fig. 8. Effect of temperature on the corrosion of the Hastelloy C-276 reactor; human urine, feces, and wipes waste feed.

in either the representative feces or urine used /9/ and no information regarding the molybdenum content in feces, urine, and wipes was available. The concentration range of nickel in this experiment ranged from 5 to 60 mg/l and that of molybdenum from 10 to 80 mg/l. These metals were also thought to have come from the reactor material.

Table 3 compares the corrosion rate of molybdenum, chromium, and nickel in different wet oxidation environments.

Table 3 Corrosion of the Hastelloy C-276 Reactor during the Oxidation of Different Feeds.

	Distilled Water Feed	NH_4OH + HAc Feed	Human Waste Feed
Element	mg/l	mg/l	mg/l
Molybdenum	4.80	18.1	45
Chromium	6.75	11.5	8.4
Nickel	2.60	15.0	7.4

(1) 184 ml of distilled water was heated at 450° C for 60 minutes.
(2) 184 ml of an NH_4OH + HAc solution was wet oxidized at 450° C for 60 minutes.
(3) 250 ml of a human urine, feces, and wipes solution was wet oxidized at 400° C for 60 minutes.

The corrosion rate of molybdenum in the presence of human wastes was higher, that of chromium was almost the same and that of nickel was lower than in the presence of the ammonium hydroxide and acetic acid model waste.

Table 4 shows the results from ESCA analysis of the suspended matter in the samples.

Nickel was found only in the sample run at 475°C. The origin of the other elements could be the raw material itself. At 250°C, the atom percent of carbon in the suspended matter was the highest which is consistent with the low carbon oxidation efficiency at this temperature (see Figure 5). At the higher temperatures, the atom percent of elements except carbon increased and this finding is also consistent with a higher carbon oxidation efficiency at these temperatures. The elemental composition of the suspended solids appeared to be independent of treatment temperatures above 250°C.

The suspended solids remaining after oxidation of urine, feces, and wipes were generally black, except for the sample oxidized at 375°C. In this case the solution was yellow and the particles were mostly off-white with some gray to black. We have no

Table 4 ESCA Analysis of Suspended Solids after Water Oxidation (atom %).

Sample and Oxid. T	C	O	Mg	P	Ca	N	F	Ni	Na	Zn	Si
400°C (NH_4OH + HAc)[1]	70	21	-	-	-	-	-	4. 1	-	-	4.0
250°C (Human Waste)[2]	67	24	3.1	1.8	1.6	1.4	1. 3	-	-	-	-
350°C	23	45	6.2	13	11	-	-	-	1.2	-	-
375°C	19	47	6.4	15	11	-	-	-	0.9	0.2	-
400°C	32	39	3.9	11	10	2.7	-	-	0.7	0.3	-
475°C	26	43	5.7	13	8.6	-	-	1.5	1.4	0.6	-

(1) The suspended solids after the wet oxidation of an ammonium hydroxide and acetic acid solution.
(2) The suspended solids after the wet oxidation of human urine, feces, and wipes.
(3) Samples were dried in a vacuum oven at 50° C.

explanation for the different appearance of the sample oxidized very close to the critical temperature of water.

SUMMARY AND CONCLUSION

Subcritical and supercritical water oxidation of CELSS model wastes were carried out using a batch type reactor. A mixture of acetic acid and ammonium hydroxide and a slurry of human feces, urine, and wipes were used as wastes. The effects of oxidation temperature and residence time on carbon and nitrogen conversion and on metal corrosion from the reactor material were studied. The temperature range studied was from 250 to 500°C and the residence time ranged from 0 to 120 minutes.

Almost complete oxidation of organic carbon in the waste feeds occurred above the critical temperature and pressure of water. On the other hand, a substantial amount of nitrogen remained in solution in the form of ammonia at temperatures from 350 to 450°C. These findings suggest that in the vicinity of 400°C, which is a little higher than the critical temperature of water, organic carbon is completely oxidized and most of the nitrogen is retained in solution. Both the oxidized form of carbon (carbon dioxide) and the ammonia can be used as nutrients by plants or algae grown in a CELSS. Other temperature ranges or methods of water oxidation cannot realize these two advantages simultaneously (Table 5).

Table 5 Comparison of Different Techniques of Wet-oxidation.

	Wet-oxidation without catalyst	Wet-oxidation with catalyst	Supercritical Water Oxidation	Low T Supercritical Water Oxidation
Temperature	110 - 310°	225 - 300°	560 - 670°	near 400°
Carbon (Oxidation)	incomplete	complete	complete	complete
Nitrogen	remains in solution as NH_4^+	gasified as N_2	gasified as N_2O and N_2	remains in solution as NH_4^+ (70-90%)
Reference	/5/	/3,5/	/8/	/This paper/

Therefore, wet oxidation temperatures near 400°C appear from this study to be desirable for a CELSS waste processor.

Regarding the percentage of ammonia remaining in solution, there was some discrepancy between the case of acetic acid and ammonium hydroxide and that of feces, urine, and wipes and therefore more experiments are needed to clarify this phenomenon. But the trends themselves appear to be identified in this work.

The Hastelloy C-276 alloy reactor corroded during WO and SCWO of wastes. The rate of corrosion depended on the type of waste being oxidized and the temperature of oxidation. The corrosion rate was generally lower above than below the critical

temperature of water. Corrosion products from a waste processor could be detrimental to the growth of plants in a CELSS.

BIBLIOGRAPHY

1. Onisko, B. L. and Wydeven, T., Wet Oxidation as a Waste Treatment in Closed Systems, Publication No. 81-ENAS-22, The American Society of Mechanical Engineers, New York, N.Y., (1981).

2. Johnson, C. C. and Wydeven, T., Wet Oxidation of a Spacecraft Model Waste, SAE Technical Paper Series, 851372, (1985).

3. Takahashi, Y. and Ohya H., Wet-Oxidation Waste Management System for CELSS, SAE Technical Paper Series, 851398, (1985).

4. Takahashi, Y., Nitta, K., Ohya, H. and Oguchi, M., The Applicability of the Catalytic Wet-Oxidation to CELSS, Adv. Space Res., Vol. 7, No. 4, pp. (4)81-(4)84, (1987).

5. Takahashi, Y. and Isobe, S., The Catalytic Wet-oxidation of Ammonium Acetate for CELSS, The 16th International Symposium on Space Technology and Science, Sapporo, (1988).

6. Timberlake, S. H., Hong, G. T., Simson, M. and Modell M., Supercritical Water Oxidation for Wastewater Treatment: Preliminary Study of Urea Destruction, SAE Technical Paper Series, 820872, (1982).

7. Hong, G. T., Fowler, P. K., Killilea, W. R. and Swallow, K. C., Supercritical Water Oxidation: Treatment of Human Waste and System Configuration Tradeoff Study, SAE Technical Paper Series, 871444, (1987).

8. Zimmermann, F. J., New Waste Disposal Process, Chemical Engineering, (August 25, 1958).

9. Carden, J. L. and Browner, R., Preparation and Analysis of Standardized Waste Samples for Controlled Ecological Life Support Systems (CELSS), NASA Cooperative Agreement NCA 2-OR260-102, NASA Contractor Report 166392, Georgia Institute of Technology (August 1982).

A-96-15437

THE C23A : FIRST STEP TO A MONITORING SYSTEM OF CELSS IN FLIGHT

Ch. Lasseur*, D. Massimino**, J.L. RENOU** and Ch. Richaud**

* Matra Espace 37, av. Louis Bréguet 78146 Vélizy-Villacoublay, FRANCE. **Service de Radioagronomie, CEN Cadarache, 13108 St Paul lez Durance, FRANCE.

ABSTRACT

Studies for every level of CELSS : Waste processing, food production, photosynthesis system, and so on..., imply an automatic system to control, command and quantify gases, water and chemical compounds. Used for many years in plant physiology studies, the C23A system monitors the analysis and quantifies gases (O2, CO2, N2, ...), physical parameters (temperature, humidity, ...) and chemical compounds (NH4+, NO3-, ...) on numerous experiments. In the new version, the architecture of the computing system is near of the space requirements. We have chosen a structure with three independent levels : acquisition, monitoring and supervision. Moreover, we use multiplexed analysers : IRGA, mass spectrometer and cheminal analyser. The multiplexing increases the accuracy of the measurements and could facilitate the spatialization. Thus the whole structure anticipates the entire separation between automation in space and control-command on ground.

INTRODUCTION

All present studies of the CELSS project, whether they are concerned with waste recycling, food production, photosynthesis system, and so on..., entail a minimum of functioning and therefore an efficient system of measurement and control-command /1, 2/. If at the present time one part of the monitoring procedures has been yet studied (being based on the known industrial process : water recycling, Bosch and Sabatier reactor, and so on...) /3, 4, 5, 6, 7, 8/, another part, the control of atmosphere and of plant cultivation, are at much less automized /9/. For the last 15 years, at the CEN Cadarache, an automatic control system has been used in research on plant gases exchanges : the C23A (chambre de culture automatique en atmosphère artificielle /10/. In order to benefit from the most recent developments in electronics and automatization we restructured our system taking into account, as far as possible, space requirements /11/ : remote control, independent functioning, multiplication of alarms and their control, multiplexing of analyzers, reliability, quality of measurements. /12/.

STRUCTURE AND FUNCTIONING

Figure 1 illustrates the architecture of the C23A system, as it stays now. It can be divided into three independent levels : input and output, automatic functioning and supervision.

Input and Output (Level 0)

It comprises all of the sensors (temperature, humidity, light, pressure, weight, as well as the different actuators (electrovalve, motor, control shutter, security devices). None of these elements are "intelligent" but are linked directly to a higher level situated a short distance away. This latter aspect enables us to avoid a part of the problem of interference.

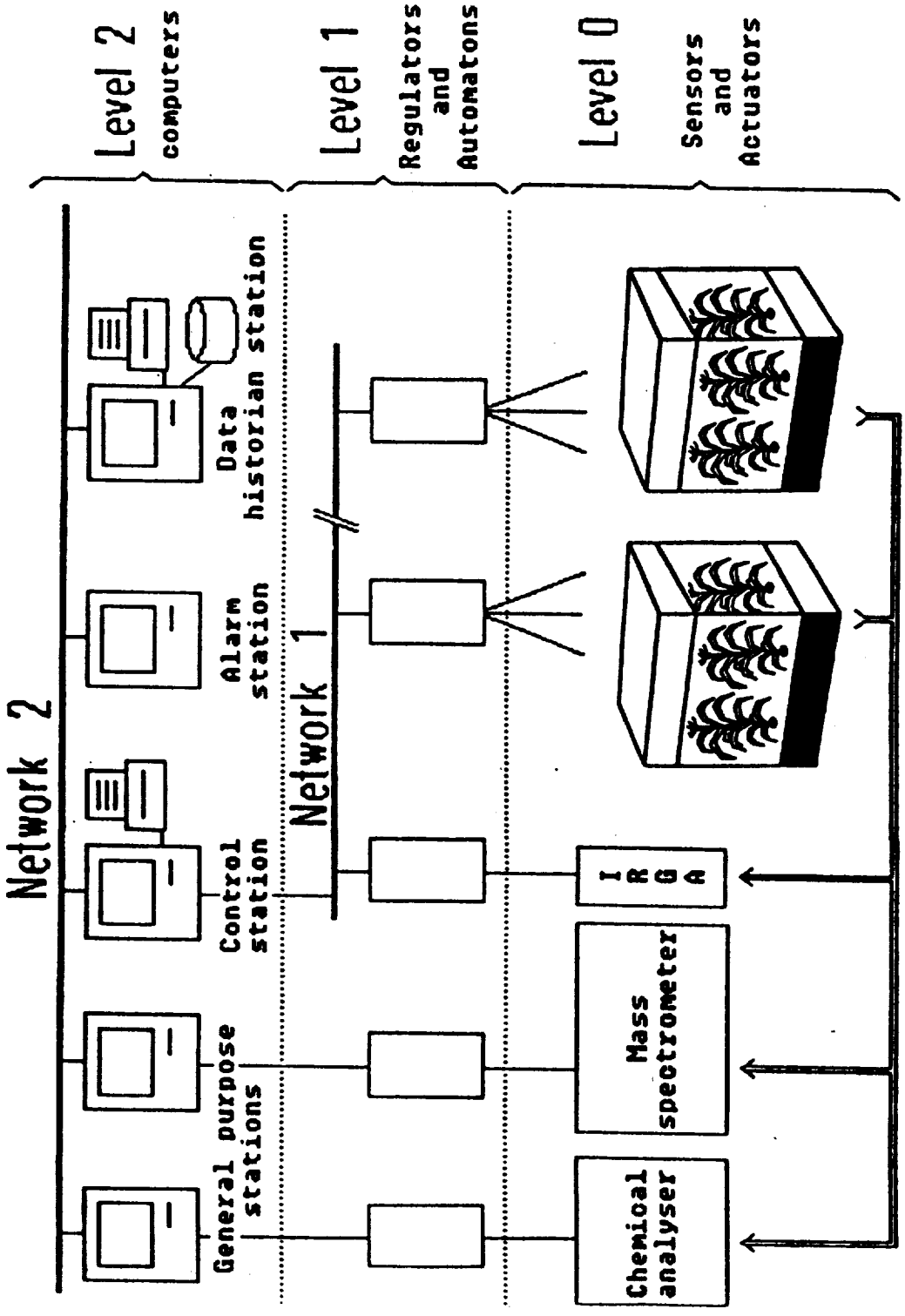

Fig. 1. Structure of the C23A system.

Automatic Functioning (Level 1)

It has the task of collecting the signals from the sensors and converting them to binary language as well as to effectuate the different functions demanded by programming and thereby to interreact with the process via level 0. The programmation of the automatic controllers is carried out by assembling macro-instructions which allow the most common arithmetical and logical functions to be carried out. They can be carried out either on the site (using a lateral keyboard) or at distance (with the help of level 2). At the present time, the frequency of measurement taking is 100 ms minimum, and the time necessary for collection, processing and resultant action is 200 ms maximum. In addition, if one uses the lateral link (network 1), absolutely any of the parameters picked up from the different points of the network can be incorporated in calculations. We thus benefit from the independence of each structure, from increased safety and the possibility of redundancy without drawbacks (the necessity of gathering two identical parameters, overloading of memories, and so on...). We shall see that this advantage exists also for level 2.

Supervision (Level 2)

Linked to the lower level by the RS232 line and capable of being as far as 6 kilometers away, this level is also divided into different sub-systems to form a network (network 2). Nevertheless, for this level, each sub-system has a specific function : control-command, data-processing, alarm centralization.

Control-Command

It enables on-line remote control configuration of all second level automatic controllers or regulators. All the parameters of level 1 devices (set-points, measurement, local memory, calculation program) can be consulted and modified in real time. Control-command can also be facilited by the use of tendency graphs showing the collected data with respect to elapsed time. The operator can thereby follow the evolution of the process in real time and react if necessary.

To simplify keeping track of the experiments, which sometimes necessitate a large number of parameters, a synthetic view can be obtained by means of animated synopses. Finally, it should be pointed out that whilst all of the parameters of the second level can be commanded from this sub-system, the access to any individual parameter can be linked to a password.

Historical Record and Storage

This sub-system is charged with saving on a hard disk or floppy the data circulating on the network. Data can have its origin in the different stations of the network, but also from the different sub-systems of level 1. Records can be taken in three different ways : unprocessed, averaged by minute or averaged by hour. In this way, and to avoid overloading memory, it is possible to correlate the speed of variation of a parameter with its frequency of storage.

Processing Station

This sub-system provides for the arithmetical and graphic processing of data collected in real time, but originating also from previously stored data. It is worth noting that the particular structure of the files was chosen to enable the use of commercially available software (Multiplan, Lotus, and so on...).

Alarm Station

It enables not only the centralization of all alarms, but also their processing. Indeed, each alarm is characterized by its origin and its degree of intensity ; the operator can thus react rapidly. It is also to be noted that the different alarms and their graduation level are defined during configuration.

The choices we have made allow us to increase the degree of automatic functioning and the reliability of our experiments. At the present time, for a single plant, we check 16 analog and 24 digital parameters (light intensity, O2, CO2, N2, humidity, pressure, mineral nutrition, transpiration, temperature) and this 24 hours a day without an operator and sometimes for periods of 6 months /13, 14/.

It is obvious that some of the technological choices made (speed of communication, type of network, choice of components, ...) do not correspond to space requirements ; nevertheless we have made an effort to guaranty a maximum of transfer toward other materials (software using high-level and structures languages).

STRUCTURE OF MULTIPLEX ANALYZERS AND RESULTS

As we saw in the description of level 0, we use a great number of sensors ; however, this sort of device is not capable of fulfilling all our analytical needs (isotope, biochemistry, measurement precision). We were thus rapidly brought to use more powerful and more complex instruments (mass spectrometer, IRGA, continuous flux, and so on...). These sorts of analyzers, when used continuously and automatically, pose several problems. Being intended for laboratory studies, they are exclusively designed with a view to taking ad hoc measurements. We were obliged to assure the totality of their automatic functioning ourselves.

Before carrying out this work, we similarly attempted to take into account a part of the space requirements : remote control, automatic calibration, temporal stability of measurements. We resolved one part of the problem by multiplexing these analyzers. Each of them being controlled by an automatic controller. It controls a multi-channel introduction system, (about 20), and each measurement channel is scanned at a specific frequency recorded in the controller. After the introduction of the analysis sample, the automatic controller converts the analyzer's output signal which itself is dependent on the concentration to be measured and carries out the various correction calculations : thermal drift, component ageing, impurity accumulation. These calculations are carried out by comparison with measurements of reference samples, one or two introduction channels being set aside for this purpose. At the present time, the precision of our measurements in O2 is $\pm$ 0.2 % on the 21.6 % present in the atmosphere, in CO2 $\pm$ 1 ppm on the 340 ppm present in the atmosphere, and ION NH4+ $\pm$ 1.5 % on the full scale.

We encountered another important drawback with this system : the need for a minimum analysis volume relatively large in comparison to that of the process being checked. Contrary to what one may imagine, this defect is not simply due to the physical properties of the device, it also concerns the structure of the introduction system. A system was therefore conceived which allows the introduction of a volume of only 0.5 ml ; this work has been patented. Finally, it should be noted that in using automatic controllers to run our equipments, we maintain a maximum degree of reliability, as well as the possibility of remote control-command and the lateral and vertical communication previously defined.

The quality of a measuring system can be judged by its precision, but the fundamental parameter of a control-command system is precisely the accuracy of its control. At the present time, for a container of 700 l, simulating photosynthesis of a 40 day wheat cover on a surface of 0.5 m2, with a 14 hour photoperiod and an illumination of 2200 ue m2/s at a CO_2 concentration of 340 ppm, the standard deviation is 3 ppm (fig. 2).

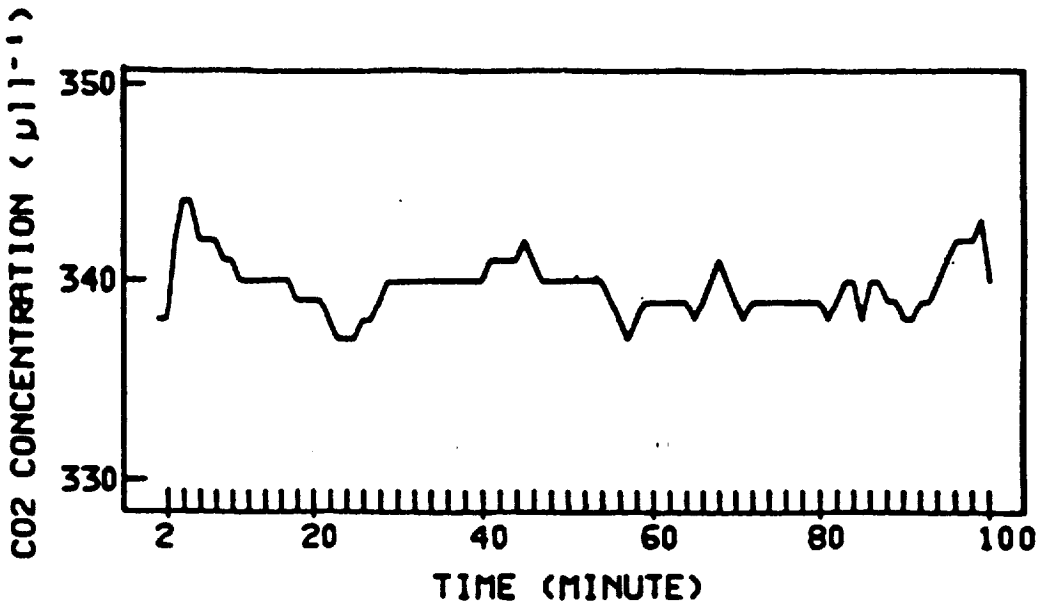

Fig. 2. CO2 concentration in a growthchamber of 700 liters containing a culture of wheat. The photosynthesis is about 880 ml of CO2 by hour and the frequency of measurements used to monitor is 15 by hour.

The sudden stopping of this photosynthesis simulation gives a maximum variation of around 20 ppm (fig. 3) spread over a maximum of 10 minutes. It should be remembered that these results were obtained by carrying out a measurement of CO2 every three minutes only. This shows clearly that the reduction in the frequency of measurement due to the multiplexing of the analyzer is not a drawback if ones uses a high performance regulator.

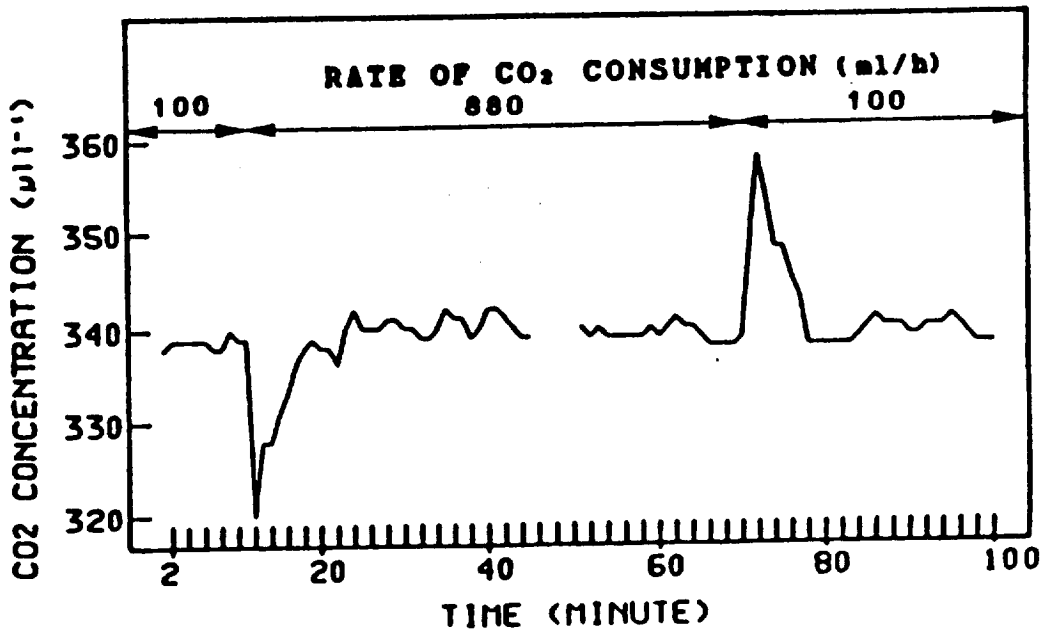

Fig. 3. CO2 concentration in a growthchamber where we have simulated sudden variations of photosynthesis. The frequency of measurements used to monitor is 20 by hour.

CONCLUSION

It's clear that we need to carry out the automatization by video control, robots (for plant cutting, seed harvesting, and so on...) and maximize the functional optimization by an expert system /15/ (a study is in progress to insert an expert software on the network). Nevertheless, the structure and the performances of the C23A have allowed to increase the level of automatization (currently we control around 250 parameters) and to tackle the problems of telemetry : remote control, quality of measurements, ... By this way, the C23A system could be a possible control system for several processes of CELSS.

REFERENCES

1. B. Moore, III, R.A., Jr. Warton and R.D. MacElroy, Controlled ecological life support systems, First principal investigators meeting, NASA CP-2247 (1982).

2. M. Oleson, R.L. Olson, Controlled ecological life support systems (CELSS), Conceptual design option study, NASA CR-177421 (August 1986).

3. R.D. MacElroy, D.T. Smernoff and H. Klein, Support systems in space travel (Topical session of XXVth COSPAR meeting, Graz, Austria) NASA CP-2378 (May 1985).

4. M. Karel, Evaluation of engineering foods for controlled ecological life support systems (CELSS), NASA CR-166359 (June 1982).

5. D.T. Smernoff, Atmosphere Stabilization and element recycle in an experimental mouse algal system, NASA CR-177402 (March 1986).

6. Lyonnaise des eaux, Matra EPT, Traitement des déchets, ESA AO/1-2019/87/NL/MA (November 1987).

7. M. Oleson, F. Slavin, R. Liening, R. Olson, Controlled ecological life support systems (CELSS), Physiochemical waste management systems evaluation, NASA CR-177422 (August 1986).

8. R.D. MacElroy, D.T. Smernoff, Regenerative life support systems in space (Topical session of XXVIth COSPAR meeting, Toulouse, France), NASA CP-2480 (June 1987).

9. R.D. MacElroy, D.T. Smernoff, J. Rummel, Controlled ecological life support systems, Design, development and use of a ground-based plant growth module, NASA CP-2479 (Juin 1987)

10. M. Andre, A. Daguenet, D. Massimino, J. Vivoli et C. Richaud, le laboratoire C23A un outil au service de la plante entière, Ann. Agron., 30 (2), 135-166 (1979).

11. Th. Blais, L. Calenge, Columbus APM utilization study, Attach pressurized module 2nd extension, final report, MATRA EPT (June 1988).

12. Ch. Lasseur, Le système C23A, nouvelle version et perspectives d'avenir, Rapport CEA n° 5455 (Juin 1988).

13. F. Bréchignac, M. André, Oxygen uptake and photosynthesis of the red macroalga, Chrondrus Crispus, in seawater, Effect of oxtgen concentration, Plant Physiol., 78, 735-738 (1985).

14. A. Gerbaud, M. André, Photosynthesis and photorespiration in whole plants of wheat, Plant Physiol., 64 (1979).

15. T. Ogina, K. Itichi, A feasibility study of an expert system for a space station and experiments in space, Space Technol., vol. 7, n° 4, 273-279 (1987).

N90-15438

EFFECT OF IODINE DISINFECTION PRODUCTS ON HIGHER PLANTS

D. Janik,* B. Macler,* Y. Thorstenson,** R. Sauer*** and R. MacElroy*

*NASA-Ames Research Center (239A-3), Moffett Field CA 94035; **Department of Genetics, University of California, Berkeley CA; ***NASA-Johnson Space Center, Houston TX.

ABSTRACT

Iodine is used to disinfect potable water on United States spacecraft. Iodinated potable water will likely be used to grow plants in space. Little is known about the effects of iodine disinfection products on plants. Seeds of select higher plants were germinated in water iodinated using the Shuttle Microbial Check Valve, and water to which measured amounts of iodide was added. Percent germination was decreased in seeds of most species germinated in iodinated water. Beans were most affected. Germination rates, determined from germination half-times, were decreased for beans germinated in iodinated water, and water to which iodide was added. Development was retarded and rootlets were conspicuously absent in bean and several other plant species germinated in iodinated water. Iodide alone did not elicit these responses. Clearly iodine disinfection products can affect higher plants. These effects must be carefully considered for plant experimentation and cultivation in space, and in design and testing of closed environmental life support systems.

INTRODUCTION

Iodine has been used to disinfect potable water on US spacecraft since Apollo /1/. A Microbial Check Valve (MCV; Umpqua Reserch Company, Myrtle Creek, OR, USA) is used to impart 2 parts per million (ppm = mg/l) of iodine to potable water /2,3/. Crews of future missions (for example, US space station) as presently conceived will reuse and recycle MCV-iodinated water. Future crews and, as such, consumers, will undoubtedly include plants.

At these concentrations, iodine can cause measurable physiological changes in human consumers and may be toxic over long periods /4/. The effects of iodinated water on plants are less well known. Plants are not known to have an iodide-based hormone system as do humans and animals. Iodine and iodide are considered by some plant physiologists to be nontoxic and possibly even non-essential to plants /5/. However, after critical review of the literature, at least one group has concluded that the more iodine there is available the more a plant will absorb, until toxic levels are ultimately reached /6/. Aquaculture data further suggest that "...no [plant] species withstands a concentration greater than 1 part of iodide in 1 million parts of solution. Indeed, at this strength the growth of peas and mustard is retarded, and any higher concentration is definitely harmful. Only when the concentration is reduced to 1 part of iodide in 5 or 10 million parts of solution has any favourable stimulatory effect been observed /6/."

We examined germination numbers and rates of seeds sprouted in glass distilled (GDW), MCV-iodinated (I2W), sodium iodide (NaIW) and potassium iodide (KIW) water.

METHODOLOGY

All glassware was multiply rinsed with Class III GDW, and where appropriate multiply rerinsed with I2W prior to use. I2W was prepared by passing GDW

through a newly-charged MCV, and was scanned from 210 to 750 nm with a scanning visible UV spectrophotometer (Shimadzu, Kyoto, Japan) for specific iodine disinfection products (IDP). I2W was stored in dark, tetrafluoroethylene (TFE) sealed, glass bottles.

Percent Germination (% GERM) Experiment

Seeds of ten higher plant species important for plant physiological experimentation, food or life support in space were obtained (Table 1; Northrup King Seed Company, Minneapolis, MN, USA). All seeds for a particular species were from the same 1988 seed lot. Abnormal-appearing seeds were discarded. Remaining seeds were equally distributed between two 250 ml Erlenmeyer flasks. Flask entrances were then covered with 0.5 mm internal mesh, TFE screens (Spectrum Medical Company, Carson, CA, USA) and secured with rubber bands. Seeds were soaked for 4 hours in either I2W or GDW, drained, and rewetted with respective solutions for 10 minutes approximately every 12 hours. Between rewettings, flasks were randomly reassembled into a tight square and placed in a protected area in a large, windowless, fluorescently-illuminated room. Upon first appearance of any primary leaves, all seeds of that species were harvested and examined for visible plant tissue (germination). % GERM's were calculated and analyzed using a standard Chi-square statistic at 99% confidence.

Germination Half-time (GERM 1/2) Experiment

Using the above techniques, multiple serial dilutions of NaIW and KIW were made up, scanned and solutions with an iodide concentration similar to I2W identified.

Seeds of Glycine max, Zea mays and Triticum aestivum were inbibed in I2W, NaIW, KIW and GDW, transferred onto TFE screens inside inverted petri plate covers, covered with petri plate bottoms, and incubated in a plant growth chamber for 5 days. Seeds were automatically photographed every 2 hours on 70 mm Kodak Tri-X film (Eastman Kodak Company, Rochester, NY, USA). Plates were maintained at 24 degrees Centigrade inside the chamber using a temperature-controlled, circulating water bath. The chamber was constantly illuminated with fluorescent light at 20 micromols/square meter-second. Photographs were analyzed using low power stereo dissecting microscopy using a slide viewing box for illumination. Cumulative % GERMS were calculated, plotted, and GERM 1/2's were determined graphically and finally verified by linear regression extrapolation.

RESULTS

I2W was determined spectrophotometrically to contain at least iodine, iodide and tri-iodide IDP species.

% GERMS were significantly lower in I2W compared to GDW exposed seeds for all species taken together, and for Glycine max (soybean), Brassica oleracea cv italica (broccoli), and Phaseolus vulgaris (pole bean) in order of decreasing significance (Table 1). Other seeds, except Raphanus sativus (raddish), showed the same trend, but were not statistically significant. Clearly, beans were most affected.

On further examination, several other differences were noted. Soybeans, pole beans and broccoli exposed to I2W germinated faster than GDW controls, while Zea mays (corn), and Brassica oleracea cv capitata (cabbage) germinated slower and were shorter than GDW controls. Soybeans, pole beans and corn exposed to I2W appeared, however, to be less developmentally mature, and to have strikingly fewer rootlets than GDW controls.

GERM 1/2's from the second experiment are summarized in Table 2. The GERM 1/2 for I2W-exposed soybeans was about half that for GDW-exposed controls. GERM 1/2's for NaIW and KIW exposed soybeans were intermediate between I2W and GDW exposed seeds. Similar differences were not observed for corn or Triticum aestivum cv yecora rojo (wheat). In this experiment, corn cultures were serendipitously retained to primary leaf formation. As noted in the first experiment, I2W-exposed corn seedlings appeared to be less developmentally mature and to have fewer rootlets than NaIW, KIW or GDW exposed seeds.

TABLE 1 Percent Germination (% GERM) of Select Seeds Sprouted in Iodinated (I2W)* and Uniodinated (GDW) Water

Species/Cultivar	% Germ I2W	% Germ GDW	Statistic Chi-sq
Glycine max	78 (41/52)	100 (52/52)	10**
Brassica oleracea cv italica	15 (15/100)	32 (32/100)	8.0**
Phaseolus vulgaris	89 (86/96)	99 (95/96)	7.8**
Zea mays	95 (40/42)	100 (42/42)	2.1
B. oleracea cv botrytis	84 (22/26)	96 (25/26)	2.0
Daucus carota	82 (82/100)	87 (87/100)	1.0
B. oleracea cv capitata	81 (81/100)	85 (85/100)	0.6
B. campestris cv rapisera	95 (95/100)	97 (97/100)	0.5
Lactuca sativa	87 (87/100)	88 (88/100)	0.1
Raphanus sativus	99 (99/100)	96 (96/100)	1.9
All species	79 (648/816)	85 (699/816)	11**

* GDW passed through Shuttle Microbial Check Valve
** Significant at 99% confidence ($p < .01$, Chi-sq > 6.63, df = 1)

TABLE 2 Germination Half-times (GERM 1/2) for select Seeds Sprouted in Iodinated (I2W)*, Iodated (NaIW and KIW)** and Uniodinated (GDW) Water

Species/Cultivar	GERM 1/2 (hours) I2W	NaIW	KIW	GDW	Statistic Z (one-tail)
G. max***	58 @ 8	71 @ 7	72 @ 11	78 @ 8	-3.5 (p<0.01)
Z. mays	26	27	25	26	n/a
T. aestivum cv yecora rojo	16	18	16	18	n/a

* GDW passed through Shuttle Microbial Check Valve
** 5 ppm iodide as sodium iodide or potassium iodide in GDW
*** N=4, @ = plus or minus one standard deviation

DISCUSSION

Higher plants are affected by IDP's. Of plants examined, soybeans, pole beans and corn were most affected. Not all affected species appeared to be affected the same way.

IDP's specifically affected seed germination, growth and development. Some but not all of these effects are attributable to iodide. However, the presence of iodine, iodide, tri-iodide and probably other IDP's in MCV-iodinated water complicates any attempt to ascribe observed differences to specific IDP's other than iodide. IDP's are unique water "contaminants" in that they are purposefully added to disinfect potable water. Further elaboration regarding their effects and toxicity is clearly warranted.

Both bean germination experiments produced an acrid, formaldehyde-like odor. It is possible that substance(s) associated with this odor could have been responsible for differences in % GERM and GERM 1/2 noted, if, for example, they were metabolic inhibitors and were produced in quantities proportional to germination rates.

Soybean germination is influenced by a number of environmental cofactors. Several merit special discussion.

Relatively pure, corrosive GDW could have caused seed or seed coat damage in controls. In the former case, differences in GERM 1/2's would be less significant. In the later case, if cell hydration were augmented, differences could be more significant.

Any bacteria present which participate in germination may have been effected by iodine disinfection products. Pure glass distilled water, iodine, and possibly some iodine disinfection products might decrease bacterial types or numbers, while iodide, triiodide and possibly some other iodine disinfection products might support or increase bacterial types or numbers. Effects, if any, on GERM % or GERM 1/2 are difficult to predict.

Humidity and aeration, while the same for experimental and control seeds, probably varied during the course of the experiments. Seeds at different developmental levels due to different germination rates could react differently to variations in humidity or oxygen, causing exaggerated results.

In neither experiment was the effect of I2W on mature plants, their progeny, or consumers of such plants examined.

ACKNOWLEDGEMENTS

DSJ and BAM performed this research while National Research Council Research Associates at NASA-Ames Research Center. This research was initiated at NASA-Johnson Space Center. D. Bubenheim provided the T. aestivum seeds. The authors thank D. Smernoff, D. Bubenheim, R. Obendorf, C. Raper, R. Gibbons, J. Hickman and W. Sisler for their suggestions and technical support.

REFERENCES

1. D. Janik, R. Sauer, D. Pierson and Y. Thorsenson, Quality requirements for reclaimed/recycled water, NASA Tech Memo #58279, NASA-Johnson Space Center, Houston TX, (Mar 1987)

2. G. Colombo, D. Putnam and R. Sauer, Microbial check valve for Shuttle, in: Proc Intersoc Conf on Environ Systems, Society of Automotive Engineers, Warrendale PA 1978, p. 1

3. G. Colombo and R. Sauer, Review of water disinfection techniques, in: Proc Intersoc Conf on Environ Systems, Society of Automotive Engineers, Warrendale PA 1987, no page number

4. D. Janik and Y. Thorstenson, Medical effects of iodine disinfection products, Final Contractor Report #B01-86, Cetus Systems Inc, Salt Lake City, UT (1986)

5. F. Salisbury and C. Ross, Plant Physiology, Wadsworth Publishing Company, Belmont CA, 1978

6. Anon, Iodine and Plant Life, Chilean Iodine Educational Bureau, London, 1950

H 90-15439

THE ROLE OF COMPUTERIZED MODELING AND SIMULATION IN THE DEVELOPMENT OF LIFE SUPPORT SYSTEM TECHNOLOGIES

Michael Modell,* Peggy Evanich,** Chau-Chyun Chen,*** Selim Anavi,*** and Jeff Mai***

* Modell Development Corporation, Framingham, MA 01701, U.S.A.
** National Aeronautics and Space Administration, Washington, DC 02546, U.S.A.
***Aspen Technology, Inc. Cambridge, MA 02139, U.S.A.

ABSTRACT

Using conventional means of process development, it would take decades and hundreds of millions of dollars to develop technology for recycling of water and solid waste for lunar missions within the next thirty years. Since we anticipate neither that amount of time nor level of funding, new methodologies for developing life support systems (LSS) technologies are essential.

Computerized modeling and simulation (CMAS) is a tool that can greatly reduce both the time and cost of technology development. By CMAS, we refer to computer methods for correlating, storing and retrieving property data for chemical species and for solving the phenomenological equations of physical/chemical processes (i.e., process conditions based on properties of materials and mass and energy balances, equipment sizing based on rate processes and the governing equations for unit operations). In particular, CMAS systems can be used to evaluate a LSS process design with minimal requirements for laboratory experimentation. A CMAS model using ASPEN PLUS is presented for a vapor compression distillation (VCD) system designed for reclaiming water from urine.

INTRODUCTION

Physical/chemical systems are expected to play a major role in reducing the resources required to sustain humans in long duration missions. In some quarters, life support technology is viewed as "pacing" technology for advanced manned missions. Such conclusions are based, in part, on acknowledgment that once-through usage of materials represents a prohibitive launch weight and an unacceptable resupply burden and, in part, on the lack of fully developed subsystems to accomplish such tasks.

Life support technology development was actively pursued by NASA during the 1960's and early 1970's. Some of those technologies are shown in Figure 1 in a conceptual design of a life support system for a Lunar base. Each of the boxes describes a life support function, under which are listed the technologies in development by NASA. During the 1970's, the emphasis was on air revitalization. Those subsystems are now fairly well developed. However, we can see from Table 1 that air consumption involves far less resources than water. From the mid 70's to mid 80's, funding for LSS technology development was cut to very low levels. Thus, we find ourselves today with an urgent need to develop, perfect and demonstrate new LSS technology for Space Station and beyond.

In the past, the development of LSS technology had been a drawn out and costly process. For example, the type of air revitalization system anticipated to be used on Space Station was developed over a period of 10 to 15 years and at a cost in the range of $20 to 30 million. At that rate, it would take decades and hundreds of millions of dollars to develop technology for recycling of water and solid waste for lunar missions. Since we anticipate neither that amount of time nor level of funding, we must find quicker and less costly ways of developing LSS technologies.

LSS TECHNOLOGY DEVELOPMENT

The goal of LSS technology development is to devise processes to meet LSS functional requirements in a cost- and resource-effective manner, and with sufficient reliability and safety so as not to endanger the crew or compromise the objectives of the mission. In general, the functional requirements for long duration manned missions are more stringent than present practices on earth. The degree of recovery of air and water on a Lunar base will be far more demanding than that required for Space Station. Waste treatment for missions that include food production by

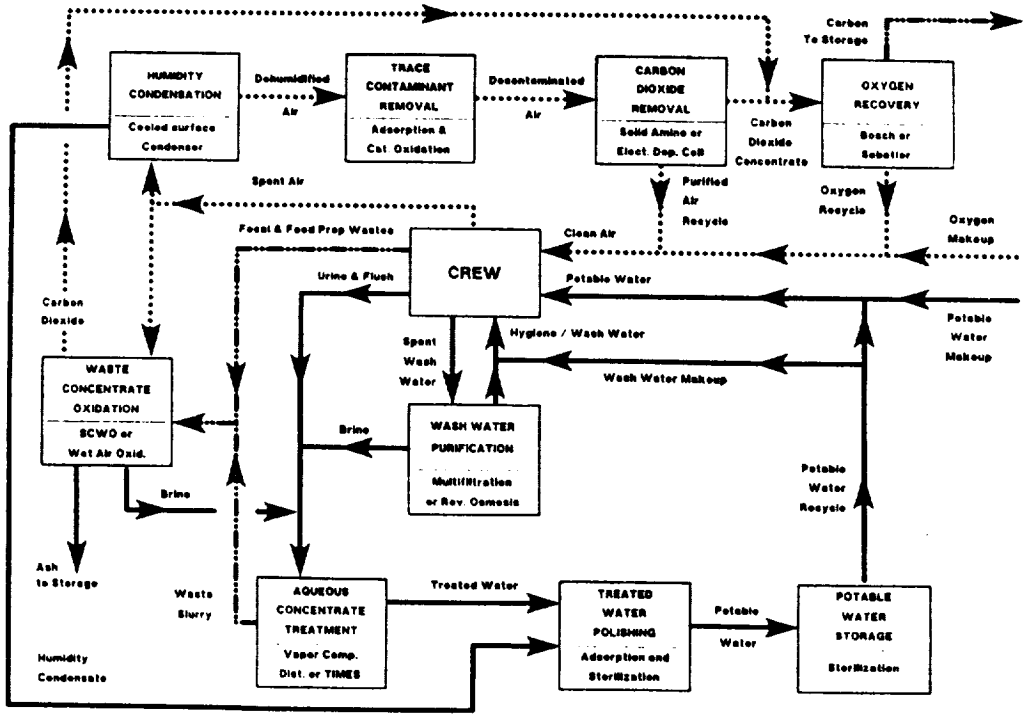

Fig. 1. A life support system for a lunar base scenario.

TABLE 1. LSS Resource Requirements

Inputs (kg/person)		Day	Year
Domestic Water		17.9	650 [1]
Clothes wash	12.5		
Shower	3.6		
Hand wash	1.8		
Atmospheric leakage		2.38	840
Drinking water		1.8	660
Metabolic oxygen		0.9	330
Food preparation water		0.7	260
Dry food solids		0.6	220
Urinal flush water		0.5	180
Totals		24.7	3,140

[1] represents 90% recycle.

plant growth will require oxidation systems that "burn" far more effectively than earth-based refuse incinerators and far more efficiently than hazardous waste incinerators. The subsystems which will be flown on future manned missions will probably not follow from existing terrestrial technology, but will have to be developed with specific space applications in mind.

In general, LSS requirements are mission-specific (e.g., oxygen recovery from carbon dioxide is less problematic if food is regenerated by plant growth). The trade-offs of resupply versus regeneration of LSS materials are somewhat sensitive to the mission scenario (e.g., the type of power generators affect the power penalty which, in turn, may impact each of the options differently). Thus, the selection of LSS subsystems for a given mission usually occurs during the mission definition phase. At that point in time, planners are usually very hesitant to select processes that are not fully developed. Their focus is primarily systems integration and their job is made considerably harder if they choose to consider technologies still under development.

Thus, we have the Catch-22 of LSS technologies. There is usually little funding available to do development work for potential missions, yet there is not enough time to develop technology for a defined mission. Hence, we must develop less costly methods of LSS technology development so that we can build capabilities prior to the definition of missions.

DEVELOPING LSS PROCESSES

Process development of physical/chemical systems has traditionally been an art rather than a discipline. There are few books written on the subject and practically no formal training offered on it at the universities. Given that process development is usually a costly and time-consuming activity, the challenge is to devise new processes as quickly and as cheaply as possible.

activity, the challenge is to devise new processes as quickly and as cheaply as possible. The tools available to the process developer are theory, empiricism, and reasoning (usually by analogy). The theory is embodied in equations governing (i) the properties (thermodynamic, kinetic and transport properties) of materials and (ii) the mass and energy balances for the unit operations. Experimentation is used to characterize those phenomena which are not adequately defined by theory or which cannot be estimated accurately by using analogies.

The conventional wisdom is that experimentation is far more expensive than calculations. Today, where algorithms are available for computer calculations of many phenomena, there is no question that computation should supercede experimentation wherever possible.

There are three levels of experimentation: laboratory scale, preprototypes and integrated testbeds. By laboratory scale we mean relatively simple experiments which are devised to evaluate parameters which cannot be estimated accurately by calculation (e.g., a bench scale reactor to obtain kinetic data). A preprototype is usually an entire system built to demonstrate the process as a functional unit in a real environment (e.g., a washwater recovery unit at a realistic scale using real wastes). It should include process control hardware and software so that safety and reliability issues are adequately addressed at the preprototype stage. Testbeds are integrated subsystems which are used to demonstrate the adequacies of interfaces in chambers which simulate the isolation of a space environment.

Preprototypes are usually very costly to design, build and test. Prior to entering this phase, the entire process should be evaluated as rigorously and as stringently as possible. For LSS applications, sufficient calculations and laboratory experiments should have been performed so that trade-off analyses can be made vis-a-vis alternatives.

In the past, a number of processes have reached the preprototype stage and subsequently have been found not to be appropriate to the LSS requirement. Whereas 15 years ago, the lack of available theory and computational capacity may have dictated more costly experimentation, it is possible today to prove technical feasibility and appropriateness of candidate processes to LSS requirements prior to building preprototypes and conducting costly experimental programs.

COMPUTERIZED MODELING AND SIMULATION

Computerized modeling and simulation (CMAS) is a tool that can greatly reduce both the time and cost of technology development. By CMAS, we refer to computerized methods for solving the phenomenological equations of physical/chemical processes (i.e., process conditions based on properties of materials and mass and energy balances, equipment sizing based on rate processes and the governing equations for unit operations). Over the past ten years, several such computerized packages have become sophisticated enough to be used to design and simulate highly complex and integrated chemical and petrochemical facilities. The one we illustrate herein is ASPEN PLUS, offered commercially by Aspen Technologies, Inc. (Cambridge, Massachusetts, USA).

CMAS systems, in general, operate as follows:

1. The inputs required are a flowsheet, compositions of inlet streams and stoichiometries of chemical reactions.
2. The user selects physical property correlations to describe the different streams, appropriate models for each of the unit operations, and design specifications and constraints.
3. The CMAS system internally calculates mass and energy balances, including self-consistent compositions and conditions of all streams.
4. The system outputs reports, in user-specified formats, which can include compositions and conditions of all streams as well as heat and power requirements of each device and unit operation.

Some of the major advances provided by CMAS systems in the past ten years are:

1. Highly sophisticated and complex correlations for physical properties of non-ideal gases, liquids, supercritical fluids, multicomponent mixtures, and aqueous solutions including concentrated electrolytes.
2. Highly efficient convergence methods to solve for multicomponent phase equilibria and simultaneous chemical equilibria of multiple reactions, even in processes with multiple recycle streams.
3. Increased speed and memory, along with reduced cost of a new generation of computers, increasing the market for CMAS systems.

The result is a powerful tool for developing LSS technology. In particular, CMAS systems can be used to evaluate a process design with minimal requirements for laboratory experimentation. Specifically, we foresee the application of CMAS in the following typical steps in process development leading up to the preprototype stage.

1. Evaluate proposed processes to determine if they warrant development. Use best case

assumptions and determine resource requirements. Are they prohibitive?
2. Propose and evaluate alternative process designs. Can reconfiguring of process steps lead to significant reductions in resource requirements?
3. Identify critical assumptions. Through sensitivity analysis, determine which steps in the process are the key to meeting performance goals.
4. Develop lab scale experimental design. Devise relatively simple experiments to demonstrate technical feasibility of key steps and to verify critical assumptions for meeting performance goals.
5. Define stable operating conditions. Develop the supervisory control logic. Define the fault tree, devise off-spec conditions, and develop responses to alarms.
6. Reevaluate potential performance and resource requirements based on laboratory results. Conduct trade-off analyses and compare to existing alternatives for meeting LSS requirements.

AN EXAMPLE: ASPEN MODEL OF A VAPOR COMPRESSION DISTILLATION (VCD) SYSTEM

VCD is considered to be a mature process for water recovery from urine, flush water and wash water concentrate. It has been under development for aerospace applications for about 25 years and is considered to be a prime candidate for deployment on the Space Station. The only existing computational model of a VCD system is the G189 thermal model to calculate the heat rejection rate /1,2,3,4,5,6/.

Process Description

Figure 2 is a schematic of the type of VCD system developed by NASA /6/. Urine and flushwater are collected and stored, usually with addition of pretreatment chemicals to reduce the carryover of ammonia. When the Storage Tank reaches a high level mark, the VCD system is activated in a batch mode. The pressure in the VCD recycle loop is reduced by opening the purge (to vacuum) valve. When the Evaporator Cylinder pressure falls to the vapor pressure of the waste at ambient temperature, the purge valve is closed. The pumps and compressor are then turned on to begin the batch. The Vapor Compressor draws vapors out of the Evaporator Cylinder, reducing that pressure and creating the driving force for vaporizing water (and volatiles) from the waste. The vapor stream leaves the Vapor Compressor at an elevated pressure. Provided that this pressure is higher than the dew point pressure of the vapor at the temperature of the Condenser Cylinder, condensate will form. The condensing surface is the outer wall of the Evaporator Cylinder. Therefore, the heat of condensation provides the heat of evaporation.

The condensate is withdrawn through the product pump and passed through a Polishing Column for posttreatment. The Ion Conductivity Monitor is a failure mode detector that activates the Diverter Valve if the condensate conductivity exceeds a set point.

As water is evaporated, the waste becomes more concentrated. Eventually, the solution reaches a saturated condition with respect to some solute and solid precipitate begins to form in the Evaporator Cylinder. In order to remove the solid and prevent clogging, the Recycle Pump provides a waste flowrate through the Evaporator Cylinder that is large relative to the evaporation rate. Thus, the recycle stream flushes the solids out of the Evaporator Cylinder and carries them to the Waste Recycle Tank, where they accumulate. As the level in the Waste Recycle Tank decreases, more feed is transferred from the Waste Storage Tank. The process continues until the level in the Storage Tank drops below a preset value.

The process is terminated and the Waste Recycle Tank is emptied (or replaced with an empty one) when the Ion Conductivity Monitor exceeds the high limit set point or the product water flow rate drops below a minimum production rate.

The fall in production rate results from the following phenomenon. As a cycle proceeds, the solute concentration in the recycle waste continues to increase with consequential decrease of the vapor pressure in the Evaporator Cylinder. (There is no external heating applied to Condenser/Evaporator Cyclinder. This "passive" control means that the cylinders always operate near ambient temperature.) The Vapor Compressor, which operates at a constant rotational speed, provides a constant compression ratio. Thus, the outlet pressure of the compressor decreases as the solute concentration increases, and the production rate falls. At some point in the cycle, the outlet pressure of the compressor will drop below the dew point pressure at the condenser temperature and the unit will cease to produce condensate.

ASPEN PLUS Model

The first step in developing a model is to translate the process flowsheet into a model block diagram. Figure 3 is an ASPEN PLUS block diagram corresponding to the flowsheet of Figure 2. Each of the boxes represents one or more unit operations in the actual process. The lines between boxes represent material streams. The dotted lines represent heat and work interactions (which are called heat and work 'streams'). The labels in the boxes correspond to block identification names supplied by the user and ASPEN PLUS unit operation types in parentheses. The stream labels are names provided by the user.

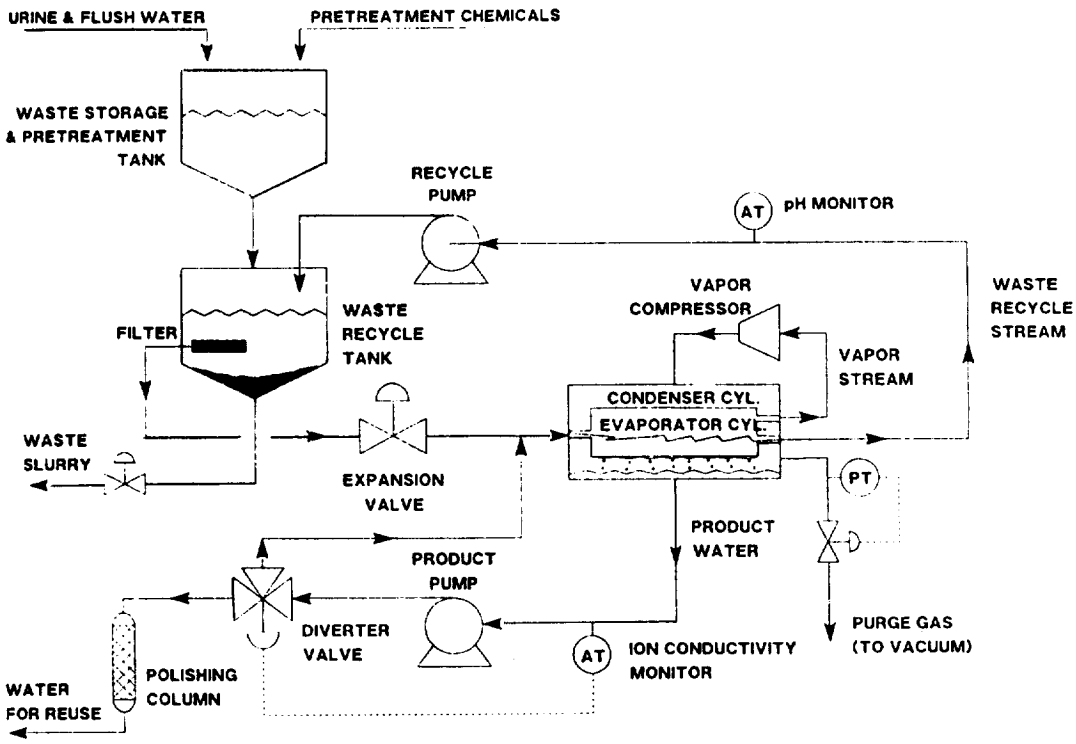

Fig. 2. Schematic of a vapor compression distillation system.

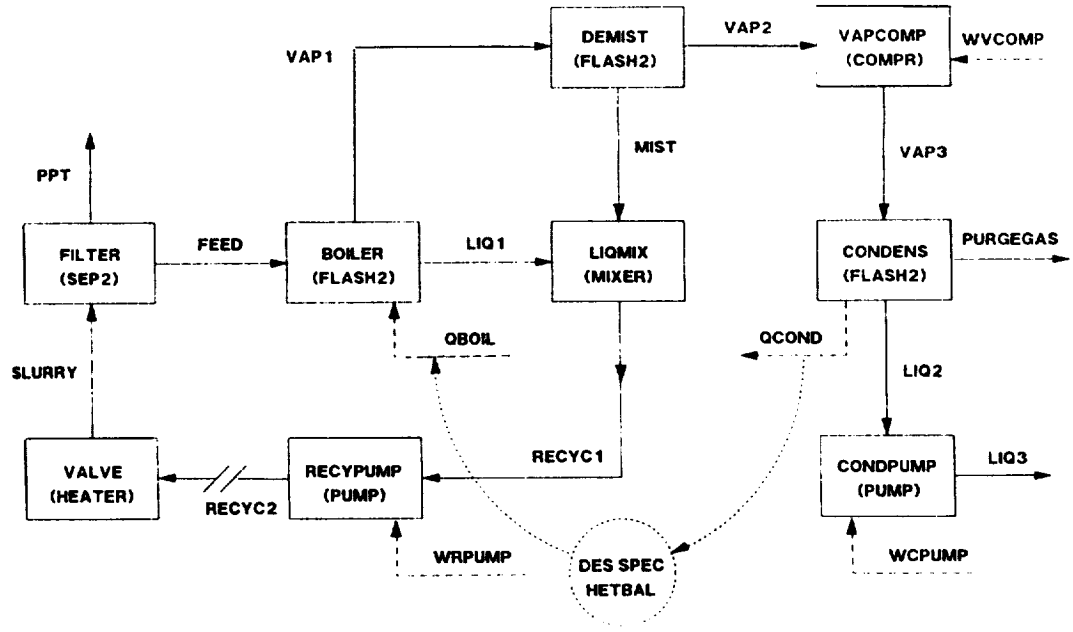

Fig. 3. ASPEN PLUS block diagram for a vapor compression distillation system.

The simulation of Figure 3 involves six types of unit operations: separators, mixers, heaters, flashers, pumps, and compressors. Examples of each are shown in Figure 4, along with the allowed inputs and outputs. In this example, the separator block is used to simply split a multiphase stream into separate phases. Mixers combine two or more streams. A mixer block performs material and energy balances. It also performs an adiabatic flash calculation on the exit stream so that if multiple phases are present, they will be at thermodynamic equilibrium. Heater blocks allow input of heat streams, while flash blocks provide for separate outlet streams for vapor, liquid and solid phases. Pumps and compressor blocks perform polyisentropic calculations for noncompressible and compressible fluids, respectively.

After generating the ASPEN PLUS block diagram, the chemical composition of the feed and physical property models need to be specified. Urine is a complex mixture of inorganic and organic compounds, as shown in Table 2 /7/. For the purpose of simulating the operation of the VCD unit, the physical properties of importance are aqueous phase solubilities and activity coefficients, and vapor pressures above the aqueous solution for water and solutes. To illustrate the methodology, we shall simplify urine composition to a five component mixture: water, sodium chloride, potassium chloride, urea and creatinine. The four solutes represent roughly 66% of the total dissolved solids typically found in urine.

The ASPEN PLUS input file for the VCD process, as described and simplified above, is shown in Table 3. The first statement is the user-defined title. [The semicolon denotes comments which are ignored by the ASPEN PLUS compiler.] Statements 2 to 4 concern default overrides for units, run time control and reports. Statements 5 to 7 define the components in terms of a user-defined name and the ASPEN PLUS database name (for those components that are present in one or more of the databases). The 'S' after component names (e.g., NACLS) indicates a solid phase. As defined in statement 8, this simulation will access the ASPEN PLUS Aqueous and Solids databases, in addition to the ASPEN PLUS pure component database (by default). For components that are not yet incorporated in one of the databases, additional property data are required. For this case, we have entered molecular weight for creatinine and urea in statements 9 to 14. Vapor pressures would have been entered here if they were known.

Statement 15 defines the default property models to be used in the simulation. SYSOP15M is used for aqueous mixtures with electrolyte and molecular solutes, as we have here. The CHEMISTRY=UREA declaration in statement 15 refers to the chemical reaction stoichiometries and equilibrium constants given in statements 16 to 26.

Statements 27 to 36 define the connectivity of blocks by input and output streams. These statements provide the simulator with the type of information shown in Figure 3. Statements 38 to 40 define the feed stream condition, while Statements 41 to 60 define each of the unit operation blocks (type of unit operation and values of independent variables, as defined in Figure 4).

Statements 61 to 67 define a Design Specification, which was given the user-defined name of HETBAL. As shown in Figure 3, this design specification relates the heat of evaporation and the heat of condensation. Alternatively, one could incorporate here a block of user-written Fortran code to describe the rate of heat transfer to and from the Evaporator and Condenser Cylinders.

Statements 68 to 71 and 72 to 73 are convergence statements used to define the method of solution of iterative processes such as the trial-and-error solution of the HETBAL design specification.

Of special interest here is the convergence block named CV1, statements 68 to 71. This convergence statement was devised to simulate the batch process by which VCD occurs. The TEAR FEED statement indicates that the stream FEED is to be the tear stream in solving for the conditions around the recycle loop (see Figure 2). The term DIRECT in statement 68 indicates that we want the iteration to proceed by direct substitution. In other words, the calculation begins by assuming the initial estimates of mass flow rates for stream FEED are correct as given in statements 38 to 40, and proceeds to calculate subsequent stream conditions around the recycle loop until it gets back to stream FEED through block FILTER. (The SEQUENCE statements of 127 to 129 give the user-defined order of calculations so that the ASPEN PLUS-generated default sequence is overridden.) If the final and initial compositions of stream FEED are not equal (within the default tolerance), then the new values of FEED are substituted directly for the old ones, and the next iteration begins. Because we have specified that a fraction of the stream entering block BOILER is to be vaporized every time this block is executed, we insure that the convergence block CV1 is never satisfied. Thus, the feed stream becomes more and more concentrated every time the calculation proceeds around the loop.

Statements 75 to 126 are Fortran statements for writing out the intermediate stage values for steps during the iterations. It is in this manner that we obtain the conditions during the batch.

For the simplified, five component mixture we used in Table 3, the results obtained by our

Fig. 4. ASPEN PLUS block inputs and outputs.

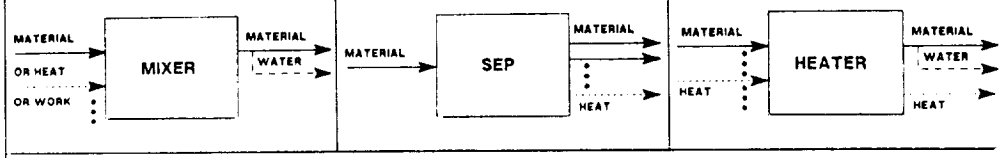

FLOWSHEET INPUTS		
Two or more material streams, or two or more heat streams, or two or more work streams.	One material stream	Any number of material streams; any number of heat streams
FLOWSHEET OUTPUTS		
One heat stream; or one work stream; or one or two material streams (second for optional water decant stream.	Two or more material streams, one heat stream optional.	One or two material streams (second for optional water decant stream); one heat stream optional.
INPUT SPECIFICATIONS		
The user may specify the outlet pressure or let it default to the minimum pressure of the inlet streams. An adiabatic flash is always performed on the product.	For each outlet stream, except the last outlet stream, the user gives one of the following specifications for each component present in the stream: 1. Fraction of the component in the inlet 2. Mole flow rate of the component 3. Mass flow rate of the component 4. Standard liquid volume flow rate of the component Any remaining flow is placed in the last outlet stream. For nonisothermal separations, the user should supply flash specifications for each outlet stream.	For a two-phase or three-phase flash, the following variables may be specified: 1. Pressure and one of the following: Temperature, Temperature Change, Degrees of Superheat, Degrees of Subcooling, Vapor Fraction, Heat Duty 2. Temperature (or Temperature Change) and one of the following: Pressure, Vapor Fraction, Heat Duty For a single phase calculation, pressure and one of the following must be specified: Temperature, Temperature Change, Heat Duty

Fig. 4 (continued). ASPEN PLUS block inputs and outputs.

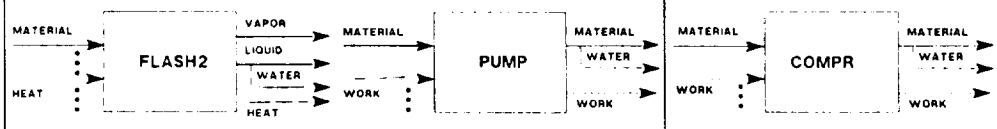

FLOWSHEET INPUTS		
One or more material streams; any number of heat streams.	One material stream; any number of work streams.	One material stream; any number of work streams.
FLOWSHEET OUTPUTS		
Two or three material streams (first for vapor, second for liquid, third for optional water decant stream); one heat stream optional.	One or two material streams (second for optional water decant stream); one work stream optional.	One or two material streams (second for optional water decant stream); one work stream optional.
INPUT SPECIFICATIONS		
Two of the following four variables must be supplied: temperature, pressure, vapor fraction, or heat duty. FLASH2 accepts any combination except vapor fraction and heat duty. If solids are present, they leave at the same temperature as the fluid phases but do not participate in the equilibrium calculations. Liquid or solids entrainment in the vapor stream may also be specified.	Either the outlet pressure, the pressure change, the pressure ratio, or the power must be specified. In addition, the efficiency must be specified. If efficiency is not specified, built-in efficiency curves for water in a centrifugal pump are used. Driver efficiency may also be specified. PUMP is designed to handle a single incompressible phase. However, the user may specify that a two-phase or three-phase flash calculation be performed to determine the outlet stream conditions and to compute the fluid density used in the pump equations.	The type of compressor is always specified. For all types of compressors and turbines, the mechanical efficiency may be specified. COMPR is designed for a single, compressible phase. However, the user may specify that two-phase flash calculations be performed to determine the outlet stream conditions and to compute the properties used in the compressor equations.

TABLE 2. An Analog Representing the Composition of Typical Human Urine (Putnam, 1970).

CHEMICAL SPECIES	FORMULA	FORMULA WEIGHT	AMOUNT (mg/l)
INORGANIC SALTS			14,157
Sodium Chloride	NaCl	58.4	8,001
Potassium Chloride	KCl	74.6	1,641
Potassium Sulfate	K_2SO_4	174.3	2,632
Magnesium Sulfate	$MgSO_4$	120.4	783
Magnesium Carbonate	$MgCO_3$	84.3	143
Potassium Bicarbonate	$KHCO_3$	100.1	661
Potassium Phosphate	K_3PO_4	212.3	234
Calcium Phosphate	$Ca_3(PO_4)_2$	310.2	62
UREA	H_2NCONH_2	60.1	13,400
ORGANIC COMPOUNDS			5,369
Creatinine	$C_4H_7N_3O$	113.1	1,504
Uropepsin (as Tyrosine)	$HO.C_6H_4.C_2H_3(NH_2).CO_2H$	181.2	381
Creatine	$HN:C(NH_2)N(CH_3).CH_2.CO_2H.H_2O$	149.2	373
Glycine	$NH_2.CH_2.CO_2H$	75.1	315
Phenol	C_6H_5OH	94.1	292
Histidine	$C_3H_3N_2.CH_2CH.(NH_2).CO_2H$	155.2	233
Androsterone	$C_{19}H_{30}O_2$	290.5	174
1-Methylhistidine	$C_3H_3N_2CH_2CH(NH.CH_3).COOH$	169.2	173
Imidazole	$C_3H_4N_2$	68.1	143
Glucose	$C_6H_7O_4(COCH_3)_5$	390.4	156
Taurine	$NH_2.CH_2.CH_2.SO_3H$	125.2	138
Cystine	$[HO_2C.CH(NH_2).CH_2S-]_2$	240.3	96
Citrulline	$NH_2CONH(CH_2)_3.CH.(NH_2).CO_2H$	175.2	88
Aminoisobutyric acid	$H_2N.CH_2$ / CH_3 >$CH.COOH$	103.1	84
Threonine	$C_4H_9O_3N$	119.1	83
Lysine	$(NH_2)_2C_6H_9.CO_2H$	146.2	73
Incloxysulfuric acid	$C_6H_5ON.H_2SO_4$	231.2	77
m-Hydroxyhippuric acid	$C_6H_4COHC(CONH.CH_2COOH)$	195.2	70
Inositol	$C_6H_{12}O_6$	180.2	70
Urobilin	$C_{33}H_{42}O_6N_4$	588.7	63
Tyrosine	$HO.C_6H_4.C_2H_3(NH_2).CO_2H$	181.2	54
Asparagine	$HO_2C.CH(NH_2).CH_2.CONH_2$	132.1	53
Organics >50 mg/l			606
ORGANIC AMMONIUM SALTS			4,131
Ammonium:			
Hippurate	$NH_4C_6H_5CO.NHCH_2.CO_2$	196.2	1,250
Citrate	$(NH_4)_3HC_6H_5O_7$	226.2	756
Glucuronate	$NH_4C_6H_9O_7$	211.1	663
Urate	$NH_4C_5H_3O_3N_4$	185.1	518
Lactate	$(NH_4)_2C_3H_4O_3$	127.1	394
L-Glutamate	$NH_2HO_2C.CHNH_2.(CH_2)_2.CO_2$	164.1	246
Asparate	$NH_4C_4H_6O_4N$	150.1	135
Formate	NH_4HCO_2	63.1	88
Pyruvate	$NH_4CH_3.CO.CO_2$	88.1	44
Oxalate	$(NH_4)_2C_2O_4$	124.0	37
Total Solutes			37,057

'pseudo-steady-state' approach are shown in Figs. 5 and 6. The vapor pressure in the Evaporator Cylinder is shown in Figure 5 as a function of water recovery. We note that the vapor pressure falls very slowly until about 80% water recovery. At 90% water recover, the vapor pressure has dropped to 10% below the initial value, while at 98%, it has dropped to 67% of the initial value.

Figure 6 is a blowup of the 90 to 100% water recovery region. Also shown are the salt precipitation curves for the four solutes. We note that these solutes begin precipitating out at 97% water recovery. [Although the four solutes chosen represent the species of highest concentration, they are not necessarily the first to precipitate out.]

The final step in the CMAS process is model validation. Given results such as those of Figure 6, a relatively few, quite simple batch distillation experiments would provide sufficient data for either validating the model or providing additional data to derive activity coefficient correlations for the molecular solutes in concentrated solutions. (ASPEN PLUS already has an excellent correlation for salt activity coefficients in dilute to concentrated solutions.)

Given a validated model, the process development could proceed in a rapid and very efficient fashion. For example, the compression ratio of vapor compression impacts the power required:

TABLE 3. ASPEN PLUS INPUT FILE FOR THE VCD SIMULATION.

```
TITLE ' SIMULATION OF A VCD UNIT WITH PSEUDO-SS APPROACH'
;
IN-UNITS ENG
;
RUN-CONTROL MAX-TIME=500
STREAM-REPORT MASSFLOW NOZEROFLOW
;
; MODEL THE FEED AS A MIXTURE OF H2O, NACL, KCL, UREA, AND
; CREATININE. NACL AND KCL DISSOCIATE TO NA+, KCL+ AND CL-
;
COMPONENTS H2O H2O/NACL NACL/NACLS NACL/KCL KCL/KCLS KCL/
      NA+ NA+/CL- CL-/K+ K+/UREAS MEA/UREA MEA/
      CREATS MEA/CREAT MEA
;
; DATABANKS ACCESSED FOR PURE COMPONENT PROPERTIES
;
DATABANKS AQUEOUS/SOLIDS
;
; PROVIDE DATA FOR COMPONENTS NOT IN ASPEN DATABANKS
;
PROP-DATA
   PROP-LIST      MW
    PVAL CREAT  113.1
    PVAL CREATS 113.1
    PVAL UREA    60.1
    PVAL UREAS   60.1
;
; ELECTROLYTE NRTL ACTIVITY COEFFICIENT MODEL USED FOR
; SOLVENT-SOLUTE INTERACTIONS IN THE AQUEOUS PHASE
;
PROPERTIES SYSOP19M CHEMISTRY=UREA
;
; SPECIFY COMPLETE DISSOCIATION OF NACL AND KCL;
; ALSO, SPECIFY SALT DISSOLUTION RELATIONSHIPS AND
; SOLUBILITY PRODUCT CONSTANTS
;
CHEMISTRY UREA
      DISS NACL  NA+ 1 / CL- 1
      DISS KCL   K+  1 / CL- 1
      SALT NACLS NA+ 1 / CL- 1
      SALT KCLS  K+  1 / CL- 1
      SALT CREATS CREAT 1
      SALT UREAS  UREA  1
      K-SALT KCLS  -2.159 -1165.
      K-SALT NACLS -3.564 -524.0
      K-SALT CREATS -4.2926
      K-SALT UREAS  -1.3359
;
; SPECIFY PROCESS FLOWSHEET
;
FLOWSHEET
   BLOCK BOILER   IN=FEED          OUT=VAP1   LIQ1 QBOIL
   BLOCK DEMIST   IN=VAP1          OUT=VAP2   MIST
   BLOCK LIQMIX   IN=LIQ1  MIST    OUT=RECYC1
   BLOCK VAPCOMP  IN=VAP2  WCOMP   OUT=VAP3
   BLOCK CONDENS  IN=VAP3          OUT=PURGEGAS LIQ2 QCOND
   BLOCK CONDPUMP IN=LIQ2  WCPUMP  OUT=LIQ3
   BLOCK RECYPUMP IN=RECYC1 WRPUMP OUT=RECYC2
   BLOCK VALVE    IN=RECYC2        OUT=SLURRY
   BLOCK FILTER   IN=SLURRY        OUT=PPT      FEED
;
; SPECIFY INITIAL FEED STREAM CONDITIONS
;
STREAM FEED TEMP=115 VFRAC=0
  MASS-FLOW H2O 1000[GM/SEC]/NACL 8.0[GM/SEC]/
   KCL 1.64[GM/SEC]/UREA 13.4[GM/SEC]/CREAT 1.50[GM/SEC]
;
; SPECIFY HEAT AND WORK STREAMS
;
DEF-STREAMS  HEAT  QBOIL   QCOND
DEF-STREAMS  WORK  WVCOMP  WCPUMP  WRPUMP
;
; SPECIFY CONDITIONS FOR EACH UNIT OPERATION BLOCK
;
BLOCK BOILER FLASH2
   PARAM TEMP=115 VFRAC=.005 ENTRN=.001
BLOCK DEMIST FLASH2
   PARAM PRES=0 DUTY=0
BLOCK LIQMIX MIXER
BLOCK VAPCOMP COMPR
   PARAM TYPE=POLYTROPIC PRATIO=2
BLOCK CONDENS FLASH2
   PARAM TEMP=125 VFRAC=0;
BLOCK RECYPUMP PUMP
   PARAM PRATIO=1.25
BLOCK CONDPUMP PUMP
   PARAM PRATIO=1.25
BLOCK VALVE HEATER
   PARAM TEMP=115 VFRAC=0
BLOCK FILTER SEP2
   FRAC STREAM=PPT COMPS=NACLS KCLS UREAS CREATS &
                  FRACS=1     1    1     1
   FLASH-SPECS FEED KODE=0
   FLASH-SPECS PPT  KODE=0
;
; DESIGN-SPEC TO MATCH DUTY OF BOILER TO CONDENS BLOCK
;
DESIGN-SPEC HETBAL
   DEFINE QCOND BLOCK-VAR BLOCK=CONDENS SENTENCE=PARAM &
      VARIABLE=QCALC
   DEFINE QBOIL BLOCK-VAR BLOCK=BOILER  SENTENCE=PARAM &
      VARIABLE=QCALC
   SPEC   'DABS(QBOIL/(.95D0*QCOND))'  TO  1D0
   TOL-SPEC  1D-4
   VARY BLOCK-VAR  BLOCK-BOILER SENTENCE-PARAM &
      VARIABLE=VFRAC
   LIMITS  .001  900
;
; USE DIRECT SUBSTITUTION FOR RECYCLE SO THAT NEW BATCH
; COMPOSITION IS NOT CHANGED BY STEADY-STATE
; CONVERGENCE METHOD
;
CONVERGENCE CV1 DIRECT
   TEAR FEED
   PARAM MAXIT=100
;
; DEFINE A CONVERGENCE BLOCK FOR THE DESIGN-SPECIFICATION
;
CONVERGENCE CV2 SECANT
   SPEC HETBAL
;
; DEFINE A FORTRAN BLOCK TO WRITE THE LIQUID AND VAPOR
; STREAM VECTORS AT EACH 'TIME INCREMENT' TO A
; SEPARATE FILE (FILE 55)
;
FORTRAN RESUL
F      REAL*8 LIQH2O,LIQNAC,LIQKCL,LIQURE,LIQCRE
F      DIMENSION IPROG(2)
F      DATA INCR / 0 /
F     DATA SUMH2O, SUMNAC, SUMURE, SUMCRE, SUMKCL /5*0D0/
F      DATA IPROG / 'ZZFO', 'RT  ' /
   DEFINE VAPH2O MASS-FLOW STREAM=VAP3 COMPONENT=H2O
   DEFINE LIQH2O MASS-FLOW STREAM=LIQ1 COMPONENT=H2O
   DEFINE LIQNAC MASS-FLOW STREAM=LIQ1 COMPONENT=NACLS
   DEFINE LIQKCL MASS-FLOW STREAM=LIQ1 COMPONENT=KCLS
   DEFINE LIQURE MASS-FLOW STREAM=LIQ1 COMPONENT=UREAS
   DEFINE LIQCRE MASS-FLOW STREAM=LIQ1 COMPONENT=CREATS
   DEFINE PRES1  STREAM-VAR STREAM=LIQ1 VARIABLE=PRESSURE
   DEFINE PRES2  STREAM-VAR STREAM=VAP3 VARIABLE=PRESSURE
   DEFINE PRES3  STREAM-VAR STREAM=LIQ2 VARIABLE=PRESSURE
F      INCR = INCR + 1
F      SUMH2O = SUMH2O + VAPH2O
F      SUMNAC = SUMNAC + LIQNAC
F      SUMKCL = SUMKCL + LIQKCL
F      SUMURE = SUMURE + LIQURE
F      SUMCRE = SUMCRE + LIQCRE
F      RECH2O = SUMH2O / (1000D0/454D0*3600D0) * 1D2
F      RECNAC = SUMNAC / (   8D0/454D0*3600D0) * 1D2
F      RECKCL = SUMKCL / (1.64D0/454D0*3600D0) * 1D2
F      RECURE = SUMURE / (13.4D0/454D0*3600D0) * 1D2
F      RECCRE = SUMCRE / (1.50D0/454D0*3600D0) * 1D2
F      WRITE(55, 8) INCR
F      WRITE(55, 9) PRES1, PRES2, PRES3
F      WRITE(55,10) VAPH2O, SUMH2O, RECH2O,
F     &             LIQNAC, SUMNAC, RECNAC,
F     &             LIQKCL, SUMKCL, RECKCL,
F     &             LIQURE, SUMURE, RECURE,
F     &             LIQCRE, SUMCRE, RECCRE
F      IF ( PRES2 .LT. PRES3 ) THEN
F        WRITE(55,12)
F        WRITE(NHSTRY,12)
F        CALL QUIT
F      ENDIF
F    8 FORMAT(/2X,'INCREMENT : ', I4 )
F    9 FORMAT( 2X,'  PRESSURES (PSIA): BOILER     = ',
F     & F10.3/ 2X,'                     COMPRESSOR = ',
F     & F10.3/ 2X,'                    CONDENSER = ',F10.3)
F   10 FORMAT (2X,'                   INCREMENTAL    TOTAL
F     &RECOVERY'2X,'                     (LB/HR)     (LB/HR)
F     &  (WT %)'/ 2X,'  H2O VAPOR      ', F10.3, 4X, F10.3,
F     & 2X,F10.3/ 2X,'  NACL SOLID PPT ', F10.3, 4X, F10.3,
F     & 2X,F10.3/ 2X,'  KCL  SOLID PPT ', F10.3, 4X, F10.3,
F     & 2X,F10.3/ 2X,'  UREA SOLID PPT ', F10.3, 4X, F10.3,
F     & 2X,F10.3/ 2X,'  CREATININE PPT ', F10.3, 4X, F10.3,
        2X, F10.3)
F   12 FORMAT (/2X,'CALCULATIONS STOPPED. REASON:
   COMPRESSOR OUTLET'
F     &/ 2X,'PRESSURE DROPPED BELOW CONDENSER PRESSURE.'/
F     &  2X,'"CONDPUMP" NOT EXECUTED.' )
;
; SPECIFY THE COMPUTATIONAL SEQUENCE
;
SEQUENCE  TOT CV1 CV2 BOILER DEMIST VAPCOMP CONDENS
  (RETURN CV2) & LIQMIX RECYPUMP VALVE FILTER RESUL
  (RETURN CV1) & CONDPUMP
```

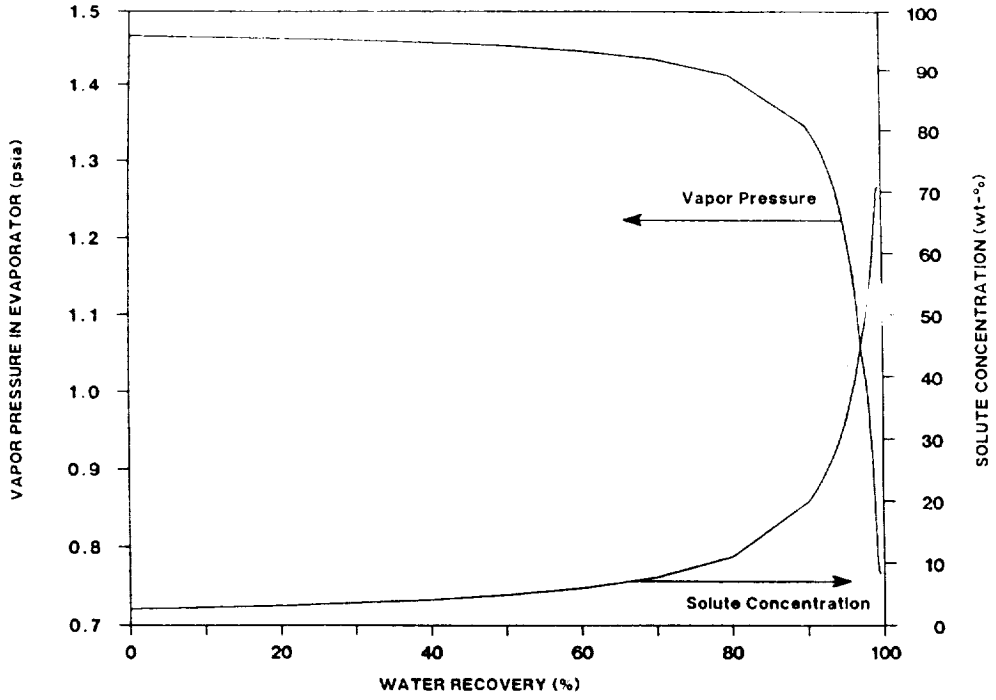

Fig. 5. ASPEN PLUS simulation results for VCD evaporator vapor pressure and solute concentration.

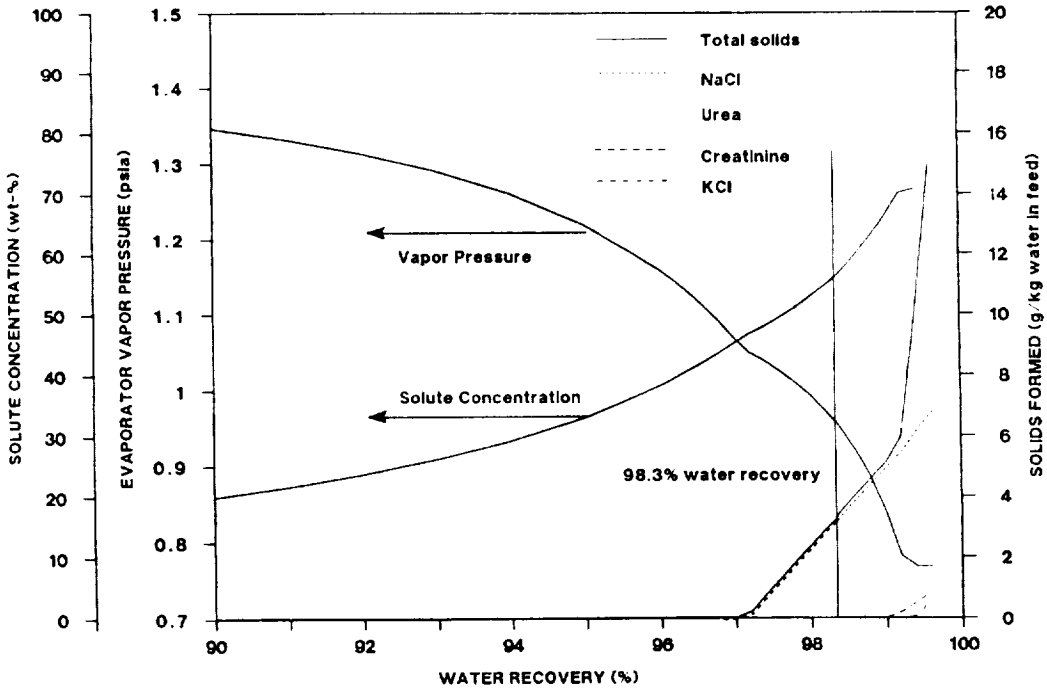

Fig. 6. ASPEN PLUS simulation results for solids precipitation in VCD.

a high compression ratio results in wasted power during the early part of the cycle when the vapor pressure is still high, but it allows one to reach a high water recovery factor near the end of the process. In other words, there is an optimum compression ratio. An ASPEN PLUS case study to locate that optimum could run in a matter of hours. Similarly, some relatively simple lab scale experiments to measure vapor pressure of solutes would allow us to calculate the carry-over organics to the condenser which, in turn, would allow us to estimate the amount of carbon needed for posttreatment.

CONCLUSIONS

We have tried to demonstrate, by example, the process of developing a CMAS model. The VCD technology is a good one for illustrating a number of points where CMAS can help to make the overall technology development effort more efficient. The necessity of generating a flowsheet and choosing unit operations to simulate the real process forces the engineer to better understand the process (e.g., what terminates the VCD process in the absence of an on-line measure of dissolved solids?). The model validation process will usually help to identify relatively simple, but very important lab scale experiments. Case studies and sensitivity analyses will provide a good assessment of which variables are truly important and which others we need not spend much time on.

As we have also seen herein, the CMAS systems developed for the chemical industry are not ideally suited to LSS technology for small colonies. Most systems designed for space life support are small and batch-operated. Although the commercial CMAS systems were designed for large, steady-state processes, we have shown that they can be readily modified to simulate batch operation.

REFERENCES

1. McDonnell Douglas Astronautics Company, Computer Aided System Engineering and Analysis (CASE/A) User's Manual, ECLSS Series, prepared for NASA under Contract NAS8-36407 (1987).

2. P.P. Nuccio, and W.J. Jasionowski, Automatic Water Recovery System, Report to the Aerospace Medical Research Laboratories under Contract AF 33(615)-2124 (1968).

3. P.P. Nuccio, Vapor Compression Distillation Module, Chemtric Report 3110 to NASA under Contracts NAS9-13714 and NAS9-14234 (1975).

4. Lockheed Missiles & Space Company, Development of a Preprototype Vapor Compression Distillation Water Recovery Subsystem, Report to NASA under Contract NAS9-15136 (1978).

5. G.S. Ellis, R.A. Wynveen, and F.H.Schubert, Preprototype Vapor Compression Distillation Subsystem, Final Report to NASA under Contract NAS9-15267, Life Systems, Inc. (1979).

6. E.M. Zdankiewicz, and F.H. Schubert, Development of an Advanced Prototype Vapor Compression Distillation Subsystem (VCDS) for Water Recovery, Final Report to NASA under Contract NAS9-16374, Life Systems, Inc. (1984).

7. D.F. Putnam, Composition and Concentrative Properties of Human Urine, Report to NASA under Contract NAS1-8954, McDonnell Douglas Astronautics Company (1970).

SECTION III

CARBON CYCLING

N90-15440

PRODUCTIVITY AND FOOD VALUE OF *AMARANTHUS CRUENTUS* UNDER NON-LETHAL SALT STRESS

Bruce A. Macler and Robert D. MacElroy

National Aeronautics and Space Administration,
Ames Research Center, Moffett Field, California, 94035, U.S.A.

ABSTRACT

Stress effects from the accumulation of metal salts may pose a problem for plants in closed biological systems such as spacecraft. This work examined the effects of salinity on growth, photosynthesis and carbon allocation in the crop plant, *Amaranthus*. Plants were germinated and grown in modified Hoagland's solution with NaCl concentrations of 0 to 1.0%. Plants received salt treatments at various times in development to assess effects on particular life history phases. For *Amaranthus cruentus* , germination, vegetative growth, flowering, seed development and yield were normal at salinities from 0 to 0.2%. Inhibition of these phases increased from 0.2 to 0.4% salinity and was total above 0.5%. 1.0% salinity was lethal to all developmental phases. Onset of growth phases were not affected by salinity. Plants could not be adapted by gradually increasing salinity over days or weeks.

Water uptake increased, while photosynthetic CO_2 uptake decreased with increasing salinity on a dry weight basis during vegetative growth. Respiration was not affected by salinity. After flowering, respiration and photosynthesis decreased markedly, such that 1.0% NaCl inhibited photosynthesis completely. Protein levels were unchanged with increasing salinity. Leaf starch levels were lower at salinities of 0.5% and above, while stem starch levels were not affected by these salinities. The evidence supports salt inhibition arising from changes in primary biochemical processes rather than from effects on water relations. While not addressing the toxic effects of specific ions, it suggests that moderate salinity *per se* need not be a problem in space systems.

INTRODUCTION

Amaranthus is a genus of broadleaf plant found throughout the world. Originally a basic food of the Aztecs and Incas, it is now widely utilized in Africa, the Mideast, southern India, southern China and Southeast Asia as well /1/. It is cultivated both for its grain and as a leafy vegetable. Amaranth grain is about 16% protein and is unusually high in lysine /2/. Vegetable amaranth may be greater than 30% protein on a dry weight basis. For vegetable use, amaranth is harvested after 3 to 6 weeks of growth, when nearly all of the plant may be eaten. Thus as a candidate for use as a crop plant in space or as part of a plant-based closed-loop life support system (CELSS), a significant advantage of amaranth is its high edibility and potentially low waste.

As a plant genus including many weed species, *Amaranthus* is generally hardy and can grow under a broad range of conditions. In the closed space environment, water and gases will undoubtedly be recycled and will be subject to the build-up of a variety of contaminants. Of concern will be the effect of metal salts that may accumulate in the plant nutrient system from repeated excess application of essential trace minerals, leachate from metalic spacecraft hardware, or residue from recycling systems. For example, excess sodium chloride may interfere with plant ion transport, metabolism and mineral nutrition, ultimately affecting growth, productivity and food value /3/. *Amaranthus* has beeen little studied with respect to salt effects. As typical of a C4 plant, a sodium requirement has been demonstrated /4/, but toxic levels have not been determined. To examine the effects of salts on *Amaranthus* , we undertook a series of experiments to quantify growth, development, photosynthesis and selected metabolites under increasing salinity stress. While the work reported here does not assess the effects of all ions, it gives a general view to the limits of total salinity in the plant growth medium.

METHODOLOGY

Amaranthus cruentus seeds, collected in Kenya during 1987, were a gracious gift of Daniel Harder, U.C. Berkeley. These were planted in equal parts perlite, peat moss and sand in 4" pots and maintained under full sunlight in a greenhouse. Plants were watered daily for the first 2 or 4 weeks with half-strength NaCl-free Hoagland's solution. Subsequently, the plants were watered daily with Hoagland's containing either 0, 0.1, 0.2, 0.5, 1.0 or 2.0% NaCl (1.0% NaCl = 0.17 M). Plants were watered until run-through was observed, allowed to stand in the solution for 5 min, then the excess solution removed.

Seed germination studies were done using 100mm petri dishes lined with glass fiber filter paper (Whatman GF/C). Dishes and filters were rinsed 10x with the appropriate salinity Hoagland's solution, seeds placed on the moist papers, dishes covered and incubated in the light at 27°C in a controlled temperature chamber. Seeds were checked daily for germination.

Photosynthesis and respiration were estimated by measurement of CO_2 uptake using an infra-red gas analyzer (IRGA, Lira Model 303). Plants were placed in 25 l. clear plexiglas and Lexan chambers under 400-500 $\mu mol/m^2s$ photosynthetic photon flux density (PFD) from cool-white fluorescent lamps. Chambers were temperature- controlled via water jackets. Gases were delivered to the chambers at 1.86 lpm.

Protein was measured by the method of Lowry, et al /5/. Starch was quantified by enzymatic hydrolysis to glucose using amyloglucosidase, followed by enzymatic determination of glucose /6/.

RESULTS

Seed Germination

Seeds were germinated in Hoagland's solution with salinities from 0 to 2.0% NaCl. *A. cruentus* germination was unaffected at salinities of 0 to 0.3% (Table 1). Seed germination was inhibited at 0.4% NaCl and above and did not occur above 0.6%.

TABLE 1 Inhibition of *A. cruentus* Germination by NaCl

Salinity:	0%	0.1%	0.2%	0.3%	0.4%	0.5%	0.6%	1.0%	2.0%
Percent germination:	68%	62%	58%	61%	40%	8%	6%	0%	0%

Average of 3 experiments of about 150 seeds each condition.

Vegetative Plant Growth.

Seedling and vegetative stage growth were similar to seed germination in their sensitivities to NaCl. Seedlings germinated in NaCl-free Hoagland's, then given Hoagland's with NaCl after one, two or four weeks of growth were severely inhibited by salinities of 0.5% and killed by salinities of 1.0% and above (Table 2). Plants did not develop tolerance to higher salinities by gradual increase in salinity over periods of weeks, but rather showed increasing inhibition. Water uptake increased on a dry weight basis with increasing salinity during vegetative growth (Table 2). Wilting was not observed at any salinity.

Flowering and Seed Development

Flowering occurred at 9 weeks after planting in plants at all non-lethal salinities and was not daylength dependent. Flowering was not inhibited by salinities to at least 1.0%. Plants grown at salinities of 0, 0.1, 0.2 and 0.5% NaCl for six weeks, then given 1.0% NaCl, flowered at the same time as controls. However, seed development was inhibited by salinities of 0.5% and above. These plants died within days of flowering.

TABLE 2 *A. cruentus* Vegetative Yield under NaCl Stress

Salinity:	0%	0.1%	0.2%	0.5%	1.0%	2.0%
Yield: (g dry wt/plant)	6.5	5.8	3.9	1.9	0.2	0.2
Water uptake: (ml/day/g dry wt)	6.4	7.0	8.5	9.8	18*	0

Plants watered with NaCl-free Hoagland's for first 2 weeks of experiment, then watered with Hoagland's at the indicated salinities. Values are averages of 2 experiments of about 10 plants each condition. *Prior to plant death.

Photosynthesis and Respiration

Plants initally on NaCl-free Hoagland's, followed by 6 weeks of NaCl-Hoagland's were assayed for photosynthesis and dark respiration by measuring CO_2 uptake and release respectively in environmentally-controlled chambers. The watering conditions were selected to provide plants before and during flowering with the same periods of salt treatment. Prior to flowering, photosynthesis decreased with increasing salinity, while respiration was unaffected (Figure 1). With the onset of flowering, photosynthesis decreased by 70% and was salinity independent from 0 to 0.5% NaCl. At 1.0% NaCl, plants showed a negative CO_2 uptake rate in the light. Respiration was inhibited 20 to 40% across all salinities tested, but was increasing with increasing salinity to 0.5%.

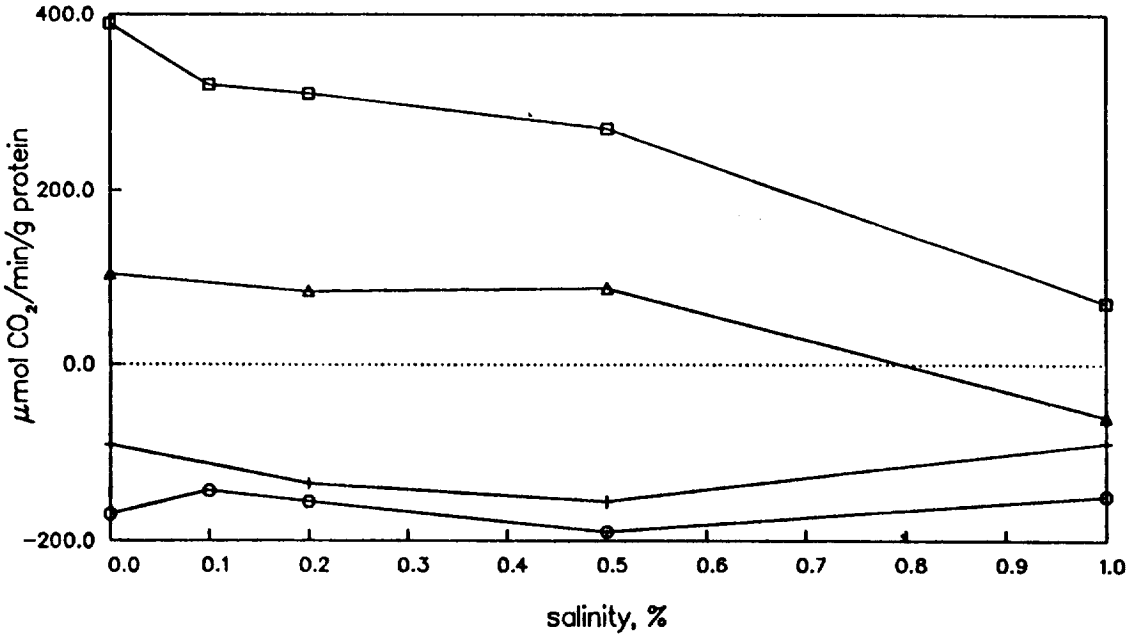

Fig. 1. Photosynthesis and respiration *vs.* salinity in *A. cruentus*. □, photosynthesis, vegetative plant; O, respiration, vegetative plant; Δ, photosynthesis, flowering plant; +, respiration, flowering plant

Protein and starch

Plants were sampled periodically throughout the experiments and assayed for protein and starch content. Protein levels in *A. cruentus* leaves were found to consistently increase at 0.1% NaCl, then decrease with increasing salinity (Table 3). Protein levels in plants treated with 1.0% or greater NaCl are those of the plants prior to beginning NaCl application and are consistent with the observed inhibition of metabolism. Protein levels in plant roots and stems appeared to be insensitive to NaCl and were the same before and after flowering. Stem and root protein levels were about half those found in leaf material. Starch levels were similar in leaves and stems at 0 and 0.2% NaCl (Table 3). Leaf starch levels were lower in plants at higher salinities, while stem starch levels were unchanged. Starch levels were constant from 6 weeks to 10 weeks, which included initiation of flowering.

TABLE 3 Protein and Starch at Different Salinities

Salinity:		0%	0.1%	0.2%	0.5%	1.0%
Protein: (mg/g dry wt)	leaf:	150	200	140	94	140
	stem:	52	51	52	55	58
Starch: (mg/g dry wt)	leaf:	49	68	52	18	21
	stem:	50	59	44	50	55

Values are averages of 3 experiments. Samples taken at 6 (vegetative), 8 (pre-flowering) and 10 (flowering) weeks of growth.

DISCUSSION

A. cruentus may be grown as a leafy vegetable or for its grain. Our work focused primarily on vegetative cultivation, since for space applications there are needs to minimize food preparation and waste recycling requirements. Also, as the data indicated, there was a marked decrease in photosynthesis and increase in respiration after flowering, which would limit air regeneration, a principal goal of a CELSS. As young vegetables, amaranth leaves in this lab were up to 20% protein and 5 to 10% starch under conditions not necessarily optimized for maximal food value. The complete mass balance yielded in addition 25% soluble materials (primarily sugars and amino acids), 40% cellulose and lignin, and 5% ash.

A. cruentus was tolerant of salinity to 0.5% NaCl, although partially inhibited by salinity above 0.2%. Plants could be grown from seed at 0.5% NaCl (although with lower germination rates), but grew much more slowly, and had lower dry weight yields. The data showed that 1.0% NaCl was lethal, inhibiting seed germination and, when added to healthy plants, suppressing photosynthesis below that level needed to replace respiratory losses. Leaf starch levels were markedly lower at 1.0% NaCl, indicating use of this for respiration prior to plant death. Since water relations and time course of development did not appear to be affected by increasing salinity, the decrease in photosynthetic CO_2 fixation may be the primary cause of decreased productivity. Kaiser, et al /8/ demonstrated these effects on photosynthetic dark reactions and ATP synthesis, but found no effect on primary photoreactions and electron transport.

From other work in this laboratory, it was found that other *Amaranthus* species, particularly *A. tricolor*, thrive at salinities to at least 1.5%, indicating that *A. cruentus* amongst members of the genus is particularly sensitive to NaCl. This suggests that salinity in the nutrient medium of a CELSS may not be a problem for some plants at the concentrations envisioned. Ballou /7/ determined for a typical CELSS that NaCl in recycled water would reach only 0.5% after 6 months of operation without any salt separation.

ACKNOWLEDGEMENTS

The authors wish to thank Ellen Moffatt, Esther Bamberg, Hanh Bui and Ellen Minor for their hours of high-quality work. This work was supported in part by the National Research Council, USA and the National Aeronautics and Space Administration.

REFERENCES

1. National Research Council, Amaranth, Modern Prospects for an Ancient Crop, National Academy Press, Washington, D.C. (1984)

2. J.P. Senft, Protein quality of amaranth grain, Rodale Res. Rep. 80-3, Rodale Press Inc, Emmaus, PA, (1980)

3. A. Lauchi and E. Epstein, Mechanisms of salt tolerance in plants, Calif. Ag. 38,18-20 (1984)

4. T. Matoh, O. Daisaku, and E. Takahashi, Effect of sodium application on growth of *Amaranthus tricolor* L., Pl. Cell. Physiol. 27, 187-192 (1986)

5. O.H. Lowry, N.J. Rosebrough, A. L. Farr, and R.J. Randall, Protein measurement with the Folin phenol reagent, J. Biol. Chem. 193, 265-275 (1951)

6. E. Raabo and T.C. Terkildsen, On the enzymatic determination of blood glucose, Scand. J. Clin. Lab. Invest.12, 402 (1960)

7. E.V. Ballou, Mineral separation and recycle in a controlled ecological life support system (CELSS), NASA contractor report #166388, NASA, Washington, D.C., March (1982)

8. W.M. Kaiser, G. Kaiser, P.K. Prachuab, S.G. Wildman and U. Heber, Photosynthesis under osmotic stress, Planta 153, 416-422 (1981)

A 90-15-491

GLOBAL DETERMINATIONS OF THE CARBON DIOXIDE EXCHANGE COEFFICIENT - COMPARISON OF WIND SPEED FROM DIFFERENT ORIGINS

J. ETCHETO and L. MERLIVAT

Université Pierre et Marie Curie, Laboratoire d'Océanographie Dynamique et de Climatologie, LODYC, Tour 14 - 2e étage, 4 Place Jussieu, 75252 Paris Cedex 05, France

ABSTRACT

The exchange coefficient of carbon dioxide between air and sea can be determined on a global scale in several ways. Geochemical methods (natural or bomb ^{14}C oceanic inventory, radon deficiency method) give global averaged values ranging between 4.8 and 6 x 10^{-2} mole . m^{-2} . yr^{-1} . μatm^{-1}. Only wind speed field based methods can monitor the space and time variations of the exchange coefficient. The average exchange coefficients obtained from wind fields range from 2.9 to 4.2 x 10^{-2} mole . m^{-2}, yr^{-1} . μatm^{-1}, always below the geochemical values. The results obtained from the SEASAT scatterometer and microwave radiometer are compared, for each ocean, averaged over three months. The SMMR overestimates the exchange coefficient nearly everywhere, but the global net flux is not changed due to a compensation of the variations of the outgasing and absorbed flux. The net CO_2 fluxes obtained using a spatially constant or variable exchange coefficient are also computed. This sensitivity test shows the importance of the spatial variability of the exchange coefficient for the net flux determination : the net flux which was - 1.17 Gtons per year with a variable exchange coefficient becomes - 0.155 when a constant exchange coefficient is assumed. We conclude by stressing the primary importance of the spatial and temporal variability of the exchange coefficient and of the concentration gradient.

INTRODUCTION

The flux of carbon dioxide exchanged between ocean and atmosphere is controlled by the air-sea concentration gradient ΔP and the exchange coefficient of the gas between the two media K : $\varphi = K . \Delta P$. The exchange coefficient itself is a combination of the transfer velocity k and the solubility s, of the gas in water with $K = k . s$.

Different attempts have been made to determine the carbon dioxide exchange coefficient on a global scale. These determinations rest on two methods :

- one based on geochemical approaches : the carbon 14 inventory (natural and artificial) in the ocean gives a mean value averaged over the global ocean and the radon deficiency method gives an estimation of the local value,

- the other one uses a relationship between the transfer velocity and the wind speed, based on wind tunnel and lake experiments, to deduce an exchange coefficient field from a wind speed field.

We will compare the various results obtained, looking in more detail into the results of the second method. We will make a test to show the consequences of assuming a spatially constant exchange coefficient on the net flux of gas exchanged between ocean and atmosphere. We will also compare the exchange coefficients determined by using wind fields obtained from the SEASAT scatterometer and microwave radiometer.

GEOCHEMICAL DETERMINATIONS

This determination can be done either from the ^{14}C naturally produced in the high altitude atmosphere or from atmospheric ^{14}C induced by nuclear explosions. For more detailed information, see Broecker et al. [1].

The principle of the natural ^{14}C determination is based on the idea that in the pre-industrial phase, the $^{14}C/^{12}C$ ratios respectively in the atmosphere, surface and deep ocean were fixed by the balance between the net influx of $^{14}CO_2$ at the air-water interface and the ^{14}C decay in the deep ocean. The Broecker et al. determination assumed the exchange coefficient and/or the concentration gradient to be spatially constant all over the global ocean. They obtained an average exchange coefficient of : (6.1 $\pm$ 1.4) x 10^{-2} mole . $m^{-2}.yr^{-1}$. μatm^{-1}. It was pointed out in [2] that the homo-

genelty hypothesis was very crude and the computation was repeated using a spatially varying exchange coefficient deduced from climatological winds by the method described in next chapter and the concentration gradient map in [1]. The resulting exchange coefficient is 5.7 x 10^{-2} mole . m^{-2} . yr^{-1}. atm^{-1}.

The method for using bomb ^{14}C is more complicated since the hypothesis of a stationary regime no longer holds. Here, the time history of the isotopic ratio in air and water is used, while the net flux of ^{12}C is still assumed to be zero. The time dependent isotopic ratios $^{14}C/^{12}C$ in the atmosphere and in the ocean are compared ; the evolution of the oceanic one is assumed to be inferred by the influx of atmospheric bomb ^{14}C. Under the same assumption of spatial homogeneity as above the average exchange coefficient is found to be : (6.1 $\pm$ 0.9) x 10^{-2} mole . m^{-2} . yr^{-1}. μatm^{-1}. This computation was redone in [2] taking into account the spatial variations as above and the sea ice coverage, and found to be 6.0x10^{-2} mole . m^{-2} . yr^{-1} . μatm^{-1}.

Finally, we should report another method using vertical profiles of radon concentration measured in the ocean. In the deep ocean the radon concentration is supposed to be in equilibrium with radium through radioactive decay. In the surface mixed layer, the radon concentration is less than its value at greater depth, this deficiency being due to the escape of the gas toward the atmosphere. This method, which assumes the exchange coefficient to be constant for several days (a rather unrealistic hypothesis), gives an average exchange coefficient of : (4.8 $\pm$ 1.2) x 10^{-2} mole . m^{-2} . yr^{-1}. μatm^{-1}, [1].

WIND FIELD BASED DETERMINATIONS

The method used here is to deduce transfer velocity from wind through a relationship determined from wind tunnel and lake experiments. The transfer velocity, k, not only depends on the wind speed, U, and sea state, but also on the sea surface temperature, varying by about a factor of three for the temperature range observed in the ocean. It is shown in [3] that for CO_2 this variation is compensated by an inverse variation of the solubility so that the exchange coefficient differs from its value at 20°C by no more than 10% in the observed temperature range. This is less than the accuracy of the relation and of the wind speed fields, so that to compute the transfer velocity at 20°C is sufficient for global studies. The most recent k(U) relationship has been given in [4] at 20°C :

$$k_{20} = 0.17\ U_{10} \qquad 0 \leqslant U_{10} \leqslant 3.6\ m.s^{-1}$$

$$k_{20} = 2.85\ U_{10} - 9.65 \qquad 3.6 < U_{10} \leqslant 13\ m\ .\ s^{-1}$$

$$k_{20} = 5.9\ U_{10} - 49.3 \qquad U_{10} > 13\ m\ .\ s^{-1}$$

where k_{20} is the liquid phase gas transfer velocity in $cm.h^{-1}$ at 20°C and U_{10} the wind speed at 10 meters height in $m.s^{-1}$. This relation is non-linear, and in particular results in a threshold effect at 3.6 m/s, the exchange being nearly blocked below this velocity. Due to this non-linearity, the transfer velocity can only be computed from high resolution wind speeds and, when averaged values are used, the variability has to be restored. All the studies described below used this relation, the limitations of which are discussed in detail in [3] and [4]. The main advantage of deducing the exchange coefficient from the wind field is that it allows the study of spatial and temporal variations on a global scale, which is completely impossible from radioactive tracers measurements : ^{14}C gives only the global mean, averaged over many years, while the measurements of radon profiles are necessarily too few to provide a monitoring of the world ocean.

A climatology of the wind speed and of its variance, with a 5°x5° resolution, obtained from the NOAA National Climatic Data Center, was used in [5]. They assumed for the wind speed a Gaussian frequency distribution having the average wind speed and variance of this climatology and computed monthly maps of the transfer velocity at 20°C. A large seasonal variation is observed in the Northern Hemisphere with small areas having a transfer velocity above 35cm . h^{-1} in January, decreasing by about a factor of three in August. The seasonal variation is weaker in the Southern Hemisphere with a few areas with a transfer velocity in excess of 30cm . h^{-1} in July while small areas in excess of 25cm . h^{-1} are observed in January. The monsoon winds give values above 30cm . h^{-1} in July.

The wind speeds at ten meters height provided by the European Meteorological Center (ECMWF) for year 1982, every 6 hours, on a 1.875° grid were used in [6] to compute monthly averaged maps of the transfer velocity at 20°C. The results for February and August are shown on Figure 1. They are qualitatively similar to those in [5], giving a global yearly averaged exchange coefficient of 2.9 x 10^{-2} mole . m^{-2} . yr^{-1} . μatm^{-1} without temperature or ice coverage correction, and are lower than the previous determinations. They also computed a map of the transfer velocity in the North Atlantic ocean during August 1978, using a climatology for temperature corrections and the wind speed measured by the SEASAT altimeter.

Two different wind data sets were used in [2]. He made temperature corrections and took into account the sea ice coverage, as deduced from climatologies. First, he used a climatology of wind speeds from the program COADS (Comprehensive Ocean - Atmosphere Data Set, 1985) on a 5.625 x 5.625°

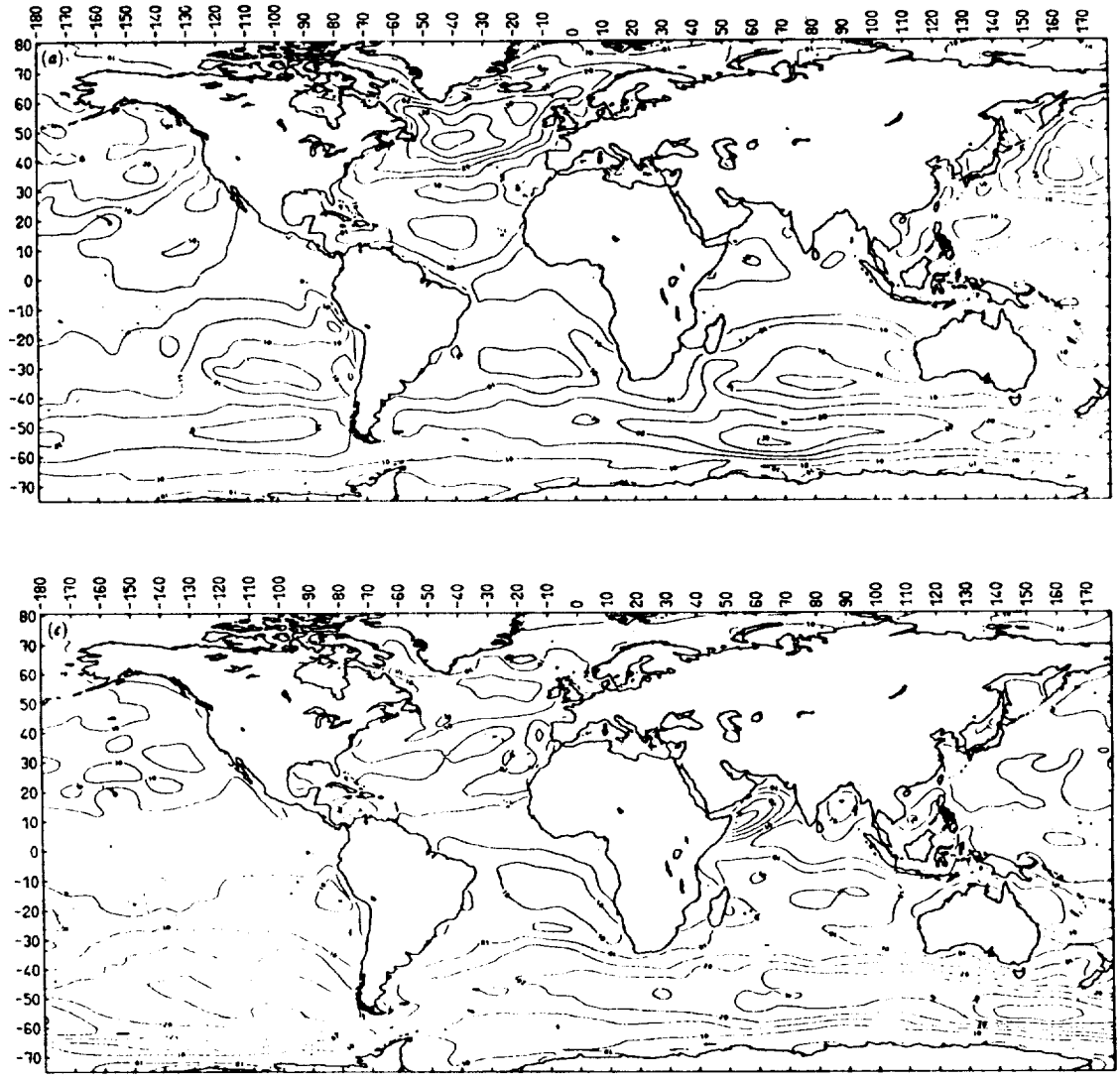

Fig. 1. Transfer velocity at 20°C during February (top) and August (bottom) 1982 deduced from ECMWF ten meters wind field, after [6].

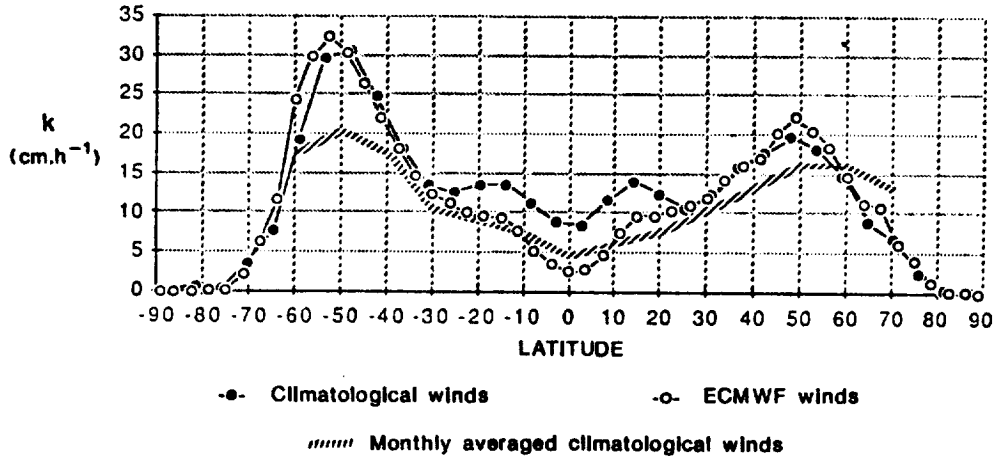

Fig. 2. Yearly zonal mean of the transfer velocity after temperature and ice coverage corrections, after [2].

grid, together with a variance map deduced from the General Circulation Model T21 of the Max Planck Institut für Meteorologie in Hamburg. Second, he used the wind speeds at 1000 mBar provided every 12 h on a 3.75 x 3.75° grid by the ECMWF for the period December 1978-November 1979, during the FGGE experiment. The monthly maps of exchange coefficient thus obtained, despite minor differences, were qualitatively in agreement, and coherent with maps previously obtained by other authors. Figure 2 shows yearly zonal means of the exchange coefficient obtained from the two wind data sets after temperature corrections and taking into account the sea ice coverage. The result has been divided by the solubility of CO_2 at 20°C in order to get units of $cm.h^{-1}$. The exchange coefficient obtained from the monthly average of the climatological winds, taking neither the variability nor the temperature or sea ice coverage into account, is shown for comparison. The two wind fields differ mainly in the equatorial region and the author attributes this difference to a lack of measurements in this region for the meteorological model while both wind fields lack measurements in the Austral Ocean. The underestimation of the exchange coefficient when the variability is neglected can be as high as a factor 1.5, the order of magnitude found in [3] for a particular case. He studied also the seasonal variation in several latitudinal zones and showed that the main variation (by a factor 3) is in the band 45 to 50° N. The variation is also large in the regions covered by sea ice in winter but it can be seen from figure 2 that in these regions the exchange coefficient is small. The yearly averaged global exchange coefficient obtained after temperature correction and taking into account sea ice coverage is 4.17×10^{-2} mole . m^{-2} . yr^{-1} . μatm^{-1} from the COADS climatology and 3.69×10^{-2} mole . m^{-2} . yr^{-1} . μatm^{-1} from the ECMWF wind speeds during the FGGE period.

The same type of analysis was done in [3], without temperature corrections, from the SEASAT scatterometer wind speed measurements integrated over the three months of the satellite lifetime (July 7 to October 9, 1978). The sea ice coverage was deduced from the altimeter signal. The resulting transfer velocity map is shown on Figure 3. The results are in qualitative agreement with previous ones. They computed the exchange coefficient averaged over three months for the various oceans. Its value on the global ocean is 3.63×10^{-2} mole . m^{-2} . yr^{-1} . μatm^{-1}. They combined this map of the exchange coefficient with the map of the air-sea concentration gradient of CO_2 given in [1] and obtained a net flux of 1.17 gigatons of carbon per year absorbed in the ocean.

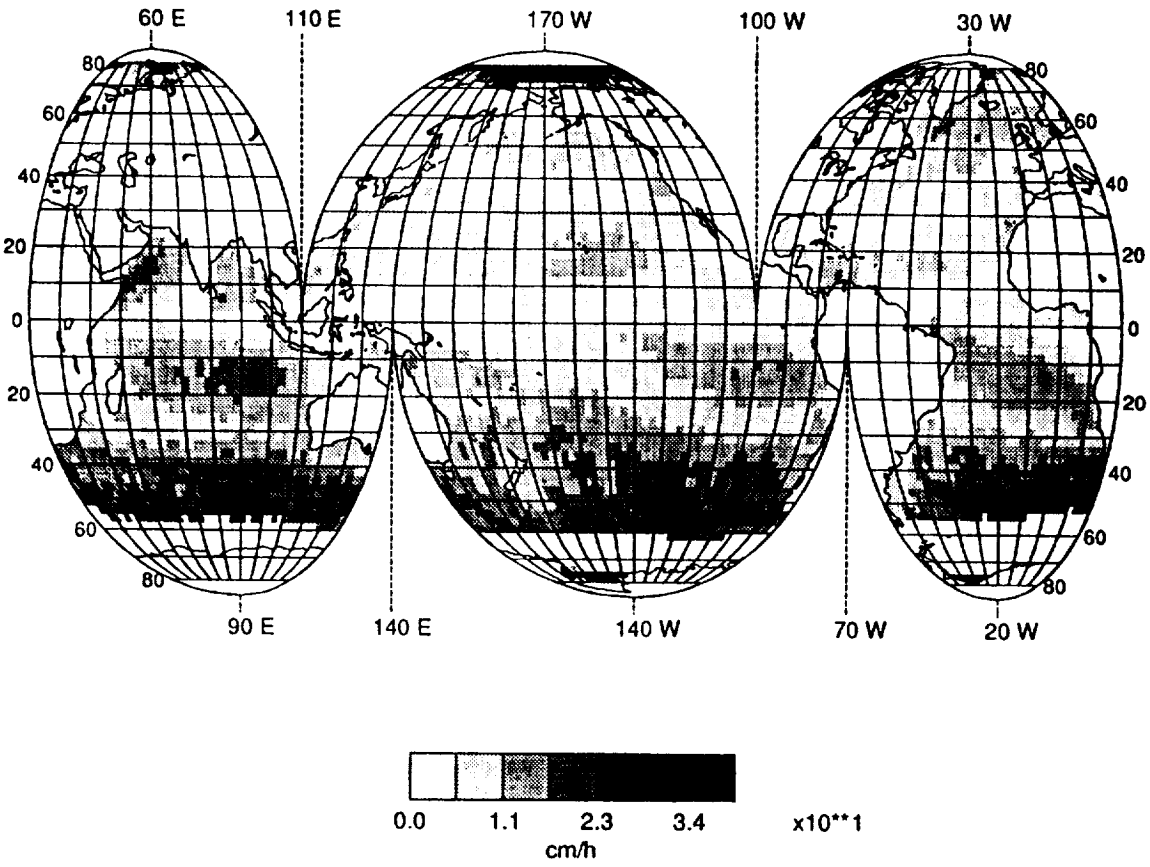

Fig. 3. Transfer velocity map for the period July 7 to October 9, 1978 deduced from the SEASAT scatterometer wind fields.

The comparison of the various determinations of the average exchange coefficient is made in [3] and their validity is discussed at length. The ^{14}C determinations are higher than the results from wind speed fields by about 40%, except the determination in [6] which is well below the others. If the wind field based determinations only are considered, the result of [3] is lower than those of [2] by 15% for the COADS climatology and by 3% for the ECMWF wind field at 1000 mBar during the FGGE period, and higher than the one in [6] for the ECMWF wind field at 10 meters in 1982 by 20%. The temperature corrections modify the average exchange coefficient by no more than a few per cent (the maximum variation of K in the ocean temperature range is 10%) and the sea ice coverage by 3%, [2]. Thus the main source of discrepancies between the various results arises from differences in the wind fields. If the same analysis is performed on various wind fields, the average exchange coefficient can be considered as representative of the wind field. Due to the non-linearity of the relations of Liss and Merlivat, this measurement emphasizes the influence of high wind speeds. It can be used as a test of the algorithms run for data reduction of spatial measurements, which are usually tested on average wind speeds. This we will do in a subsequent section of this paper to compare the SEASAT scatterometer and SMMR wind speed fields, but before that we will test the influence of assuming a spatially uniform exchange coefficient on the determination of the carbon dioxide net flux.

INFLUENCE OF A SPATIALLY VARYING EXCHANGE COEFFICIENT

To get an insight into the influence on the determination of the net CO_2 flux of assuming a constant exchange coefficient all over the world, as is frequently done for global modelling of carbon dioxide, we will take the approach used in [3]. We will use the map of the air-sea concentration gradient of CO_2 from [1] and combine it with the exchange coefficient map of [3]. We will then compute the flux exchanged in the various oceans and the global net flux, and compare it to the results obtained when a constant exchange coefficient, equal to the average exchange coefficient in [3], is used. This should be taken as a sensitivity test only and can in no way be considered as representative of the reality, since the combination of the Broecker et al. map, a crude yearly average, with a three month average of the exchange coefficient does not take into account the seasonal variations, which are of primary importance for the flux ([2], [3], [6]). The results which are highly dependent on the map of air-sea concentration gradient used, are shown in table 1.

TABLE 1. Comparison of Constant Versus Varying Exchange Coefficient

	OUTGASING				ABSORPTION				NET FLUX			
	area (10^6 km^2)		10^2 x K (mole.m^{-2}.yr^{-1}.µatm^{-1})	flux (Gtons.yr^{-1})	area (10^6 km^2)	10^2 x K (mole.m^{-2}.yr^{-1}.µatm^{-1})	flux (Gtons.yr^{-1})	area (10^6 km^2)	10^2 x K (mole.m^{-2}.yr^{-1}.µatm^{-1})	flux (Gtons.yr^{-1})
Atlantic ocean	33.20	var	3.20	0.132	41.5	2.70	-0.340	74.7	2.92	-0.208
		cst	3.63	0.194		3.63	-0.417		3.63	-0.224
Indian ocean	19.9	var	3.03	0.106	29.6	3.99	-0.142	49.6	3.60	-0.036
		cst	3.63	0.123		3.63	-0.129		3.63	-0.005
Pacific ocean	55.0	var	2.33	0.584	46.6	3.67	-0.164	146.8	2.76	0.420
		cst	3.63	0.974		3.63	-0.162		3.63	0.812
Antarctic ocean	0	var			57.3	6.81	-1.350	57.3	6.81	-1.350
		cst				3.63	-0.738		3.63	-0.738
Global ocean	108.2	var	2.73	0.822	175.1	4.52	-1.995	328.4	3.63	-1.174
		cst	3.63	1.292		3.63	-1.447		3.63	-0.155

The limit of the Antarctic Ocean has been taken to be 40°S. The global net flux is significantly changed : 0.16 gigatons of carbon per year absorbed by the ocean instead of 1.17. The reason for that is that generally the outgasing regions are low latitude areas with a weak exchange coefficient, while the absorbing regions are high latitude areas with a large exchange coefficient. Hence, to take a constant exchange coefficient everywhere tends to enhance the outgasing and decrease the absorption. This is true everywhere except in the absorbing part of the Atlantic Ocean : all the north Atlantic Ocean down to latitude of 10°N is absorbing, including tropical and subtropical latitudes where the exchange coefficient is weak, well below the global average. During the arctic summer, the exchange coefficient in the north Atlantic is above the global average only north of 40°N.

The determining factors for this change in net flux are :

- the large decrease of the flux absorbed in the Antarctic Ocean (-0.61 Gtons) due to a decrease of the exchange coefficient by nearly a factor of two in the region where two third of the world absorption occurs

- to a lesser extent, the increase of the outgasing in the Pacific Ocean (+0.39 Gtons) where the exchange coefficient has increased by more than 50% in the region where two third of the outgasing occurs.

The effect on the net flux is very large because it is the result of the difference between an outgasing flux and an absorbed flux of similar magnitudes, so that a variation of 50% on each flux can result in a variation of one order of magnitude in the difference. We should stress again that this is completely dependent on the concentration gradient map used, both for the definition of the outgasing and absorbing regions and for the magnitude of the fluxes. One should note that the same effect would appear for the temporal variations, especially seasonal, since both the concentration gradient and the exchange coefficient have large seasonal variations. This has been shown for particular examples in [3] and [6].

Thus no reasonable global modelling of the carbon dioxide can be made without taking into account the spatial and temporal variations of the exchange coefficient and of the concentration gradient of carbon dioxide at the air-sea interface. For the former only the determination from wind fields can provide this information. It explains the significance of this method.

COMPARISON OF SEASAT SMMR AND SCATTEROMETER WIND FIELDS

We will now compare the results obtained using wind fields determined from the SEASAT scatterometer (SCATT) and the SEASAT micro-wave radiometer (SMMR).

The SEASAT satellite was launched in June 1978 in a quasi-circular orbit having an inclination of 108 degrees, a period of 101 minutes and an altitude of approximately 800 km. It carried, among other instruments, a microwave radiometer and a scatterometer. We used the wind data obtained from these two devices after reduction by F. Wentz ([7], [8]) for the period July 7 to October 9, 1978.

The scatterometer measured in two swaths, 600 km wide, one on each side of the track between 150 and 750 km (we did not use the nadir measurements) and, after data reduction, one wind speed value was obtained for each 100x100 km square in the swath.

The SMMR measured in one 600 km wide swath on one side of the track, approximatly from the subtrack to 600 km starboard. We used the wind speeds given for a 85x85 km square using a combination of the brightness temperatures at 10.7 H/37V/21V gigahertz. The sea ice coverage was determined from the 6.6V brightness temperature : when this temperature was above 172° K over the ocean, the radiometer was assumed to be looking at sea ice. The sea ice coverage was determined for each month, using the measurements during a six days period in the middle of the month : July 13 to 18, August 18-23, September 7-22. The data for each month were cleaned using the corresponding sea ice coverage. The data had to be masked when they were at less than 350 kilometers from large land masses or sea ice. For "small islands" or peninsulas, defined approximatly as being less than 3° wide either in latitude or in longitude, the mask is only 120 kilometers wide. The data flagged as bad or questionable from an algorithmic point of view (eg. brightness, temperature out of the usual range, heavy rain, no solution found by the algorithm ...) and the measurements made in masked area are suppressed. Then the average of the transfer velocity in a square the size of which can be specified and during a given time is computed, giving a map of averaged transfer velocities on a grid. These results are integrated in space, weighted by the area of the square concerned after removing the area covered with land or sea ice. The September sea ice coverage was used for this integration. It results in an average exchange coefficient per ocean, after multiplying by the solubility of carbon dioxide at 20°C for a salinity 35°/$_{oo}$, that is 33 mole.m^{-3}.μatm^{-1}, separately for the outgasing and absorbing areas, as defined in [1]. This has been done in [3] for the scatterometer, averaging over the lifetime of the satellite and using a 10° grid. In order to make a comparison, we did exactly the same for the SMMR data and the results are shown in table 2. The exchanged fluxes have also been computed for comparison, using the concentration gradient map of [1]. The same reservations as above about the significance of these fluxes are valid here.

The wind speeds obtained from the SMMR are compared to those obtained from the scatterometer in [8]. They concluded that between 3 and 17 $m.s^{-1}$, the difference between the two data sets was nearly zero, while the SMMR underestimated the low wind speeds (below 3 $m.s^{-1}$) and overestimated the high wind speeds (above 17 $m.s^{-1}$), by 1 to 2 $m.s^{-1}$. The effect of this underestimation below 3 $m.s^{-1}$ has no effect on the transfer velocity since at these wind speeds the gas exchange is blocked anyway. On the other hand, the overestimation at high wind speeds is effective and the exchange coefficient is increased in all regions, except in the outgasing area of the Atlantic Ocean where it is not changed. The global average exchange coefficient is increased by 13% while in [8] it is reported that the global average wind speed is changed by about 1% only ; this reflects the effect of wind speed dependent biases on the exchange coefficient. The "equivalent wind speed", corresponding to an exchange coefficient of 4.09×10^{-2} $mole.m^{-2}.yr^{-1}.\mu atm^{-1}$ is 8.3 ms^{-1}, on which a 13% difference corresponds to 1 $m.s^{-1}$. This seems to indicate that the overestimation of the

TABLE 2. Comparison Of SMMR And Scatterometer Data

		OUTGASING			ABSORPTION			NET FLUX		
		area (10^6 km^2)	10^2 x K (mole.m^{-2}. yr^{-1}.µatm^{-1})	flux (Gtons.yr^{-1})	area (10^6 km^2)	10^2 x K (mole.m^{-2}. yr^{-1}.µatm^{-1})	flux (Gtons.yr^{-1})	area (10^6 km^2)	10^2 x K (mole.m^{-2}. yr^{-1}.µatm^{-1})	flux (Gtons.yr^{-1})
Atlantic ocean	SCATT	33.2	3.20	0.132	41.5	2.70	-0.340	74.7	2.92	-0.208
	SMMR	32.5	3.21	0.123	36.8	2.90	-0.291	69.3	3.05	-0.167
Indian ocean	SCATT	19.9	3.03	0.106	29.6	3.99	-0.142	49.6	3.60	-0.036
	SMMR	19.0	3.45	0.118	29.5	4.17	-0.148	48.5	3.89	-0.030
Pacific ocean	SCATT	55.0	2.33	0.584	46.6	3.67	-0.164	146.8	2.76	0.420
	SMMR	54.3	2.82	0.757	46.0	4.07	-0.180	144.4	3.27	0.577
Antarctic ocean	SCATT	0			57.3	6.81	-1.350	57.3	6.81	-1.350
	SMMR				56.7	7.63	-1.484	56.7	7.63	-1.484
Global ocean	SCATT	108.2	2.73	0.822	175.1	4.52	-1.995	328.4	3.63	-1.174
	SMMR	105.7	3.05	0.999	169.0	5.02	-2.102	318.8	4.09	-1.104

SMMR wind speed, with respect to that by scatterometer, does exist at wind speeds lower than reported in [8]. The fact that in the Antarctic Ocean, where the exchange coefficient is about twice what it is elsewhere ("equivalent velocity" 12.6 m.s^{-1}), the increase is only 12% (no more than in other regions) confirms this tendency. There could be also an effect of the variance. The variance of the SMMR data is larger than the one of the scatterometer data and this could change the transfer velocity when it is close to the points of non linearity of the k(U) relationship. And finally, one should notice that the area of the regions concerned is slightly smaller for the SMMR data than it is for the scatterometer data. This is a consequence of the mask applied to the measurements 350 km off land or ice, which results in regions without measurements which are not considered in the integration.

As far as the exchanged flux is concerned, it is increased by about the same amount as the exchange coefficient, as would be expected, except in the Atlantic Ocean where it is decreased even in the outgasing area where the exchange coefficient is increased. A possible explanation is that the difference between the SMMR and the scatterometer varies spatially probably depending on latitude. The pressure gradient map used to compute carbon dioxide fluxes has a dependence on latitude which differs in the Atlantic Ocean from that in other oceans, and this could be the reason for this surprising behavior of the flux. Another factor for decreasing the flux is that the aera has decreased, by as much as 11% in the absorbing region, thus decreasing the exchanged flux. This change in area is particularly large in the Atlantic Ocean where the coast lines are relatively close to each other, resulting in a masked area larger compared to the global area than in other oceans. The results for the global net flux is nearly the same as the one from the scatterometer because both the outgasing flux and the absorbed flux are increased by about the same amount and they compensate.

CONCLUSION

The average exchange coefficient of carbon dioxide between air and sea can be determined on a global scale either from geochemical measurements or from global wind speed fields.

The first class of determinations cannot give access to the spatial and temporal variability of the exchange coefficient. They give results about 40% larger than those of the second class.

The second class of determinations is able to monitor the space and time variations of the exchange coefficient, through a relationship between wind speed and transfer velocity.

We have shown, through a sensitivity test, the importance of these variations for determining the net CO_2 flux on a global scale. This test concerns only the spatial variability, since there has been no attempt up to now to map the seasonal variation of the pressure gradient on a global scale.

We have also compared the SEASAT wind speed measurements made simultaneously by two instruments, the microwave radiometer and the scatterometer.

The SMMR has a tendency to underestimate the low wind speeds (in the range where the CO_2 exchange is blocked) and to overestimate the high wind speeds, compared to the scatterometer. It results in an overestimate of the global average exchange coefficient by 13%, but does not change the global net flux.

REFERENCES

1. Broecker, W.S., J.R. Ledwell, T. Takahashi, R. Weiss, L. Merlivat, L. Memery, T.H. Peng, B. Jähne and K.O. Munnich, Isotopic versus micrometeorologic ocean CO_2 fluxes : a serious conflict, J. Geophys. Res., 91, 10517-110527, 1986.

2. Monfray, P., Echanges océan/atmosphère du gaz carbonique : variabilité avec l'état de la mer, Thesis, Université de Picardie, 1987.

3. Etcheto, J. and L. Merlivat, Satellite determination of the carbon dioxide exchange coefficient at the ocean-atmosphere interface : a first step, J. Geophys. Res., in press, 1988.

4. Liss, P. and L. Merlivat, Air-sea gas exchange rates : Introduction and synthesis, in The Role of Air-Sea Exchange in Geochemical Cycling, Adv. Sci. Inst. Ser., Ed. P. Buat-Ménard, D. Reidel Pub. Co., 1986.

5. Erickson, D.J. and R.A. Duce, On the global transfer velocity field of gases with a Schmidt number of 600, Searex Newslett., 10, 7-10, 1987.

6. Thomas, F., C. Perigaud, L. Merlivat and J.F. Minster, World scale monthly mapping of the CO_2 ocean-atmosphere gas transfer coefficient, Phil. Trans. R. Soc., A 325, 71-83, 1988.

7. Wentz, F.J., S. Peteherych and L.A. Thomas, A model function for ocean radar cross sections at 14.6 GHz, J. Geophys. Res., 89 (C3), 3689-3704, 1984.

8. Wentz, F.J., L.A. Mattox and S. Peteherych, New algorithms for microwave measurements of ocean winds : Applications to SEASAT and the Special Sensor Microwave Imager, J. Geophys. Res., 91 (C2), 2289-2307, 1986.

ACKNOWLEDGEMENTS

We thank J.C. Magenham and A. Ozieblo for providing the programming assistance. This work was done under CNES contract 86/CNES/1227 and E.E.C. contract EV4C-0065-F.

CARBON CYCLING BY CELLULOSE-FERMENTING NITROGEN-FIXING BACTERIA

S. B. Leschine and E. Canale-Parola

Department of Microbiology, University of Massachusetts,
Amherst, MA 01003, USA

ABSTRACT

The most abundant organic materials on Earth are plant polysaccharides such as cellulose and hemicelluloses. Inasmuch as vast quantities of these polymers are present in anaerobic environments (e.g., in soils and sediments), anaerobic microorganisms that ferment plant polysaccharides play a central role in carbon cycling on the planet as a source of CO_2 and, indirectly, of CH_4. Cellulose-fermenting bacteria from soil and pond sediment were isolated in a medium (incubated in N_2) which lacked a source of combined nitrogen. The isolates had the ability to utilize atmospheric N_2 as the nitrogen source for cell growth. Nitrogenase (the enzyme which catalyzes the reduction of N_2 to ammonia) was demonstrated by means of the acetylene reduction test in these isolates and in several previously described anaerobic cellulolytic bacteria isolated from various natural environments. Thus, cellulose-fermenting bacteria that fix N_2 may be widespread and may play a role in nitrogen cycling as well as in carbon cycling on a global scale. Knowledge of the physiology and ecology of these organisms is crucial to detailing the mechanisms producing local sources and sinks of atmospheric gases, interpreting data obtained using space-based sensors, and understanding the effects of atmospheric warming on fermentations as major sources of CO_2 and CH_4.

INTRODUCTION

Key processes of biogeochemical cycles are mediated by microorganisms. For example, an important step in the global carbon cycle is the microbial degradation of cellulose, the most abundant organic material on Earth /1/. Photosynthesis yields annually up to 1.5×10^{11} tons of dry plant material worldwide, almost half of which consists of cellulose /2/. For life to continue on Earth, the carbon present in this polymer must be reintroduced into the atmosphere in the form of CO_2.

A substantial amount of cellulose (5-10%) is degraded in anaerobic environments /2/. Anaerobic activity occurs in proximity to the surface in soils, composts, and freshwater, marine, and estuarine sediments, indicating that aerobic conditions normally prevail only in a thin crust /2/. In anaerobic environments, cellulose is initially decomposed by cellulose-fermenting microorganisms yielding CO_2, H_2, organic acids, and ethanol. Some products of cellulose fermentation serve as growth substrates for other bacteria which produce acetate, CO_2, and H_2. These products are then converted to CH_4 by methanogenic bacteria. Thus, as a source of CO_2 and, indirectly, of CH_4, anaerobic cellulolytic microorganisms play a major role in carbon cycling on the planet (Fig. 1). Although the microbiota involved directly and indirectly in cellulose degradation in the rumen has been studied extensively /3,4/, relatively little is known about the complex interactions among free-living microorganisms involved in the anaerobic degradation of cellulose in other natural habitats /2/. The distribution of anaerobic cellulolytic bacteria in nature is largely unknown.

Due primarily to recent interest in the potential use of cellulolytic bacteria for alcohol fuel production from biomass, several species of anaerobic cellulolytic bacteria from sediments, compost, and sewage sludge have been described /5-11/. The long-term goal of our research is to advance understanding of the physiology and ecology of these microorganisms. Mostly, we have studied strains of a *Clostridium* species (referred to as "C strains") that we isolated from the sediment of a freshwater swamp. These strains actively ferment not only cellulose but also components of the hemicellulosic portion of biomass (e.g., xylan, pentoses), forming primarily ethanol, acetic acid, H_2, and CO_2 /5/. Information obtained from these studies may help us predict the response of cellulose-fermenting bacteria to current global warming and probable altered precipitation patterns. For example, if anaerobic cellulose

degradation is enhanced and the rate of CO_2 and CH_4 production is increased, there will be a positive feedback on the rate of climate change by this microbial activity /12,13/.

Environments rich in cellulose are frequently deficient in nitrogen (e.g., peat soils, agricultural wastes, composts). Thus, cellulose-fermenting bacteria that satisfy their nitrogen requirements through the fixation of N_2 would be expected to have a strong selective advantage over those which require a source of combined nitrogen. Moreover, such microorganisms might be expected to play a major role in nitrogen cycling, as well as in carbon cycling, on a global scale. However, it has not been determined whether cellulose is widely used as an energy source by nitrogen-fixing bacteria. This is surprising given the abundance of cellulose and the suggestion /14/ that nitrogen fixation by free-living heterotrophic bacteria in natural ecosystems is limited by the availability of oxidizable growth substrates. Waterbury and coworkers /15/ have shown that cellulose serves as a growth substrate for a nitrogen-fixing aerobic bacterium which exists in a symbiotic relationship with shipworms. Their findings demonstrate that these two complex physiological processes, nitrogen fixation and cellulose degradation, can be performed by a single bacterium. A major objective of our research was to determine whether free-living anaerobic cellulolytic bacteria that are widespread in terrestrial environments fix nitrogen when they utilize cellulose as the fermentable substrate for growth.

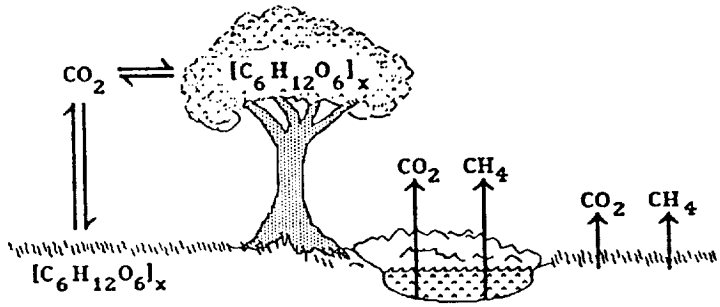

1. Cellulose ⇨ Organic Acids + Ethanol + CO_2 + H_2
2. Organic Acids, Ethanol ⇨ Acetate + CO_2 + H_2
3. Acetate ⇨ CO_2 + CH_4; CO_2 + H_2 ⇨ CH_4

CELLULOSE ⇨ CO_2 + CH_4

Fig. 1. Role of cellulose-fermenting bacteria in carbon cycling. Cellulose $[(C_6H_{12}O_6)_x]$, a major product of the photosynthetic fixation of CO_2, is fermented by anaerobic cellulolytic bacteria (step 1). Ethanol and the acidic products of cellulose fermentation serve as growth substrates for other bacteria which produce acetate, CO_2, and H_2 (step 2). Methanogenic bacteria produce CH_4 from acetate or by reduction of CO_2 with H_2 (step 3). In anaerobic environments, the complete dissimilation of cellulose results in the formation of CO_2 and CH_4.

ISOLATION OF NITROGEN-FIXING CELLULOSE-FERMENTING BACTERIA

Four strains of anaerobic cellulolytic bacteria were isolated from forest soil and freshwater mud using a procedure that selected for nitrogen-fixing strains /16/. Enrichment cultures were prepared by serially diluting soil or mud samples into anaerobic culture tubes containing a liquid growth medium, designated "MW-C". This medium (which was similar to one described by Daesch and Mortenson /17/) lacked a source of combined nitrogen, included cellulose (ball-milled Whatman No. 1 filter paper; 0.6%, dry wt/vol) as the fermentable substrate, was prereduced /18/, and was maintained in an N_2 atmosphere. After 7-14 days of incubation at 30°C, enrichment cultures showed significant disappearance of cellulose. Spent medium and remaining cellulose fibers from enrichment cultures were serially diluted into melted cellulose soft agar medium in tubes. The contents of these tubes were poured onto plates of agar medium within an anaerobic chamber. After 2-4 weeks of incubation, colonies surrounded by zones of clearing appeared in the otherwise opaque medium. These colonies were transferred by streaking onto plates of cellobiose agar medium, and restreaked several times to obtain pure cultures. Colonies were then transferred into liquid cellulose medium (MW-C) to confirm whether the isolate was cellulolytic. Three strains (B1A, B1B, and B1C) were isolated from mud from the bottom of a shallow pond (Beaver's Pond, Shutesbury, Massachusetts) and one (strain B3B) from forest soil near Beaver's Pond.

CHARACTERIZATION OF NITROGEN-FIXING CELLULOLYTIC ISOLATES

The isolates resembled one another morphologically (Fig.2). All were motile curved rods measuring 0.6 to 0.8 µm x 3 to 6 µm. Under the growth conditions used, spores were never observed either within cells or free in culture supernatant fluids. Cells of all four strains stained gram-negative. Electron microscopy of thin sections of strain B1A cells /16/ showed that the cytoplasmic membrane was surrounded by a multilayered cell wall that differed from typical cell walls of most gram-negative anaerobic bacteria (eg., those of most *Bacteroidaceae* /19/), but resembled those of other gram-negative mesophilic cellulolytic bacteria /5,20/. All isolates were obligately anaerobic and fermented polysaccharides, hexoses, and pentoses that are commonly present in plant materials. None of the strains utilized maltose, glycerol, or amino acids as fermentable substrates. Further phenotypic and genotypic characterization of the isolates is required to determine their taxonomic position.

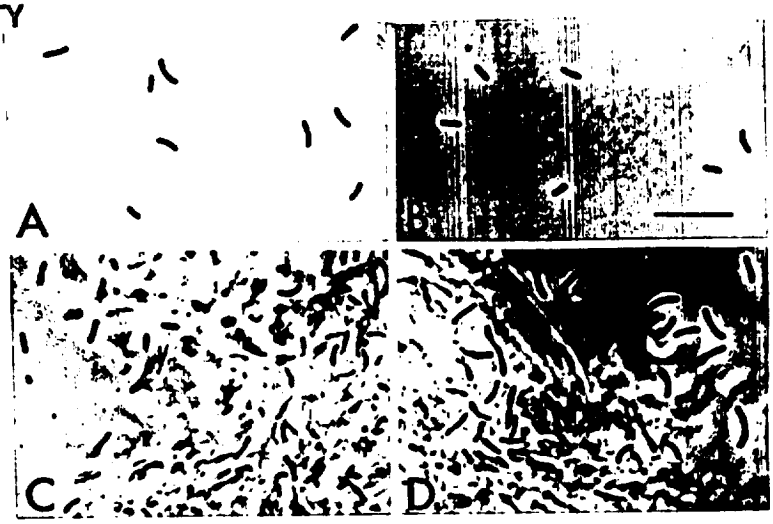

FIG. 2 A-C. Phase-contrast photomicrographs of nitrogen-fixing cellulolytic isolates (wet-mount preparations), strains (A) B1A, (B) B1B, (C) B1C, and (D) B3B. Cells were cultured to late-exponential phase in a cellobiose-containing medium. Cells of strains B1C (C) and B3B (D) are entangled in cellulose fibers introduced into the culture along with the inoculum (a 7-day culture in cellulose medium). Scale bar, 10 μM.

The presence of nitrogenase in the isolates was demonstrated by means of the acetylene reduction test /21/. Cells reduced acetylene to ethylene (e.g., 1310 nmol/h/mg cell protein) when growing in medium MW-C but not when growing in the same medium supplemented with 0.2% NH_4Cl. Inasmuch as the isolates grew in a medium lacking combined nitrogen and containing cellulose as the fermentable substrate, it was concluded /16/ that they utilized this polysaccharide as the energy source for N_2 fixation.

NITROGENASE ACTIVITY IN OTHER CELLULOSE-FERMENTING BACTERIA

Several previously described anaerobic cellulolytic species [*Clostridium* strain C7, from mud of a freshwater swamp in Woods Hole, Massachusetts, U.S.A. /5/;*Clostridium papyrosolvens*, from estuarine sediments of the River Don in Aberdeenshire, Scotland /6/; strain JW-2, from wetwood of an elm in Amherst, Massachusetts, U.S.A. /20/] were cultured in a defined, cellulose-containing medium /16/. The previously described cellulolytic species, as well as the new isolates, reduced acetylene to ethylene when grown in this medium, but not when grown in the same medium supplemented with NH_4Cl, a result that indicated the presence of nitrogenase in these bacteria. Moreover, growth in a cellobiose-containing medium lacking combined nitrogen was dependent on N_2 /16/. No growth occurred when cultures were incubated in an argon atmosphere. These observations indicated that N_2 served as the nitrogen source for the growing cells. Thus, cellulolytic bacteria from a variety of environments synthesized active nitrogenase and apparently incorporated N_2 into cell material during growth. Although other cellulolytic bacteria may possess nitrogenase /15,22/, this is the first demonstration of nitrogen fixation during the anaerobic degradation of cellulose. Our finding of nitrogenase activity in cellulose-fermenting bacteria isolated from a variety of environments is consistent with the view /16/ that nitrogen-fixing cellulolytic bacteria are widespread in nature.

DISCUSSION

In the study described above, we did not attempt to enumerate nitrogen-fixing cellulolytic bacteria in specific terrestrial environments. The results of such experiments, if performed using classical methods involving viable counts, probably would not be meaningful because these bacteria often adhere to or are entangled in cellulose fibers (e.g., Fig. 2C,D). Furthermore, the growth requirements of diverse nitrogen-fixing cellulolytic bacteria are not known. Future studies aimed at identifying cellulolytic species in their natural environments and estimating their activities will be conducted with the use of oligonucleotide probes complementary to ribosomal ribonucleic acid (rRNA) sequences unique to members of groups of cellulose-fermenting organisms. Since the probes are complementary to rRNAs, and actively growing cells may contain more than 10^4 ribosomes /23/, each a potential probe target, single cells may be labeled and identified by *in situ* hybridization and microautoradiographic procedures /24/. This method permits the identification of single cells microscopically (cultivation is not required) and offers a very powerful tool to identify the presence of members of particular bacterial groups in natural ecosystems. The metabolic activity of populations of cellulolytic bacteria in natural samples may be estimated by measuring the amount of probe bound to bulk extracted rRNA. Since the rRNA content of cells is proportional to growth rate over a wide range of growth rates /25/, the amount of group-specific probe hybridized per unit of biomass would provide an estimate of the metabolic activity of that group /24,26/. Results of these studies will contribute to our understanding of the diversity of cellulose-fermenting nitrogen-fixing bacteria, their quantitative contribution to cellulose breakdown and nitrogen fixation, their potential for improving soil fertility, and the effect of atmospheric warming on their activity.

ACKNOWLEDGMENTS

We thank T. A. Warnick for expert technical assistance. This work was supported by National Science Foundation grant BSR-8708469 and by U. S. Department of Energy contract DE-FG02-88ER13898.

REFERENCES

1. E. B. Cowling and W. Brown, Structural features of cellulosic materials in relation to enzymatic hydrolysis, in: Advances in Chemistry Series 95, ed. G. J. Hajny and E. T. Reese, American Chemical Society, Washington 1969, p. 152.

2. L. G. Ljungdahl and K.-E. Eriksson, Ecology of microbial cellulose degradation, in: Advances in Microbial Ecology, Vol. 8, ed. K. C. Marshall, Plenum Press, New York 1985, p. 237.

3. R. E. Hungate, The Rumen and its Microbes, Academic Press, New York, 1966.

4. M. J. Wolin and T. L. Miller, Interactions of microbial populations in cellulose fermentation, Fed. Proc. 42, 109 (1983)

5. S. B. Leschine and E. Canale-Parola, Mesophilic cellulolytic clostridia from freshwater environments, Appl. Environ. Microbiol. 46, 728 (1983)

6. R. H. Madden, M. J. Bryder, and N. J. Poole, Isolation and characterization of an anaerobic, cellulolytic bacterium, *Clostridium papyrosolvens* sp. nov., Int. J. Syst. Bacteriol. 32, 87 (1982)

7. W. D. Murray, L. Hofmann, N. L. Campbell, and R. H. Madden, *Clostridium lentocellum* sp. nov., a cellulolytic species from river sediment containing paper-mill waste, System. Appl. Microbiol. 8, 181 (1986)

8. W. D. Murray, L. C. Sowden, and J. R. Colvin, *Bacteroides cellulosolvens* sp. nov., a cellulolytic species from sewage sludge, Int. J. Syst. Bacteriol. 34, 185 (1984)

9. G. B. Patel, A. W. Khan, B. J. Agnew, and J. R. Colvin, Isolation and characterization of an anaerobic, cellulolytic micro-organism, *Acetivibrio cellulolyticus* gen. nov., sp. nov., Int. J. Syst. Bacteriol. 30, 179 (1980)

10. E. Petitdemange, F. Caillet, J. Giallo, and C. Gaudin, *Clostridium cellulolyticum* sp. nov., a cellulolytic mesophilic species from decayed grass, Int. J. Syst. Bacteriol. 34, 155 (1984)

11. J. Sukhumavasi, K. Ohmiya, S. Shimizu, and K. Ueno, *Clostridium josui* sp. nov., a cellulolytic, moderate thermophilic species from Thai compost, Int. J. Syst. Bacteriol. 38, 179 (1988)

12. J. E. Hobbie and J. M. Melillo, Role of microbes in global carbon cycling, in: Current Perspectives in Microbial Ecology, ed. M. J. Klug and C. A. Reddy, American Society for Microbiology, Washington 1984, p.389.

13. A. E. Linkins, J. M. Melillo, and R. L. Sinsabaugh, Factors affecting cellulase activity in terrestrial and aquatic ecosystems, in: Current Perspectives in Microbial Ecology, ed. M. J. Klug and C. A. Reddy, American Society for Microbiology, Washington 1984, p.572.

14. R. Brouzes, J. Lasik, and R. Knowles, The effect of organic amendment, water content, and oxygen on the incorporation of $^{15}N_2$ by some agricultural and forest soils, Can. J. Microbiol. 15, 899 (1969)

15. J. B. Waterbury, D. B. Calloway, and R. D. Turner, A cellulolytic nitrogen-fixing bacterium cultured from the gland of Deshayes in shipworms (*Bivalvia: Teredinidae*), Science 221, 1401 (1983)

16. S. B. Leschine, K. Holwell, and E. Canale-Parola, Nitrogen fixation by anaerobic cellulolytic bacteria, Science, in press.

17. G. Daesch and L. E. Mortenson, Effect of ammonia on the synthesis and function of the N_2-fixing enzyme system in *Clostridium pasteurianum*, J. Bacteriol. 110,103 (1972)

18. R. E. Hungate, A roll tube method for cultivation of strict anaerobes, in: Methods in Microbiology, Vol. 3B, ed. J. R. Norris and D. W. Ribbons, Academic Press, New York 1969, p. 117.

19. L. V. Holdeman, R.W. Kelley, and W. E. C. Moore, Anaerobic gram-negative straight, curved and helical rods, in: Bergey's Manual of Systematic Bacteriology, Vol. 1, ed. N. R. Krieg and J. G. Holt, Williams and Wilkins, Baltimore 1984, p. 602.

20. J. E. Warshaw, S. B. Leschine, and E. Canale-Parola, Anaerobic cellulolytic bacteria from wetwood of living trees, Appl. Environ. Microbiol. 50, 807 (1985)

21. J. R. Postgate, The acetylene reduction test for nitrogen fixation, in: Methods in Microbiology, Vol. 6B, ed. J. R. Norris and D. W. Ribbons, Academic Press, New York 1972, p. 343.

22. M. Bogdahn and D. Kleiner, Inorganic nitrogen metabolism in two cellulose-degrading clostridia, Arch. Microbiol. 145, 159 (1986)

23. H. Bremer and P. P. Dennis, Modulation of chemical composition and other parameters of the cell by growth rate, in: *Escherichia coli* and *Salmonella typhimurium*, Cellular and Molecular Biology, Vol. 2, ed. F. C. Neidhardt, American Society for Microbiology, Washington 1987, p.1527.

24. S. J. Giovannoni, E. F. DeLong, G. J. Olsen, and N. R. Pace, Phylogenetic group-specific oligodeoxynucleotide probes for identification of single microbial cells, J. Bacteriol. 170, 720 (1988)

25. L. J. Ingraham, O. Maaloe, and F. C. Neidhardt, Growth of the Bacterial Cell, Sinauer Associates, Sunderland, Mass., U.S.A. 1983.

26. D. A. Stahl, B. Flesher, H. R. Mansfield, and L. Montgomery, Use of phylogenetically based hybridization probes for studies of ruminal microbial ecology, Appl. Environ. Microbiol. 54, 1079 (1988)

A90-15443

EFFECT ON ATMOSPHERIC CO_2 FROM SEASONAL VARIATIONS IN THE HIGH LATITUDE OCEAN

Tyler Volk

Earth Systems Group, Department of Applied Science, New York University, New York, NY 10003, U.S.A.

ABSTRACT

Data from the North Pacific gyre, Bering Sea, and North Atlantic show large seasonal fluctuations in the pCO_2 of surface waters. The seasonal variation in these high latitudes apparently has a generic pattern: higher surface water pCO_2 in winter and lower in summer. Satellite data will eventually help decipher the relative effects of temperature and biological production in the seasonal carbon cycle, but as yet little work has been done on what possible role the seasonality of pCO_2 in the high latitudes might have on the average value of atmospheric pCO_2. Here I develop a model that shows the average value for atmospheric pCO_2 depends upon the ratio of the rates at which the ocean/atmosphere system moves toward equilibrium values during the summer and winter conditions of the high latitude ocean.

SEASONALITY OF PCO_2 IN THE HIGH LATITUDE OCEAN SURFACES

Data for two sites off Iceland in the north Atlantic shows an important seasonal pattern in many properties of the surface waters /1/. The pCO_2 is lower in the summer than in the winter, which is the opposite the trend expected if the surface temperature, being relatively high in summer, were the determining factor. The nutrients, such as phosphate and nitrate, are relatively low in the summer months, apparently a result of photosynthesis, which removes CO_2 from the surface water as well as nutrients. Higher nutrients in winter are due to a lack of photosynthesis and increased exchange between surface and deep waters. This cycle of nutrients corresponds to a cycle in the organic matter, which controls the seasonality of surface pCO_2. This cycle has been modeled by Peng et al. /2/.

Data from the Bering Sea /3,4/ exhibits a qualitatively similar seasonal cycle. There pCO_2 in the water drops from approximate equilibrium with atmospheric pCO_2 in March and April to become about 50% undersaturated by May and June. The close correspondence in the seasonal cycles of pCO_2 and nitrate content of the surface waters is strong evidence that the reduction in nutrients by photosynthesis is the main factor responsible for reducing the pCO_2 by incorporating carbon into organic tissues.

The same pattern occurs over a broad region of the northern Pacific /5,6/. Four of the five large sectors of the high latitude Pacific have higher surface water pCO_2 in winter months and lower pCO_2 in summer months. Again, this trend is opposite that due to the temperature forcing upon CO_2 solubility and generally agrees with the cycle of organic carbon shown by the nutrients. The importance of nutrients in the seasonal cycle differs from the dominance of temperature in determining the annually-averaged sign of the disequilibrium between ocean and atmosphere in many ocean surface regions /7/.

The question of possible effects from this seasonality on atmospheric CO_2 arises because of the critical role of the high latitude surface ocean in partitioning of carbon dioxide between the ocean and atmosphere /8-11/. These studies used box models to explore the possibility of different steady states, but one study by Wenk and Siegenthaler /11/ is particularly relevant here. They performed a transient calculation to see how the system moved from one state to the other. They found a strictly exponential transient between the states and reasoned why this should be so. The reason was that the transient essentially involved moving an "excess" or a "deficit" of CO_2 with a particular exchange rate between the combined atmosphere and surface boxes and the deep ocean box.

MODEL CONSIDERATIONS

It is instructive to follow this reasoning to examine what the average atmospheric pCO_2 would be if the ocean circulation and surface temperatures and nutrients oscillated between two states, perhaps corresponding to the seasonal variation. Here we consider the seasons as two distinct states, switched instantaneously between one and the other in a repeating cycle. Each state can be characterized by an equilibrium condition, which is the state of the ocean and atmosphere if particular values of ocean circulation, gas exchange coefficients, and distributions of temperatures and chemical properties like nutrients and alkalinity were held for a sufficiently long period of time. In a model with three ocean boxes, equilibrium was approached with a time constant of about 250 years /11/.

Consider, then, two states "a" and "b", which differ primarily in the "summer" and "winter" conditions of their high latitude waters. The two equilibrium values of atmospheric pCO_2 for the total ocean/atmosphere system are, respectively, $P_{eq,a}$ and $P_{eq,b}$. During the time interval when conditions have the equilibrium state $P_{eq,a}$, assume the atmosphere relaxes toward $P_{eq,a}$ with a time constant of k_a^{-1}. Similarly, during the time interval when the equilibrium state of atmosphere is $P_{eq,b}$, assume the atmosphere relaxes toward $P_{eq,b}$ with a time constant of k_b^{-1}. The two governing differential equations are therefore:

$$\frac{dP}{dt} = k_a (P_{eq,a} - P) \qquad \text{during interval } P_{eq} = P_{eq,a} \qquad (1a)$$

$$\frac{dP}{dt} = k_b (P_{eq,b} - P) \qquad \text{during interval } P_{eq} = P_{eq,b} \qquad (1b)$$

Since we consider that state "b" corresponds to the time when the high latitude ocean surface waters are in their winter condition, which has higher surface pCO_2 than during their summer condition, $P_{eq,b}$ is greater than $P_{eq,a}$. Atmospheric pCO_2 at the end of each interval where $P_{eq} = P_{eq,b}$ will be the highest P of the seasonal cycle (P_{max}), while P at the end of each interval where $P_{eq} = P_{eq,a}$ will be the lowest P of the seasonal cycle (P_{min}). This means P_{max} is the initial condition for the beginning of every interval $P_{eq} = P_{eq,a}$ and P_{min} is the initial condition at the beginning of every interval $P_{eq} = P_{eq,b}$. Solving equations (1a,b) with these initializing conditions gives

$$P = P_{eq,a} + (P_{max} - P_{eq,a})\, e^{-k_a t} \qquad \text{during interval } P_{eq} = P_{eq,a} \qquad (2a)$$

$$P = P_{eq,b} + (P_{min} - P_{eq,b})\, e^{-k_b t} \qquad \text{during interval } P_{eq} = P_{eq,b} \qquad (2b)$$

Assuming the equilibrium states and time constants can be known, equations (2a,b) have four unknowns: P for the two time intervals, P_{min}, and P_{max}. However, two additional equations come from continuity of the value of P at the two times when P_{eq} is discontinuous: when P_{eq} switches from $P_{eq,a}$ to $P_{eq,b}$ and when P_{eq} switches from $P_{eq,b}$ to $P_{eq,a}$.

$$P = P_{min} = P_{eq,a} + (P_{max} - P_{eq,a})\, e^{-k_a t^*} \qquad \text{at point when } P_{eq} \text{ switches from } P_{eq,a} \text{ to } P_{eq,b} \qquad (3a)$$

$$P = P_{max} = P_{eq,b} + (P_{min} - P_{eq,b})\, e^{-k_b t^*} \qquad \text{at point when } P_{eq} \text{ switches from } P_{eq,b} \text{ to } P_{eq,a} \qquad (3b)$$

The time t^* is the length of the interval during which $P_{eq} = P_{eq,a}$, and here is also equal to the interval during which $P_{eq} = P_{eq,b}$. In this system where the alternation of $P_{eq,a}$ and $P_{eq,b}$ forms a seasonal cycle, $t^* = 0.5$ yr.

Defining $\phi = k_b t^*$ and $\alpha = k_a/k_b$, we can solve for P_{min} and P_{max} using equations (2a,b) and (3a,b):

$$P_{min} = \frac{P_{eq\,a} + [P_{eq\,b}\,(1-e^{-\phi}) - P_{eq\,a}]\, e^{-\alpha\phi}}{1-e^{-\phi(1+\alpha)}} \qquad (4a)$$

$$P_{max} = P_{eq,b} + (P_{min} - P_{eq,b})\, e^{-\phi} \qquad (4b)$$

It is convenient to define $\Delta P_{eq} = P_{eq,b} - P_{eq,a}$ to be able to express P_{min} and P_{max} in terms of $P_{eq,a}$ and ΔP_{eq}. Then

$$P_{min} = P_{eq,a} + \gamma \Delta P_{eq} \quad (5a)$$

$$P_{max} = P_{eq,a} + \lambda \Delta P_{eq} \quad (5b)$$

$$\text{where } \gamma = \frac{e^{\phi} - 1}{e^{(1+\alpha)\phi} - 1} \quad , \quad \lambda = \frac{e^{(1+\alpha)\phi} - e^{\alpha\phi}}{e^{(1+\alpha)\phi} - 1} \quad (5c)$$

We are interested in the average atmospheric pCO_2, defined here as $P_{av} = (P_{min}+P_{max})/2$:

$$P_{av} = P_{eq,a} + 0.5\,(\gamma+\lambda)\,\Delta P_{eq} \quad (6)$$

For the special case where the summer and winter time constants are identical ($\alpha = 1$), $P_{av} = P_{eq,a} + 0.5\,\Delta P_{eq}$. A way of thinking about this is that the atmosphere is between the two equilibrium states, with summer and winter high latitude conditions about equally important in determining the atmospheric pCO_2. However, as is most certainly the case, if the summer equilibration time is greater than that of the winter, in other words k_a is less than k_b, then P_{av} is closer to that of the winter equilibrium state, $P_{eq,b}$. This is shown graphically in Figure 1a. As a limiting case, if $k_a = 0$, then $P_{av} = P_{eq,b}$. In Figure 1a with P_{av} as a function of α, any variation in ϕ if ϕ is less than about 1 does not significantly affect the relation between P_{av} and α.

Another property of this system of potential interest is the oscillation relative to its maximum possible. This quantity, $(P_{max}-P_{min})/\Delta P_{eq}$ is

$$\frac{P_{max} - P_{min}}{\Delta P_{eq}} = \lambda - \gamma \quad (7)$$

The time scale for gas exchange of CO_2 between the ocean surface and atmosphere is of the order of year to years. That it is at least a year is evident from the fact that strong seasonality in the pCO_2 of surface waters exists. However, adjustment of the entire ocean/atmosphere system to changes in high latitude surface waters takes longer, on times scales of hundreds of years /11/. The relaxation time of about 250 years followes equilibration of the atmosphere and surface ocean, and thus this time may not be appropriate for the seasonal cycle. However, here we have only assumed that there exists some time constant which applies during the seasonal cycle. It is therefore appropriate to examine the behavior of the system from k^{-1}=1 yr. to k^{-1} = 100 yr., or since $\phi = k_b t^*$ and t^*=0.5 yr.≈1.0, we need to examine values of ϕ approximately between 0.01 and 1.0.

Figure 1 shows how varying ϕ affects $(P_{max}-P_{min})/\Delta P_{eq}$ with three different values of α. As qualitatively expected, large values of ϕ (which correspond to small values of the relaxation time, k^{-1}) yield large atmospheric CO_2 fluctuations. Since the changes in surface water nutrients in the glacial/interglacial models is approximately that observed during the seasonal cycle in the high latitudes, it is reasonable that the difference between $P_{eq,a}$ and $P_{eq,b}$ is on the order of the glacial/interglacial atmospheric CO_2 changes, about 60 µatm /8-11/. If $\phi \approx 1$, figure 1 shows that atmospheric CO_2 would vary as a significant fraction of the difference between $P_{eq,b}$ and $P_{eq,a}$, but the air-sea gas exchange coefficient is too low to allow such rapid, large changes. Thus, smaller values of ϕ seem more likely, but this can be tested by running models of the ocean/atmosphere system in transient modes.

CONCLUSIONS

Even though the ocean/atmosphere system moves toward equilibrium over time scales of hundreds of years, this work indicates that seasonality in the high latitudes could affect the steady-state average value of atmospheric CO_2. This effect would exist if the equilibration rates differ between the summer and winter conditions. The fact that the two hemispheres of Earth are in opposite seasons would not affect this result. Winter conditions certainly have faster rates of exchange between the atmosphere and ocean (higher gas exchange coefficients during high latitude winters than summers /12/) and faster rates of exchange between the surface and deep waters (deep convection during winter and stratification during summer /2/). This indicates that seasonality could affect the global average atmospheric pCO_2 by moving this average closer to that of the long-term equilibrium conditions of the winter surface water states. This finding suggests phenomena that should be explored further by converting the steady-state box models into models with time-dependent seasonality in the high latitudes.

ACKNOWLEDGEMENT

Work supported by NASA Grant NAGW-850 to New York University.

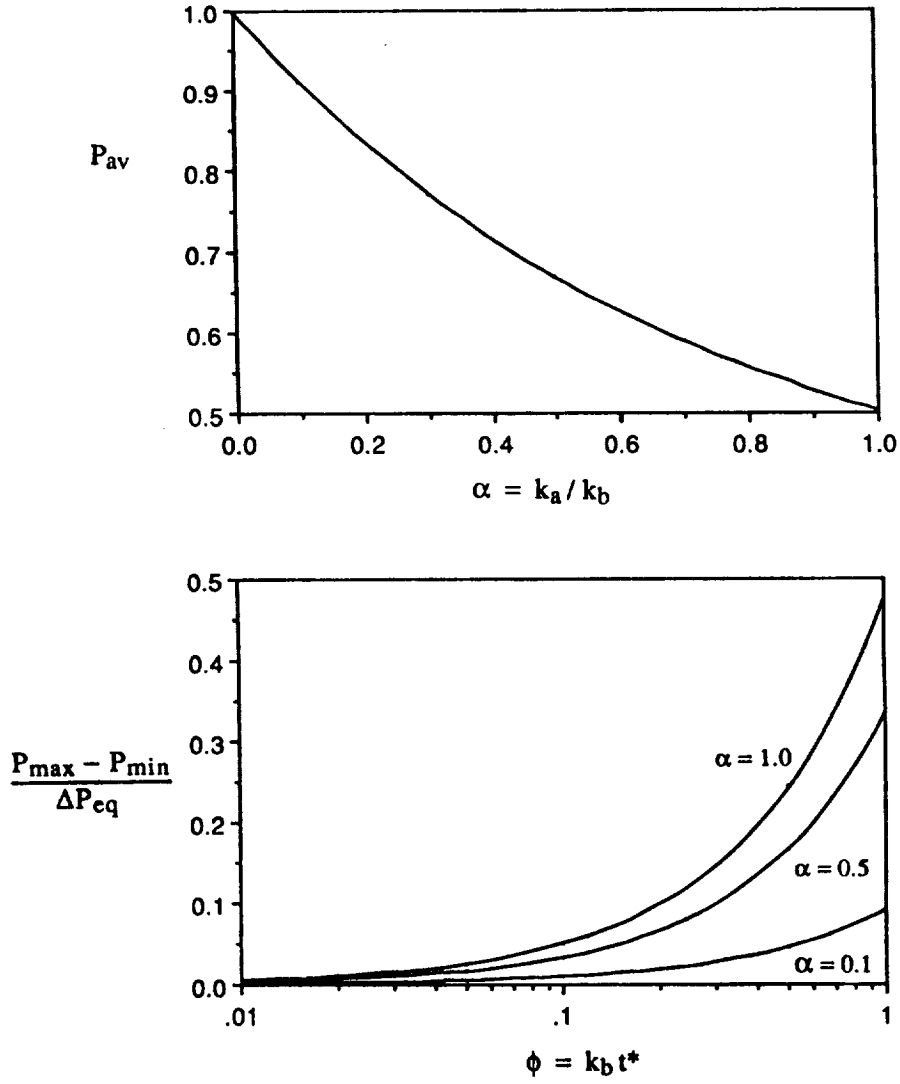

Fig. 1. Variation of atmospheric CO2 (top) and its seasonal variation (bottom) as a function of the parameters derived from the rates of change towards equilibrium during winter (k_b) and summer (k_a).

REFERENCES

1. Takahashi, T., J. Olafsson, W. S. Broecker, J. Goddard, D. W. Chipman and J. White, Seasonal variability of the carbon-nutrient chemistry in the ocean areas west and north of Iceland, *J. Mar. Res. Inst.*, *9*, 20–36 (1985).

2. Peng, T.-H., T. Takahashi and W. S. Broecker, Seasonal variability of carbon dioxide, nutrients, and oxygen in the northern North Atlantic surface water: observations and a model, *Tellus*, *39B*, 439-458 (1987).

3. Codispoti, L. A., G. E. Friederich, R. L. Iverson and D. W. Hood, Temporal changes in the inorganic carbon system of the south-eastern Bering Sea during spring 1980, *Nature*, *296*, 242-245 (1982).

4. Codispoti, L. A., G. E. Friederich and D. W. Hood, Variability in the inorganic carbon system over the southeastern Bering Sea during spring 1980 and spring-summer 1981, *Continental Shelf Res.*, *5*, 133-160 (1986).

5. Takahashi, T., J. Goddard, S. Sutherland, D. W. Chipman and C. C. Breeze, Seasonal and geographic variability of carbon dioxide sink/source in the oceanic areas: Observations in the North and Equatorial Pacific Ocean, 1984–1986 and global summary, *Rep. MRETTA 19X–89675C*, 66 pp., Carbon Dioxide Res. Div., U. S. Dep. of Energy, Washington, D. C.,1986.

6. Takahashi, T., J. Goddard, S. C. Sutherland, G. Mathieu, and D. W. Chipman, Assessment of carbon dioxide sink/source in the north Pacific Ocean: Seasonal and geographic variability, 1986-1987, Progress Report for Contract 19X-89675C to U. S. Dept. of Energy, Washington, D. C., 1988.

7. Volk, T., and Z. Liu, Controls of CO_2 sources and sinks in the earth scale surface ocean: temperature and nutrients, *Global Biogeochemical Cycles*, *2*, 73-89 (1988).

8. Volk, T. and M. I. Hoffert, Ocean carbon pumps: analysis of relative strengths and efficiencies in ocean-driven atmospheric CO_2 changes, in *The Carbon Cycle and Atmospheric CO_2 : Natural Variations Archean to Present*, Geophys. Mongr. Ser., vol. 32, ed. E. T. Sundquist and W. S. Broecker, AGU, Washington., D. C. 1985, p. 99.

9. Ennever, F. K. and M. B. MacElroy, Changes in atmospheric CO_2: factors regulating the glacial to interglacial transition, in *The Carbon Cycle and Atmospheric CO_2 : Natural Variations Archean to Present*, Geophys. Mongr. Ser., vol. 32, ed. E. T. Sundquist and W. S. Broecker, AGU, Washington., D. C. 1985, p. 154.

10. Toggweiler, J. R. and J. L. Sarmiento, Glacial to interglacial changes in atmospheric carbon dioxide: the critical role of ocean surface waters in high latitudes, in *The Carbon Cycle and Atmospheric CO_2 : Natural Variations Archean to Present*, Geophys. Mongr. Ser., vol. 32, ed. E. T. Sundquist and W. S. Broecker, AGU, Washington., D. C. 1985, p. 163.

11. Wenk, T., and U. Siegenthaler, The high-latitude ocean as a control of atmospheric CO_2, in *The Carbon Cycle and Atmospheric CO_2 : Natural Variations Archean to Present*, Geophys. Mongr. Ser., vol. 32, ed. E. T. Sundquist and W. S. Broecker, AGU, Washington., D. C. 1985, p. 185.

12. Etcheto, J. and L. Merlivat, this issue.

SECTION IV

BIOFERMENTOR DESIGN AND OPERATION

N90-15444

DESIGN FOR A BIOREACTOR WITH SUNLIGHT SUPPLY AND OPERATIONS SYSTEMS FOR USE IN THE SPACE ENVIRONMENT

Kei Mori*, Haruhiko Ohya**, Kanji Matsumoto**, Hiroyuki Furuune***, Kyôko Isozaki***, and Peter Siekmeier***

*Keiô University, Hiyoshi 3-14-1, Kôhoku-ku, Yokohama 223, Japan
**Yokohama National University, Tokiwadai, Hodogaya-ku, Yokohama 240, Japan
***La Forêt Engineering and Information Service Co., Toranomon 2-7-8, Minato-ku, Tokyo 105, Japan

ABSTRACT

An experiment was carried out to determine the characteristics of an operations system that can support fast cultivation of algae at high densities in the weightlessness of space.

The experiment was conducted in glass bioreactor tanks, in which light was supplied by radiator rods connected to optical fiber cables. The illumination areas of the tanks were 2600 cm^2, 6000 cm^2, and 9200 cm^2 per liter of solution. The characteristics of O_2-CO_2 gas exchange, concentration and separation of chlorella in the growth medium, dialysis of ionic salts in the growth medium, etc. were examined.

Chlorella ellipsoidea was used in the experiment, yielding the following results:

(1) By increasing the ratio of illumination area to volume, growth rates of up to approximately 0.6 g/L·h could be obtained in a highly concentrated solution (one that contains 20 g/L or more of algae).
(2) The most suitable proportions of carbon dioxide and oxygen gases for growing algae quickly at high concentrations were found to be 10% CO_2 and 10% O_2 (by volume).
(3) There was a high optimum concentration for fast cultivation, and the data obtained resembled the theoretical curve postulated by P. Behrens *et al.*
(4) It was possible to exchange carbon dioxide and oxygen using gas-permeable membrane modules.
(5) It was possible to separare the chlorella from the growth medium and recycle the medium.

INTRODUCTION

A system for space use similar to the one described in this experiment, which will consist of a bioreactor and a solar light collection system, will be able to filter most of the harmful ultraviolet and infrared radiation from sunlight and transfer the concentrated visible light through optical fiber cables to illuminate cultivation tanks. Visible light can also be obtained by passing artificial light, such as light from xenon lamps, through lenses and filters and then into optical fibers [1-4]. This photosynthetic bioreactor system may prove practical not only for red, green, and blue-green algae and photosynthetic bacteria, but also for cell cultures from higher plants.

A previous CELSS paper described the planning and construction of a photosynthetic bioreactor system using the same solar light collection and transmission system and also a silicon membrane module, a CO_2-O_2 gas exchange device, and an acrylic bioreactor tank. Short-time operation experiments were carried out, and a simulation was done to determine the specifications of a system which would allow one person to survive in space [5].

In this experiment, a glass tank was designed and constructed, and a carbon dioxide and oxygen gas exchange device, an ion dialyser, and a filter to separate the culture from the growth medium were fitted to the tank. This operations experiment incorporated an automatic regulation device which received information from DO, DCO_2, pH, and temperature sensors and used it to control other devices. By investigating the characteristics of each device, the optimum parameters for increasing and maintaining the yield of algae were determined.

METHODOLOGY

The Design of a Photosynthetic Bioreactor System using a Solar Light Collection Device [6-8]

The complete system. The bioreactor system for use in space consists of 5 major components (as shown in Figure 1):

(1) Tank illumination subsystem
(2) Light supply subsystem

(3) CO_2 supply and O_2 collection subsystem
(4) Culture supply and separation subsystem
(5) Nutrient supply and recycling subsystem

All of these components operate within a closed system consisting of the tank, a network of tubes, and several devices which are necessary to monitor the DO, DCO_2, pH, temperature, light intensity, etc. of the growth environment [9-11]. The system must be capable of operating for long periods of time without maintenance.

Bioreactor design. The glass photosynthetic bioreactor which we developed and built for this experiment is shown in Figure 2. With this sysrem, solar light or light from a xenon lamp can be transmitted through optical fibers either directly into the tank, or indirectly into light radiator rods, where it can be dispersed very precisely throughout the medium. The radiator rods are protected by glass tubes, but tubes of other materials such as plastic, polymer, and quartz can also be used. This setup also makes it possible to disinfect the tank with steam or chemicals.

This particular bioreactor system has the following advantages:
(1) Since the illumination area can be changed by altering the density of the radiator rods in the tank, the setup allows for a greater degree of freedom than that obtained with previous photosynthetic bioreactors.
(2) It is possible to disperse solar or xenon light, from which ultraviolet and infrared radiation has been removed, with arbitrary intensity and quality.

Hence, it is possible to achieve fast growth at high concentration by dispersing large amounts of light with a spectrum similar to that of sunlight into a closed bioreactor system; it should therefore be possible to design a compact and productive system for a space station.

The solar light collection and transmission system. We recently developed a flat-dome solar collecting system (shown in Figure 3) which is similar to the one which is being planned concentrate it by a factor of 10,000, and focus it into the input end of an optical fiber cable. The focal points of different wavelengths of light are at different distances from the lens: the focal point of ultraviolet light is closest to the lens, followed by the focal points of the visible wavelengths, and the focal point of infrared light is farthest from the lens Hence, it is possible to choose a particular range of wavelengths depending on the placement of the optical fiber input end.

Of course, light from xenon lamps can also be transmitted through optical

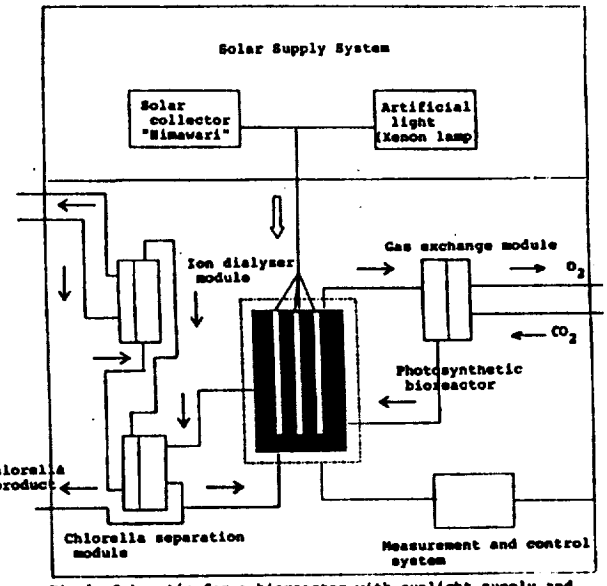

Fig.1 Schematic for a bioreactor with sunlight supply and operations system for use in the space environment.

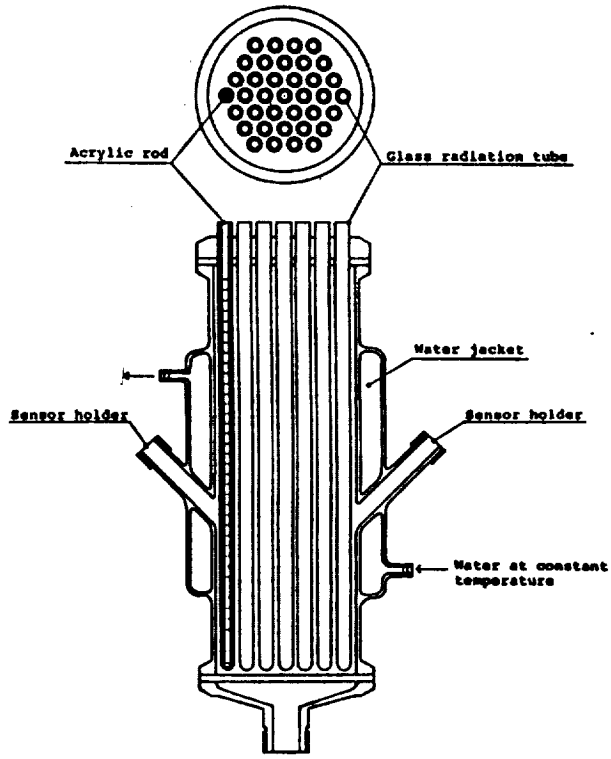

Fig.2 Photosynthetic Bioreactor

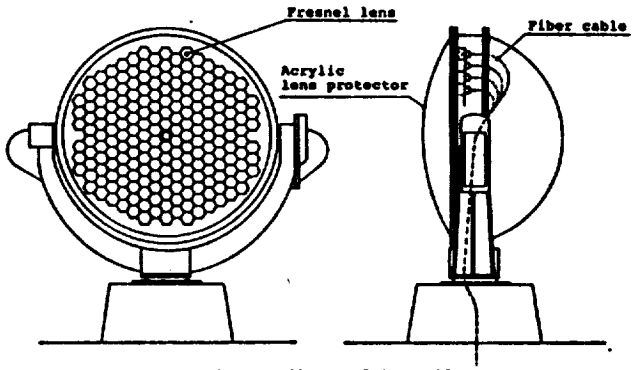

Fig.3 Solar light collector "Himawari" (terrestrial type for experimentation)

fibers afterusing reflecting mirrors and filtersto cut infrared and ultraviolet radiation; it is thus possible to provide the system with stable high-quality light. A xenon lamp unit for supplying artificial solar rays is shown in Figure 4. Figure 5 shows the spectrum of light from the solar light collecting device and the xenon lamp. This system can provide light with a stable quality and intensity for photosynthesis experiments.

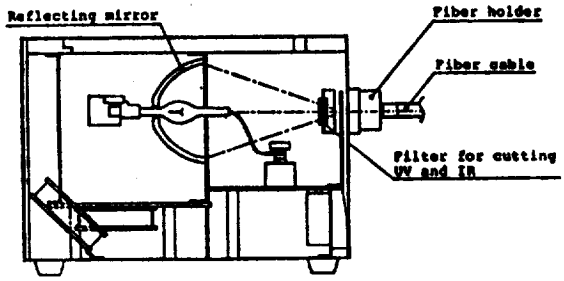

Fig.4 Artifitial light source (xenon lamp)

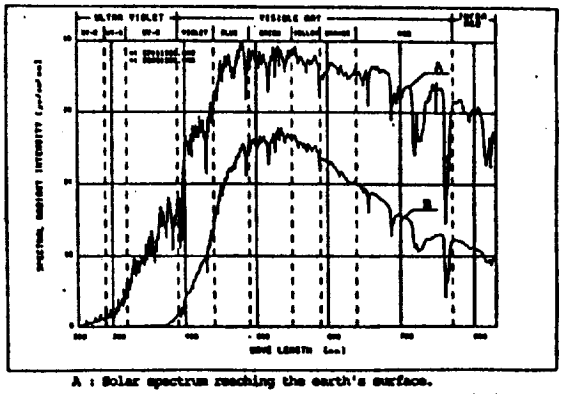

A : Solar spectrum reaching the earth's surface.
B : The same spectrum after passing through a Himawari Light Collector of 60% transmissivity.

Spectrum delivered by the Himawari Light Collector on the earth.

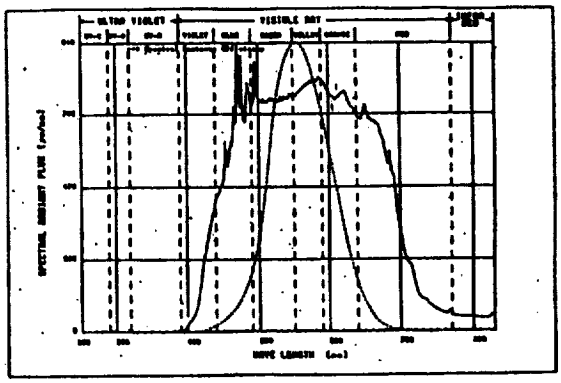

Spectrum delivered by the filtered xenon lamp.

Fig.5 Comparison of the spectra of the Himawari Light Collector and the xenon lamp.

Methods and Materials

A diagram of the operations system used in this experiment is shown in Figure 6. The algal culture used in the experiment was C. ellipsoidea. The composition of the culture medium was as follows: in 1 liter, 5 g KNO_3; 2.5 g $MgSO_4 \cdot 7H_2O$; 1.25 g KH_2PO_4; 0.028 g $FeSO_4 \cdot 7H_2O$; and 1 mL A_5 solvent. The temperature of the medium was kept at 25°C during the experiment.

A xenon lamp was used to provide light resembling sunlight in space, and the light was fed into the bioreactor by optical fibers. The experimental methods are described below.

The photosynthetic bioreactors. The bioreactors used in the experiment consisted of glass tanks of three different sizes (diameters 40 mm, 34 mm, and 28 mm; height 250 mm) and light radiator rods (plastic fibers with a diameter of 3 mm) with glass protection tubes (outside diameter 10 mm, inside diameter 8 mm). These three bioreactors had radiation areas of 2600 cm^2/L, 6000 cm^2/L, and 9200 cm^2/L. (In the case of the bioreactor with a radiation area of 9200 cm^2/L, plastic fibers were inserted directly into the chlorella culture without the use of protective tubes.) The gas used was a combination of varying amounts of carbon dioxide, oxygen, and nitrogen, and a gas flow of about 1 vvm was administered from the bottom of the tank. For each bioreactor tank, the light intensity, initial concentration, and gas composition were varied, and changes in the growth rate (g/L·h) were measured.

Gas exchange devices. The gas exchange module used (manufactured by Mitsubishi Rayon Corp.) contained polypropylene membranes. The chlorella solution was circulated inside the membranes, and a mixture of carbon dioxide, oxygen, and nitrogen gas was circulated outside the membranes. The rate of exchange of carbon dioxide and oxygen between the gas side and the liquid side was calculated from the changes in the concentration of dissolved oxygen (DO) and the concentration of dissolved carbon dioxide (DCO_2).

Chlorella filtration. Two different filtration devices were used to separate the chlorella culture from the growth medium in order to investigate the filtration characteristics of the chlorella: a 0.45 μm microfilter module, and an ultrafiltration device (with a molecular mass of separation of 15,000 to 20,000).

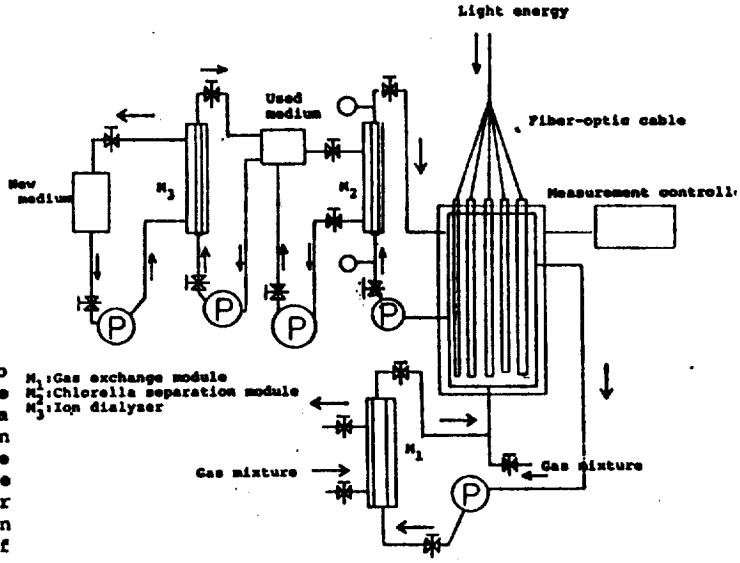

Fig.6 Schematic of operation system used for experimentation.

Determination of ion dialysis characteristics. Samples of chlorella medium taken after growth at high concentrations for long periods of time and then passed through the 0.45 μm membrane filter module were dialysed with new medium (the volume of the new medium used was four times that of the used medium) using a hollow-fiber type dialyser (Kawasumi Laboratories, Inc. KF-101). The new and used growth medium samples, as well as the growth medium obtained after dialysis, were used to grow chlorella on an undulating platform with an average illumination of 3000 Lx; the rates of chlorella growth were compared. The growth medium samples were also placed in an ultrasound-emitting tank (40 kHz ± 2 kHz) for a certain amount of time. The granularity distribution and the chlorella growth rates before and after being placed in the tank were determined, and the effect of the sound waves was investigated.

Measurement and control devices. Concentration of chlorella was determined from the dry weight of a sample. For concentrations of 1 g/L or less, the light absorption at 660 nm was used to calculate the dry weight.
To determine the light intensity, an OMA (Princeton Applied Research model 1450) was used, and the intensity of visible light (380 nm-780 nm) was obtained by integration and converted into watts.

To determine the composition of the gas, oxygen gas was measured by the solid zirconium electric charge method, and carbon dioxide was measured with a gas analyser (manufactured by Able Corp.) by the undispersed infrared absorption method.

EXPERIMENTAL RESULTS

Photosynthetic Bioreactor Tests

The goal of this experiment was to determine growth characteristics resulting from different initial concentrations of chlorella and various gas compositions, given a constant light intensity. Figures 7, 8, and 9 show the growth characteristics for tanks having illumination areas of 9200, 6000, and 2600 cm^2/L. The 9200 cm^2/L tank was given a constant 10% supply of CO_2, and the concentration of oxygen was varied.

For each tank, there was an optimum initial concentration of chlorella, which was found to be near the equilibrium point. With increased light intensity, the most suitable initial concentration was found to shift to a higher value. With bioreactors having a larger illumination area per unit volume, a higher rate of growth was possible, and with an illumination area of 9200 cm^2/L and a concentration of 20-60 g/L, the rate was found to be between 0.4 g/L·h and 0.6 g/L·h. The results show that P. Behrens' model of productivity based on his experiments with *Senedesmus* holds even at higher concentrations [12].

The effects of changes in the amounts of carbon dioxide, oxygen, and nitrogen on the growth rate with an illumination area of 9200 cm^2/L are shown in Table 1. It is apparent that if the percentage of carbon dioxide is made higher or lower than 10 vol%, the rate of growth decreases, and the same holds true for oxygen. The gas composition which yields the highest growth rate is $CO_2:O_2:N_2$ = 10%:10%:80% (by volume). This is independent of the light intensity and is especially evident at high concentrations.

We centrifuged a high-concentration sample grown for a short time under optimum conditions for 20 minutes at 3000 rpm,

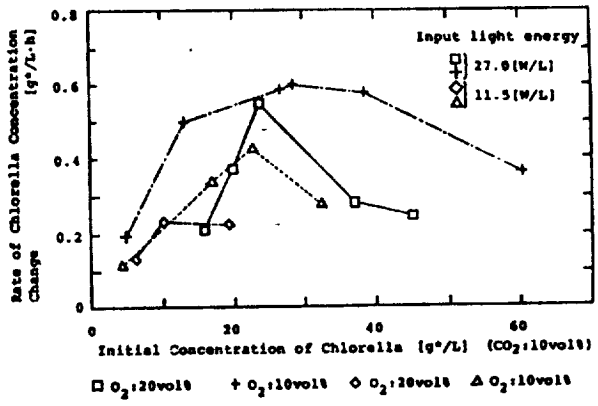

Fig.7 Relationship between rate of change of chlorella concentration and initial concentration of chlorella in new medium (illumination area of 9200cm^2/L).

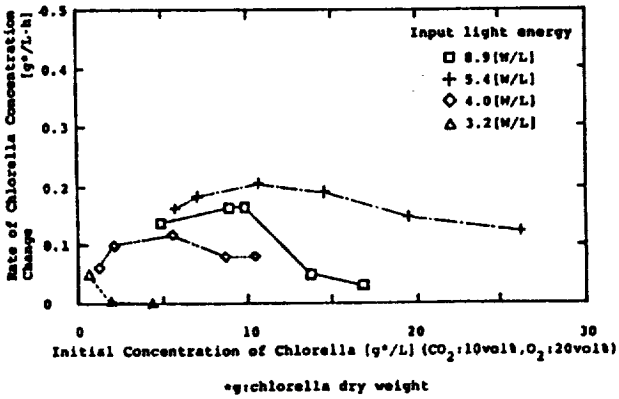

Fig.8 Relationship between rate of change of chlorella concentration and initial concentration of chlorella in new medium (illumination area of 6000cm^2/L).

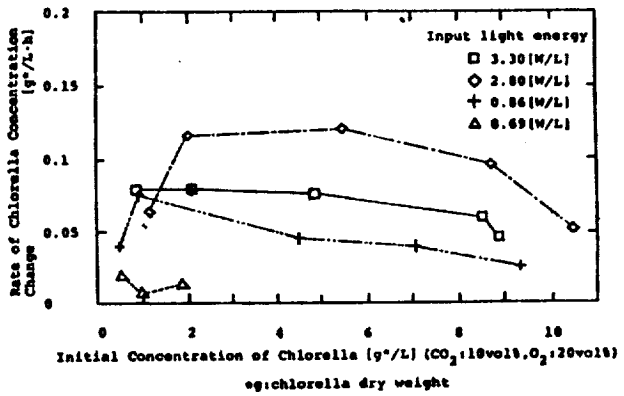

Fig.9 Relationship between rate of change of chlorella concentration and initial concentration of chlorella in new medium (illumination area of 2600cm^2/L).

obtaining a greenish fluid. When examined with a spectrometer, peaks at 663 and 432 nm were evident, indicating the presence of chlorophyll a and chlorophyll b. The growth curve obtained by cultivating chlorella in this used culture medium on an undulating platform is shown in Figure 10. There was a large difference in the growth rates of chlorella in the new culture medium and in the used culture medium, influenced by the concentration of minerals and other recycled substances. It is apparent that inorganic salts are the limiting factor for short-term high-density growth.

Table 1 Effect of Input Gas Proportions on the Rate of C. ellipsoidea Concentration Change (illumination area of 9200cm^2).

Rate of C. ellipsoidea concentration change (g*/L·h)	Initial concentration of C. ellipsoidea (g*/L)	Temperature (°C)	Flow rate:0.06~0.15L/min (1vvm) CO_2 (vol%)	O_2 (vol%)	N_2 (vol%)
0.132	27.27	25	0	100	0
0.16	28.13	25	0	50	50
0.306	26.67	25	0	10	90
0.294	27.93	25	10	50	40
0.426	30.67	25	5	10	85
0.268	34.13	25	20	10	70
0.6	28.7	25	10	10	80

*g:chlorella dry weight

Gas Exchange Tests

Simulation of concentration change in the chlorella culture.

Figure 11 shows a curve representing CO_2 and O_2 concentrations in a chlorella culture supplied with gas containing 10 mol% CO_2. If photosynthetic processes are stopped, (e.g. by the absence of light), the concentration of dissolved CO_2 increases with time as a result of the CO_2 supplied to the system until it levels out at the saturation point (C_A). If light is restored to the system, the concentration of the CO_2 decreases until the rate of CO_2 use is approximately equal to the rate of CO_2 supply (C_{AL}). In the absence of light, the concentration of O_2 in the liquid levels out at the saturation point. If light is restored to resume photosynthesis, the liquid becomes supersaturated with O_2. In this case, the equilibrium concentration of oxygen can be determined by the sum of the amount of oxygen which escapes from the tank and the amount of oxygen that can be collected with a membrane.

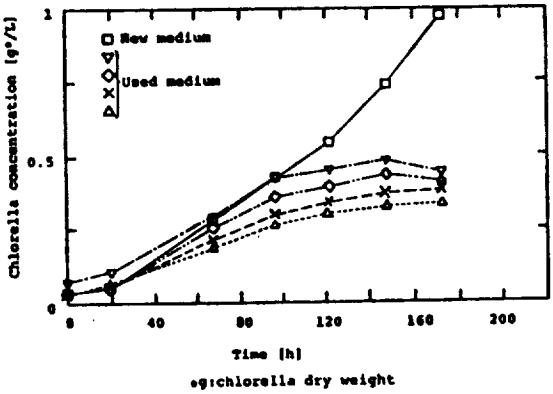

*g:chlorella dry weight

Fig.10 Comparison of chlorella growth curves obtained with used medium and with new medium.

Supply of carbon dioxide. The concentration of carbon dioxide in the solution while in a state of darkness can be expressed as follows:

$$dC_{AL}/dt = K_L \cdot a \cdot (C_A - C_{AL}) \qquad (1)$$

Here, C_A is the CO_2 concentration in the solution at the saturation point, C_{AL} is the CO_2 concentration in the solution, K_L is the mass transfer coefficient, and a is the area of the liquid-gas interface (which is equal to $A \cdot \varepsilon / V$, where A is the area of the membrane, ε is the porosity of the membrane, and V is the volume of the liquid in the tank).

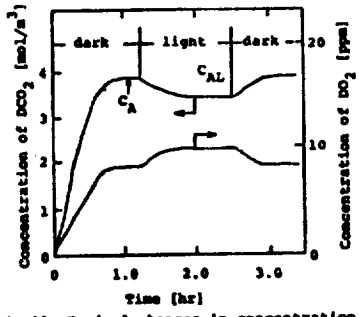

Fig.11 Typical changes in concentration of dissolved CO_2 and O_2.

We conducted experiments in which we changed the following factors which we thought might influence the value of K_L: the concentration of CO_2 in the gas, the pressure of the gas, the flow rate of the gas, the density of chlorella, and the flow rate of the surrounding liquid. It was found that the first four factors did not affect the value of K_L, but K_L was affected by the flow rate of the surrounding liquid. In Figure 12, the relationship between the Sherwood value Sh (= $K_L d_h/D$), oxygen collection h contains the liquid flow, is shown. Here, d_h (the radius of the hollow fibers in the membrane) = 200 μm, D (the dissolution constant of water) = 1.9¥10^{-9} m^2/s, n (the viscosity of water) = 9.0¥10^{-7}m^2/s, and v is the flow rate inside the hollow fibers.

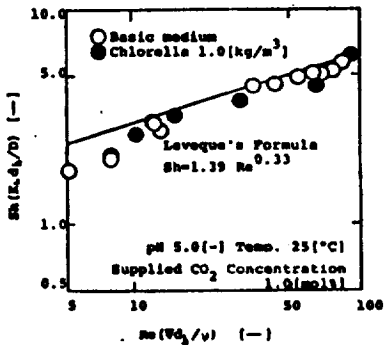

Fig.12 Relationship between values of the Re and Sh functions.

The straight line in the graph shows the Leveque model which can be applied to flow through tubes, and it is evident that the flow of plain growth fluid and also of growth fluid containing chlorella corresponds fairly closely with the predicted flow.

Collection of oxygen through membranes. The concentration of dissolved O_2 can be calculated by the following formula:

$$dC_{BL}/dt = [K_A C_{AL} S/a] - [K_L' a (C_B - C_{BL})] - O_2(g)/V \qquad (2)$$

Rate of photosynthesis — Rate of membrane oxygen collection — Rate of emission of oxygen from the tank

Here, C_{BL} is the O_2 concentration in the liquid, K_L' is the mass transfer coefficient for O_2, C_B is the concentration of oxygen at saturation, and $O_2(g)$ represents the oxygen which is emitted from the tank.

Under normal conditions, the amount of oxygen produced by photosynthesis can be expressed as the sum of the amount of oxygen collected with the membrane and the amount of oxygen escaping from the top of the tank. From the results of the experiment, it was shown that the amount of oxygen collected with the membrane increased with the flow of the surrounding liquid, given a constant photosynthetic rate. The relationship of the membrane oxygen collection ratio (rate of oxygen collection through the membrane / rate of photosynthetic oxygen production) to the Re value is shown in Figure 13. In the graph, Σ represents the total rate of oxygen collection through the membrane and Σ represents the rate of collection of dissolved oxygen which passes through the membrane and rises as gas, where $K_L'=K_L$. It is thought that the difference is due to bubbles of oxygen in the surrounding liquid which escape as bubbles from the membrane due to the pressure difference between the liquid and the gas.

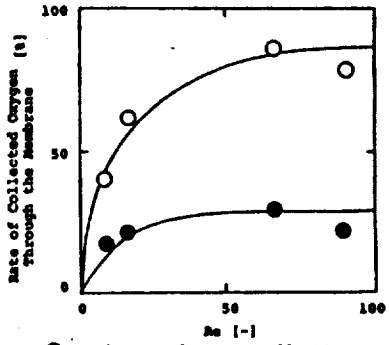

Fig.13 Relationship between the oxygen collection rate and Re value.

In Figure 13, it is shown that on earth, about 80% of the oxygen can be collected with a membrane, but it is thought that in the absence of gravity, all of the oxygen bubbles will circulate around the surrounding liquid, so that nearly 100% can be collected.

Membrane area necessary to support one human. A human requires 620 L of oxygen per day. It is thought that if 620 L of carbon dioxide is given to the system, all of the necessary oxygen can be produced. The rate at which CO_2 passes through the system is related to other factors by the following equation:

$$J = K_L \cdot e \cdot A (C_A - C_{AL}) \qquad (3)$$

The rate of supply of CO_2 is 620 L per day (i.e. $J = 2.94 \times 10^{-4}$ mol/s). The necessary membrane area, as shown in Equation 3, depends on the difference between the CO_2 concentration of the medium and the CO_2 concentration at saturation point as well as the mass transfer coefficient. In Figure 14, the relationship between the membrane area necessary to administer the amount of carbon dioxide necessary to support a human for a day and the CO_2 concentration difference is shown using the Reynolds value (which influences the mass transfer coefficient) as a parameter. Using this graph, it is possible to obtain the necessary membrane area under various operation conditions.

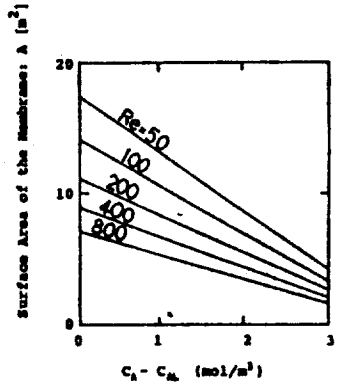

Fig.14 Effect of Re and the gas-liquid difference in CO_2 concentration on the necessary membrane area.

Tests on Chlorella Separation Characteristics

The results of these tests are shown in Figure 15. Initially, the rate of flow through the microfilter (MF) was unusually high, but it dropped quickly. The ultrafilter (UF) had a low but constant flow rate. The chlorella adhered to the microfilter, resulting in a low chlorella collection rate. It is thought that with the microfilter, chlorella not only collected on the surface, but also became clogged inside. The ultrafilter showed a buildup of chlorella only on the surface. Clearly, it is necessary to take into account the concentration, cellular size, and granularity of a culture when choosing porous hollow fiber filters, ceramic filters, etc.

Ion Dialysis Tests

The growth curves obtained by cultivating chlorella on an undulating platform with (1) culture medium which has been passed through a 0.45 μm membrane filter (used culture medium), (2) new culture medium, and (3) dialysed medium, are shown in Figure 16. The growth curves obtained with the new medium and the dialysed medium are about the same, unlike the difference between the new medium and the old medium. This is thought to be a result of constant ion supply through the dialysis membrane.

Table 2 shows the chlorophyll distribution in the used culture medium, the dialysed culture medium, and the new culture medium. The growth curve for the used culture medium showed low rates of growth, and the spectrum of pigments (extracted using acetone) shows low levels of chlorophyll a (663 nm) and chlorophyll b (432 nm). The new culture medium and the dialysed culture medium both show high levels of pigment density.

Figure 17 shows the growth curve of chlorella which has been exposed to ultrasonic waves. There were practically no effects noticed after exposure to ultrasound for 10 or 20 minutes. There was no change in granularity, and there was no damage from the ultrasonic exposure. The cell wall of *Chlorella* is hard, and it is difficult to damage it by ultrasound waves, so in order, to make it possible for humans to digest, it is necessary to dry the cells and then physically destroy the cell walls with a homogeniser. However, ultrasound may be useful for removing chlorella which sticks to the bioreactor system.

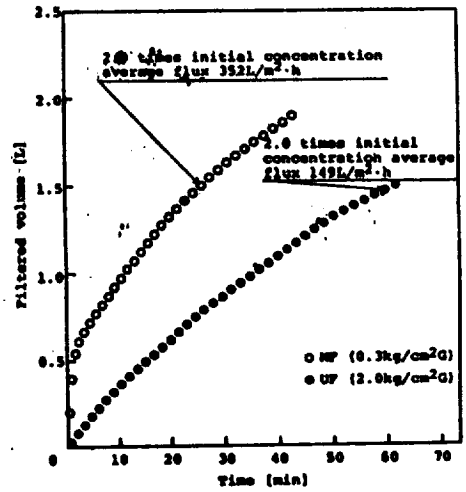

Initial volume: 3.0[L]
Effective membrane surface (one side): 0.10[m²]
Chlorella concentration: 2.0[g*/L]
*g:chlorella dry weight

Fig.15 Comparison of MF and UF permeability

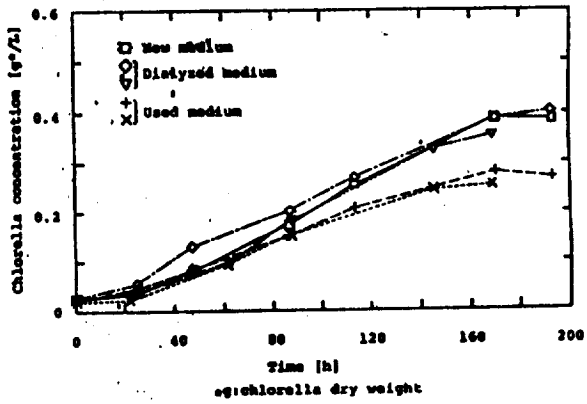

*g:chlorella dry weight

Fig.16 Comparison between chlorella growth in ion dialysed medium and used medium.

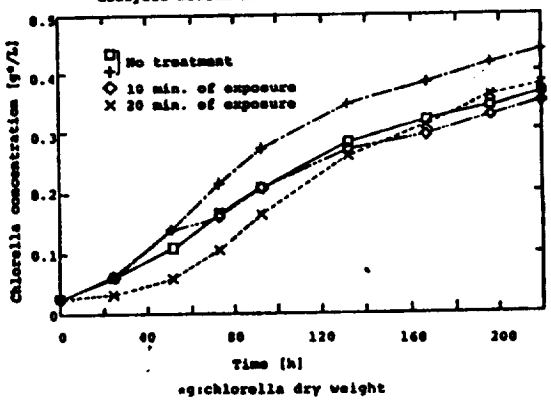

*g:chlorella dry weight

Fig.17 Growth curves of chlorella exposed to ultrasonic waves.

CONCLUSIONS

The following implications for the characteristics and the feasibility of a photosynthetic bioreactor which can grow algae quickly at high concentrations follow from this experiment:

(1) By increasing the illumination area per unit volume, a growth rate of up to around 0.6 g/L·h could be obtained.

(2) For high density and high speed growth, the optimum amounts of carbon dioxide and oxygen were 10 vol% CO_2 and 10 vol% O_2.

(3) At the optimum density for high speed, high-density growth, a growth curve resembling that predicted by P. Behrens' model was obtained.

(4) It was possible to administer carbon dioxide gas and collect oxygen gas using gas exchange modules.

(5) It was possible to separate chlorella from its growth medium and recycle the old growth medium.

We can think of various bioreactor system setups for space use, such as a life-support system for CELSS and a system for experiments with cells of higher plants. We are planning to conduct continuous operations system experiments for long periods of time in order to verify our results.

Table 2 Comparison between chlorophyll concentration of used medium, ion dialysed medium, and original medium.

Medium	Total concentration of chlorophyll (μg/mg*)	Chlorophyll a (μg/mg*)	Chlorophyll b (μg/mg*)
Used medium	5.0	2.8	2.2
Ion dialysed medium	24.0	17.0	7.0
Original medium	32.0	23.0	9.0

*mg:chlorella dry weight

REFERENCES

1) K. Mori, "A Lighting System for Supplying Visible Solar Light with Fiber-Optic Cables," 14th National Congress of the Illuminating Engineering Institute of Japan, Apr. 3, 1981 (in Japanese).

2) K. Mori, N. Tanatsugu and M. Yamashita, "Visible solar-ray supply system for space station," Acta Astronautica, Vol. 13, No. 2, p. 71 (1985)

3) K. Mori (inventor), "Apparatus for Collecting and Transmitting Solar Energy," U.S. Patent No. 4,461,278.

4) M. Oleson and R. L. Olson, "Conceptual design option study-controlled ecological life support system (CELSS), NASA Contractor Report 177421, Contract NAS2-11806 (June 1986)

5) K. Mori, H. Ohya, K. Matsumoto and H. Furuune, "Sunlight Supply and gas exchange systems in microalgal bioreactor," Adv. Space Res. vol. 7, pp. 447-452 (1987)

6) K. Mori et al., "An Experimental System for an Ecologically Controlled Environment Space Station Symposium," The Japan Society for Aeronautics and Space Sciences, Jun. 27, 1983 (in Japanese).

7) K. Mori, "Photoautotrophic bioreactor using visible solar rays condensed by Fresnel lenses and transmitted through optical fibers," Biotechnology and Bioengineering, No. 15, p. 331 (1986) John Wiley and Sons, Inc.

8) K. Mori (inventor), "Photoradiator," Japanese Patent Applications No. 78,809/82, 78,810/82, 97,459/82, 99,775/82.

9) R. D. Johnson, "A closed life-support system for space colonies," 77-ENAS-18 (1978), ASME publication

10) David T. Smernoff, Robert A. Wharton Jr. and M. Averner, "Operation of an Experimental Algal Gas Exchanger for use in a CELSS," NASA Conference Publication 2480 (1987).

11) R. D. Gafford and D. E. Richardson, "Mass Algal Culture in Space Operation," Journal of Biochemical and Microbiological Technology and Engineering, vol. II, no. 3, pp 299-311 (1960).

12) P. Behrens, K. Arnett, R. Glandue, J. Cox, D. Lieberman and R. Radmer, "Algal Culture Studies for CELSS," NASA Contractor Report 177448, Contract NAS2-12115 (June 1986).

N90-15445

CLOSED AND CONTINUOUS ALGAE CULTIVATION SYSTEM FOR FOOD PRODUCTION AND GAS EXCHANGE IN CELSS

*Mitsuo OGUCHI, Koji OTSUBO, Keiji NITTA**
*Atsuhiro SHIMADA, Shigeo FUJII, Takashi KOYANO, Keizaburo MIKI***

* Space Technology Research Group, National Aerospace Laboratory,
7-44-1 Jindaiji-Higashimachi, Chofu, Tokyo 182, Japan
** Corporate Research & Development Laboratory, Toa Nenryo Kogyo K.K.
3-1 Nishitsurugaoka 1-Chome, Ohimachi, Iruma-gun, Saitama 354, Japan

ABSTRACT

In CELSS (Controlled Ecological Life Support System), utilization of photosynthetic algae is an effective means for obtaining food and oxygen at the same time. We have chosen Spirulina, a blue-green alga, and have studied possibilities of algae utilization. We have developed an advanced algae cultivation system, which is able to produce algae continuously in a closed condition.
Major features of the new system are as follows.
(1) In order to maintain homogeneous culture conditions, the cultivator was designed so as to cause a swirl on medium circulation.
(2) Oxygen gas separation and carbon dioxide supply are conducted by a newly designed membrane module.
(3) Algae mass and medium are separated by a specially designed harvester.
(4) Cultivation conditions, such as pH, temperature, algae growth rate, light intensity and quantity of generated oxygen gas are controlled by a computer system and the data are automatically recorded.
This equipment is a primary model for ground experiments in order to obtain some design data for space use.
A feasibility of algae cultivation in a closed condition is discussed on the basis of data obtained by use of this new system.

INTRODUCTION

To realize the long duration living of human beings in space, we have to transport the various necessary materials such as food, gases, water and so on. However, this way is expensive and has problems about consumption of restricted resources in the earth. So to solve those problems, CELSS has been earnestly studied in recent years.

Oxygen and food are indispensable materials for maintaining a living environment for human beings and animals. Then, microalgae having higher photosynthetic ability are one of the most important components of CELSS in point of air regeneration and food production. Especially, Spirulina is considered to be a good candidate because of the following distinctive features.

① High food value and easy digestion.
② Rapid growth and easy harvest.
③ High utilization efficiency of CO_2.

From the reasons of mentioned above, we have been experimenting with closed gas systems since 1986 /1/. As we had obtained a confirmation for photosynthetic algae utilization through this effort, we have been studying a closed and continuous algae cultivation system.

DESIGN OF SYSTEM

Algae cultivation in a weightless environment has lots of problems compared with ground cultivation. In industrial algae cultivation which cultivates algae mass only as food, to supply enough carbon dioxide and light energy for algae, the culuture solution is well agitated by means of bubbling air in an opened type cultivation pool. However, those methods can not be used in a weightless environment. Considering utilization efficiency in space, a tank type closed cultivator seems to be most suitable.

Construction of system

The closed and continuous algae cultivation system is composed of three parts, a main body, an instrumental panel and a computer system. This system could be worked either automatically or manually.

Figure 1 shows the schematic flow diagram. Culture solution is circulated by p-2 pump (using a roller or centrifugal pump) through the bypass line which is made of silicone rubber tube. The solution is pumped out at the top of the cultivation tank and flows in from three inlets at the bottom of the cultivation tank. The flow rate is from 0.6 to 3 liter/min.

A thermo-sensor and pressure-sensor are set on the top of the cultivation tank. An optical density(O. D.)-sensor, a pH-sensor and a heater are set on the bypass line. Two hollow fiber membrane modules used as an oxygen separator and a carbon dioxide supplier are also set on the bypass line. Oxygen gas is separated from the culture solution through the membrane module and pumped to a tank by a vacuum pump, P-1. The concentration and quantity of separated oxygen gas are measured by an O_2 analyzer and a gas flow meter. In order to check the concentration of CO_2 contained in separated gas, a CO_2 analyzer is also used. Carbon dioxide gas is supplied from the CO_2 tank to the culture through the membrane module.
All of those indicators are set on an instrumental panel.

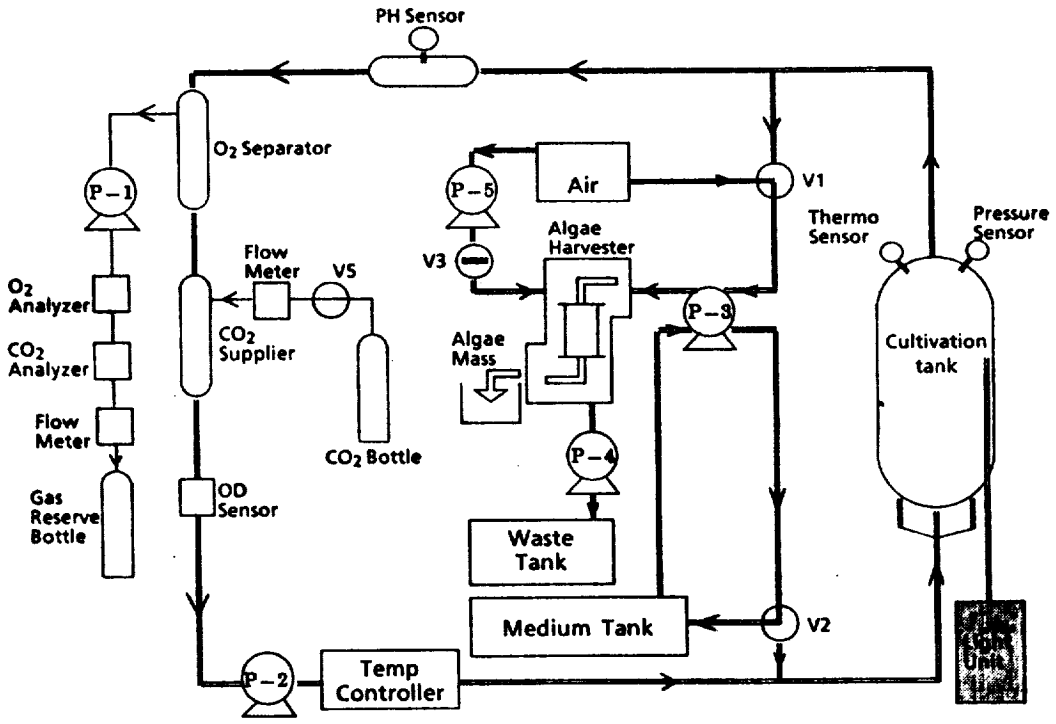

Fig. 1 The schematic flow diagram of the system

The specifications of this system is shown in Table 1.

TABLE 1 Specifications of Cultivation System

Cultivation tank	I.D. 180 DIA × 370 H (mm)
Lighting source	Halogen lamp (50w×3)
Light supply methods	Bundled plastic optical fiber and Acrylic optical rod
Sensors	Pressure, Temperature, pH, Optical density, Oxygen, Carbon dioxide and Gas mass flow
Gas separator	Hydrophobic porous type membrane module
Controllers	Pressure, Temperature and pH
Instrument panel	530 W×600 D×1500 H (mm)
Computer	Personal computer Program language : Basic Program size : 140KB
Total power	400 w (max : 700 w)

Apparatus

Cultivation tank. The cultivation tank is made from acrylic resin and has a round shaped top and bottom in order to facilitate the collection of generated oxygen gas. The tank is 180 mm inner diameter × 370 mm height and an inner volume is about 6 liter. Two kinds of cultivation tank have been made. Although the outer shape is similar, one has three bundles of optical fibers and the other has three acrylic optical rods to provide light energy.

The bundle of optical fibers is made up of about 30 plastic optical fibers each with a diameter of 2 mm and a pointed head cut at an angle of 45 degrees so that the light leaks uniformly. Likewise, the optical rod has grooves cut around its surface at varying depths and intervals. The light is supplied through the bundle of optical fibers or the acrylic optical rod from three halogen lamp units. The maximum light intensity is about 10,000 lux.

The bottom inlets have an angle against the vertical axis so that the culture flow swirls in the cultivation tank and keeps the Spirulina culture homogeneous.

Gas separator. As a gas separator, a hydrophobic porous type hollow fiber membrane module has been used in this experiment. A previous type module and a new designed one are shown in Fig. 2. Until now, the previous type which is commercially available for medical use as in Fig. 2 (a) has been used. But because both the inlet and outlet are at right angles, those especially the outlet were gradually clogged by growing algae mass. In order to prevent the clogging, a new module with a U-typed hollow fibers as shown in Fig. 2 (b) is designed. The major feature of new module is to use re-usable hollow fibers which are constructed so as to be removed easily.
The characteristics of the hollow fibers is shown in table 2.

Optical density-sensor. A diode laser and photo detector are used as the O.D.-sensor. A glass cell connected to the bypass line is fastened just between the diode laser and the photo detector. The wavelength of diode laser is 780nm and the dimensions of the diode laser and the photo detector are 25mm (W) × 25mm (H) × 55mm (L) respectively.

Algae harvester. The algae harvester is made of six cylindrical filters (the bore of 3mm, the length of 30cm, the pore size of 10μm(×3) and 30μm(×3)). The filters are mounted on a board, size of 25.5cm (W) × 18cm (D).

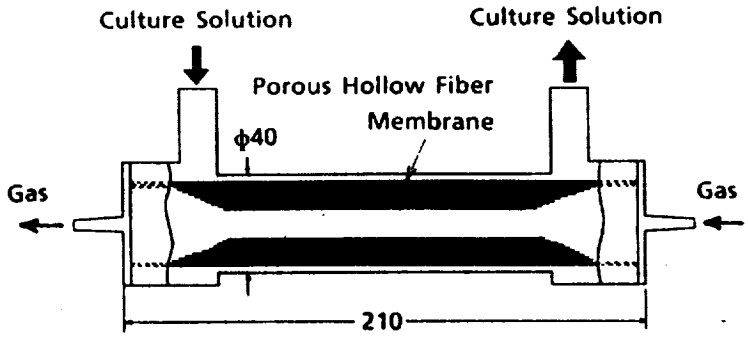

(a) Gas separator used medical type in the market

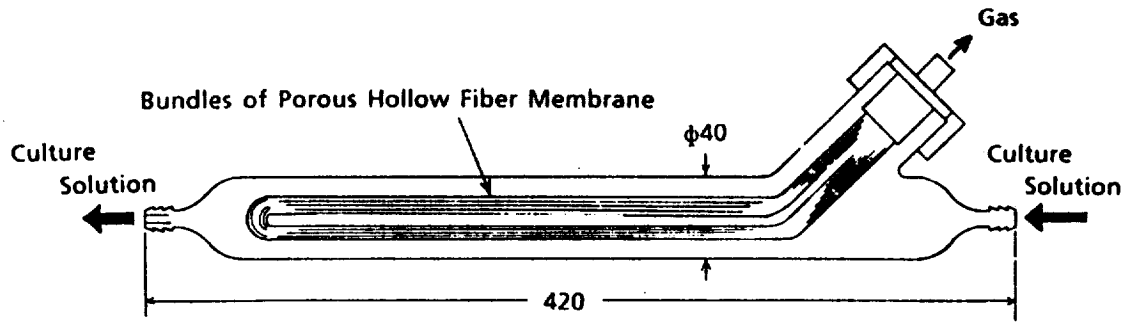

(b) New designed gas separator

Fig. 2 The Illustrations of Membrane Module

TABLE 2 Characteristics of Porous Hollow Fiber Module

Material	Polypropylene
Inner diameter	200 μm
Wall thickness	22 μm
Porosity	45 %
Pore Size	0.036 μm
Gas flux	7×10^4 l/m^2 hr 0.5atm
Bubble point	12.5 kg/cm^2
Effective area	0.3 m^2

Operation for culturing. Algae cultivation is controlled by means of four operational modes using a computer system. Manual operation is also possible.
Electric valves, valve-1 and valve-2, are set on the sub-line connected to the bypass line. When valve-1 is opened and pump-3 is run, the Spirulina culture flows into the algae harvester. When valve-2 is opened and p-3 is run, the medium is added to the bypass line from the medium tank.
The four modes of operation of valve-1 and valve-2 are as follows:

	valve-1	valve-2	P-3	P-4	P-5
I) Ordinary	Closed	Closed	Off	Off	Off
II) Harvest	Open	Open	On	On	On
III) High pressure	Open	Closed	On	On	On
IV) Low pressure	Closed	Open	On	Off	Off

Ordinary mode. Usually the system runs in ordinary mode. Both valve-1 and valve-2 are closed and culture is neither harvested nor medium added.

Harvest mode. When algae growth and O.D. value reaches the maximum, valve-1 and valve-2 are opened and the culture flows into the harvester. Then the medium is filtrated through the filter to the waste tank by pump-4. After filtration, electric valve-3 is opened and the algae mass is blown out by pump-5 while the fresh medium is added to the culture to keep the internal pressure constant.

High pressure mode. When the value of the internal pressure of the cultivation tank is over the maximum, only valve-1 is opened and the culture flows into the algae harvester until the pressure decreases to the ordinary level.

Low pressure mode. When the value of the internal pressure of the cultivation tank is under the minimum, only valve-2 is opened and the medium flows into the bypass line until the pressure increases to the ordinary level.

A computer system is set to control these four modes, and also the pH value by switching the electric valve-5.
All data obtained by sensors are recorded in the computer and transcribed into a graph.

RESULTS AND DISCUSSION

The species of Spirulina used in these experiments are Spirulina maxima, Spirulina oscillatoria and Spirulina subsalsa. The culture is maintained in a liquid culture medium /2/.
The cultivation system runs in the following conditions. Light intensity at 3,000 to 10,000 lux, temperature at 30 °C, pH at 8.6 to 10.5, internal pressure at 0.01 to 0.10 kgf/cm^2, O.D. at 10 to 30 %. P-2 speed at 820 to 2,000 ml/min.

There were no problems observed regarding computer control of pH, pressure, O.D. and data logging. Figure 3 shows the data obtained by culturing S. subsalsa in the closed and continuous cultivation system. The concentration of separated oxygen gas increased gradually and reached a value of 32 % after 108 hours culture. All through this experiment, the separated oxygen gas was pumped from the culture constantly at a mean flow rate of 200 ml/min by vacuum pump. In order to keep internal pressure stable, the valve for CO_2 supply was opened and CO_2 gas was pumped into the culture continuously.

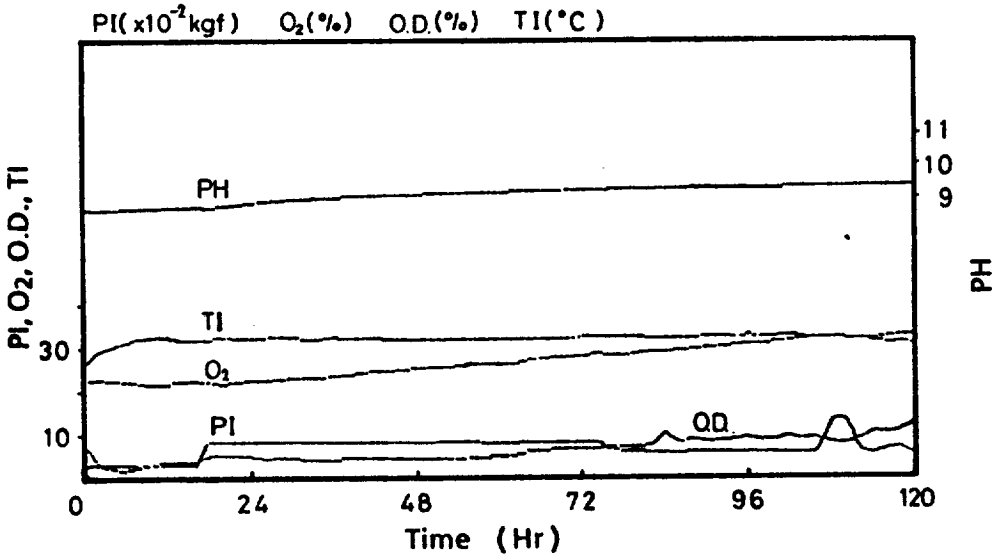

Fig. 3 Some of data obtained from the cultivation system
The line shows pH, Temperature, O_2 concentration, O.D. and Pressure.

Though S. subsalsa culture was not bacteria free, no serious bacteria contamination problems occurred in long continuous culture as compared with other algae cultures. For maintaining good algae growth and constant oxygen production, S. subsalsa would be a good candidate for algae culturing in space.

Apparatus

Light supply method. The light intensity in the early culturing stage showed a value of about 10,000 lux near the part of the optical fibers and rods and about 5,000 lux at the surface of the tank wall.
Since the optical rods are directly submerged in the culture solution so as not to create dead space, algae mass tended to adhere to the cut part of the surface of the rod. As a result of this phenomenon, the light supplying efficiency dropped and took more time than the culture using the optical fibers.

O.D.-sensor. Generally, algal growth is monitered by measuring optical density of culture solution at a wavelength around 680nm in a spectrophotometer. On the other hand, the O.D. value at 560nm seems to have better response for Spirulina growth check /3/. However, a compact photoelectric sensor with a wavelength of around 560nm, which is applicable in this cultivation system, could not be found.
Then a photoelectric sensor with a wavelength of 660nm as a compact O.D.-sensor was obtained. But the photoelectric sensor did not work well due to the unstable response.

Therefore, a diode laser with a wavelength of 780nm was tried as O. D.-sensor and it showed a good response to algal growth. Figure 4 shows the relationship between the value obtained with diode laser and algal dry weight. The O.D. value is not directly proportional to the algal dry weight. However, the amount of algal biomass in the sample could be roughly estimated by its O.D. value.

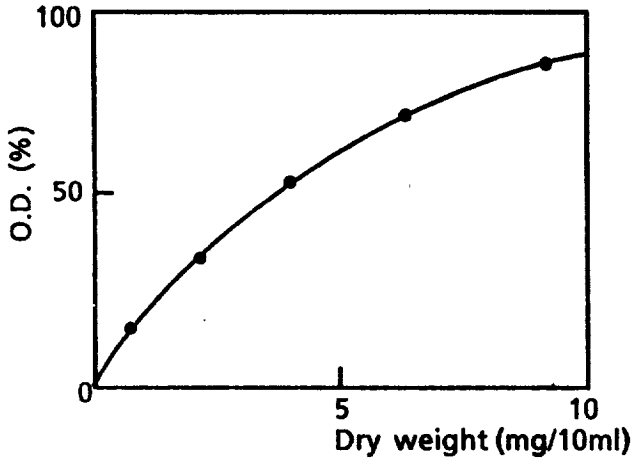

Fig. 4 The relation between the O.D. value obtained with Diode laser and algal dry weight

Algae harvester. Cylindrical filters are used as the Spirulina harvester. Since Spirulina is filamentous algae, it is easily harvested compared with Chlorella. The diameter of the cylindrical filter used in this experiment is 3mm. If the diameter of the filter is larger than this, the algae mass does not flow out when blown by air. Spirulina culture was concentrated more than 16 times by this harvester. About 1g dry weight of algae mass was harvested on a run. In good culture condition, no clogging was observed after repeated harvests.
It would be possible to clean the algae mass with water using this harvester if additional pumps and filters were attached.

Influence of circulation pump. When S. maxima culture was circulated by a centrifugal pump, the culture did not show good growth because of its high shearing effect on the algae. However, no bad effect was observed for the growth rate of S. subsalsa culture circulated by the centrifugal pump. It's partly because S. subsalsa is smaller than S. maxima and its spiral-shape is tight.

The bellows pump, which is neither a centrifugal nor roller type, generates no friction and is capable of moving liquid containing some air. So it seemed to be better than the centrifugal type for algae culture. But the S. subsalsa culture did not show good growth when the culture was circulated by the bellows pump. Otherwise, no problem was observed for S. maxima culture when it was circulated by the bellows pump at the flow rate of 1,120 ml/min.
But as the circulating speed of the bellows or the roller pump was comparatively slow in comparison to the centrifugal one, some problems still remained about gas separation.

Figure 5 shows the effect of circulation on the growth of S. maxima using a stirrer as a reference culture and three kinds of pumps (bellows, centrifugal and roller pump).

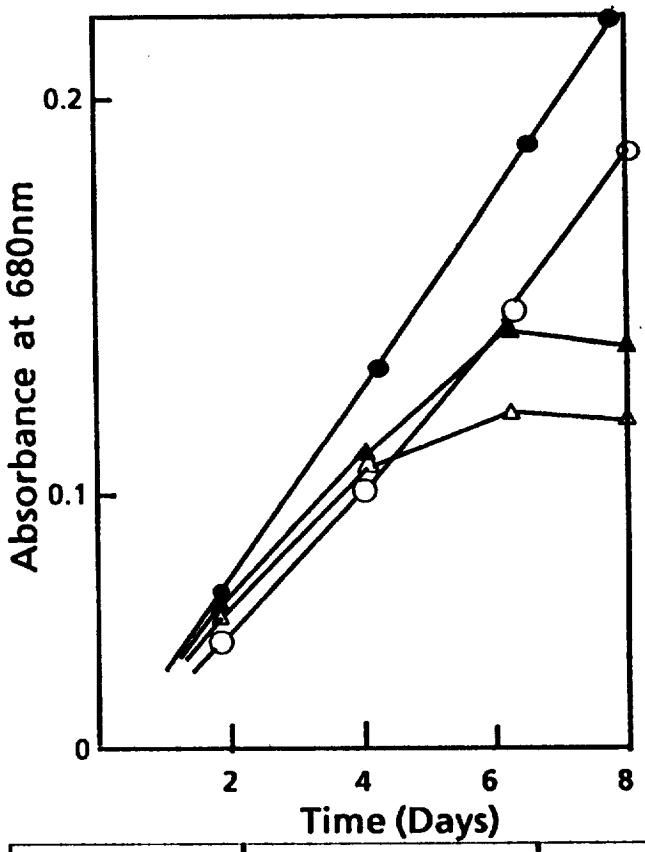

Symbol	Methods	Circulation rate
●	Stirrer	–
○	Bellows pump	1,120 ml/min
▲	Centrifugal pump	1,800 ml/min
△	Roller pump	1,200 ml/min

Fig. 5 Effect of Circulation on the Growth of S. maxima

Gas separator. As for this experiment, the newly designed membrane module has no algae clogging problem at the inlet and outlet of the module.
According to the straight culture solution flow, the circulation speed has increased about one liter/min over the previous type.
But other problems have occurred.

Algae growth was shown by monitoring O.D. at 780nm with a diode laser. Gradual increase of the pH value was observed together with the O.D. value increase as shown in Fig. 3. However, the O.D. value of this experiment was a little lower than in the batch culture because of Spirulina cell adhesion to the hollow fibers of the membrane modules. In the batch culture, S. subsalsa grew rapidly as shown in Fig.6, but in cultures circulated through the hollow fibers, algae tended to clog.

As a result, the O.D. value was not as high as the batch culture. One reason why algae clogged is that S. subsalsa produces poly-saccharide, and another is the design of the membrane module and the solution circulating speed. Because of its adhesion problem, we did not succeed in keeping a long (months) continuous culture of S. subsalsa in this cultivation system. Improvements in membrane module design will decrease that problem and then more oxygen could be obtained from S. subsalsa culture.

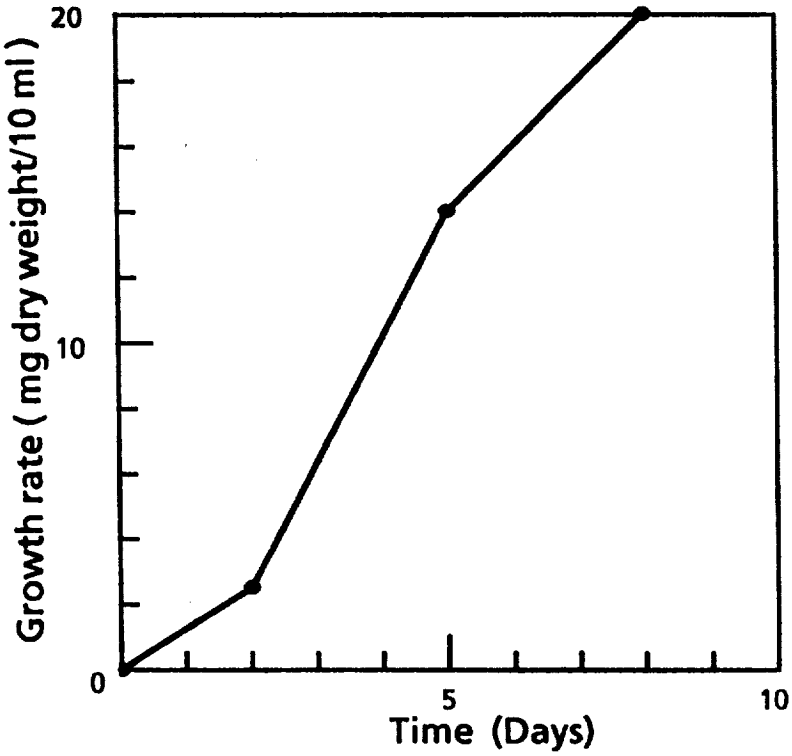

Fig. 6 Growth curve of S. subsalsa. in the batch culture

After those experiments, a gas recovering test which used the same equipment already reported /1/ was tried. The test experiments were started after the concentration of dissolved oxygen decreased to some degree. Pure oxygen gas was supplied at the rate of 30 ml/min for 10mimutes.

The results are shown in Fig. 7. Fig. 7 (a) shows the concentration of recovered oxygen gas using the previous type membrane module and Fig. 7 (b) shows the result using the new type. The effective area of membrane is $0.3m^2$ for both of them.

As is evident from Fig. 7, the peak value of recovered oxygen is almost the same. But, the rate of decrease is quite different. Two reasons are considered. The first reason is the new type has smaller contact surfaces, because the hollow fibers are inserted in a bundle. On the other hand, the hollow fibers of the previous type are set uniformly in the case. Therefore, the previous type has wider contact surfaces than the new one. The flow rate of the recovered gas was about 80 to 100 ml/min in the previous type and it was about 30 to 50 ml/min in the new one.

The second reason is the drop of the gas recovering efficiency because when fiber length becomes longer, the drag on the gas stream in the fibers is stronger than on the shorter fibers in same membrane area. A few solutions to those problems have already been found out.

Problems and improvements

Cell adhesion. S. maxima culture adhered neither to the cultivation tank nor to the bypass line under environmental conditions favorable to growth. But when the culture became high density,

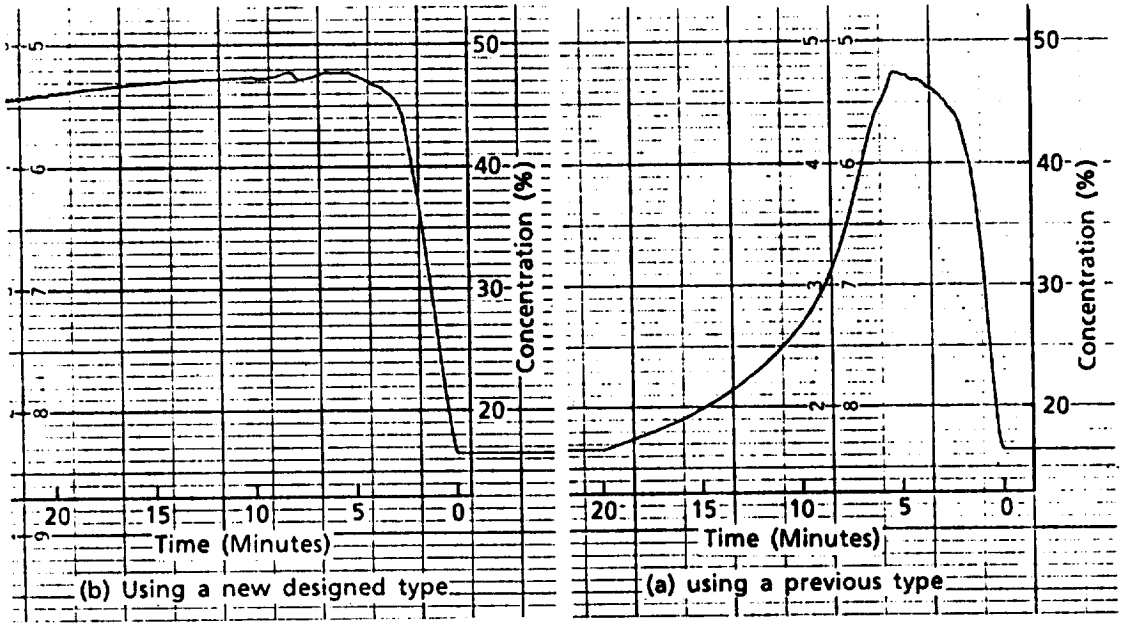

Fig.7 The Concentration of Recovered O_2 Gas

some adhesion occurred, especially to the hollow fibers. S. subsalsa is more adhesive because of the production of poly-saccharide.

Bacteria contamination. Spirulina culture has less bacteria contamination than Chlorella culture because of high alkalinity of the medium. S. subsalsa culture has no problem with contamination by bacteria. But S. maxima culture was sometimes affected by the contamination of bacteria. Culture growth is not good under serious bacteria contamination, especially when algae are sheared by the pump. Some improvements are needed to keep the culture system aseptic.

Algae harvester. In order to automatically keep long continuous culture, treatment of algae after harvest and recycling of culture filtrate is required. The algae harvester also needs more improvements to be used for long term because it did not work so smoothly when applied to S. maxima culture.

CONCLUSION

Oxygen recovery and the algae harvesting method are the main technical problems if algae are cultivated in a micro gravity environment because gas and liquid do not separate naturally. This cultivation system is a primary model (for ground experiments), constructed considering conditions in a state of weightlessness. We could recover oxygen gas from Spirulina culture and add carbon dioxide into the culture medium through membrane modules while keeping the internal pressure of the cultivation tank constant. And algae mass was harvested in a closed system. While it may be no problem to conduct short period experiments with this system in a micro gravity environment if the size of the system is allowed, it is still difficult to keep Spirulina culture in good condition for a long time. Bacteria contamination and cell adhesion are the last problems. These problems must be overcome to keep the culture stable for a long time in space.

REFERENCES

1. M. Oguchi, K. Otubo, K. Nitta and S. Hatayama, Food production and gas exchange system using blue-green alga (Spirulina) for CELSS Adv. Space Res. 7, # 4, 7 - 10 (1987)
2. G. Clement, Ann. Nutr. Alim. 29, # 5, 477 - 488 (1975)
3. L. V. Venkataraman, Bluegreen alga Spirulina, Central Food Technological Research Institute, Mysore 570013 (India) 1983.

N90-15446

GAS BUBBLE COALESCENCE IN REDUCED GRAVITY CONDITIONS

B.G. Thompson* and W.S.C. Brooks**

* Biotechnology Department, Alberta Research Council, P.O. Box 8330, Postal Station F, Edmonton, Alberta, Canada T6H 5X2
**SED Systems Inc., P.O. Box 1464, Saskatoon, Saskatchewan, Canada S7K 3P7

ABSTRACT

The effects of low gravity, as produced by a reduced gravity aircraft, the KC135, on the formation and coalescence of gas bubbles were examined over a range of gas-liquid ratios and with various medium constituents. These effects will influence design considerations of fermentors operating in reduced gravity conditions.

INTRODUCTION

Fermentors operating in reduced gravity conditions will be used for a number of functions. They will be used in controlled ecological life support systems (CELSS) or biological life support systems (BLSS) for photosynthetic and nonphotosynthetic organism growth, for basic research purposes, and may be used as feedstock producing units for biopharmaceutical production systems.

A single fermentor design is unlikely to be of generic use in space. Different designs will be required to take into account operational condition requirements. Only certain fermentor designs will be usable dependent on application. These applications include:

1. Examinations of the effects of low gravity on organisms. Many fermentors impart mass transfer through active mixing systems. The combination of positive accelerative forces and shear imparted by the mixing system and the negative accelerative forces imparted by the resident liquid in the bioreactor make these types of fermentors unsuitable for the investigation of the effects of reduced gravity on organisms.

2. Examinations of organisms requiring high rates of mass transfer for growth. Conversely, fermentors without active mixing systems such as those that rely soley on diffusion or slow perfusion for mass transfer, while possibly being suitable for uses as above, will not have mass transfer rates to support organism growth under most microgravity operating conditions.

3. Examinations of organisms living at gas-liquid interfaces. Fermentors that separate the gas and liquid phases with gas permeable membranes will not allow the growth of organisms that need to grow at an interface.

The bubble coalescence experiments described will be the basis for an actively mixed gas-liquid fermentor design that will allow high mass transfer rates and enable the cultivation of organisms that must grow at a gas-liquid interface.

Fermentors operating under reduced gravity will vary from those operating under unit gravity /1/. Phases of differing density at unit gravity tend to separate spontaneously in finite periods of time in the absence of other accelerating forces. In reduced gravity the absence of gravity induced accelerations will cause this spontaneous separation to cease. Similarly thermally driven macroscopic convection in monophase conditions will also cease in reduced gravity conditions.

Gas transfer in a fermentor is important for both photosynthetic and nonphotosynthetic organisms. Organisms require the removal of waste by-product gases and normally require a specific gas or gases for metabolic purposes. In aerobic organisms the waste gas is usually carbon dioxide and the gas required for metabolism is usually oxygen. However other gases such as nitrogen, hydrogen, hydrogen sulphide, methane, and other gaseous hydrocarbons may serve as metabolic substrates or be waste by-products.

Gas transfer from a gas phase to an organism or visa versa is generally governed by the following equation:

$$\frac{dg}{dt} = KA(C^*-C) \qquad [1]$$

where $\frac{dg}{dt}$ = gas transfer rate

K = some gas transfer coefficient
A = interfacial surface area between gas and liquid
C*= gas concentration at interface of gas and liquid
C = bulk liquid gas concentration

C is determined by the equilibrium of the gas uptake rate by the organism, ds/dt, and the gas transfer rate, dg/dt. C* is a function of gas solubility and the partial pressure of the gas in the gas phase. The equilibrium A in a continually mixed gas/liquid fermentor is determined by the balance of bubble coalescence and bubble breakup. Both of these processes are effected by the viscosity of the medium in the fermentor and the presence of surface active agents and particulate matter. In fermentors where the gas and liquid phase are separated by a gas permeable membrane, A is constant. K in any fermentor is dependent on the net resistance to gas transfer between the gas phase and the surface of the microorganism.

Thompson and Ward /1/ examined the effects of varying the functions that govern gas bubble coalescence rates on the performance of a mixed phase microgravity fermentor and found that this rate was a critical factor in accessing reactor performance. Similarly, factors effecting K in microgravity need to be determined.

This paper describes a series of experiments undertaken on a reduced gravity aircraft, the KC135, in order to study the effects of reduced gravity on gas bubble formation and on the factors that effect gas bubble coalescence.

MATERIALS AND METHODS

The experiment was undertaken on a KC135 aircraft which provides an environment with accelerations of 10-2 to 10-3 g for periods of up to 30s. The bubble generation apparatus used is shown in a simplified form in Figure 1. In this system, gas liquid mixtures contained in a 30 mL ampoule (B, Figure 1) were subjected to a controlled instantaneous acceleration as the ampoule impacts on a stationary surface (A, Figure 1). The ampoule is driven by a spring action (C, Figure 1) activated by a hand pulled plunger (D, Figure 1). The ampoule was attached to the plunger mechanism. Agitation impulses ranged from 0.3 Kg.m/s to 0.03 Kg.m/s dependent on the mass contained in the sample ampoule. The force was roughly equivalent to dropping the ampoules 5 m. onto a solid surface. The resulting gas-liquid mixture was then examined over time using a two camera video system operating at 90 angles to each other. Camera speed was 30ms/frame. Initial bubble size distributions prior to coalescence (about 100 ms) and net bubble deceleration rates were observed. In order to minimize the residual effects of gravity that are primarily in the vertical axis, bubble decelerations were only measured in the horizontal axis. Bubbles were selected that had initial velocities within 10% of each other. The gas-liquid mixtures consisted of air as the gas phase and water as the liquid phase. The liquid phase was modified with additives including glycerol, yeast (Saccharomyces cerevisiae, 2 X 10^7 cells/mL) and a non-ionic surface active agent (Antifoam C, 0.1% v/v). A total of 180 trials over a 3 day period were obtained for different gas-liquid mixtures.

RESULTS

The experimental conditions resulted in four different event periods (Figure 2). The first period was a near instantaneous acceleration when the sample ampoule impacts the surface and the momentum in the fluid causes the violent agitation of the gas-liquid solution. This phase lasted 100ms. By the end of this period, bubble formation was complete, although turbulence was still present. Bubble breakup had completely ceased by the end of this period. The second period was a bubble deceleration period. Due to the viscosity of the fluid and the lack of acceleration forces the bubbles rapidly came to a stop within a localized region of the sample. Concurrent with this period was a period where the bubbles underwent coalescence events due to collision. Once relative bubble motion ceased, bubble coalescence largely ceased. The final phase identified was that of relative domain motions where regions of the sample would move relative to each other. In this case, bubbles within a domain had no relative velocity. Occasionally bubbles at the edge of two domains would

coalesce as a result of net relative domain velocities. This phase continued until the liquid viscosity totally dampened the motion or until the end of the parabola when g loads of approximately 2 were experienced causing virtually instantaneous (< 30 ms) gas-liquid phase separation.

Bubble Size Distribution

The distribution of bubble size was measured immediately after agitation occurred and prior to coalescence events. Figures 3a and 3b show the distributions found with water-air mixtures. Thirty-eight trials were performed with this system. Two general distributions were observed. The sizes represent bubble diameters as observed uncorrected for magnification effects of the sample tube. The effects of components added to the liquid phase of the system on bubble size distribution are found in Figures 4, 5, and 6. The addition of surfactant to the system resulted in a net distribution of bubbles with diameters smaller than the distributions caused by the addition of yeast or glycerol. The surfactant trial bubble size distributions fell between the two air-water distributions.

Deceleration

Deceleration versus bubble diameters at differing viscosities are found in Figure 7. As bubble diameters increase at any one viscosity, decelerations increase. For constant bubble diameters, increasing viscosity increases deceleration. As well, increasing viscosity increases the rate at which deceleration increases as bubble diameter increases.

DISCUSSION

The results presented here impact on gas transfer in low gravity fermentors in several ways:

1. Initial Interfacial Surface Area

   The composition of the gas-liquid mixture in the ampoule determined the initial interfacial surface area obtained from a near instantaneous accelerative event. As a result, the design of microgravity fermentation units will necessarily have to take in account initial medium composition and changes in medium composition during a fermentation. The initial bubble size distributions determined after a point accelerative event demonstrate that when compared to the water-air distribution found in Figure 3a, additives, whether viscosifying agents, surfactants or particulate matter, have a deleterious effect on interfacial surface area. When compared to the water-air bubble distribution found in Figure 3b, the addition of surfactant actually increases interfacial surface area. In this case, this has the effect of increasing gas transfer in a fermentation.

   The effects of different concentrations of these additives on bubble distribution were not determined. It will be necessary to examine specific concentration dependent effects on bubble size distribution prior to fermentor design.

   The two distributions obtained for water-air mixtures are unexplained. It may be that water has the correct physical properties under the force applied to display either distribution, dependent on other external conditions such as quality of gravity, pressure, and/or temperature.

2. Interfacial Surface Area Over Time

   The degree of which coalescence will occur will determine the net instantaneous interfacial surface area at any time. Most coalescence has been demonstrated to occur during that period (Figure 2) in which bubbles have velocities relative to each other. As shown in Figure 7, both bubble size and viscosity affect the deceleration experienced by a bubble as it moves through the liquid. This was in general agreement with Stokes law pertaining to bubbles or droplets of one fluid in another. Medium conditions will therefore also effect the time period in which coalescence will occur.

3. K, Gas Transfer Coefficient

   The gas transfer coefficient is dependent on several factors. If there is a net velocity difference between the gas and liquid phases, oxygen is carried away from the bubble surface in a non-diffusion mediated manner. As well, this net velocity difference sweeps the surface of the bubble, reducing the stability of the bubble surface. This has the tendency to increase K. When relative gas-liquid motion cease, as in the domain motion phase described above, bubble surfaces are not renewed and gas transfer occurs primarily by diffusion. This will lower gas transfer.

CONCLUSION

The results presented here indicate that initial medium conditions and changes in those conditions during fermentation will affect gas transfer in a microgravity fermentor. They also demonstrate that at the point in which most bubble coalescence ceases, ensuring that the interfacial surface area, A, remains constant, gas transfer may be inhibited by another process effecting K, the gas transfer coefficient. The net gas transfer in the system will be determined by a balance of factors effecting A and K.

ACKNOWLEDGMENTS

The authors would like to acknowledge the assistance of D. Cain and S. Hollemeyer in experimental design and T. Malcolm in data analysis. The further assistance of NRCC-Space Division, the Canadian Astronaut Corp., SED Systems Inc. and the Alberta Research Council is also acknowledged.

REFERENCES

1. B.G. Thompson, and D. Ward. Acta Astronautica 13(3):105-117 (1986)

FIGURES

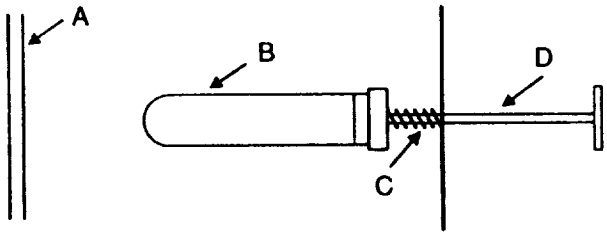

Fig. 1. Agitation mechanism for system. The plunger, D, is pulled against the resistant force of the spring, C. When this is released, it accelerates the sample ampoule B into C stationary surface, A.

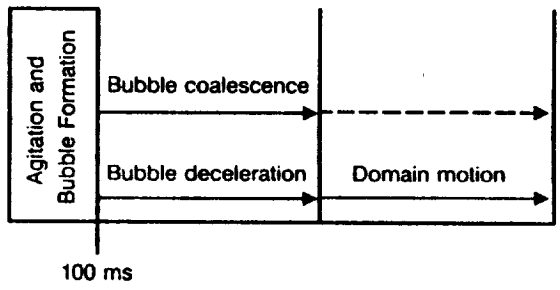

Fig. 2. The four event periods found after gas-liquid mixing in the sample ampoule.

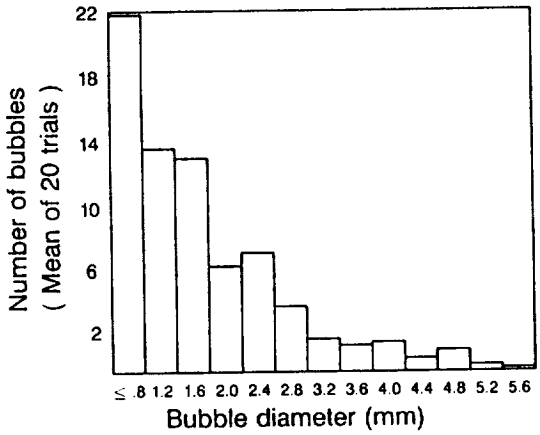

Fig. 3a. First distribution of bubbles with respect to bubble diameter in a water-air mixture.

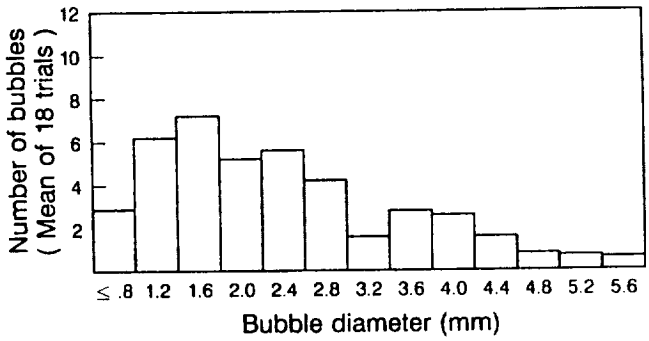

Fig. 3b. Second distribution of bubbles with respect to bubble diameter in a water-air mixture.

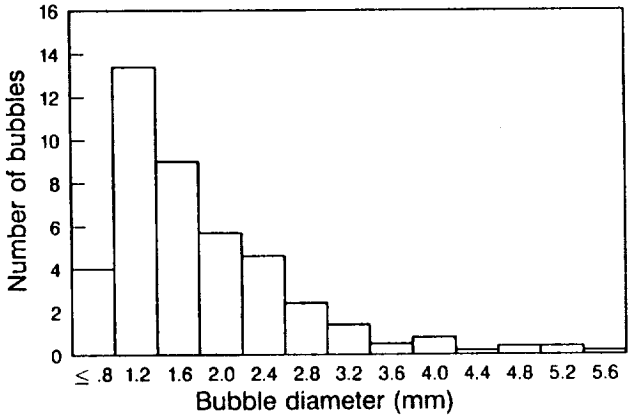

Fig. 4. Distribution of bubbles with respect to bubble diameter in a 0.1% v/v antifoam/water-air mixture.

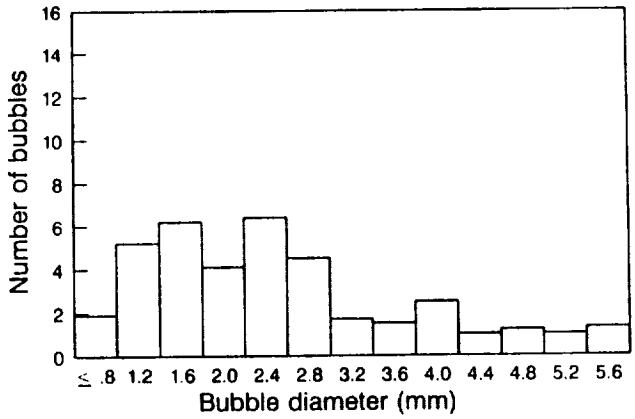

Fig. 5. Distribution of bubbles with respect to bubble diameter in a yeast/water-air mixture.

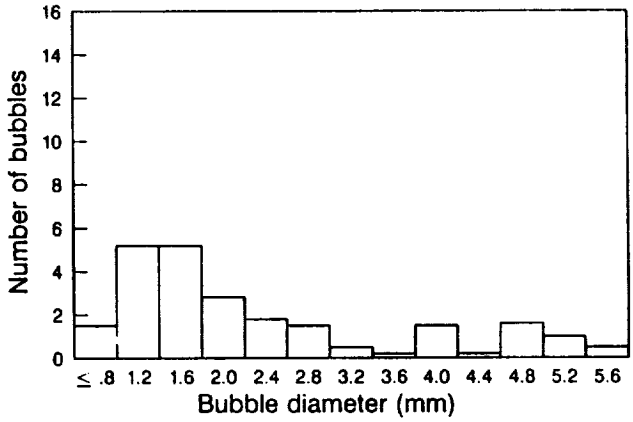

Fig. 6. Distribution of bubbles with respect to bubble diameter in a 14% v/v glycerol/water-air mixture.

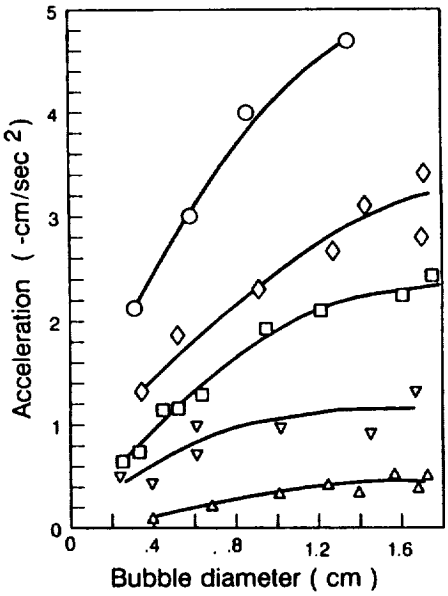

Fig. 7. Acceleration vs. bubble diameter in various glycerol/water-air mixtures. Relative viscosity at solutions:

N90-15497

PHASE SEPARATED MEMBRANE BIOREACTOR: RESULTS FROM MODEL SYSTEM STUDIES.

Petersen G.R.,* Seshan P.K.,* Dunlop E.H.**

* Jet Propulsion Laboratory, 4800 Oak Grove Drive Pasadena CA 91109, U.S.A. ** Department of Chemical Engineering ,Colorado State University Fort Collins CO 80523, U.S.A.

ABSTRACT

The operation and evaluation of a bioreactor designed for high intensity oxygen transfer in a microgravity environment is described. The reactor itself consists of a zero headspace liquid phase separated from the air supply by a long length of silicone rubber tubing through which the oxygen diffuses in and the carbon dioxide diffuses out. Mass transfer studies show that the oxygen is film diffusion controlled both externally and internally to the tubing and not by diffusion across the tube walls. Methods of upgrading the design to eliminate these resistances are proposed. Cell growth was obtained in the fermenter using Saccharomyces cerevisiae showing that this concept is capable of sustaining cell growth in the terrestial simulation.

INTRODUCTION

The use of a bioreactor as a fermenter in Controlled Ecological Life Support Systems (CELSS) will likely occur in the food production or waste processing subsystems. It is anticipated that a design for a fermenter for an operational CELSS will be developed from models flown and tested on STS missions.

Probable areas of use

There are three possible places a CELSS-type bioreactor could be used:

i. As redundancy or backup for the conventional food production systems that would be available in space. It is clear that several systems could be developed, probably using plants and/or animals. However there is always the problem of catastrophic crop failure and if there is not enough stored food and it would be necessary to activate emergency rations of food. One possible source of this is microbial food which can be made available in two or three days. We have done preliminary studies that show that in reasonable sized fermenters it is possible to produce adequate quantities of edible types of biomass, for example yeast, that can be processed into the necessary food components.

ii. As supplements to conventional food production. The limiting amino acids for human nutrition are tryptophan and lysine. One of the deficiencies in human foods such as wheat and similar materials is very easily satisfied by microbial sources. Many bacteria, and some yeasts, could provide the necessary amounts of lysine, methionine and tryptophan. This is just one example of a supplement and others may be possible. Also an analysis of human food balances reveals that even when using wheat and high quality foods humans are still short of carbohydrate. It is possible that it will always be necessary to have some calories from microbial carbohydrates.

iii. The area of that will probably have first application for the bioreactor is the production of valuable commodities (in this case, food) from inedible plant waste. It is a consistent observation for all plants that about 50% of biomass is inedible. Of the inedible biomass, about 40% is comprised of cellulosics and about 20-30% is found in hemicellulosics (pentose sugars). These two components are readily separated with mild hydrolysis and fractionation methods. The further hydrolysis of these

components into monosaccharides suitable for direct use or fermentation by microorganisms provides additional food sources for CELSS food production subsystems.

APPARATUS AND METHODS

The main problem with carrying out fermentations in microgravity is of course that the bubbles will not rise in the fermenter thus preventing gas - liquid disengagement /1/. One reasonable solution is to avoid the need to solve the separation problem by not having a gas phase to disengage. The apparatus is designed to explore this concept for high- rate oxygen-transfer intensive microbial growth in a CELSS environment.

The gas and liquid phases are kept separate when the reactor contains about 10% by volume of silicone tubing in a zero-headspace fermentation configuration and passing the gas (air or oxygen) through the inside of the tubes. Oxygen and carbon dioxide are highly permeable to silicone rubber and diffuse rapidly through it. It is also possible to have liquid silicones saturated with oxygen passing through the tubes to act as oxygen carriers. Carbon dioxide can be readily removed from the off-gasses by adsorption in a sink such as monoethanolamine. A potentially attractive alternative to a fixed CO2 sink is reversible adsorption by redox-switched absorbers such as substituted metallocenes and quinones /2/.

Such a system is essentially gravity-independent and can be readily examined under terrestial conditions.

The terrestial model tested was constructed from plexiglass in the form of a cylinder containing a total of 8.7 liters volume. The working volume was about 7.7 liters, the other liter being occupied by tubing and support frames. Thus 88% was available for culture. The flowsheet is shown in figure 1.

150 feet of silicone tubing was wound round a support frame. The tubing had an internal diameter of 0.104 inches and an external diameter of 0.192 inches.

Stirring was provided to the center of the liquid by a marine impeller revolving at 200-400 revolutions per minute. Air flow to the inside of the tube could be varied by a mass flow controller from 2.5 to 20 liter per minute gas flow at an applied pressure of between 3 and 10 psig.

A 1.5% innoculum of Saccharomyces cerevisiae PEP4 was added to a synthetic medium (Yeast carbon base- YCB) supplemented with YM(1%) and 0.1% tryptone. It is thus a relatively rich media.

As this test fermenter is not capable of being autoclaved due to the plexiglass construction, a standard operating procedure was developed and followed. It takes about two days to sterilize the whole reactor. First, the reactor is cleaned with clean water and then assembled. It is filled and left overnight with a 10% solution of alcohol, and rinsed thoroughly the next day with sterile distilled water. It is then filled again with 3% hydrogen peroxide solution, left overnight and rinsed with several washes of sterilized deionized water. The media is introduced by adding two liters of nutrient broth to the bioreactor, followed by four liters of sterile distilled water, 500 mls of a stock solution of YCB without glucose. 125 mls of 40% glucose is added to yield 10 milligram per ml solution of sugar i.e. excess sugar.

100 ml of an overnight culture of the yeast are added. The head space is removed by adding enough YM broth to fill up the reactor, and then all the probes are inserted; the oxygen probe, the pH probe, the temperature probe, after we have rinsed each one of them out with alcohol. The air lines are connected and stirring is started to initiate the whole experiment. We remove a sample of culture immediately to measure the starting glucose concentration and then sample periodically with a hypodermic needle and syringe through stoppers that are in the top of the bioreactor. Contamination was only a problem on one run.

Oxygen transfer measurements were made by degassing the fermenter with nitrogen and following the rise of dissolved oxygen on a chart recorder as air was reintroduced through the tubes. Measurements were made with a New Brunswick galvanic oxygen probe.

RESULTS & DISCUSSION

Yeast growth

In order to evaluate the reactor under actual growth conditions,cultures of yeast were grown under a variety of of reactor conditions. Figure 1A was an initial run at low gas pressure but high flow rate. There was no attempt to control pH or temperature. The data showed us that the apparatus and sterilization techniques could be employed to culture yeast cells. The effect of lowering the flowrate by one half and increasing the pressure is shown in figure 1B. Again, the system worked well and the rate of cell growth increased as is shown by the quicker depletion of oxygen (20 hours vs. 30 hours).

Since oxygen was apparently supplied at adequate levels, an attempt was made to evaluate the lower working point of the apparatus. The time at which oxygen depletion occurred as a function of reactor conditions was used as the basis for evaluating the lower working limit of the apparatus. The initial experiment in this series is shown in figure 2. With only 50 feet of tubing, 7.5 psig. and 1 liter/min flowrate,the reactor reached oxygen depletion after about 14-15 hours. However, the possibility that glucose depletion was the cause for lowered oxygen consumption could not be ruled out. In the experiment shown in Figure 3, the flowrate was lowered even more and the glucose measurements were taken more frequently. The results showed that glucose depletion had not occurred simultaneously with oxygen depletion. This indicates that the cells are growing at a rate that was a direct function of oxygen supply. The other observation was that by lowering the flowrate to 0.5 liter/min, the point at which oxygen was depleted was shifted to 16-17 hours. This is slightly higher than the value shown in Figure 2 and is consistent with the fact that airflow was half that of the value used in the Figure 2 experiment.
The cells are still healthy and normal. The maximum cell count is 1.3 grams per liter. This is not a high density, but it is encouraging for our first design.

These simple experiments showed the following:

1. The reactor could be sterilized, operated and maintained using the simple equipment employed(i.e. no temperature or pH control) to provide meaningful results.

2. Oxygen limitation can be reached in in a relatively short time permitting quick analysis of the system.

3. Measurements of oxygen transfer rates will need to be conducted in order to estimate actual maximum operating limits.

Oxygen transfer studies

The oxygen transfer data from the step response studies were analyzed by the method of Ruchti et al. /3/, and expressed as the product of the overall mass transfer coefficient and the surface area per unit volume of reactor, Kla.
The measurements were taken for a range of air flowrates and stirrer speeds. and are given in Table 1.

The biological experiments demonstrated that modest cell dry weights could be obtained with this design of fermenter before oxygen limitation was reached. While these results are encouraging they clearly are not adequate for a practical system. To overcome the inherent limitation of the preliminary equipment design, the oxygen transfer studies were initiated. The values of Kla obtained were some 50-100 times lower than in conventional stirred fermenters operating under terrestial conditions. They correspond to oxygen transfer intensities of around 0.04 kgO2/m3/hr. Figure 4 is an attempt to show the interaction between exponential cell growth in the absence of oxygen limitation for a range of doubling time from 1 to 4 hours. This is indicated by the solid lines. The broken lines show the cell mass that can be supported, at 50% carbon conversion,for differing oxygen transfer intensities of between 1 and 5 kgO2/hr/m3. It shows that for cell dry masses of likely importance in this project that oxygen limitation will dominate under most conditions and should thus be the focus of future studies.

Three main effects can be expected to contribute to the low oxygen transfer intensities observed in this study:-

a. film diffusion resistance in the tube containing the gas
b. external film diffusion into the bulk liquid
c. oxygen diffusion across the silicone tubing wall

For laminar flow of the gas and liquid, resistances a and b above will be reduced as the flowrate past the tubes is increased while resistance c will be unchanged. From fluid mechanics it is known that the mass transfer coefficient will vary inversely with the square root of the flowrate. A common way of therefore assessing the relative importance of the contributions is to plot the reciprocal of Kla vs. the reciprocal of the square root of the flowrate, extrapolate to zero on the axis i.e. infinite velocity which removes the film resistance and compare the magnitude of the residual mass transfer coefficient /4/.

$$1/Kla = 1/(\text{velocity, internal})^{0.5} + 1/(\text{velocity, external})^{0.5} + \text{membrane diffusion resistance} \quad (1)$$

Figure 5 shows this procedure for the internal flowrate variation experiment. The graph shows a marked slope implying that indeed the internal diffusion resistance in the tube is substantial and that major improvements in oxygen transfer can be expected simply by increasing the flowrate, perhaps with recycle, through the tubes.

The residual mass transfer resistances can now be subtracted out and the effect of external film resistances examined. Figure 6 shows the same kind of graph, this time produced by changing the stirrer speed. Again a substantial slope is observed with the regression line passing through the origin of the graph. i.e. at infinite stirrer speed the mass transfer coefficient becomes infinite. The interpretation of this is that the external fluid resistances are extremely high compared to which any resistance from the oxygen diffusion across the membrane is negligible.

These results are very reassuring as they imply that redesign of the equipment can be done in ways that will result in very substantial increases in oxygen transfer efficiency that will permit large increases in cell mass to be obtained long before the diffusion resistances in the tubes themselves start to become important.

The reactor will be reconfigured to reflect these findings.

CONCLUSIONS

1. Yeast can be successfully grown in a phase separated fermenter that should be capable of operation independent of gravity.

2. The current design limitations can be overcome and will result in substantial increases in oxygen transfer intensities which in turn will support greater cell masses to provide a practical test facility for a CELSS test bed.

REFERENCES

1.Seshan P.K., Petersen G.R., Beard B.J., Dunlop E.H. "Design Concepts for Bioreactors in Space in CELSS " NASA Technical Manual 88215 (1986).

2.Bell W.L.,Miedaner A.,Smart J.C.,Dubois D.L., Drostow C.E. "Synthesis and Evaluation of electroactive CO2 carriers". NASA SAE Technical Paper Series. Paper 881078. 1988

3.Ruchti G.,Dunn I.J.,Bourne JR. "Comparison of Dynamic Oxygen Electrode Methods for the Measurement of Kla", Biotech. Bioeng. 23 277-290 (1981).

4.Dunlop E.H., Williams R., "Physicochemical aspects of Protein bound substances. Part II- kinetics of removal." Medical & Biological Engineering 16 350-362 (1978).

TABLE 1 Mass transfer coefficients (Kla) as a function of system variables.

Airflow Rate (lit/min)	Stirrer Speed (rpm)	Kla (hr-1)
9.5	325	4.20
7.5	325	2.75
5.0	325	2.64
2.5	325	2.08
7.5	275	3.47
7.5	275	2.75
7.5	225	2.77
7.5	110	1.97
7.5	155	1.29

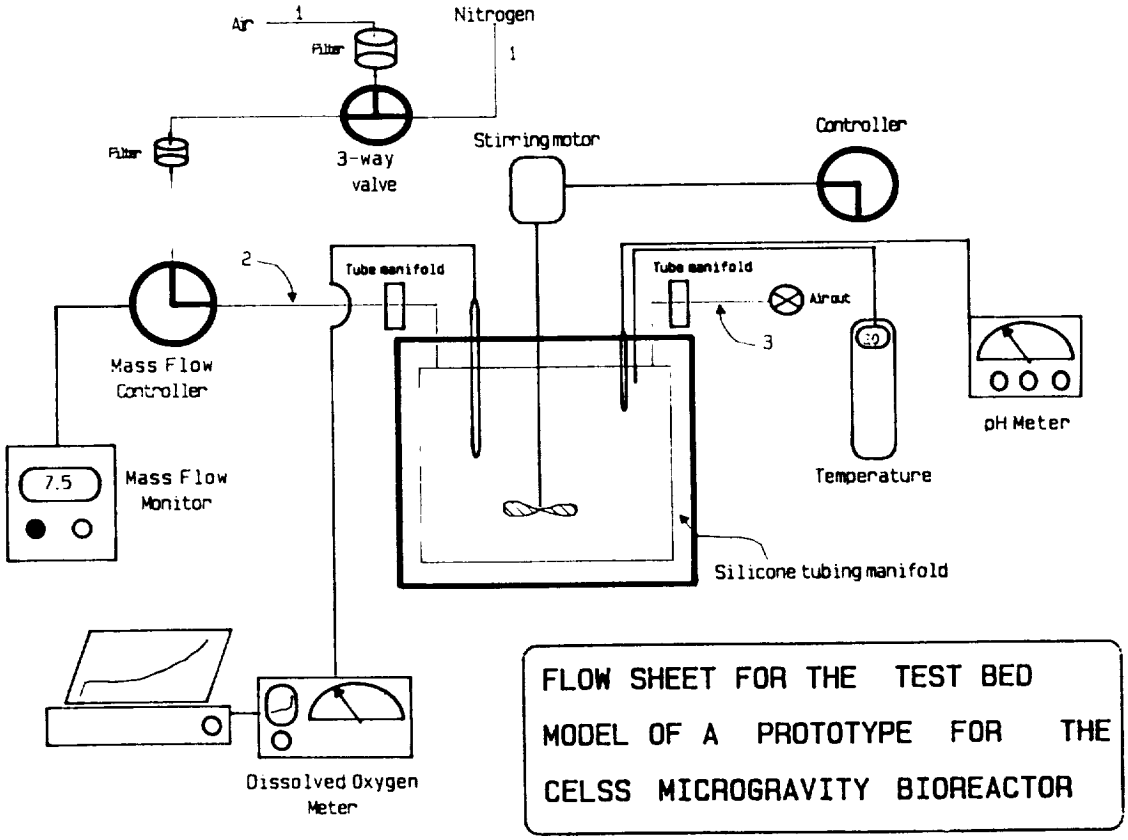

Fig. 1 Flowsheet for terrestial simulation of the fermenter configured to measure oxygen transfer intensity and model yeast growth.

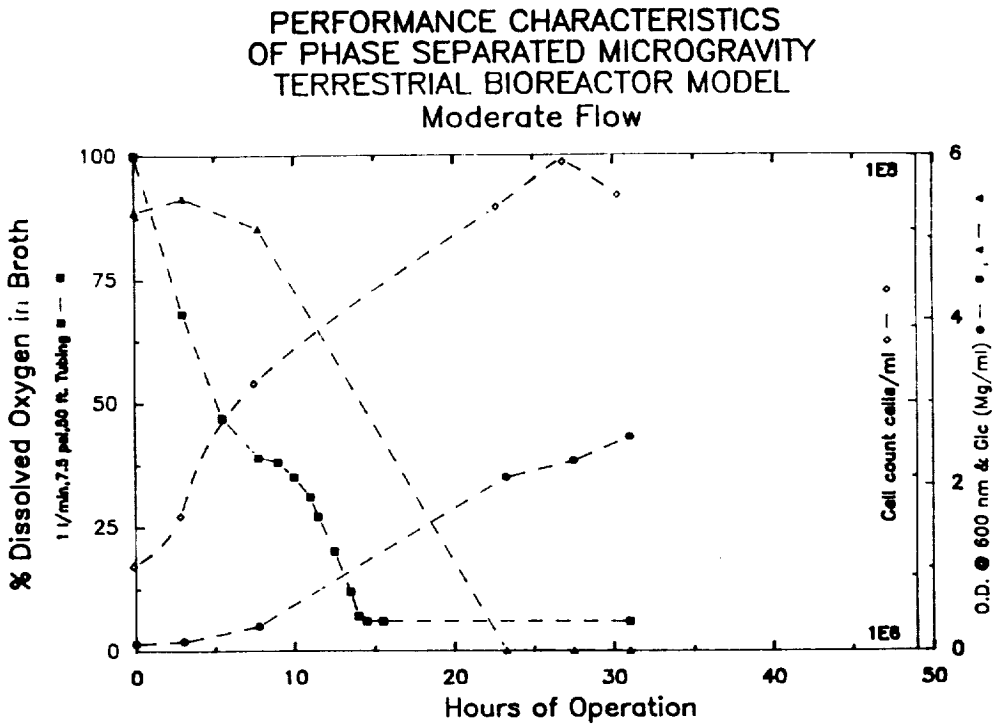

Fig. 2. Initial evaluation of the fermenter. The lowest working point of the fermenter was established. With only 50 feet of tubing, 7.5 psig. and 1 liter/min flowrate the reactor reached oxygen depletion after about 14-15 hours.

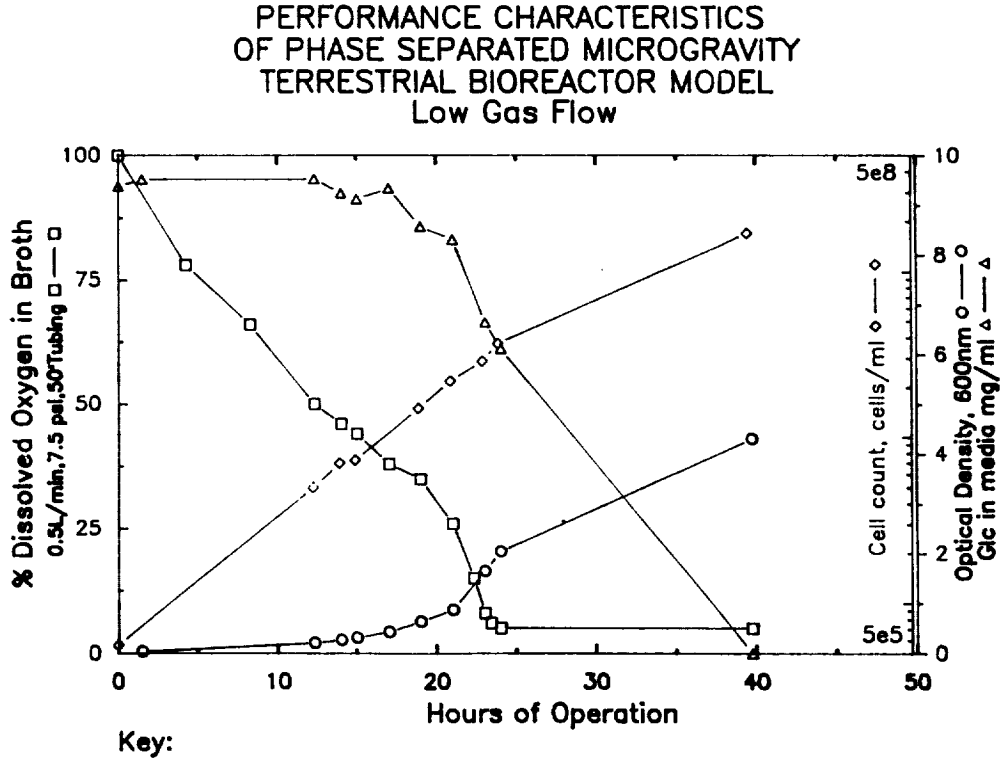

Fig. 3. At even lower flowrate glucose depletion does not occur simultaneously with oxygen depletion, indicating that the cells are growing at a rate that was a direct function of oxygen supply.

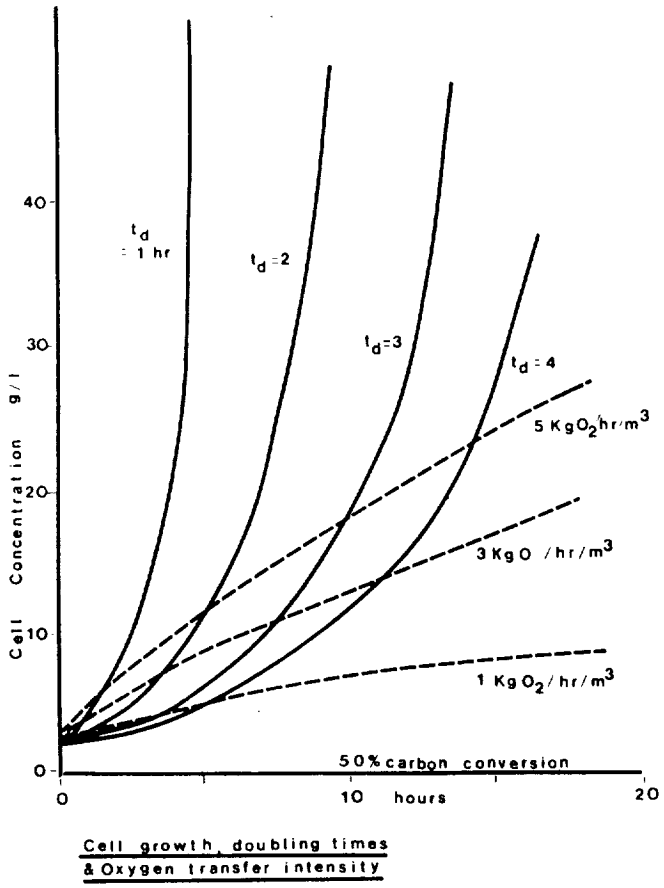

Cell growth, doubling times & Oxygen transfer intensity

Figure 4

Fig. 4. The interaction between exponential cell growth in the absence of oxygen limitation for a range of doubling time from 1 to 4 hours can be seen. This is indicated by the solid lines. The broken lines show the cell mass that can be supported, at 50% carbon conversion, for differing oxygen transfer intensities of between 1 and 5 kgO2/hr/m3. It shows that for cell dry masses of likely importance in this project that oxygen limitation will dominate under most conditions and should thus be the focus of future studies.

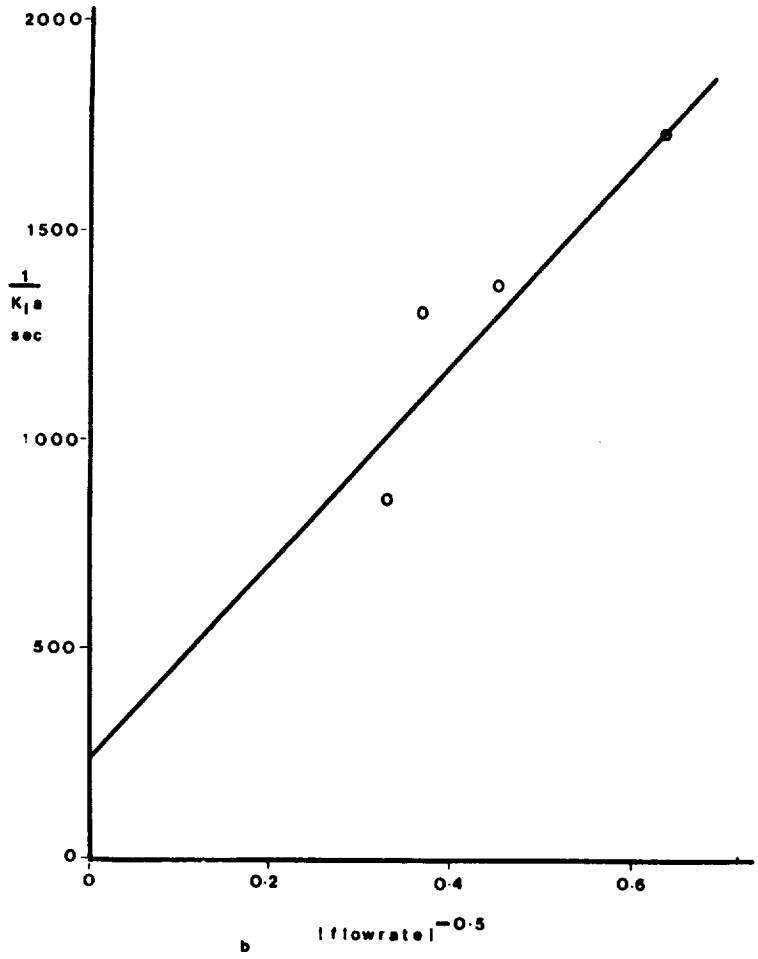

Figure 5

Fig. 5. The procedure for assessing the internal flowrate resistances The graph shows a marked slope implying that indeed the internal diffusion resistance in the tube is substantial and that major improvements in oxygen transfer can be expected simply by increasing the flowrate.

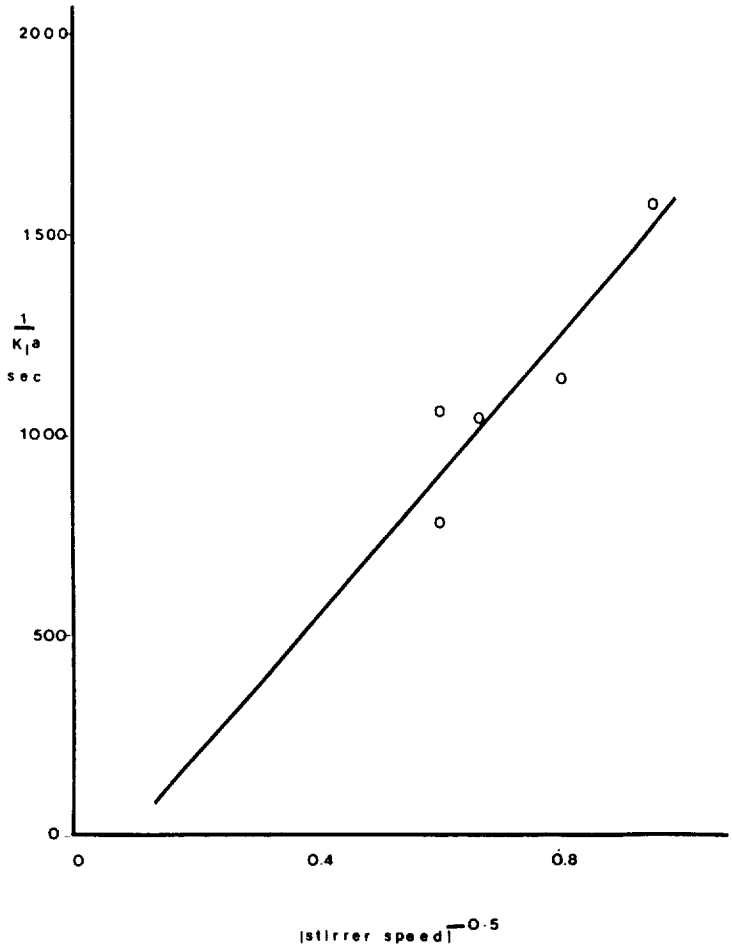

Figure 6

Fig. 6. The residual mass transfer resistances from figure 6 are subtracted out and the effect of external film resistances examined by changing the stirrer speed. Again a substantial slope is observed with the regression line passing near the origin of the graph. i.e. at infinite stirrer speed the mass transfer coefficient becomes infinite implying that the external fluid resistances are extremely high compared to which any resistance from the oxygen diffusion across the membrane is negligible.

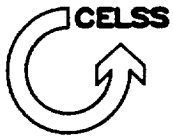

APPENDIX

Controlled Ecological Life Support Systems (CELSS)
A Bibliography of CELSS Documents Published as NASA Reports

1. Johnson, Emmett J.: Genetic Engineering Possibilities for CELSS: A Bibliography and Summary of Techniques. NASA CR-166306, March 1982.

2. Hornberger, G.M. and Rastetter, E.B.: Sensitivity Analysis as an Aid in Modelling and Control of (Poorly-Defined) Ecological Systems. NASA CR-166308, March 1982.

3. Tibbitts, T.W. and Alford, D.K.: Controlled Ecological life Support System: Use of Higher Plants. NASA CP-2231, May 1982.

4. Mason, R.M. and Carden, J.L.: Controlled Ecological Life Support System: Research and Development Guidelines. NASA CP-2232, May 1982.

5. Moore, B. and MacElroy, R.D.: Controlled Ecological Life Support System: Biological Problems. NASA CP-2233, May 1982.

6. Aroeste, H.: Application of Guided Inquiry System Technique (GIST) to Controlled Ecological Life Support Systems (CELSS). NASA CR-166312, January 1982.

7. Mason, R.M.: CELSS Scenario Analysis: Breakeven Calculation. NASA CR-166319, April 1980.

8. Hoff, J.E., Howe, J.M. and Mitchell, C.A.: Nutritional and Cultural Aspects of Plant Species Selection for a Controlled Ecological Life Support System. NASA CR-166324, March 1982.

9. Averner, M.: An Approach to the Mathematical Modelling of a Controlled Ecological Life Support System. NASA CR-166331, August 1981.

10. Maguire, B.: Literature Review of Human Carried Microbes' Interaction with Plants. NASA CR-166330, August 1980.

11. Howe, J.M. and Hoff, J.E.: Plant Diversity to Support Humans in a CELSS Ground-Based Demonstrator. NASA CR-166357, June 1982.

12. Young, G.: A Design Methodology for Nonlinear Systems Containing Parameter Uncertainty: Application to Nonlinear Controller Design. NASA CR-166358, May 1982.

13. Karel, M.: Evaluation of Engineering Foods for Controlled Ecological Life Support Systems (CELSS). NASA CR-166359, June 1982.

14. Stahr, J.D., Auslander, D.M., Spear, R.C. and Young, G.E.: An Approach to the Preliminary Evaluation of Closed-Ecological Life Support System (CELSS) Scenarios and Control Strategies. NASA CR-166368, July 1982.

15. Radmer, R., Ollinger, O., Venables, A. and Fernandez, E.: Algal Culture Studies Related to a Closed Ecological Life Support System (CELSS). NASA CR-166375, July 1982.

16. Auslander, D.M., Spear, R.C. and Young, G.E.: Application of Control Theory to Dynamic Systems Simulation. NASA CR-166383, August 1982.

17. Fong, F. and Funkhouser, E.A.: Air Pollutant Production by Algal Cell Cultures. NASA CR-166384, August 1982.

18. Ballou, E. V.: Mineral Separation and Recycle in a Controlled Ecological Life Support System (CELSS). NASA CR-166388, March 1982.

19. Moore, B., III, Wharton, R. A., Jr., and MacElroy, R.D.: Controlled Ecological Life Support System: First Principal Investigators Meeting. NASA CP-2247, December 1982.

20. Carden, J. L. and Browner, R.: Preparation and Analysis of Standardized Waste Samples for Controlled Ecological Life Support Systems (CELSS). NASA CR-166392, August 1982.

21. Huffaker, R. C., Rains, D. W. and Qualset, C. O.: Utilization of Urea, Ammonia, Nitrite, and Nitrate by Crop Plants in a Controlled Ecological Life Support System (CELSS), NASA-CR 166417, October 1982.

22. Gustan, E. and Vinopal, T.: Controlled Ecological Life Support System: Transportation Analysis. NASA CR-166420, November 1982.

23. Raper, C. David, Jr.: Plant Growth in Controlled Environments in Response to Characteristics of Nutrient Solutions. NASA CR-166431, November 1982.

24. Wydeven, T.: Composition and Analysis of a Model Waste for a CELSS. NASA Technical Memorandum 84368, September 1983.

25. Averner, M., Karel, M., and Radmer, R.: Problems Associated with the use of Algae in Bioregenerative Life Support Systems. NASA CR-166615, November 1984.

26. Radmer, R., Behrens, P., Fernandez, E., Ollinger, O., Howell, C., Venables, A., Huggins, D. and Gladue, R.: Algal Culture Studies Related to a Closed Ecological Life Support System (CELSS). NASA CR-177322, October 1984.

27. Wheeler, R. and Tibbitts, T.: Controlled Ecological Life Support System: Higher Plant Flight Experiments. NASA CR-177323, November 1984.

28. Auslander, D., Spear, R., Babcock, P. and Nadel, M.: Control and Modeling of a CELSS (Controlled Ecological Life Support System). NASA CR-177324, November 1984.

29. Karel, M. and Kamarei, A.R.: Feasibility of Producing a Range of Food Products from a Limited Range of Undifferentiated Major Food Components. NASA CR-177329, April 1984.

30. MacElroy, R.D., Smernoff, D.T., and Klein, H.: Life Support Systems in Space Travel. (Topical Session of XXVth COSPAR meeting, Graz, Austria) NASA CP-2378, May 1985.

31. MacElroy, R.D., Martello, N.V., Smernoff, D.T.: Controlled Ecological Life Support Systems: CELSS '85 Workshop, NASA TM-88215, January 1986.

32. Tibbitts, T.W.:Controlled Environment Life Support System: Calcium-Related Leaf Injuries on Plants. NASA CR-177399, March 1986.

33. Tibbitts, T.W., Wheeler, R.M.: Controlled Environment Life Support System: Growth Studies with Potatoes, NASA CR-177400, March 1986.

34. Babcock, P.S.: Nonlinear System Controller Design Based on Domain of Attraction: An Application to CELSS Analysis and Control, NASA CR-177401, March 1986.

35. Smernoff, D.T.: Atmosphere Stabilization and Element Recycle in an Experimental Mouse-Algal System, NASA CR-177402, March 1986.

36. Oleson, M., Olson, R.L.: Controlled Ecological Life Support Systems (CELSS): Conceptual Design Option Study, NASA CR-177421, August 1986.

37. Oleson, M., Slavin, F., Liening, R., Olson, R.: Controlled Ecological Life Support Systems (CELSS): Physiochemical Waste Management Systems Evaluation, NASA CR-177422, August 1986.

38. Knox, J.: A Method of Variable Spacing for Controlled Plant Growth Systems in Spaceflight and Terrestrial Agriculture Applications, NASA CR-177447, February 1987.

39. Radmer, P., Arnett, K., Gladue, R., Cox, J., Lieberman, D.: Algal Culture Studies for CELSS, NASA CR-177448, February 1987.

40. Karel, M., Nakhost, Z.: Utilization of Non-Conventional Systems for Conversion of Biomass to Food Components, NASA CR-177449, February 1987.

41. MacElroy, R.D., Smernoff, D.T., Rummel, J.: Controlled Ecological Life Support Systems: Design, Development and Use of a Ground-Based Plant Growth Module, NASA CP-2479, June 1987.

42. MacElroy, R.D., Smernoff, D.T.: Regenerative Life Support Systems ,in Space, (Topical Session of XXVIth COSPAR meeting, Toulouse, France), NASA CP-2480, June 1987.

43. Tremor, J.W., MacElroy, R.D.: Report of the First Planning Workshop for CELSS Flight Experimentation, NASA CP-10020, November 1988.

NASA
National Aeronautics and Space Administration

Report Documentation Page

1. Report No.	2. Government Accession No.	3. Recipient's Catalog No.
NASA CP-10040		

4. Title and Subtitle
Controlled Ecological Life Support Systems:
Natural and Artificial Ecosystems

5. Report Date
December 1989

6. Performing Organization Code

7. Author(s)
Editors: Robert D. MacElroy, Brad G. Thompson,[1]
Theodore W. Tibbitts,[2] and Tyler Volk[3]

8. Performing Organization Report No.
A-89105

10. Work Unit No.
199-61-12

9. Performing Organization Name and Address
Ames Research Center
Moffett Field, CA 94035

11. Contract or Grant No.

13. Type of Report and Period Covered
Conference Publication

12. Sponsoring Agency Name and Address
National Aeronautics and Space Administration
Washington, DC 20546-0001

14. Sponsoring Agency Code

15. Supplementary Notes
Point of Contact: Robert D. MacElroy, Ames Research Center, MS 239-4, Moffett Field, CA 94035
(415) 694-5573 or FTS 464-5573
[1]Alberta Research Council, Edmonton, Alberta, Canada. [2]University of Wisconsin, Madison, Wisconsin. [3]New York University, New York, New York.

16. Abstract

The scientists supported by the NASA-sponsored Controlled Ecological Life Support Systems (CELSS) program have played a major role in creating a Committee on Space Research (COSPAR) section devoted to the development of bioregenerative life support for use in space.The series of 22 papers in this volume were sponsored by Subcommission F.4 and presented at the 27th COSPAR, held in Espoo, Finland, July 18-29, 1988. The papers deal with many of the diverse aspects of life support, and with outgrowth technologies that may have commercial applications in fields such as biotechnology and bioengineering. In addition to those papers presented by U.S. scientists, researchers from France, Canada, Japan, and the Soviet Union contributed to the sessions, and their presentations have been included in this volume.

17. Key Words (Suggested by Author(s))	18. Distribution Statement
Life support systems, Plant productivity, Closed ecosystems, Simulation modeling, Waste recycling, Carbon cycling, Gas exchange, Biofermentors, Algae	Unclassified–Unlimited Subject Category–54

19. Security Classif. (of this report)	20. Security Classif. (of this page)	21. No. of Pages	22. Price
Unclassified	Unclassified	199	A09

NASA FORM 1626 OCT 86

For sale by the National Technical Information Service, Springfield, Virginia 22161